

**Analysis of the ontogeny of
regional endothermy in Pacific
bluefin tuna (*Thunnus orientalis*)
and the effects of feed restriction
in yellowtail kingfish (*Seriola
lalandi*)**

by
Arif Malik

Thesis
Submitted to Flinders University
for the degree of

Doctor of Philosophy
College of Science and Engineering

31/7/2019

CONTENTS

Declaration	6
Acknowledgements	7
Summary	10
Chapter 1 – General introduction	12
1.1.1. Thermoregulation in vertebrates	13
1.1.2. Regional endothermy in fishes.....	14
1.1.3. Red muscle endothermy in fishes.....	14
1.1.4. Visceral endothermy in fishes	15
1.1.5. Cranial endothermy in fishes	16
1.1.6. Regulation of mitochondrial abundance by PGC-1 α	16
1.1.7. Bluefin tunas	17
1.1.8. Amberjacks	18
1.1.9. Project aims	19
1.1.10. Thesis structure.....	20
Chapter 2 - Regulation of the ontogenetic transition from ectothermy to regional endothermy in pacific bluefin tuna (<i>Thunnus orientalis</i>): anatomy and physiology	25
Abstract.....	26
2.1. Introduction	28
2.1.1. Regional endothermy in fishes	28
2.1.2. Tuna classification and distribution	28
2.1.3. The life history of Pacific bluefin tuna.....	29
2.1.4. Regional endothermy in bluefin tunas	31
2.1.5. Aims	32
2.2. Materials and Methods.....	33
2.2.1. Fish specimens	33
2.2.2. Estimating the age of the PBT specimens	33
2.2.3. Temperature measurements	34
2.2.4. Fish sampling for histology	35
2.2.5. Red muscle distribution and mass measurements.....	36
2.2.6. Confirmation of the species identity of our PBT specimens	37
2.2.7. Statistical analyses.....	38
2.3. Results	39
2.3.1. Fish growth and age determination	39
2.3.2. Red muscle distribution and ontogeny	41
2.3.3. Relationships between tissue temperature, body size and ambient water temperature	46
2.3.4. Proliferation of the red muscle rete blood vessels with increasing fish body size and decreasing ambient water temperature.....	49
2.3.5. Proliferation of the visceral rete blood vessels with increasing body size and decreasing ambient water temperature.....	56
2.4. Discussion.....	59
2.4.1. PBT can significantly elevate their red muscle temperature above the ambient water temperature at a minimum body size of ~29 cm FL	59
2.4.2. PBT can significantly elevate their red muscle temperature above the ambient water temperature at a minimum age of approximately 5.5 months....	60
2.4.3. Scaling of body mass with fork length	64
2.4.4. Anatomy of the red muscle.....	64
2.4.5. Anatomy of the red muscle retia.....	67
2.4.6. Anatomy of the visceral retia	68
2.4.7. Cranial temperature elevation	71

2.4.8. Conclusions.....	72
-------------------------	----

Chapter 3 - Regulation of the ontogenetic transition from ectothermy to regional endothermy in pacific bluefin tuna (*Thunnus orientalis*): Biochemistry and molecular biology73

Abstract.....	74
3.1. Introduction.....	77
3.1.1. Regional endothermy in tunas.....	77
3.1.2. The effects of muscle type on mitochondrial abundance and aerobic metabolic capacity in fishes.....	77
3.1.3. The effects of muscle type on glycolytic capacity in fishes.....	78
3.1.4. The effects of body size on mitochondrial abundance and aerobic metabolic capacity in fish skeletal muscle.....	78
3.1.5. The effects of body size on the glycolytic capacity of skeletal muscle fibres of fishes.....	79
3.1.6. The effects of decreasing water temperature on mitochondrial abundance and aerobic metabolic capacity in fish skeletal muscle.....	79
3.1.7. The effects of decreasing water temperature on glycolytic capacity in fish muscle.....	80
3.1.8. Aims.....	81
3.2. Materials and Methods.....	82
3.2.1. Fish specimens.....	82
3.2.2. Citrate synthase enzyme activity analysis.....	82
3.2.3. Cytochrome c oxidase enzyme activity analysis.....	83
3.2.4. Pyruvate kinase enzyme activity analysis.....	84
3.2.5. Primer design for polymerase chain reaction.....	84
3.2.6. RNA extraction and cDNA synthesis.....	85
3.2.7. Conventional polymerase chain reaction.....	86
3.2.8. Cloning of the PCR products in <i>E. coli</i>	88
3.2.9. Gene expression analysis using qRT-PCR.....	89
3.2.10. Statistical analyses.....	90
3.3 Results.....	91
3.3.1. The effects of muscle type and body size on citrate synthase enzyme activity.....	91
3.3.2. The effects of muscle type and body size on cytochrome c oxidase enzyme activity.....	93
3.3.3. The effects of muscle type and body size on pyruvate kinase enzyme activity.....	96
3.3.4. The effects of muscle type and body size on the amount of protein extracted per g tissue.....	98
3.3.5. The effects of muscle type and body size on the citrate synthase transcript abundance, expressed as copies per g tissue.....	101
3.3.6. The effects of muscle type and body size on the cytochrome c oxidase subunits I and IV-1 transcript abundances, expressed as copies per g tissue.....	105
3.3.7. The effects of muscle type and body size on the pyruvate kinase transcript abundance, expressed as copies per g tissue.....	107
3.3.8. The effects of muscle type and body size on β -actin transcript abundance, expressed as copies per g tissue.....	108
3.3.9. The effects of muscle type and body size on total RNA extracted per g tissue.....	113
3.4. Discussion.....	115
3.4.1. The effect of muscle type on citrate synthase enzyme activity.....	115
3.4.2. The effect of fish body size on citrate synthase enzyme activity.....	116
3.4.3. The effect of muscle type on cytochrome c oxidase enzyme activity.....	118
3.4.4. The effect of fish body size on cytochrome c oxidase enzyme activity.....	120
3.4.5. The effects of temperature on citrate synthase and cytochrome c oxidase enzyme activities.....	121
3.4.6. The effect of muscle type on pyruvate kinase enzyme activity.....	121

3.4.7. The effect of fish body size on pyruvate kinase enzyme activity.....	123
3.4.8. The effect of muscle type on citrate synthase transcript abundance	123
3.4.9. The effect of body size on citrate synthase transcript abundance	125
3.4.10. The effects of muscle type on the transcript abundances for cytochrome c oxidase subunits I and IV-1	126
3.4.11. The effects of body size on the transcript abundances for cytochrome c oxidase subunits I and IV-1	127
3.4.12. The effect of muscle type on pyruvate kinase transcript abundance ..	128
3.4.13. The effect of body size on pyruvate kinase transcript abundance	128
3.4.14. Conclusions.....	129

Chapter 4 - Roles of the PGC-1 transcriptional co-activators in red muscle endothery in Pacific bluefin tuna (<i>Thunnus orientalis</i>)	131
Abstract.....	132
2.1. Introduction	134
4.1.1. The PGC-1 transcriptional coactivator family in mammals.....	134
4.1.2. PGC-1 α in mammals	134
4.1.3. Muscle fibre types in mammals	135
4.1.4. Regulation of PGC-1 α in mammals.....	136
4.1.5. PGC-1 β in mammals.....	136
4.1.6. PGC-1 α and PGC-1 β in fishes	137
4.1.7. The role of the PGC-1 family of transcriptional co-activators in regionally endothermic fishes.	138
4.1.8. Aims	140
4.2. Materials and Methods.....	141
4.2.1. Fish sampling	141
4.2.2. RNA extraction and cDNA synthesis.....	141
4.2.3. Primer design for cloning a PGC-1 α cDNA from PBT red muscle using conventional polymerase chain reaction	142
4.2.4. Conventional polymerase chain reaction for cloning a PGC-1 α cDNA from PBT red muscle.....	144
4.2.5. Cloning of the PGC-1 α PCR product in <i>Escherichia coli</i>	144
4.2.6. Quantitative real time polymerase chain reaction	145
4.2.7. Preparation of the standards for qRT-PCR	146
4.2.8. Preparation of the samples for qRT-PCR.....	146
4.2.9. Statistical analyses.....	147
4.3. Results	149
4.3.1. Sequence analysis of a PGC-1 α cDNA from PBT red muscle	149
4.3.2. Phylogenetic analysis of the PBT PGC-1 α amino acid sequence.....	154
4.3.3. The effects of tissue type and fish size on PGC-1 α transcript abundance	158
4.3.4. The effects of tissue type and fish size on PGC-1 β transcript abundance	158
4.3.5. The effect of tissue type and fish size on PPAR α transcript abundance	160
4.3.6. The effect of tissue type and fish size on MCAD transcript abundance	160
4.3.7. The effect of tissue type and fish size on β -actin transcript abundance	160
4.3.8. Correlation analyses between PPAR α , MCAD, PGC-1 α and PGC-1 β transcript abundances	165
4.3.9. Correlation analyses between CS, COXI, COXIV, PGC-1 α and PGC-1 β transcript abundances	167
4.4. Discussion.....	169
4.3.1. Sequence analysis of a PGC-1 α cDNA from PBT red muscle	169
4.3.2. The effects of tissue type and body size on PGC-1 α transcript abundance	171
4.3.3. The effects of tissue type and body size on PGC-1 β gene expression.	172
4.3.4. The effects of tissue type and body size on PPAR α gene expression..	173
4.3.5. The effects of tissue type and body size on MCAD gene expression ...	174

4.3.6. The effects of tissue type and body size on transcript abundance of β -actin.....	175
4.3.7. Transcript abundances for PPAR α and MCAD are strongly correlated with transcript abundances for the PGC-1 transcriptional coactivators.....	176
4.3.8. Correlations of the PGC-1 transcriptional co-activators with the genes that encode the mitochondrial marker enzymes citrate synthase and cytochrome c oxidase.....	177
4.3.9. Conclusions.....	179

Chapter 5 - The effects of feed restriction on aerobic and glycolytic metabolic capacity in yellowtail kingfish (<i>Seriola lalandi</i>) farmed at suboptimal water temperatures.....	181
Abstract.....	182
5.1. Introduction.....	185
5.1.1. Yellowtail kingfish distribution and aquaculture.....	185
5.1.2. The effects of water temperature on YTK physiology.....	186
5.1.3. Diet of cultured YTK.....	186
5.1.4. Fish skeletal muscle structure and metabolism.....	188
5.1.5. Effects of fasting and feed restriction on mitochondrial abundance and aerobic metabolic capacity in fishes.....	189
5.1.6. Effects of fasting on glycolytic metabolic capacity in fishes.....	190
5.1.7. Peroxisome proliferator-activated receptor-gamma coactivator 1-alpha in mammals.....	190
5.1.8. The effects of fasting on PGC-1 α gene and protein expression in the skeletal muscle and liver of fishes.....	191
5.1.8. Aims.....	192
5.2. Materials and Methods.....	193
5.2.1. Fish culture.....	193
5.2.2. Fish tissue sampling.....	193
5.2.3. Citrate synthase enzyme activity analysis.....	194
5.2.4. Cytochrome c oxidase enzyme activity analysis.....	195
5.2.5. Pyruvate kinase enzyme activity analysis.....	195
5.2.6. RNA extraction and cDNA synthesis.....	196
5.2.7. Primer design for cloning a PGC-1 α cDNA from YTK red muscle using conventional polymerase chain reaction.....	197
5.2.8. Conventional polymerase chain reaction for cloning a PGC-1 α cDNA from YTK red muscle.....	197
5.2.9. Cloning of the PGC-1 α PCR product in <i>Escherichia coli</i>	200
5.2.10. Quantitative Real Time-Polymerase Chain Reaction.....	201
5.2.11. Determining the amplification efficiency for the qPCR primers.....	202
5.2.12. Statistical analyses.....	202
5.3. Results.....	204
5.3.1. Fish growth.....	204
5.3.2. Effects of tissue type and feed restriction on CS enzyme activity.....	206
5.3.3. Effects of tissue type and feed restriction on COX enzyme activity.....	209
5.3.4. Effects of tissue type and feed restriction on PK enzyme activity.....	209
5.3.5. Effects of tissue type and feed restriction on the amount of protein extracted per g tissue.....	210
5.3.6. Effects of tissue type and feed restriction on CS transcript abundance.....	213
5.3.7. Effects of tissue type and feed restriction on COXI transcript abundance.....	216
5.3.8. Effects of tissue type and feed restriction on PK transcript abundance.....	216
5.3.9. Cloning and sequence analysis of a PGC-1 α cDNA from YTK red muscle.....	217
5.3.10. Phylogenetic analysis.....	224
5.3.11. Effects of tissue type and feed restriction on PGC-1 α transcript abundance.....	226

5.3.12. Effects of tissue type and feed restriction on PPAR α transcript abundance.....	228
5.3.13. Effects of tissue type and feed restriction on MCAD transcript abundance.....	228
5.4. Discussion.....	230
5.4.1. Fish growth.....	230
5.4.2. Effects of tissue type and restricted feeding on CS enzyme activity	230
5.4.3. Effects of tissue type and restricted feeding on COX enzyme activity ..	232
5.4.4. Effects of tissue type and restricted feeding on PK enzyme activity	233
5.4.5. Effects of tissue type and restricted feeding on CS transcript abundance	234
5.4.6. Effects of tissue type and restricted feeding on COXI transcript abundance.....	235
5.4.7. Effects of tissue type and restricted feeding on PK transcript abundance	237
5.4.8. Sequence analysis of a PGC-1 α cDNA cloned from YTK red muscle ..	238
5.4.9. Effect of tissue type and feed restriction on PGC-1 α transcript abundance	240
5.4.10. Effects of tissue type and feed restriction on PPAR α transcript abundance.....	244
5.4.11. Effects of tissue type and feed restriction on MCAD transcript abundance.....	245
5.4.12. Conclusions.....	246
Chapter 6 - Conclusions and future directions	248
References	256
Appendices	272

DECLARATION

I certify that this thesis does not incorporate without acknowledgment any material previously submitted for a degree or diploma in any university; and that to the best of my knowledge and belief it does not contain any material previously published or written by another person except where due reference is made in the text.

Signed.....

Date.....

ACKNOWLEDGEMENTS

To my supervisor, Associate Professor Kathy Schuller, thank you for your guidance, patience and for giving me a clip round the ear to whip me into shape throughout every step of my PhD. A PhD is hard work and is not always an enjoyable experience but working with you has been fantastic. I would like to extend my thanks to my co-supervisor, Associate Professor Charlie Huveneers and adjunct supervisor Associate Professor David Stone.

I am extremely grateful to Professor Kathy Dickson and Associate Professor Takashi Kitagawa. Not only was their knowledge invaluable during our collaboration in Japan but they made our collaboration an enjoyable one. I would also like to thank Charles Farwell, Ethan Estess, Dr Yoshinoi Aoki, Dr Marty Wong and everyone who contributed to the bluefin tuna project and made my time spent overseas exceptionally fun.

To my fellow PhD student Christopher Waterman, as much as it pains me to say it, your friendship has been a huge support during my PhD and the quick lunches and beer breaks have been invaluable. I'd also like to thank Dr Sarmad Al-Asadi, Krishna-Lee Currie, Simone Jaenisch, Ben Crowe and Jess Buss for sharing all the fun associated with being PhD students.

I would like to thank my housemates Emily and Shaun (Prawny) for their support/ridicule during most of my PhD. Having a happy home life helped keep me sane and I'm glad to have you as my second family.

To my girlfriend Kiarra, thank you for sharing the last few months (the most stressful months!) of my PhD with me. Your support at the end gave me the final push I needed to get me over the line.

To my high school friend Dr Hayden Burdett. Without your suggestion all those years ago to submit a university application and just "see what happens" none of this would have happened. Words can't describe how grateful I am for that little nudge in the right direction.

Finally, I'd like to thank my parents. For always having faith in me even when I had no faith in myself and for encouraging and supporting me every step of the way during the past few crazy years. None of this would have been possible without you.

I acknowledge the contribution of the Australian Government Research Training Program Scholarship for its contribution to my candidature

In memory of
Ryan James Meese (Meesey)
10/3/1983 – 3/12/2016
&
Felix
200? – 21/4/2018

SUMMARY

Early in their post-larval development, tunas undergo an ontogenetic transition from ectothermy to regional endothermy but it is largely unknown when this occurs or how it is regulated. In bluefin tunas, the tissues that are endothermic are the red ('slow-twitch', predominantly aerobic) skeletal muscle, the viscera and the cranium (eye/brain). We observed a linear increase in the red muscle temperature elevation above the ambient temperature in juvenile Pacific bluefin tuna (PBT, *Thunnus orientalis*). More specifically, we estimated that significant temperature elevation in the red muscle of juvenile PBT occurs at a minimum body size of approximately 29 cm fork length (FL), corresponding to an age of approximately 5.5 months. The red muscle mass of the PBT specimens scaled slightly less than isometrically with increasing body mass (BM) indicating that increasing red muscle mass as a proportion of total BM was not the explanation for the increasing red muscle temperature elevation with increasing body size. Similarly, the activity per g tissue of mitochondrial marker enzymes either decreased or remained constant with increasing body size. This suggested that the development of red muscle endothermy in PBT is not a result of an increase in mitochondrial abundance and therefore heat generated by an increase in the aerobic metabolic activity in the red muscle. Instead, increasing temperature elevation in the red muscle above the ambient water temperature correlated well with the proliferation of red muscle counter-current heat-exchanging blood vessels known as *retia mirabilia* (singular = rete). Similarly, increasing temperature elevation in the viscera of PBT correlated well with increases in the proliferation of the visceral rete. Together these findings indicate that it is likely that the development of the *retia* is the most important factor supporting the development of regional endothermy in PBT. The temperature elevation we observed in the red muscle of our PBT specimens with increasing body size was not paralleled with an increase in the transcript abundance of peroxisome proliferator-activated receptor-gamma (PPAR gamma) coactivator-1 α (PGC-1 α), a master regulator of mitochondrial biogenesis and function in mammals, with increasing body size. This suggests that the function of PGC-1 α may be different in fishes than it is in mammals.

Yellowtail kingfish (YTK, *Seriola lalandi*) is an important aquaculture species in South Australia but in winter it suffers from impaired feed digestion due to suboptimal water temperatures. It was found that CS and COX enzyme, per g tissue, were 57% and 20% greater, respectively, in the liver of feed restricted YTK compared to satiated YTK. This suggested that the aerobic metabolic capacity of the liver increased in response to feed restriction. This did not correspond with an increase in PGC-1 α transcript abundance. Therefore, it is unlikely that the feed restriction-induced increase in mitochondrial abundance was a result of regulation by PGC-1 α .

CHAPTER 1 – General introduction

1.1.1. Thermoregulation in vertebrates

Vertebrates can regulate their body temperature in response to changes in the temperature in their surrounding environment (Seebacher, 2009). There are two broad types of thermoregulation, behavioural and physiological. Behavioural thermoregulation is dependent on externally generated heat whereas physiological thermoregulation involves internally generated heat. Ectothermic vertebrates, i.e., amphibians and reptiles and most fishes, have little to no internal physiological sources of heat and cannot generate sufficient metabolic heat to warm their bodies and instead use external heat sources to maintain their body temperature. This is particularly important for fishes because water conducts heat 25 times more effectively than air (Castellini, 2018). This means that heat flows out of a warm object in cold water much more efficiently than it does when that same object is in air (Castellini, 2018).

Ectotherms can regulate their body temperature through behavioural modification (Glanville and Seebacher, 2006, Seebacher, 2000, Seebacher and Grigg, 2001). Examples of behavioural modification include reptiles basking in the sunlight to directly use heat produced by the sun to maintain close to optimal body temperatures and fishes adjusting their vertical position in the water column to utilise the change in water temperature to maintain their internal body temperature (Porter and Gates, 1969, Freitas et al., 2015). Advantages of not having the requirement of generating heat by metabolic processes are that ectotherms can invest a greater percentage of their energy into growth and reproduction and they can survive for long periods of time without feeding.

In contrast, endothermic vertebrates (mammals and birds) maintain relatively stable body temperatures that are higher than the surrounding environment by adjusting metabolic heat production in response to varying environmental temperature (Ruben, 1995). Endotherms can also adjust their ability to retain heat by flattening/raising their fur and feathers to trap heat in small air cells within their structure (Speakman and Król, 2010). Endothermy provides a stable thermal environment for optimal enzyme activity and reduces vulnerability to fluctuations in external temperature (Ruben, 1995, Lovegrove, 2012). This has allowed endotherms to spread and occupy a large range of

environmental niches. However, endothermy is energetically expensive, meaning that birds and mammals must feed more frequently than similarly sized ectotherms (Buckley et al., 2012). As stated above, an ectotherm can go for long periods of time without feeding. In contrast, a small endothermic animal may be starving within a day of lacking food (Wang et al., 2006). The most widely accepted explanation for the evolution of endothermy has been the selection for an enhanced aerobic capacity to sustain physical exertion for longer periods of time (Clarke and Portner, 2010). A consequence of high levels of physical activity resulting from a high aerobic capacity is a greater metabolic production of heat. Thus, it is likely that the increase in aerobic capacity gave rise to endothermy.

1.1.2. Regional endothermy in fishes

Most fishes are ectothermic (Dickson and Graham, 2004). However, some display regional endothermy (Dickson and Graham, 2004). This is enabled by conserving metabolic heat in only some of their tissues to maintain elevated temperatures above the temperature of their environment while other tissues are still ectothermic (Dickson and Graham, 2004, Davenport et al., 2015). Regionally endothermic fishes include the tunas, billfishes, lamnid sharks, the common thresher shark (*Alopias vulpinus*) and the opah (*Lampris guttatus*) (Dickson and Graham, 2004, Sepulveda et al., 2005, Wegner et al., 2015). Fishes with regional endothermy have elevated temperatures in either their red ('slow-twitch', oxidative) muscle fibres, eyes, brain, viscera, or only some of these tissues (Dickson and Graham, 2004).

1.1.3. Red muscle endothermy in fishes

There are two predominant types of muscle fibres in the skeletal muscle of fishes, the "slow twitch", oxidative red muscle fibres and the "fast-twitch", glycolytic white muscle fibres (Johnston et al., 2011). The red muscle fibres are very abundant in mitochondria and are used for endurance type activity, such as long migrations and are resistant to fatigue. In contrast, white muscle fibres are much less abundant in mitochondria and are more glycolytic (Roy et al., 2014). They are used for short intense bursts of powerful activity, such as

pursuing prey and fatigue more quickly. Muscular contraction generates heat as a by-product.

In tunas and lamnid sharks, heat generated by the repeated contraction of the red muscle is conserved by vascular counter-current heat exchangers, called *retia mirabilia* (singular = rete), to reduce convective heat loss at the gills. (Bernal et al., 2001a). Venous blood, which is cooled as it passes through the gills to draw oxygen from the water, passes by warm outgoing arterial blood and heat transfer occurs thereby warming the cooled blood. A proposed advantage of red muscle endothermy is enhanced sustainable (i.e. aerobic), cruise-type swimming performance (Dickson and Graham, 2004).

Early in their post-larval development, tunas undergo an ontogenetic transition from ectothermy to regional endothermy but it is largely unknown when this occurs or how it is regulated. Dickson (1994) showed that black skipjack tuna (*Euthynnus lineatus*) start life as ectotherms but could significantly elevate the temperature of their red muscle above ambient water temperature at a minimum body size of ~21 cm FL. Similarly, Kubo et al. (2008) showed that Pacific bluefin tuna (*Thunnus orientalis*) could achieve this feat at a minimum body size of ~55 cm FL. There are no other studies that we know of that have pin-pointed the timing of this important ontogenetic transition.

1.1.4. Visceral endothermy in fishes

Elevation of visceral temperatures in tunas and lamnid sharks involves retention of metabolic heat produced during the digestion and absorption of food in a process known as specific dynamic action (SDA) or dietary induced thermogenesis (Dickson and Graham, 2004). The site of heat production for visceral endothermy is the pyloric caeca in tunas (Carey et al., 1984) and the spiral valve intestine in lamnid sharks (Carey et al., 1981). Tunas and lamnid sharks conserve the heat produced through SDA through visceral counter current heat exchanging blood vessels, as is true for red muscle endothermy (Carey et al., 1981, Fudge and Stevens, 2005). Visceral endothermy increases the activity of digestive enzymes allowing regionally endothermic fishes to digest more nutrients per day than can individuals from closely related species (Newton et al., 2015). A proposed advantage of visceral endothermy is

improved rates of nutrient digestion and assimilation in cooler waters (Dickson and Graham, 2004).

1.1.5. Cranial endothermy in fishes

It has been proposed that in tunas the source of heat for cranial endothermy may be the frequent contraction of the highly aerobic ocular muscles or the heat produced by the central nervous system, though the true mechanism is unknown (Block, 2011, Sepulveda et al., 2007). The heat for cranial endothermy is conserved by heat exchanging, cranial *retia* that protect the eyes and brain from heat loss (Block and Finnerty, 1994, Bushnell et al., 1992). The source of heat for cranial endothermy in lamnid sharks is much better understood. These fishes utilise heat generated within the red muscle to warm their brain and eyes. The warm blood from the red muscle enters the myelonal vein and flows towards the brain where the heat is retained by the cranial *retia* (Wolf et al., 1988). It has been proposed that the dependence of cranial endothermy on heat generated by the red muscle in lamnid sharks means that cranial endothermy evolved after, or in association with, red muscle endothermy (Dickson and Graham, 2004). Unlike tunas and lamnid sharks, billfishes such as swordfish (*Xiphias gladius*) have highly specialized extraocular muscles that are modified into a thermogenic organ that warms just the brain and eyes up to 10-15°C above ambient water temperatures (Carey and Robison, 1981, Carey, 1982, Block, 1987a). A proposed advantage of cranial endothermy is enhanced vision in cooler waters allowing better perception of prey (Fritsches et al., 2005).

1.1.6. Regulation of mitochondrial abundance by PGC-1 α

In mammals, the peroxisome proliferator-activated receptor-gamma (PPAR gamma) coactivator-1 α (PGC-1 α) was first identified as an activator of the transcription factor peroxisome proliferator-activated receptor-gamma (PPAR γ), hence its name (Puigserver et al., 1998). Since its initial discovery, PGC-1 α has been shown to be an important transcriptional coactivator that coordinates the up-regulation of mitochondrial biogenesis and function (e.g. β -oxidation) in mammals by interacting with transcription factors such as PPAR α , estrogen related receptor- α (ERR α) and nuclear respiratory factors (NRF) 1

and 2 (Lin et al., 2005a, Arany, 2008, Liu and Lin, 2011). It is uncertain if PGC-1 α has the same role in fishes as it does in mammals. The reason for this uncertainty is because the PGC-1 α amino acid sequence is highly conserved among vertebrates except for the ray-finned fishes, a subclass of the bony fishes (LeMoine et al., 2010a). In the ray-finned fishes, the NRF-1, PPAR γ and MEF2c transcription factor binding domains are interrupted by various insertions including serine (S)-rich and glutamine (Q)-rich insertions (Wu et al., 1999, Michael et al., 2001, LeMoine et al., 2010a). Thus, it is questionable as to whether PGC-1 α coordinates the up-regulation of mitochondrial biogenesis and function in fishes, as it does in mammals.

1.1.7. Bluefin tunas

Bluefin tunas are the largest species of tuna (Froese and Pauly, 2018). They are highly sought after fishes, as their flesh is popular in high-end sushi and sashimi restaurants (Bergin and Haward, 1996, Porch, 2005). Bluefin tunas are extremely economically valuable fish and are often auctioned off at selective fish markets in Japan, such as the famous Tsukiji fish market (Miyake et al., 2010). For example, in January 2018, a record US\$3.1 million was paid at the Toyosu market (incorporating the former Tsukiji fish market) for a single, wild-caught, bluefin weighing 278 kg (613 lbs) that was caught off the northern coast of Japan's Aomori prefecture (<https://edition.cnn.com/2019/01/05/asia/giant-tuna-sets-record-at-japan-auction/index.html>). There are three species of bluefin tuna, Pacific bluefin tuna (PBT, *Thunnus orientalis*), Atlantic bluefin tuna (ABT, *Thunnus thynnus*) and southern bluefin tuna (SBT, *Thunnus maccoyii*) (Tseng et al., 2011). Due to the popularity of bluefin tuna for human consumption the populations of these fishes have declined severely from overfishing (Safina and Klinger, 2008, Matsuda et al., 1998). For example, the spawning stock biomass (SSB) of ABT peaked in the mid-1970s and then declined until 1991 due to overfishing before the population became steady (ICCAT, 2017). As a result, PBT, ABT and SBT are currently listed as vulnerable, endangered and critically endangered, respectively, on the International Union for Conservation of Nature and Natural Resources (IUCN) Red List of Threatened Species (<https://www.iucn.org/resources/conservation-tools/iucn-red-list-threatened-species>) (Collette et al., 2011a, Collette et al., 2011b, Collette et al., 2014).

Farming and strict catch quotas have slowed the decline of the bluefin tuna populations (ICCAT, 2017). The aquaculture of bluefin tunas is generally dependent on capturing these fishes as juveniles and then fattening them in sea cages along the Pacific coast of Mexico and the southern coast of Japan (for PBT), in the Mediterranean Sea (for ABT) and the Spencer Gulf of South Australia (for SBT) (Miyake et al., 2010, Mylonas et al., 2010, Kirchhoff et al., 2011). In more recent times, there has been a push to establish more sustainable methods of producing bluefin tuna for human consumption, through aquaculture based captive breeding (Sawada et al., 2005, Masuma et al., 2008, De Metrio et al., 2010, Bubner et al., 2012, Tsuda et al., 2012, Okada et al., 2014, Yúfera et al., 2014, Endo et al., 2016). There has been limited success with breeding these fishes in captivity. Mostly there has been success breeding PBT in captivity (Sawada et al., 2005). After 23 years of research, scientists at the Kindai University (Osaka, Japan) completed the life cycle of captive-bred PBT under aquaculture conditions in the summer of 2002 (Sawada et al., 2005). The challenges facing the breeding of these fishes in captivity include trauma by collision with the tanks or net wall of their sea cages, cannibalism in larval and juvenile stages and their high mortality in the cold water temperatures experienced during the winter when the fish are maintained in sea cages (Sawada et al., 2005).

1.1.8. Amberjacks

The amberjacks are popular recreational and commercially sought after fish that, like the bluefin tunas, have high-quality flesh that is popular for sushi and sashimi (Jirsa et al., 2011). Several amberjacks, including yellowtail kingfish (YTK, *Seriola lalandi*), are farmed, predominantly in sea-cages (Premachandra et al., 2017, Kolkovski and Sakakura, 2004, CST, 2016, Norwood, 2017, Benetti et al., 2005, Kingfish-Zeeland, 2018). For example, Japanese yellowtail (*Seriola quinqueradiata*) is farmed in Japan, Almaco jack (*Seriola rivoliana*) near Hawaii and greater amberjack (*Seriola dumerili*) in Japan, the Mediterranean and Vietnam (Webster and Lim, 2002, Benetti et al., 2005, Naomasa et al., 2013, Sicuro and Luzzana, 2016). YTK is farmed in sea cages in Australia, New Zealand, Mexico, Chile and Hawaii as well as in indoor facilities in the Netherlands (Premachandra et al., 2017, Kolkovski and

Sakakura, 2004, CST, 2016, Norwood, 2017, Benetti et al., 2005, Kingfish-Zeeland, 2018).

The culture of YTK in countries such as Australia, New Zealand and Chile depends on the rearing of larvae/fingerlings produced in a hatchery from captive brood stock (Kolkovski and Sakakura, 2004, Orellana et al., 2014, CST, 2016). In contrast, the culture of Japanese yellowtail and greater amberjack in Japan is reliant, mainly, on the on-growing of readily available wild-caught juveniles (Kolkovski and Sakakura, 2004). YTK is a valuable aquaculture species in a rapidly expanding industry in Australia. For example, in 2018, sales volumes increased from the previous year by 15% while sales revenue grew 18%, supported by continued improvement in selling prices (CST, 2018). In Australia, YTK aquaculture takes place predominantly in South Australia but there has been some expansion into New South Wales and Western Australia as well (Norwood, 2017).

1.1.9. Project aims

The aims of this project were:

1. To determine the effects of fish body size/age on the development of regional endothermy in PBT and to estimate the minimum body size for significant temperature elevation in the red muscle
2. To ascertain the effects of fish body size/age on the development of red muscle and visceral *retia* in PBT
3. To determine the effect of fish body size/age on mitochondrial abundance/aerobic metabolic capacity in red muscle and white muscle during the development of regional endothermy in PBT
4. To determine whether PGC-1 α is involved in the development of regional endothermy in PBT by investigating the effect of fish body size/age on PGC-1 α transcript abundance in red muscle and white muscle during the development of regional endothermy in PBT
5. To determine the effects of feed restriction on mitochondrial abundance/aerobic metabolic capacity in the red muscle, white muscle and liver of juvenile YTK

6. To determine the effects of feed restriction on the transcript abundance of PGC-1 α and genes involved in β -oxidation in red muscle, white muscle and liver of juvenile YTK

Aims 1-3 will provide insight into how the ontogenetic transition from ectothermy to regional endothermy occurs at the anatomical, physiological and molecular levels in PBT. Additionally, Aim 4 will identify whether the role of the PGC-1 transcriptional coactivators have any involvement in the up-regulation of mitochondrial biogenesis and function in during this transition. Collectively, these aims will identify which anatomical, physiological and/or molecular changes are the driving force for the transition from ectothermy to regional endothermy in PBT. The final aims (5 and 6) address the second topic in this thesis and will provide new knowledge into the effects of feed restriction on the aerobic metabolic capacity in the red muscle, white muscle and liver of juvenile YTK.

1.1.10. Thesis structure

This thesis consists of a general introduction (see above), four results chapters and a general discussion. The results chapters have been formatted as draft manuscripts for submission to scientific journals. Chapters 2, 3 and 4 explore the ontogenetic transition from ectothermy to regional endothermy at the anatomical, physiological and molecular levels. However, at the beginning of this project it was unknown if tuna tissue would become available. Therefore, the work done on YTK was done due to the uncertainty of getting tissue from tuna and has been included in this thesis despite the dissimilar topic. The titles and authors' names, affiliations and contributions to the draft manuscripts are as follows:

Chapter 2

Regulation of the ontogenetic transition from ectothermy to regional endothermy in Pacific bluefin tuna (*Thunnus orientalis*): Anatomy and Physiology

A. Malik¹, K. Dickson², T. Kitagawa³, K. Fujioka⁴, C. Farwell⁵, E. Estess⁵, Kathryn Schuller¹

¹College of Science and Engineering, Flinders University, Adelaide, South Australia, Australia

²College of Natural Sciences and Mathematics, California State University Fullerton, California, USA

³Atmosphere and Ocean Research Institute, University of Tokyo, Kashiwa, Chiba, Japan

⁴National Research Institute of Far Seas Fisheries, Shizuoka, Japan

⁵Monterey Bay Aquarium, Monterey, California, USA

Key words: Pacific bluefin tuna, *Thunnus*, regional endothermy, *retia mirabilia*, temperature elevation

Proposed journal: Journal of Experimental Biology

A. Malik helped to devise the project, collected the PBT tissue samples, confirmed the identity of the specimens through DNA sequencing, analysed the red muscle content/distribution of the PBT specimens and wrote the manuscript. K. Dickson contributed to the design and implementation of the research, collected the PBT tissue samples, performed the temperature measurements and the histological analyses and contributed her expertise to the writing of the final manuscript. T. Kitagawa contributed to the design and implementation of the research and contributed his expertise to the writing of the final manuscript. K. Fujioka supplied the PBT the specimens and contributed his expertise to the writing of the final manuscript. C. Farwell and E. Estess provided knowledge and assistance in handling the live PBT specimens. K. Schuller devised the project, participated in the collection of the tissue samples, advised on the analyses, and contributed her expertise and advice on the writing of the final manuscript.

Chapter 3

Regulation of the ontogenetic transition from ectothermy to regional endothermy in Pacific bluefin tuna (*Thunnus orientalis*): Biochemistry and molecular biology

Arif Malik¹, Kathryn Dickson², Takashi Kitagawa³, Ko Fujioka⁴, Kathryn Schuller¹

¹College of Science and Engineering, Flinders University, Adelaide, South Australia, Australia

²College of Natural Sciences and Mathematics, California State University Fullerton, California, USA

³Atmosphere and Ocean Research Institute, University of Tokyo, Kashiwa, Chiba, Japan

⁴National Research Institute of Far Seas Fisheries, Shizuoka, Japan

Key words: Pacific bluefin tuna, *Thunnus orientalis*, regional endothermy, mitochondria, citrate synthase, cytochrome *c* oxidase, pyruvate kinase

Proposed journal: Comparative Biochemistry and Physiology Part B: Biochemistry and Molecular Biology

A. Malik helped to devise the project, collected the PBT tissue samples, analysed the enzyme activity and gene expression of the tissue samples and wrote the manuscript. K. Dickson contributed to the design and implementation of the research, collected the PBT tissue samples and contributed her expertise to the final manuscript. T. Kitagawa contributed to the design and implementation of the research and contributed his expertise to the final manuscript. K. Fujioka supplied PBT the specimens and contributed his expertise to the final manuscript. K. Schuller devised the project, contributed her expertise and supported in the writing of the final manuscript

Chapter 4

Roles of the PGC-1 transcriptional co-activators in red muscle endothermy in Pacific bluefin tuna (*Thunnus orientalis*)

A. Malik¹, K. Dickson², T. Kitagawa³, K. Fujioka⁴, Kathryn Schuller¹

¹College of Science and Engineering, Flinders University, Adelaide, South Australia, Australia

²College of Natural Sciences and Mathematics, California State University Fullerton, California, USA

³Atmosphere and Ocean Research Institute, University of Tokyo, Kashiwa, Chiba, Japan

⁴National Research Institute of Far Seas Fisheries, Shizuoka, Japan

Key words: Pacific bluefin tuna, *Thunnus*, regional endothermy, mitochondria, temperature elevation, PGC-1 α , PPAR α , MCAD

Proposed journal: Comparative Biochemistry and Physiology Part B: Biochemistry and Molecular Biology

A. Malik helped to devise the project, collected the PBT tissue samples, cloned the PGC-1 α gene, analysed the gene expression of the tissue samples, and wrote the manuscript. K. Dickson collected the PBT tissue samples and contributed her expertise to the final manuscript. T. Kitagawa contributed his expertise to the final manuscript. K. Fujioka supplied PBT the specimens. K. Schuller devised the project, contributed her expertise and supported in the writing of the final manuscript

Chapter 5

The effects of feed restriction on aerobic and glycolytic metabolic potential in yellowtail kingfish (*Seriola lalandi*) farmed in suboptimal water temperatures

A. Malik¹, D.A.J Stone^{1,2}, L. Kuerschner¹, Kathryn Schuller¹

¹College of Science and Engineering, Flinders University, Adelaide, South Australia, Australia

²South Australian Research and Development Institute, South Australian Aquatic Sciences Centre, West Beach, South Australia

Key words: Yellowtail kingfish, *Seriola*, feed restriction, mitochondria, temperature, PGC-1 α , citrate synthase, cytochrome *c* oxidase

Proposed journal: Comparative Biochemistry and Physiology Part B: Biochemistry and Molecular Biology

A. Malik helped to devise the project, collected the YTK tissue samples, cloned the PGC-1 α gene, analysed the enzyme activities and gene expression from the tissue samples and wrote the manuscript. D.A.J Stone devised the project and contributed his expertise to the final manuscript. L. Kuerschner maintained the fish and implemented the feeding treatments. K. Schuller, advised on the analyses, contributed her expertise and advice on the writing of the final manuscript

CHAPTER 2 - Regulation of the ontogenetic transition from ectothermy to regional endothermy in pacific bluefin tuna (*Thunnus orientalis*): anatomy and physiology

Abstract

Tunas are unusual fishes because they are regional endotherms. Regionally endothermic fishes can elevate the temperature of their red ('slow-twitch', predominantly aerobic) skeletal muscle, cranium (eye plus brain) and/or viscera above the ambient water temperature by conserving metabolic heat. Here we show that young Pacific bluefin tuna (PBT, *Thunnus orientalis*) juveniles begin to elevate their red skeletal muscle temperature (T_{RM}) above the ambient water temperature (T_a) at a minimum body size of ~29 cm fork length (FL), corresponding to a minimum age of ~5.5 months and that the thermal excess ($T_{RM} - T_a$) increases with increasing fish size up to an impressive 14.2°C in one of the largest specimens we studied (61.2 cm FL and 5,200 g body mass (BM)). Red muscle mass increased with increasing body size but the ratio of red muscle mass to BM decreased. Thus, disproportionately increasing red muscle mass relative to BM cannot explain the increasing red muscle temperature elevation we observed in these fish as they grew larger. In contrast, increasing red muscle temperature elevation was strongly positively correlated with increasing proliferation of the red muscle *retia*. These are networks of specialized blood vessels interposed between the red muscle and the gills that conserve the metabolic heat generated by the repeated contraction of the red muscle. We also observed small elevations of the visceral and cranial temperatures in some of the larger individuals we studied. The visceral temperature elevations were paralleled by increasing proliferation of the visceral rete. This rete conserves the heat generated by specific dynamic action. Overall, we conclude that increasing proliferation of the red muscle *retia* and the visceral rete underpins the increasing capacity for temperature elevation in the red muscle and visceral tissues in young PBT juveniles.

Abbreviations

Pacific bluefin tuna, PBT; Atlantic bluefin tuna, ABT; Southern bluefin tuna, SBT, Specific dynamic action, SDA; Fork length, FL; Body mass, BM; Cytochrome *c* oxidase subunit 1, COXI

2.1. Introduction

2.1.1. Regional endothermy in fishes

Early in their post-larval development, tunas undergo an ontogenetic transition from ectothermy to regional endothermy but it is largely unknown when this occurs or how it is regulated (Dickson, 1994, Kubo et al., 2008). In fishes, regional endothermy is defined as the ability to elevate and maintain certain regions of the body at temperatures above the ambient water temperature (T_a), by conserving metabolic heat (Dickson and Graham, 2004). In bluefin tunas, the tissues that are endothermic are the red ('slow-twitch', predominantly aerobic) skeletal muscle, the viscera and the cranium (eye/brain). Proposed advantages of regional endothermy in fishes include: (a) thermal niche expansion into cooler waters; (b) enhanced cruise-type (i.e. sustainable, aerobic) swimming performance; (c) faster rates of nutrient digestion and assimilation leading to faster growth and (d) improved vision in cooler/deeper waters leading to greater success in the capture of prey (Carey et al., 1984, Block et al., 1993, Dickson and Graham, 2004).

2.1.2. Tuna classification and distribution

Tuna larvae and very young juveniles are restricted to warm tropical waters presumably because they are functioning as ectotherms and have not yet developed the capacity for regional endothermy (Reglero et al., 2014, Kitagawa et al., 2010, Fujioka et al., 2018b). In contrast, older tuna juveniles and adults can be found either in warm tropical or cool temperate waters, depending upon the species. Tunas are bony fishes (class Osteichthyes) belonging to the tribe Thunnini within the family Scombridae (Dickson and Graham, 2004). The tribe Thunnini consists of the genera *Allothunnus*, *Auxis*, *Euthynnus*, *Katsuwonus* and *Thunnus*. The genus *Thunnus* is further subdivided into the subgenus *Thunnus* (the bluefin group) and the subgenus *Neothunnus* (the yellowfin group). Atlantic bluefin tuna (ABT, *Thunnus thynnus*), Pacific bluefin tuna (PBT, *Thunnus orientalis*) and southern bluefin tuna (SBT, *Thunnus maccoyii*) belong to the bluefin group and are the most cool-water tolerant of all of the tunas. The older juveniles and adults in this group spend most of their lives foraging at higher latitudes in cool temperate waters but like all tunas they return to warm tropical waters, at lower latitudes,

to spawn and hatch their eggs (Reglero et al., 2014). The present study focuses on one of the bluefin tuna species, namely Pacific bluefin tuna (PBT).

2.1.3. The life history of Pacific bluefin tuna

There are two known spawning grounds for PBT. The first is in the waters surrounding the Ryukyu Archipelago to the south of the Japanese main island of Kyushu and the second is in the Sea of Japan to the west of the Japanese main island of Honshu (Fig. 2.1) (Kitagawa et al., 2006b, Fujioka et al., 2018a). PBT spawn in these waters in the summer months of April to June and July to August, respectively. Once hatched, the larvae and young juveniles disperse to their winter feeding grounds off the west coast of Kyushu Island in the East China Sea and off the south coast of Honshu Island in the north-western Pacific Ocean. The larvae/juveniles travelling from the more southerly spawning ground are assisted in their dispersal by the Kuroshio Current. This is a warm current that travels northwards from the Ryukyu archipelago before splitting into an eastern extension (also known as the Kuroshio Extension) that carries the larvae and young juveniles to their feeding grounds off the south coast of Honshu Island and a western extension (also known as the Tsushima Current) that carries them to their feeding grounds off the west coast of Kyushu Island.

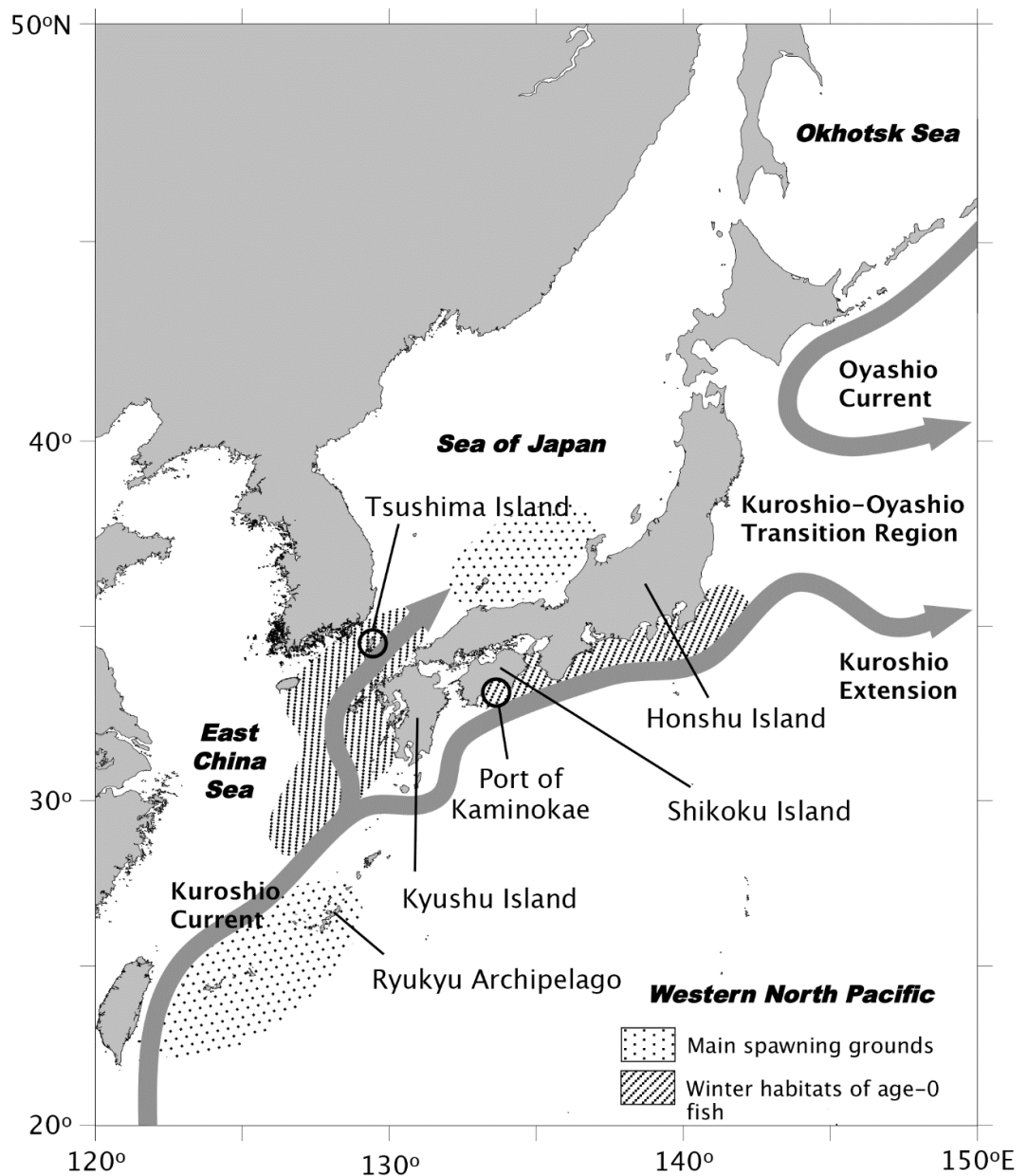


Fig. 2.1. Map of the western North Pacific Ocean showing the sampling locations (open circles) for the Pacific bluefin tuna (PBT) specimens used in this study. The map also shows a schematic illustration of the main ocean currents around Japan (broad grey arrows). The stippled areas are the known hatching grounds for PBT larvae and the dashed areas are the habitats for age-0 PBT juveniles (Kitagawa et al., 2006b, Fujioka et al., 2018a).

2.1.4. Regional endothermy in bluefin tunas

In bluefin tunas, there are three types of regional endothermy, commonly referred to as red muscle endothermy, visceral endothermy and cranial endothermy (Gunn and Block, 2001, Marcinek et al., 2001, Dickson and Graham, 2004). In the red muscle, the source of the heat that warms the tissue is the repeated contraction of the red ('slow-twitch', predominantly aerobic) muscle fibres. These power the continuous swimming that is characteristic of tunas. Tunas swim continuously because they are negatively buoyant and they are ram ventilators, i.e., they require water continuously flowing over their gills to obtain oxygen (Dickson and Graham, 2004). In most fish species, the red muscle is located in a narrow wedge just beneath skin. In tunas, on the other hand, it is located in cones deep within the body, close to the vertebral column (Graham and Dickson, 2000). This more medial location of the red muscle in tunas reduces conductive heat loss across the body surface. The heat generated by the repeated contraction of the red muscle is conserved by *retia mirabilia* ('wonderful nets') (Dickson et al., 2000, Stevens, 2011). These are networks of arterioles and venules arranged as counter-current heat exchangers. In these networks, the warm blood exiting the muscle in the venules, transfers heat to the cool blood entering the muscle in the arterioles. This reduces convective heat loss at the gills. In the tuna species belonging to the genera *Auxis*, *Euthynnus* and *Katsuwonus* there are two different types of red muscle *retia*, the lateral and the central (Dickson and Graham, 2004, Graham and Dickson, 2000). The bluefin tunas have only the lateral. The lateral *retia*, consist of epaxial and hypaxial halves on either side of the fish and they are located between the red muscle and the major subcutaneous arteries and veins that run along the sides of the fish (Carey and Teal, 1966, Dickson and Graham, 2004). In this study, we will refer to these lateral *retia* simply as red muscle *retia* (singular = rete).

In addition to red muscle endothermy, bluefin tunas also exhibit visceral and cranial endothermy (Dickson and Graham, 2004). In the viscera, the source of the heat that warms the tissue is specific dynamic action (SDA). SDA is the heat generated by the processes of digestion and assimilation of nutrients, following a meal (Fitzgibbon et al., 2007). In the cranium, the heat source is, most likely, either the frequent contraction of the highly aerobic ocular muscles

or the heat produced by the central nervous system (Block, 1987b, Block and Finnerty, 1994, Dickson and Graham, 2004, Sepulveda et al., 2007). Like the red muscle, both the viscera and the cranium have heat-exchanging blood vessels arranged as *retia*. These are referred to as visceral and cranial *retia*, respectively.

2.1.5. Aims

Firstly, this study aimed to determine when, at what minimum body size and age, PBT juveniles begin to significantly elevate their red muscle, visceral and cranial tissue temperatures above the ambient water temperature. Secondly, we aimed to determine how this temperature elevation is related to the ontogenetic development of the anatomical features that support the development of regional endothermy in fishes. To this end, we measured the maximum temperatures in the red muscle, viscera and cranium in young PBT juveniles of different sizes/ages and compared the tissue temperatures with the ambient water temperature and we analysed the mass of red muscle relative to the mass of the fish as well as the extent of proliferation of the red muscle and visceral *retia* in different sized fish.

2.2. Materials and Methods

2.2.1. Fish specimens

Four groups of young Pacific bluefin tuna (PBT, *Thunnus orientalis*) juveniles caught in Japanese waters were used in this study. The first [18.5 – 21.2 cm fork length (FL), 71 – 142 g body mass (BM), n = 21] was obtained from fishermen operating offshore from the port of Kaminokae (Kochi Prefecture, Shikoku Island) on the 2nd of August 2016 (late summer) (Fig. 1). The fish were caught in small batches, using barbless hooks and maintained alive in ambient seawater in the baitwell of a commercial fishing boat for a period of no more than one hour prior to sampling. The second [33.3 – 42.6 cm FL, 750 – 1,700 g BM, n = 10] and third [57.5 – 62.5 cm FL, 4,050 – 5,350 g BM, n = 4] were obtained from a sea cage farm located approximately 1 km offshore from the town of Imazato (Nagasaki Prefecture, Tsushima Island) on the 28th of November 2016 (late autumn) and the 27th of March 2017 (early spring), respectively. The fish was hooked individually from the sea cage, using a pole and line with a barbless hook. The fourth [42.2 – 47.5 cm FL, 1,500 – 2,200 g BM, n = 5] was caught by a fisherman operating off the south coast of Honshu Island in late October 2016. The fish in Groups one through three were obtained alive whereas those in Group four had been frozen whole. The fish in Groups two and three had been maintained on the sea cage farm on a diet of anchovies, sardines and round herring and were fed to satiation once or twice a day since October and May 2016, respectively.

2.2.2. Estimating the age of the PBT specimens

The age of our PBT specimens was estimated using the von Bertalanffy growth function, with values for PBT obtained from Shimose et al. (2009). The von Bertalanffy growth function relates FL in cm to age in years and can be written as follows: $L_t = L_\infty(1 - e^{-K(t-t_0)})$, where L_t = FL at age t , L_∞ = the asymptotic FL, K = the growth coefficient, t = age in years, and t_0 = the theoretical age when length is equal to zero (Chen et al., 1992). Using the values for PBT obtained from Shimose et al. (2009), this equation becomes $L_t = 249.6(1 - e^{-0.173(t+0.254)})$.

2.2.3. Temperature measurements

The fish in Groups one through three were used for the temperature measurements. Individual fish were caught one by one and subjected to the temperature measurements described below. The measurements were made immediately following the capture of each fish and while it was still alive. The fish were transferred to a seawater-moistened, vinyl-covered, foam cradle for tissue temperature measurements. During the tissue temperature measurements, the fish were not sedated. Instead, the fish's eyes were covered with a soft, seawater-moistened cloth to keep it calm. This was done to prevent the body temperature being increased by the increased physical activity resulting from being stressed. Ethics approval for all fish handling procedures was obtained from the Institutional Animal Care and Use Committee of California State University-Fullerton (Protocol No. 16-R-07). The temperature measurements were made using an Omega[®] copper-constantan type T thermocouple attached to an Omega[®] model HH506R digital thermometer (Omega[®] Technologies). The maximum temperature was determined for the red muscle, the viscera and the cranium. For the red muscle, the thermocouple probe was inserted slowly into the body at a position just dorsal to the epaxial lateral blood vessels and approximately 40-50% of FL from the fish's snout. The probe was inserted until it contacted the vertebral column and then slowly withdrawn towards the skin. The maximum temperature was recorded at a point slightly shallower than the vertebral column. For the viscera, the probe was inserted into the visceral cavity and the maximum temperature was recorded in the more anterior portion of this cavity. For the cranium, the probe was inserted into the ocular cavity behind the eye where the ocular muscles and the optic nerve are located. Immediately following the tissue temperature measurements, the same thermocouple/thermometer was used to measure the ambient water temperature (T_a). To ensure the accuracy of the temperature measurements, the thermocouple/thermometer had been calibrated against a mercury thermometer. For the fish in Groups two and three (the intermediate-sized and largest fish), extra precautions were taken to prevent overheating of the tissues during the temperature measurements. To do this, ambient sea water was pumped in through the fish's mouth and out across its gills using a length of clear, flexible, PVC tubing (13 mm internal diameter, 16 mm external diameter)

attached to a 12 V submersible pump (Rule 500 GPH) powered by dry cell batteries, at a flow rate of 32 litres min⁻¹. The flow of water maintained the supply of oxygen to the fish's gills and kept its heart beating and blood circulating during the temperature measurements. In addition, the fish was kept calm by covering its eyes with a soft, seawater-moistened cloth and supporting its body in a sea-water moistened, vinyl-covered, foam cradle.

2.2.4. Fish sampling for histology

Immediately following the temperature measurements, the fish was euthanized, weighed using a spring balance and then dissected for the histology samples. The histology samples were taken only from the left side of the body to ensure that the right side remained intact for the muscle distribution analyses (see below). For the histology analyses, samples were taken of the red muscle *retia*, with some of the skin and red muscle still attached for orientation, at a position approximately 40-50% of FL from the snout of the fish, just posterior to the insertion of the pectoral fin. Samples were also taken of the visceral rete. Each sample was placed in a labeled histology cassette which was subsequently immersed in 10% (v/v) neutral buffered formalin (pH 7.4) (Wako Pure Chemical Industries Ltd., Japan). For processing for microscopy, the tissue samples were rinsed in 0.1 M phosphate buffer, then dehydrated in a series of increasing concentrations of ethanol finishing with at least two changes of 100% (v/v) ethanol. Paraffin is poorly soluble in ethanol. Therefore, the samples were then immersed in xylene, which is miscible with both ethanol and paraffin, to replace the ethanol (clearing). Finally, the samples were vacuum infiltrated and embedded in paraffin wax. Following this, the embedded samples were sectioned using a rotary microtome (Microm HM325 microtome) to produce 5- μ m-thick sections that were subsequently mounted on glass slides and stained with hematoxylin and eosin (Humason, 1979). The slides were examined and photographed using an Olympus SZ40 microscope fitted with a Kodak video camera and Q Capture Pro software. To quantify their size, the lengths of the blood vessels constituting the red muscle *retia* and the total cross-sectional area of the blood vessels constituting both the red muscle *retia* and the visceral rete were measured using ImageJ software (<https://imagej.nih.gov>). The lengths of the red muscle rete blood vessels were measured from the axial margin of the large lateral subcutaneous

artery and vein to the lateral border of the red muscle, in all images in which the rete blood vessels were clearly visible. In addition, to obtain cross sections of the rete blood vessels segments of the red muscle *retia* were also embedded and the number of rows of vessels in each rete were measured in each cross section. Prior to the measurements for each section, the scale was set in Image J using the ruler in the image (Schneider et al., 2012). The visceral rete blood vessels were cut in cross-section and montages of multiple images were created using the merge function in Adobe Photoshop in order to visualize the whole rete and to measure the total visceral rete cross-sectional area.

2.2.5. Red muscle distribution and mass measurements

Whole fish, or fish that had been partially dissected to remove the histology samples (see above), were used for these measurements. For the smallest fish, eleven of the twenty specimens caught on the 2nd of August 2016 (Group one fish, see above) and partially dissected for the histology samples were used. For the intermediate-sized fish, the five fish that had been caught and frozen whole in late October 2016 (Group four fish, see above) were used. For the largest fish, the four specimens that had been caught on the 27th of March 2017 (Group three fish, see above) and partially dissected for the histology samples were used. Only one side of the Groups one and three fish had been dissected to remove the histology samples and therefore the other side remained intact for the muscle distribution analyses. The partially dissected fish had been carefully arranged back into their original shape before being frozen at -20°C in preparation for the muscle distribution analyses. To analyse the distribution of the red muscle along the length of the fish, the whole or partially dissected fish were removed from the freezer and sectioned using a bandsaw while still frozen. The bandsaw was used to cut the fish into 2-cm-thick cross-sections, commencing immediately posterior to the operculum and continuing until little red muscle remained visible, in the area of the finlets. The head, tail and each cross-section were photographed alongside a scale bar, and the resulting images were analysed using Image J software (Schneider et al., 2012). For each cross-section, the total cross-sectional area and the area occupied by the red muscle were determined. The values for adjacent sides of neighbouring cross-sections were averaged together to correct for any tissue

losses as a result of the band-sawing procedure and the values so obtained were averaged between the anterior and posterior sides of each cross-section to correct for any differences in red muscle area between different planes within each cross-section. To determine the mass of red muscle in each section at different positions along the body, the area values for each cross-section were multiplied by the width of each cross-section (i.e. 2 cm) to obtain volume values and the volume values were converted to mass values by multiplying them by published tuna muscle density values (Magnuson, 1973, Magnuson, 1978).

2.2.6. Confirmation of the species identity of our PBT specimens

Different tuna species can be difficult to distinguish from one another when they are very young (Matsumoto et al., 1972, Chow et al., 2003, Pedrosa-Gerasmio et al., 2012). Thus, we confirmed the species identity of the PBT specimens we sampled using a modification of the method described by Ward et al. (2005). This method uses the nucleotide sequence variation in the mitochondrial cytochrome c oxidase subunit 1 (COXI) gene to differentiate between different fish species. DNA was extracted from 25 mg of PBT red muscle (previously stored in RNA/later[®], Ambion[®]) using a QIAamp[®] DNA mini kit. In the first step of this procedure, the tissue was homogenised, in 180 µL of the ALT buffer supplied with the kit, for 4 min using a Retsch MM40 bead mill set at a frequency of 30 Hz. All other procedures were as described by the manufacturers of the kit. To determine the species of origin, the extracted DNA was used as the template for polymerase chain reaction (PCR). Each 50 µL PCR reaction contained 1 µg of PBT red muscle DNA, 200 µM dNTPs (Promega), 2.5 units of *Taq* DNA polymerase (New England Biolabs), 5 µL of 10x ThermoPol[®] Buffer (New England Biolabs) and 0.2 µM of the relevant forward and reverse PCR primers. The sequences of the forward and reverse primers were 5'-TCAACCAACCACAAAGACATTGGCAC-3' and 5'-AGACTTCTGGGTGGCCAAAGAATCA-3', respectively. The PCR cycling conditions were as follows: one cycle of denaturation at 95°C for 3 min followed by 30 cycles of denaturation at 95°C for 3 s, annealing at 55°C for 30 s and extension at 68°C for 1 min followed by a final extension at 68°C for 5 min. The PCR cycling was done in a Hybaid PX2 thermal cycler (Thermo Scientific). The resulting PCR products were purified using the Wizard[®] SV Gel and PCR

Clean-Up System (Promega), following the manufacturer's instructions and their nucleotide sequences were determined using Sanger sequencing by the Australian Genome Research Facility (AGRF). Finally, the sequences were used to perform nucleotide BLAST searches of the GenBank nucleotide database (available at <http://www.ncbi.nlm.nih.gov/>). The BLAST searches retrieved COXI nucleotide sequences from various tuna species. The top five hits, each with 99% identity to our sequences, were from PBT. Various tuna sequences from the GenBank database and our sequences were aligned using ClustalX2 (Larkin et al., 2007) and then the Neighbor-Joining method (Saitou and Nei, 1987), implemented using MEGA6 (Tamura et al., 2013), was used to infer the relationships between these sequences. The sequences obtained from the samples we collected, grouped most closely together with the five other PBT COXI sequences that had previously been deposited in the GenBank database and they were clearly separated from the COXI sequences from the other tuna species (Appendix 1). Thus, we confirmed that the species that we were studying was indeed PBT.

2.2.7. Statistical analyses

All graphs, the linear, power and polynomial trend lines that were fitted to the data and their corresponding R^2 values were generated using Microsoft Excel (Excel 2013). Scaling coefficients that describe the relationship of fish FL or BM to a given variable were obtained by plotting the \log_{10} of the variable of interest against the \log_{10} of FL or BM and obtaining the slope value from the linear regression performed in Microsoft Excel (Excel 2013). The slope value was the scaling coefficient. The standard error was calculated through linear regression analysis of the log transformed data performed using the IBM® SPSS Statistics version 22.0 software package (IBM, New York, USA).

2.3. Results

2.3.1. Fish growth and age determination

Four groups of young PBT juveniles were used in this study. The Group one fish, the smallest fish, ranged in size from 18.5 to 21.2 cm FL and 71 to 142 g BM. The Group two fish, the intermediate-sized fish, ranged in size from 33.3 to 42.6 cm FL and 750 to 1,700 g BM. The Group three fish, the largest fish, ranged in size from 57.5 to 62.5 cm FL and 4,050 to 5,350 g BM. The Group four fish, additional intermediate-sized fish, ranged in size from 42.2 to 47.5 cm FL and 1,500 to 2,200 g BM. Taking all of these fish all together, BM increased exponentially with increasing FL with a scaling coefficient (mean \pm SE) of 3.38 ± 0.04 indicating slightly greater than isometric scaling of BM with increasing FL (Fig. 2.2). By substituting the smallest and largest FL for each group of fish into the von Bertalanffy growth function, with values for PBT from Shimose et al. (2009), the ages of the fish were estimated to be 2 to 3 months for the Group one fish, 6 to 8 months for the Group two fish, 15 to 16 months for the Group three fish and 8 to 10 months for the Group four fish.

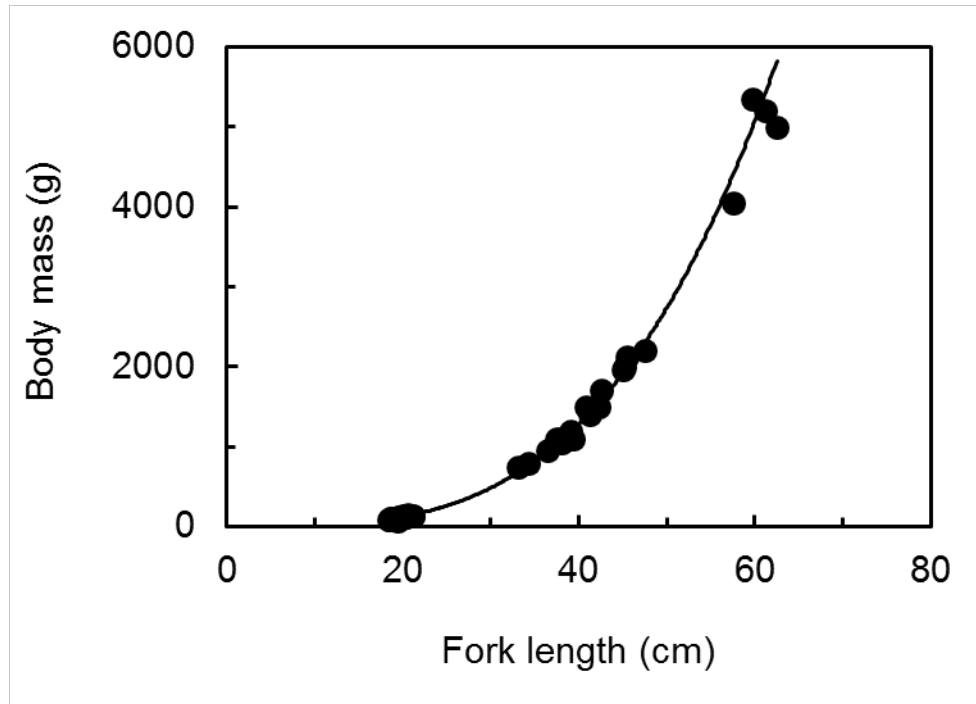


Fig. 2.2. The relationship between body mass (BM) and fork length (FL) in young juvenile PBT specimens sampled in the waters of Japan. The relationship is described by the equation $BM = 4.86 \times 10^{-3} FL^{3.38}$, $R^2 = 0.99$, $n = 41$.

2.3.2. Red muscle distribution and ontogeny

Fig. 2.3 shows examples of cross-sections through the body of small, intermediate-sized and large individuals to illustrate the distribution and ontogeny of their red muscle. Regardless of the size of the fish, the red muscle had the more medial distribution that is typical of tunas.

Fig. 2.4 shows how the amount of red muscle varied along the length of the body of the fish. In the smallest (~20 cm FL), intermediate-sized (~45 cm FL) and largest (~60 cm FL) fish, the maximum red muscle area, expressed as a percentage of the whole body cross-sectional area, was reached at 52, 46 and 49% of FL, respectively, from the snout of the fish. Thus, regardless of the size of the fish, the maximum amount of red muscle was reached at approximately 50% of FL from the snout of the fish.

Fig. 2.5 shows how the total mass of red muscle varied in relation to the size of the fish. The average total red muscle mass as a percentage of the average total BM was $5.79 \pm 1.4\%$ when all of the fish were taken all together. In Fig. 2.5A, the total mass of red muscle is shown to increase with increasing FL with a scaling coefficient of 3.10 ± 0.09 . Thus, there was slightly greater than isometric scaling of red muscle mass with increasing FL. In Fig. 2.5B, the total mass of red muscle is shown to increase with increasing BM with a scaling coefficient of 0.90 ± 0.24 . Thus, there was slightly less than isometric scaling of red muscle mass with increasing BM. Figs. 2.5C and 2.5D show that red muscle mass, expressed as a percentage of total body mass, decreased with increasing FL with a scaling coefficient of -0.35 ± 0.08 and with increasing BM with a scaling coefficient of -0.10 ± 0.02 . Thus, when the data were expressed this way, it became apparent that the red muscle mass as a proportion of the total BM decreased as the fish grew larger.

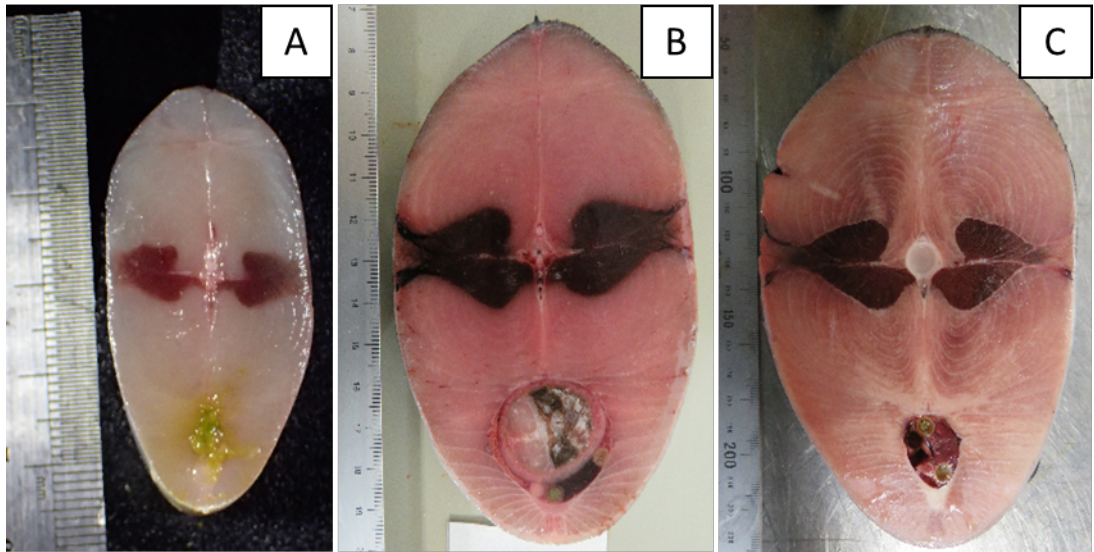


Fig. 2.3. Transverse body sections, taken at ~50% of FL, in young juvenile PBT specimens of different sizes, i.e., (A) 18.5 cm FL and 110 g BM, (B) 45.5 cm FL and 2,120 g BM and (C) 59.7 cm FL and 5,350 g BM.

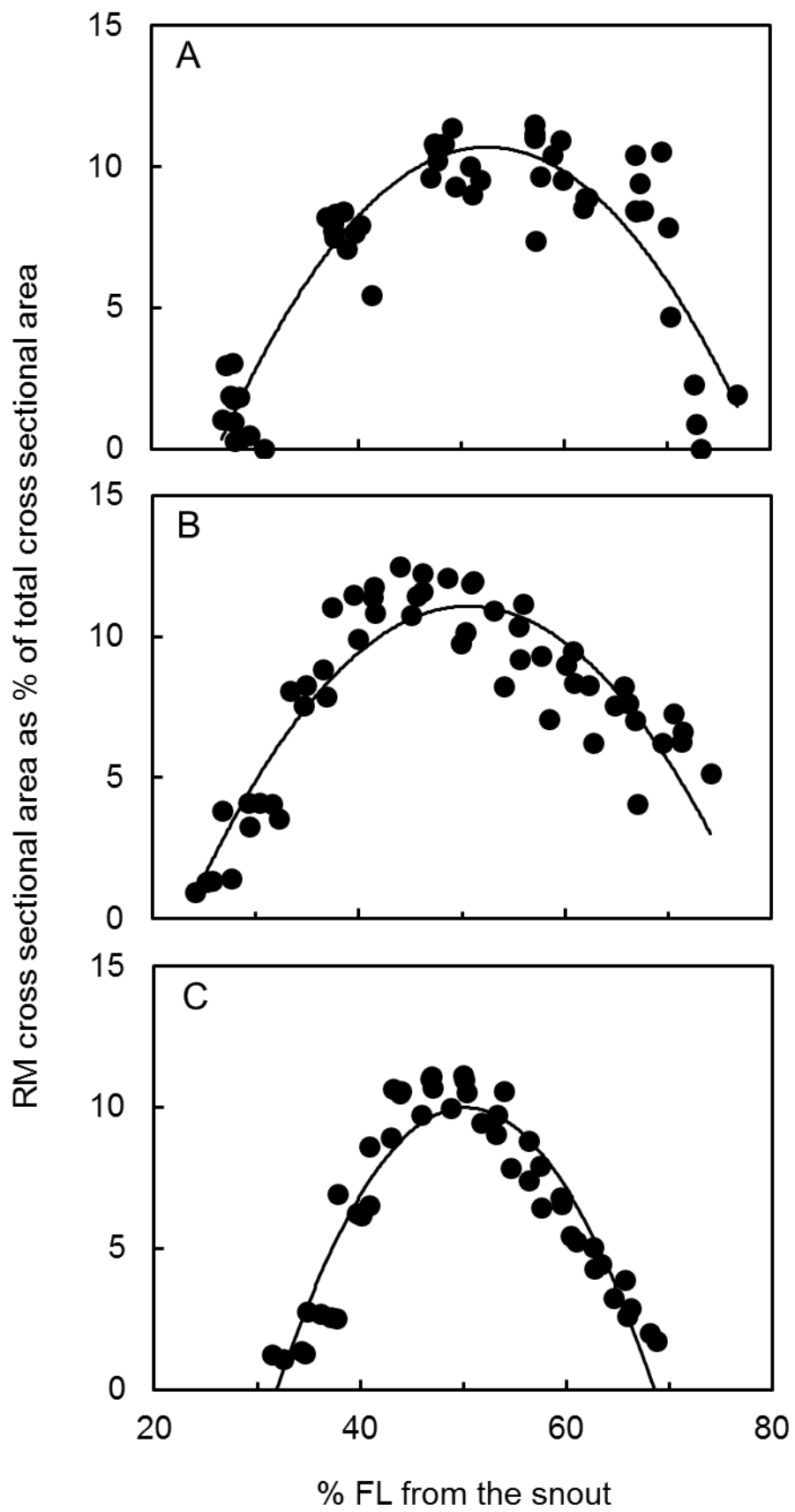


Fig. 2.4. Red muscle distribution along the length of the body in small juvenile PBT specimens of different sizes, i.e., (A) ~20 cm FL (n = 11), (B) ~45 cm FL (n = 5) and (C) ~60 cm FL (n = 4). The red muscle cross-sectional area as a percentage of the total cross-sectional area is plotted as a function of the relative position of the cross-section along the length of the body (% of FL from the snout). The curves represent the best-fitting polynomial functions for all of the fish within each size class.

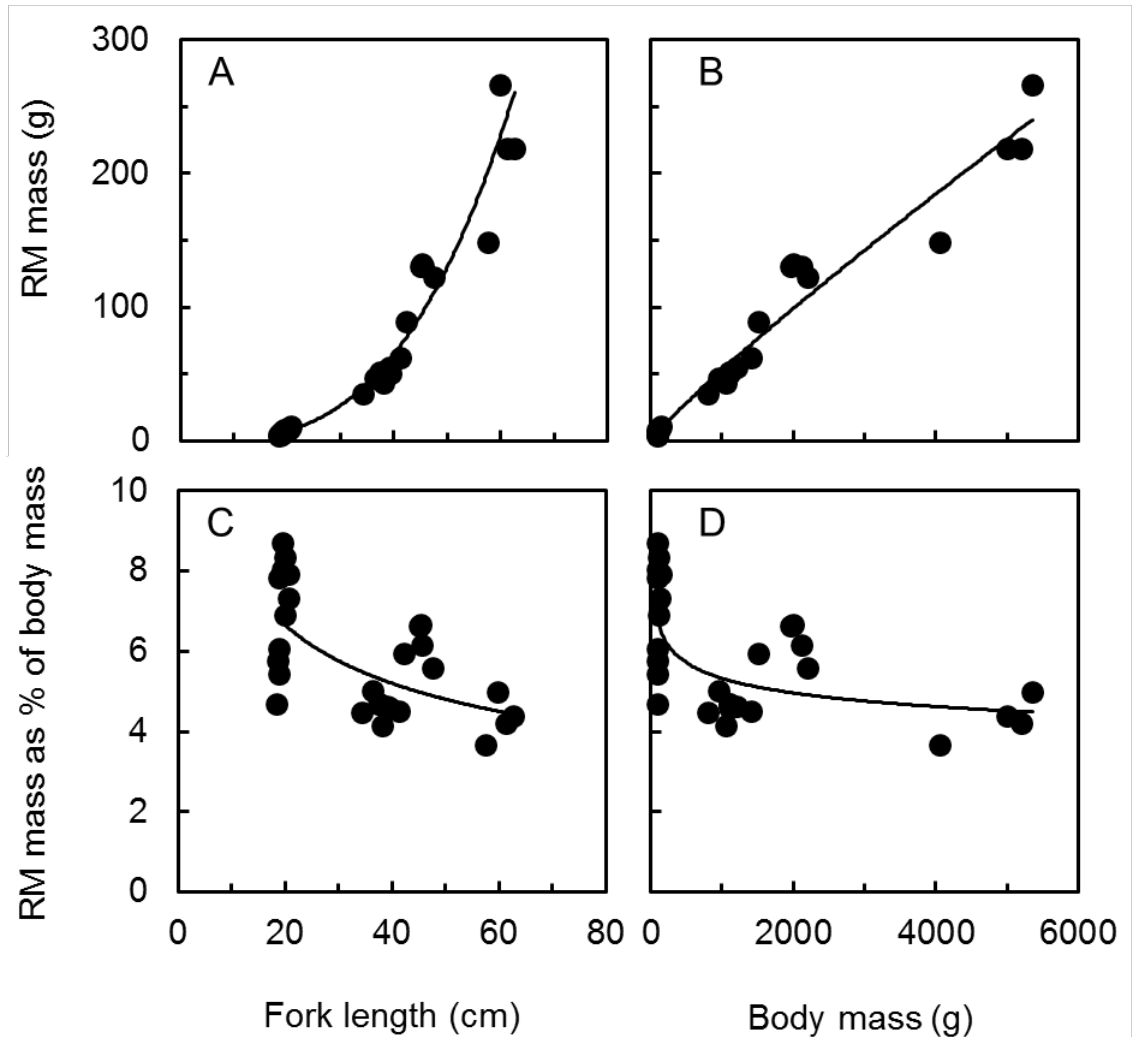


Fig. 2.5. The relationships between red muscle mass, fork length (FL) and body mass (BM) in young PBT specimens of different sizes ($n = 28$). The best-fitting power functions for the data in the different panels are: (A) $y = 7.1 \times 10^{-4}FL^{3.10}$, $R^2 = 0.98$; (B) $y = 1.1 \times 10^{-1}BM^{0.90}$, $R^2 = 0.98$; (C) $y = 19.3FL^{-0.35}$, $R^2 = 0.41$; (D) $y = 10.8BM^{-0.10}$, $R^2 = 0.40$.

2.3.3. Relationships between tissue temperature, body size and ambient water temperature

Fig. 2.6 shows how the maximum red muscle, visceral and cranial temperatures varied with varying body size and with varying water temperature in our young PBT specimens. For the smallest fish (~20 cm FL), caught in August (late summer) at an average ambient water temperature (T_a) of 29.4°C, the mean maximum red muscle temperature (T_{RM}) was 30.5°C. For the intermediate-sized fish (~40 cm FL), caught in November (late autumn) at an average T_a of 20.4°C, the mean maximum T_{RM} was 25.4°C. And for the largest fish (~60 cm FL), caught in March (early spring) 2017 at an average T_a of 15.8°C, the mean maximum T_{RM} was 26.9°C. Thus, the decrease in T_{RM} was small compared with the decrease in T_a and because of this, the mean thermal excess ($T_{RM} - T_a$) for the red muscle increased from 1.1°C in the smallest fish to 4.9°C in the intermediate-sized fish to 11.1°C in the largest fish (Fig. 2.6B). Thus, the thermal excess for the red muscle increased with increasing fish size and with decreasing T_a . The maximum thermal excess for the red muscle for any of the fish we studied was an impressive 14.2°C, observed in a specimen with a size of 61.2 cm FL.

In contrast to the thermal excess values for the red muscle, the thermal excess values for the viscera and the cranium were much more modest (Figs. 2.6A and B). The mean maximum visceral temperature (T_v) decreased with decreasing T_a from 30.0°C for the ~20 cm FL fish to 22.2°C for the ~40 cm FL fish to 19.3°C for the ~60 cm FL fish (Fig. 2.6A). Thus, T_v closely mirrored T_a but with a small elevation of the visceral temperature in the largest fish. Specifically, the thermal excess for the viscera was 0.6°C for the ~20 cm FL fish, 1.8°C for the ~40 cm FL fish and 3.5°C for the ~60 cm FL fish (Fig. 2.6B). Similarly, the maximum cranial temperature (T_c) for the three size classes of fish decreased with increasing fish size and with decreasing T_a from 29.9°C for the ~20 cm FL fish to 21.8°C for the ~40 cm FL fish to 17.8°C for the ~60 cm FL fish (Fig. 2.6A). This resulted in thermal excess values for the cranium of only 0.5°C for the ~20 cm FL fish, 1.3°C for the ~40 cm FL fish and 2.0°C for the ~60 cm FL fish (Fig. 2.6B). Thus, the cranial thermal excess values were the smallest of all for the three different tissue types. In summary, T_{RM}

remained relatively constant as the fish grew larger and this resulted in increasing thermal excess values for the red muscle as the water temperature cooled. In contrast, T_V and T_C decreased essentially in parallel with the declining T_a except for T_V in some of the larger fish which was somewhat elevated. In the red muscle, the highest thermal excess value recorded was 14.2°C whereas in the viscera and the cranium it was only 5.1°C and 2.7°C , respectively.

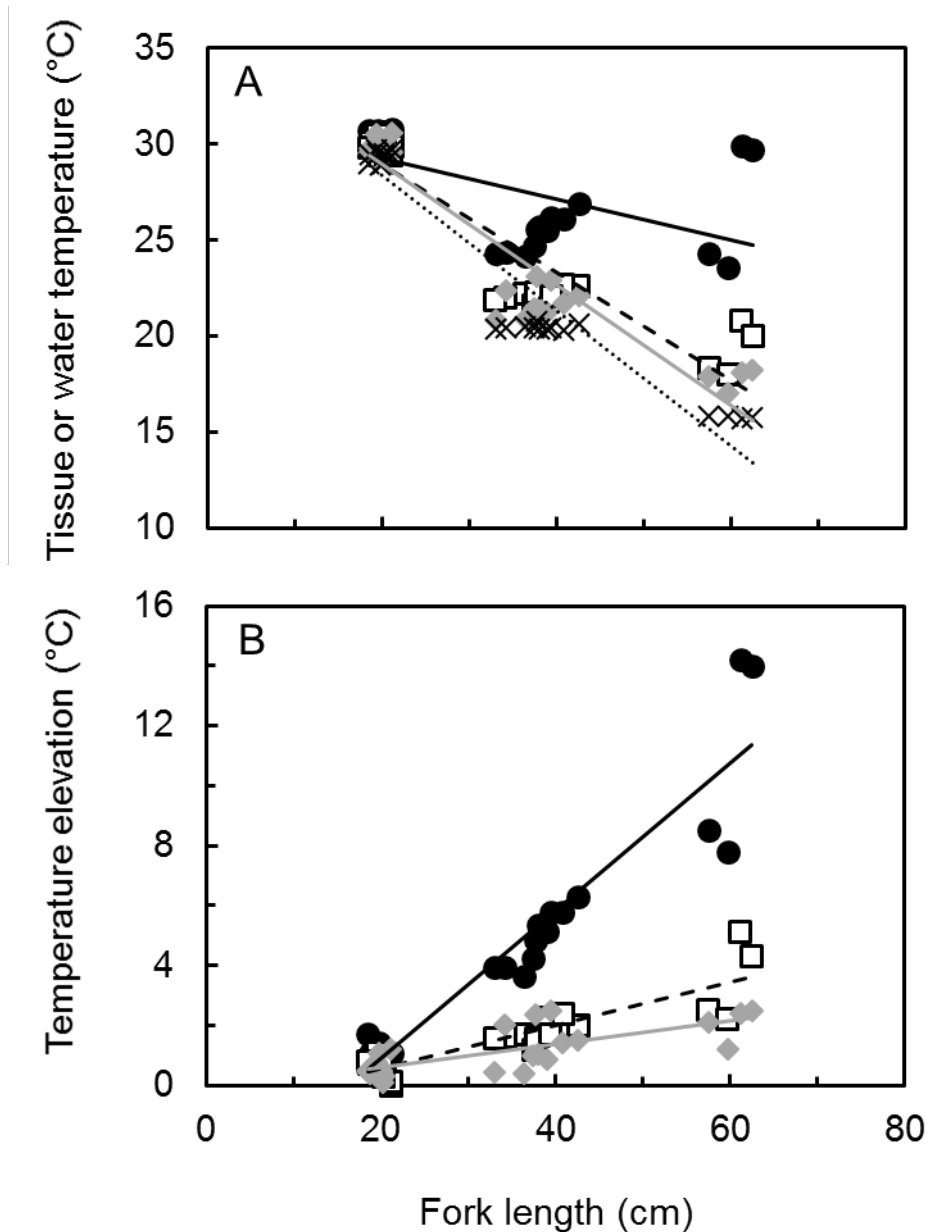


Fig. 2.6. The effects of increasing fish size and decreasing T_a (× with a dotted line) on maximum T_{RM} (● with solid black lines), T_V (■ with dashed lines) and T_C (◆ with solid grey lines) in young PBT specimens of different sizes caught in the waters of Japan in August and November 2016 and in March 2017. In Panel A, the relationships between temperature and FL are described by the equations: $T_{RM} = -0.11FL + 31.42$, $R^2 = 0.29$; $T_V = -0.29FL + 34.56$, $R^2 = 0.80$, $T_C = -0.32FL + 35.21$, $R^2 = 0.87$; and $T_a = -0.36FL + 35.42$, $R^2 = 0.88$. In Panel B, the relationships between temperature elevation and FL are described by the equations: $T_{RM} = 0.25FL - 4.01$, $R^2 = 0.90$; $T_V = 0.07FL - 0.86$, $R^2 = 0.78$; and $T_C = 0.04FL - 0.20$, $R^2 = 0.13$. Measurements were made on 25 specimens in total with 10 at ~20 cm FL, 10 at ~38 cm FL and 4 at ~60 cm FL.

2.3.4. Proliferation of the red muscle rete blood vessels with increasing fish body size and decreasing ambient water temperature

Fig. 2.7 shows an example of how the red muscle rete blood vessels proliferated with increasing fish body size and with decreasing T_a . Fig. 2.7A shows a macroscopic view of a cross-section through the body of a small PBT specimen (18.5 cm FL) with a box highlighting the location of the red muscle rete blood vessels. The rete blood vessels are located between the red muscle and the large subcutaneous artery and vein that run just beneath the skin along the lateral line of the fish. Fig. 7B shows a microscopic view of the boxed in region in Fig. 7A and Fig. 7C shows a higher magnification of this same region. It is apparent from these three figures that the red muscle rete consists of epaxial and hypaxial halves connected to the corresponding major lateral arteries and veins running along the length of the body of the fish and connecting the red muscle blood circulation to the gills. Figs. 7D, E and F show longitudinal-sections of the rete blood vessels in examples of small (18.5 cm FL), intermediate-sized (37.4 cm FL) and large (61.2 cm FL) PBT specimens whereas Figs. 7G, H and I show the corresponding cross-sections. It is clear that the width of the rete (in the longitudinal sections) and the number of individual rete blood vessels (in the cross-sections) increases substantially with increasing fish size. In particular, the difference between the smallest and intermediate-sized fish is especially striking with relatively little proliferation in the smallest fish (Fig. 2.7D) but considerable proliferation in the intermediate-sized fish (Fig. 2.7D). Fig. 7J shows a higher magnification of Fig. 7I highlighting the individual arterioles (with the thicker walls) and venules (with the thinner walls) that make up the rete and showing how they are interspersed with one another to facilitate heat exchange.

In Fig. 2.8A, data are presented for the quantification of the average lengths of the blood vessels that make up the red muscle rete. The quantification was done using samples taken from the region of the body of the fish that contained the maximum amount of red muscle, i.e., at approximately 50% of FL from the snout. It is clear from the figure that there was a very strong correlation ($R^2 = 0.97$) between the average vessel length and increasing fish body size. Thus, there is a quantitative as well as a qualitative increase in the proliferation of

the red muscle rete blood vessels as the fish grow larger. In Fig. 2.8B, data are presented for the maximum number of red muscle rete blood vessel rows. It is evident from the figure that, like the average red muscle rete blood vessel length, there was a very strong correlation ($R^2 = 0.91$) between the maximum number of red muscle rete vessel rows and increasing fish body size. Fig. 2.8C shows that there is a strong positive correlation ($R^2 = 0.85$) between the maximum number of red muscle rete blood vessel rows and the thermal excess in the red muscle. This indicates that the increasing thermal excess in the red muscle is due to the increasing proliferation of the red muscle rete blood vessels with increasing body size.

Fig. 2.9 shows that there was a strong positive correlation between the red muscle temperature elevation and the age of the fish ($R^2 = 0.85$). Together with the strong correlations we observed between red muscle rete length/the maximum number of red muscle rete blood vessel rows and the thermal excess in the red muscle, this provides strong evidence that the increase in thermal excess in the red muscle with increasing age is due to the proliferation of the red muscle *retia*.

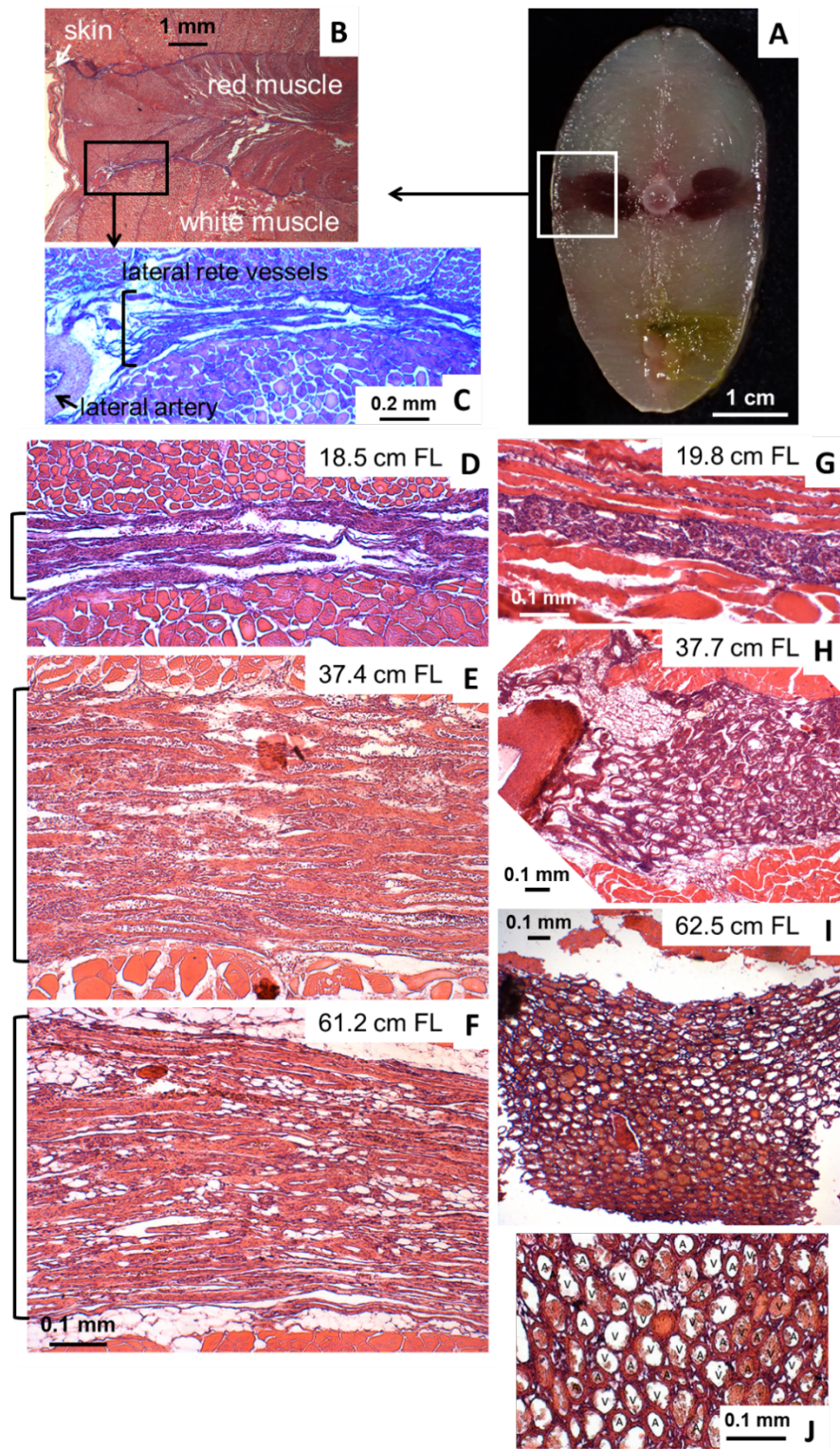


Fig. 2.7 The effect of increasing body size on the length of the red muscle rete blood vessels. (A) Transverse section of a 18.5 cm FL PBT specimen. (B) Higher magnification of box in A, showing the epaxial and hypaxial red muscle *retia*. (C) Higher magnification of the hypaxial portion of the red muscle rete (box in B). (D-F) Longitudinal sections of the hypaxial portion of red muscle rete (bracketed) from three PBT specimens (18.5, 37.4 and 61.2 cm FL, respectively) all at the same magnification. (G-I) Cross-sections of the red muscle rete blood vessels from three PBT specimens (19.8, 37.7 and 62.5 cm FL, respectively). (J) Higher magnification of I, showing alternating thicker-walled arterioles (A) and thinner walled venules (V).

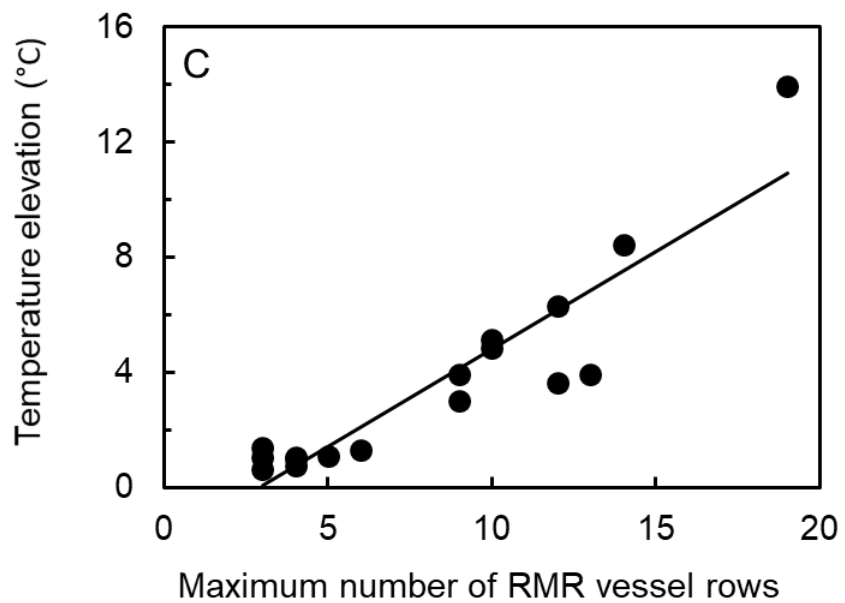
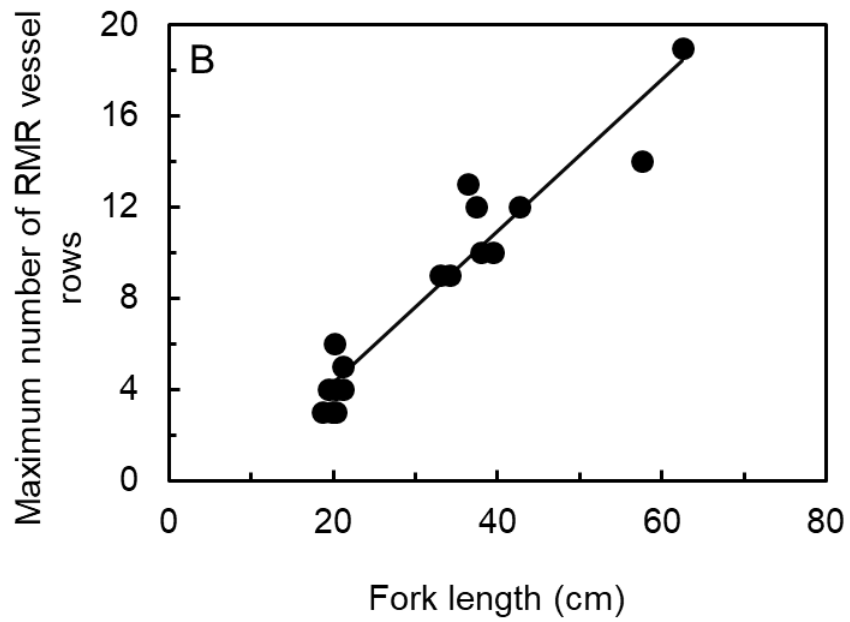
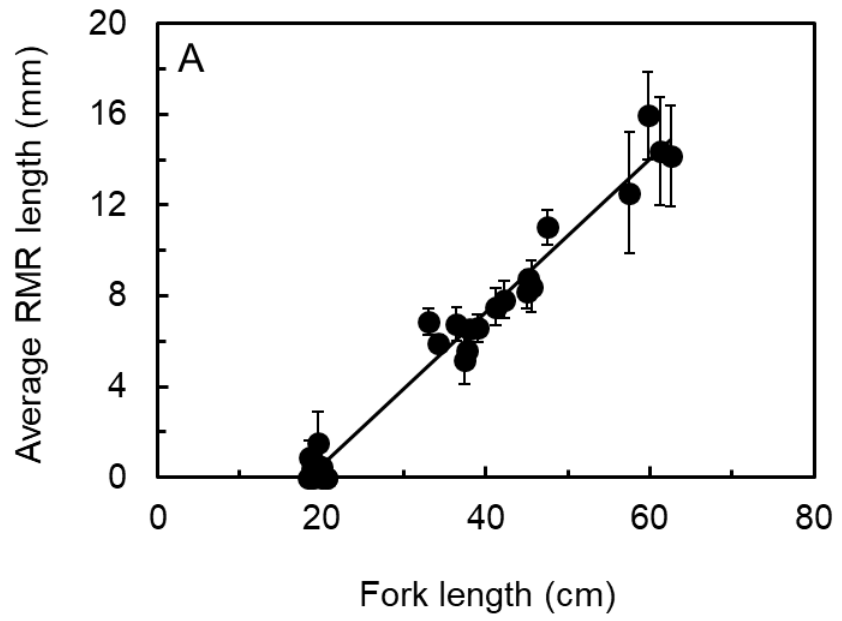


Fig. 2.8 The effect of body size (measured as FL) on (A) the average (\pm the standard deviation (SD)) length of the red muscle rete (RMR) blood vessels and (B) the maximum number of RMR vessel rows in the region of the maximum amount of red muscle. The equation describing the data in panel A is $\text{RMR length} = 0.34\text{FL} - 6.15$ ($R^2 = 0.97$, $n = 28$) and in panel B it is $\text{RMR vessel rows} = 0.33\text{FL} - 2.35$ ($R^2 = 0.91$, $n = 17$). Panel C shows the relationship between the maximum number of RMR vessel rows and red muscle temperature elevation in young PBT specimens of different sizes. The equation that describes the relationship is $\text{temperature elevation} = 0.68\text{RMR vessel rows} - 1.97$, $R^2 = 0.85$, $n = 17$.

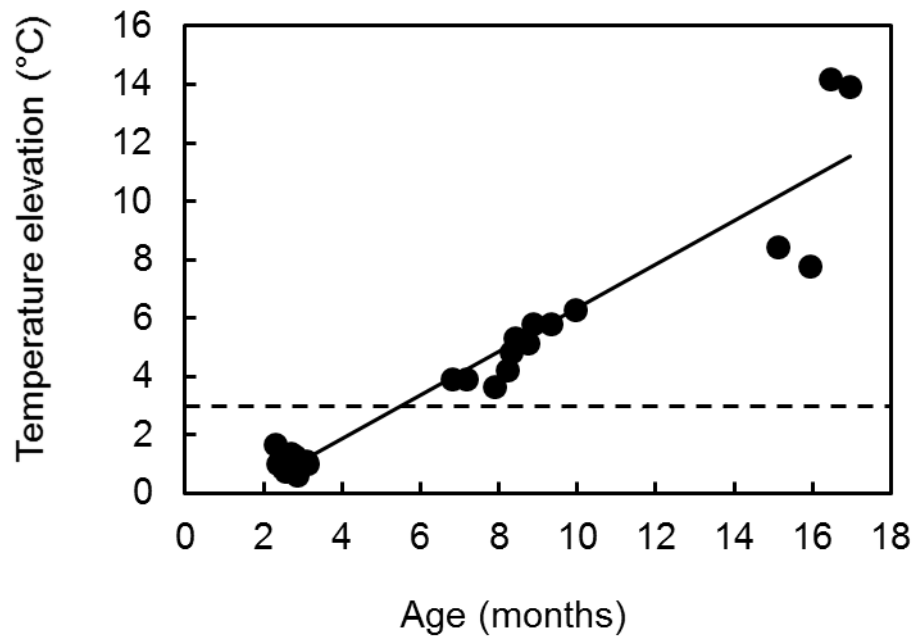


Fig. 2.9. The relationship between fish age and red muscle temperature elevation above the ambient water temperature in young PBT specimens of different sizes. The ages were estimated using the von Bertalanffy growth function with values for PBT obtained from Shimose et al. (2009). The dotted line represents the point where the tissue temperature elevation above the ambient water temperature is 3°C. This was used to determine the minimum body size and age at which PBT displays red muscle endothermy. This cutoff was chosen based on the study by Dickson (1994).

2.3.5. Proliferation of the visceral rete blood vessels with increasing body size and decreasing ambient water temperature

Fig. 2.10 shows how the total cross-sectional area occupied by the blood vessels of the visceral rete increases with increasing fish size and decreasing T_a in four different PBT specimens ranging in size from 21.1 to 57.5 cm FL. The total cross-sectional area occupied by the blood vessels of the visceral rete increased from 0.9 to 2.0 mm² in the smallest fish to 8.4 to 12.9 mm² in the intermediate-sized fish to 25.7 mm² in the largest fish. It can also be seen that the number of blood vessels within the rete increased considerably with increasing fish size. In Fig. 2.11A, data are presented for the quantification of the total cross-sectional area occupied by the visceral rete blood vessels. It is clear that the average cross-sectional area increases linearly and steeply with increasing fish body size. Thus, there is a quantitative as well as a qualitative increase in the total cross-sectional area occupied by the visceral rete blood vessels as the fish grow larger. Fig. 2.11B shows that there was a weak positive correlation ($R^2= 0.46$) between the cross-sectional area of the visceral rete and the thermal excess within the visceral cavity. This indicates that the increasing thermal excess in the viscera is due to the increasing proliferation of the red muscle rete blood vessels with increasing body size.

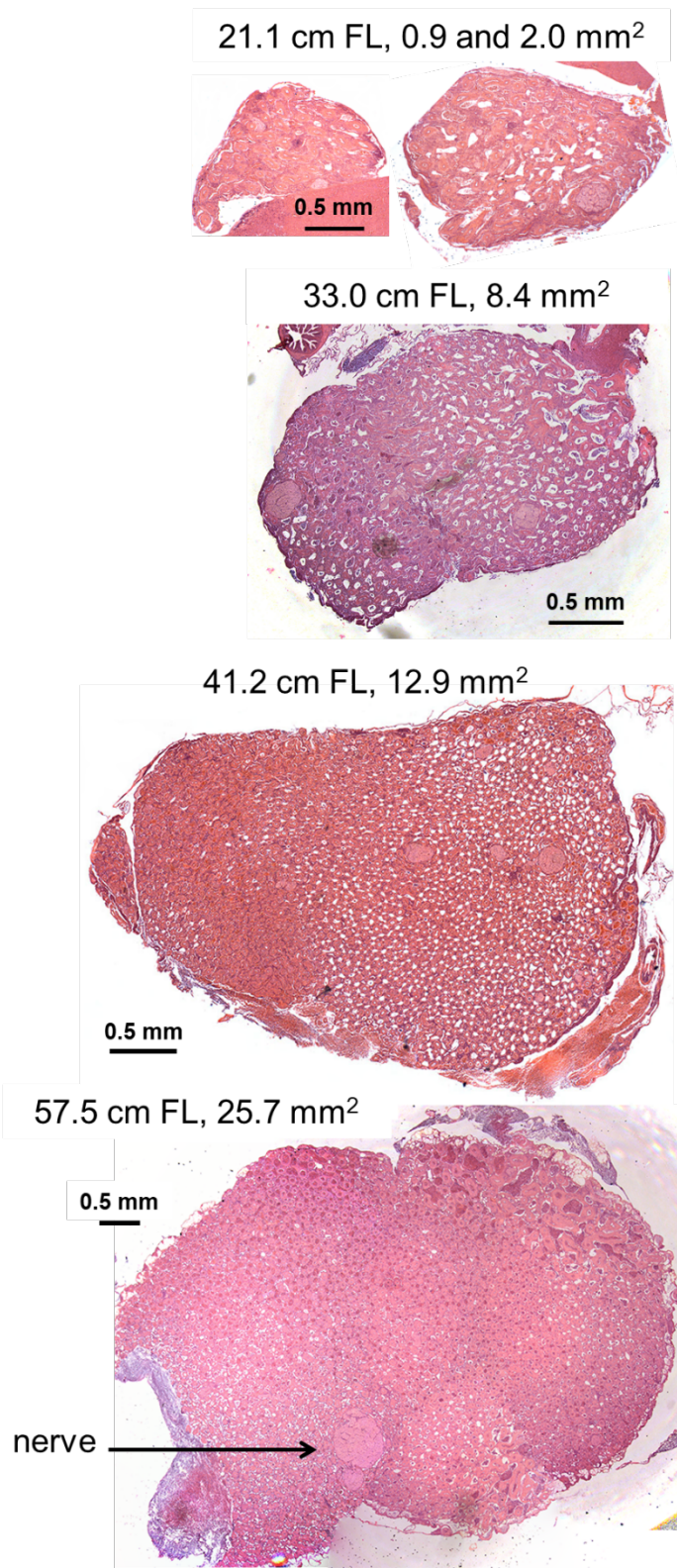


Fig. 2.10 Micrographs of cross-sections of the visceral rete from four PBT specimens of different sizes. FL and visceral rete cross-sectional area are indicated above each micrograph.

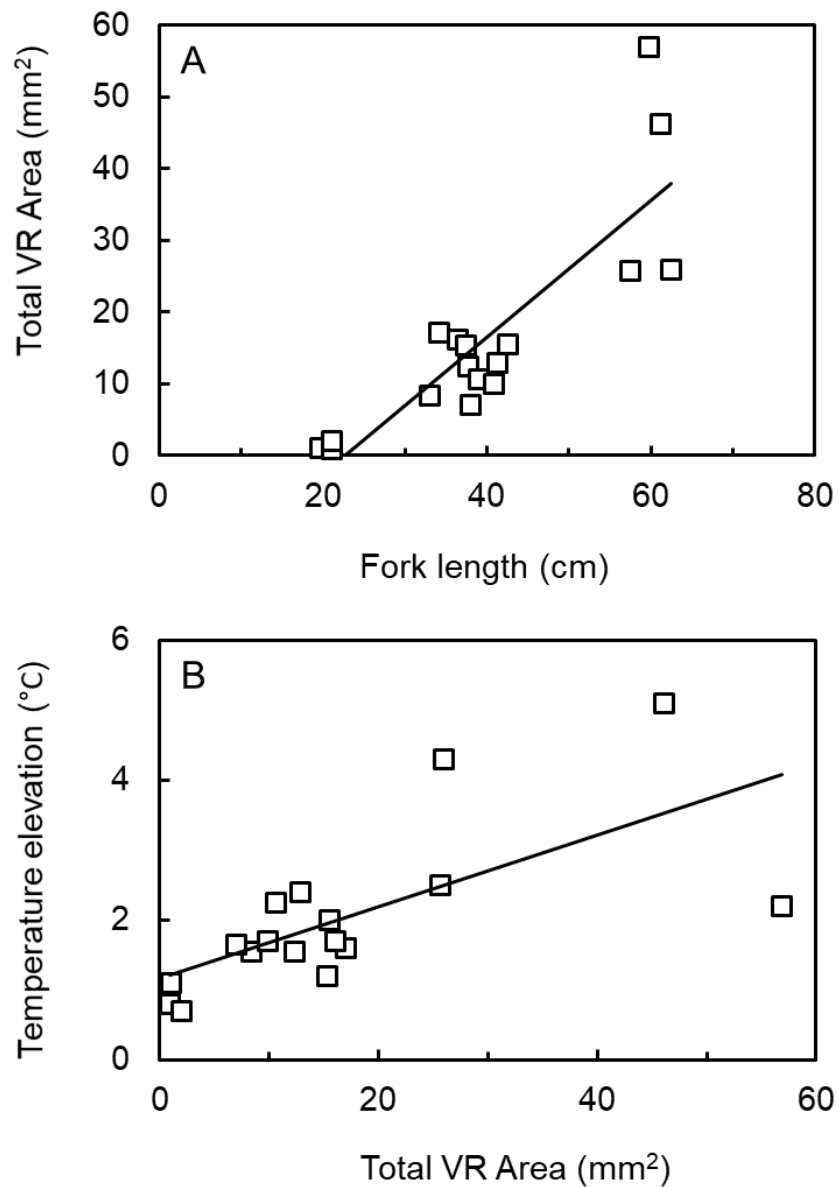


Fig. 2.11. Panel A shows the effect of increasing body size (measured as FL) on the total visceral rete (VR) cross-sectional area in young PBT specimens of different sizes. The equation that describes the relationship is $VR\ area = 0.95FL - 21.54$ ($R^2 = 0.72$, $n = 17$). Panel B shows the relationship between total VR cross-sectional area and visceral temperature elevation in young juvenile PBT specimens of different sizes. The equation that describes the relationship is $temperature\ elevation = 0.05VR\ area + 1.16$ ($R^2 = 0.46$, $n = 17$).

2.4. Discussion

2.4.1. PBT can significantly elevate their red muscle temperature above the ambient water temperature at a minimum body size of ~29 cm FL

In the literature, there is a dearth of studies investigating the ontogeny of endothermy in tunas (Dickson, 1994, Dickson et al., 2000, Kubo et al., 2008). Thus, it is largely unknown when they make the transition from ectothermy to regional endothermy. Dickson (1994) showed that black skipjack tuna (*Euthynnus lineatus*) could significantly elevate their T_{RM} above T_a at a minimum body size of ~21 cm FL and Kubo et al. (2008) showed that PBT could achieve this feat at a minimum body size of ~55 cm FL. Based on comparisons with various ectotherms, Dickson (1994) proposed a minimum thermal excess ($T_{RM} - T_a$) of 3°C as evidence of red muscle endothermy. By substituting this value into the equation that describes the relationship between red muscle thermal excess and fish FL in the fish we studied (Fig. 2.6B), we determined a minimum body size for significant red muscle temperature elevation of 29 cm FL in our young PBT specimens. This is much smaller than the size estimated for this species by Kubo et al. (2008). There could be several reasons for this. Firstly, the dataset of Kubo et al. (2008) was incomplete in that the three specimens that showed evidence of red muscle temperature elevation were the largest that they had available. Thus, there were no larger fish to confirm the trend. Additionally, there was a considerable size gap between the largest fish and the next largest (~55 cm compared with ~34 cm FL) in the study of Kubo et al. (2008). Thus, their dataset lacked continuity. In addition, Kubo et al. (2008) used temperature sensors that had been implanted into the body of the fish (in the red muscle, the white muscle and the peritoneal cavity, which is equivalent to the visceral cavity). Thus, their sensors may not have been positioned in the warmest part of the respective tissues. Any or all of these differences may be important but the most important is most likely the different ambient water temperatures (T_a) in our study compared with the study of Kubo et al. (2008). In our study, the largest fish (57.5 to 62.5 cm FL), with T_{RM} elevations of 7.8 to 14.2°C, were caught at T_a values of only 15.8°C. In contrast, in the study of Kubo et al. (2008), fish of a similar size (54.5 to 55.5 cm FL), with red muscle temperature elevations of

only 2.6 to 4.4°C, had been maintained at T_a values of 22.8°C, i.e., a considerably higher ambient water temperature than in our study. Thus, there was less scope for significant red muscle temperature elevation above T_a in the study of Kubo et al. (2008) because of the higher T_a in that study.

It is interesting to compare the red muscle temperature elevations we observed in our small/young tuna specimens with those observed in larger/older tuna specimens. In the largest of our small tuna specimens (~60 cm FL and ~5 kg BM), the red muscle temperature elevations we observed ranged from 7.8°C to 14.2°C, above an average T_a of 15.8°C. In their pioneering work done in the late 1960s, Carey and Teal (1969) measured maximum red muscle temperatures in a total of 121 large (68 – 362 kg) specimens of Atlantic bluefin tuna (ABT), caught at various locations to obtain a wide range of ambient water temperatures. Using their data, they derived the following equation: red muscle temperature = $[0.25 \times T_a (\text{°C})] + 24.94(\text{°C})$. Using this equation, the red muscle temperature elevation in one of these large ABT specimens at an ambient water temperature of 15.8°C would have been 13.1°C. This is very similar to the value we observed for our largest PBT specimens. This suggests that our largest PBT specimens (~60 cm FL and ~5 kg BM) had already developed their full capacity for red muscle endothermy. To confirm this, measurements will need to be made on larger PBT specimens.

2.4.2. PBT can significantly elevate their red muscle temperature above the ambient water temperature at a minimum age of approximately 5.5 months.

In the wild, PBT spawn mainly in the waters surrounding the Ryukyu Archipelago in the months of April to June each year (Kitagawa et al., 2006a, Kitagawa et al., 2010, Fujioka et al., 2018a, Fujioka et al., 2018b) (Fig. 2.1). Subsequently, their larvae disperse, with the aid of the Kuroshio Current and the Tsushima Warm Current, to the feeding grounds for age-0 PBT juveniles in the East China Sea off the north-west coast of Kyushu Island and in the western North Pacific Ocean off the south coast of Shikoku Island. PBT juveniles caught off the south coast of Shikoku Island in the months of July to August have been estimated, using otolith analysis, to be 2 to 3 months of age and their sizes have been shown to range from 16.7 to 30.0 cm FL (Tanaka et

al., 2006). In our study, the youngest fish were caught in this same location and at this same time of year and their sizes were within the same range. Thus, our youngest fish were most likely 2 to 3 months of age. Based on our temperature measurements, these fish were unable to elevate their body temperature above the ambient water temperature. Thus, PBT juveniles of this size (~20 cm FL and ~2-3 months of age) are functioning as ectotherms. This is consistent with their geographical restriction to the warm waters of the Kuroshio Current

The Group two fish were obtained in late November, in the same year that they hatched. Thus, they were most likely 6 to 8 months of age. The Group three fish had hatched in 2015 and we sampled them in late March 2017. Thus, the members of this group were most likely 22 to 24 months of age. Wild-caught PBT at 22 to 24 months of age, have body sizes ranging from 55.4 to 68.1 cm FL (Itoh, 2001). This compares well with the body size range (57.5 to 62.5 cm FL) we observed for our Group three fish.

To check the age estimates made using our knowledge of the life history of these fish and to obtain the minimum age at which PBT can significantly elevate their red muscle temperature above the ambient water temperature, we used the von Bertalanffy growth function, with constants for PBT obtained from Shimose et al. (2009). Using this equation, we estimated the ages of our three groups of fish to be 2 to 3 months for the Group one fish, 6 to 10 months for the Group two fish and 15 to 16 months for the Group three fish (Fig. 2.11). The ages for the Groups one and two fish were similar to the ages predicted using the life history method but the calculated age for the Group three fish was substantially younger than predicted using the life history method. Thus, we conclude that for these oldest fish, the natural history based estimate of their age is more accurate than the estimate based on the von Bertalanffy growth function. In summary, we estimate the age of the Group one fish to be 2 to 3 months of age, the Group two fish to be 6 to 8 months of age and the Group three fish to be 22 to 24 months of age. Thus, PBT undergoes the transition from ectothermy to regional endothermy between the ages of approximately 2 months and 2 years.

As already mentioned, the proposed minimum temperature elevation for evidence of red muscle endothermy in tunas is 3°C (Dickson, 1994). Thus, we used this value together with the von Bertalanffy growth function, to estimate the minimum age for significant red muscle temperature elevation in our PBT specimens. Using this approach, we found an age of 5.5 months. Thus, 5.5 months is the minimum age for evidence of red muscle endothermy in PBT.

Our estimate of 5.5 months for the onset of red muscle endothermy in PBT makes sense in terms of the geographical distribution of this species in relation to the ambient water temperature. For example, in the waters to the south and east of the Japanese main islands of Shikoku and Honshu, the median T_a experienced by free-ranging age-0 (i.e. <12 months of age) PBT juveniles, as determined using archival tags implanted in their peritoneal cavity, was found to be 27.6°C in July (mid-summer) compared with 17.0°C in May (late spring/early winter) (Fujioka et al., 2018a). Based on previous estimates (Tanaka et al., 2006), the fish implanted with the tags would have been 2 to 3 months of age when they were first caught and released in July/August and those of them that were recaptured in May of the following year would have been 12 months of age. Thus, if the transition from ectothermy to regional endothermy in PBT occurs at approximately 5.5 months of age, as we have estimated, this would correspond to the months of October to November. If this is correct, then the transition from ectothermy to regional endothermy, at least in the red muscle, occurs during the period just before T_a declines relatively sharply from a median of 23°C in November to a median of 18°C in January of the following year. This suggests that declining T_a may be the signal that triggers the onset of the development of regional endothermy. Alternatively, an endogenous signal, generated independently of any external environmental influences, may be the trigger. Future research is warranted to address this question.

The relatively warm water temperatures experienced by age-0 PBT juveniles along the southern coasts of Shikoku and Honshu Islands are due to the influence of the Kuroshio Current and seasonal variations in the path of this current strongly influence the geographic distribution of these fish (Fujioka et al., 2018a). The Kuroshio Current is a warm, low nutrient current that flows

north-eastwards along the southern coasts of Shikoku and Honshu Islands (Mizuno and White, 1983, Kawai, 1998) (Fig. 2.1). Age-0 PBT juveniles are found predominantly on the inshore side of this current, and/or along the current front, but their distance from the shore varies with seasonal variations in the current's offshore displacement (Fujioka et al., 2018a). In summer and autumn, when the Kuroshio Current is close to the coast, age-0 PBT juveniles inhabit predominantly near-coastal waters. In contrast, in winter, when the Kuroshio Current moves eastwards, away from the coast, these fish are found more widely distributed, both inshore and further offshore. The distribution of age-0 PBT juveniles in relation to the path of the Kuroshio Current has been linked to various oceanographic factors, including the current's speed (Fujioka et al., 2018a). Very young (~2 months of age and 21.0 to 24.5 cm FL) PBT have been found to swim at a speed of 0.6 – 0.7 m/s (Noda et al., 2016). This is substantially slower than the speed (1.0 – 1.5 m/s) of the Kuroshio Current, as it flows along the southern coasts of Shikoku and Honshu Islands (Nitani, 1975). Thus, the observation that age-0 PBT juveniles caught and released to the south of Shikoku and Honshu Islands are restricted to the coastal waters inshore from the Kuroshio Current, is presumably because of the high energetic costs that would be incurred by swimming directly within the current (Fujioka et al., 2018a). This suggests that increasing swimming prowess, associated with increasingly more frequent and powerful contractions of the skeletal muscles may be the signal that initiates the transition from ectothermy to regional endothermy. This warrants further investigation.

Another interesting finding of the tagging study mentioned above, is that age-0 PBT juveniles tracked to the south of Shikoku and Honshu Islands, substantially increased their daily travel distance as they made the transition from summer to winter (Fujioka et al., 2018a). There was also a dietary shift to more active prey and from smaller prey items, such as zooplankton and squid, to larger prey items, such as small fishes, when the PBT juveniles reached approximately 25 cm FL (Shimose et al., 2013, Kitagawa and Fujioka, 2017). This suggests that perhaps a dietary shift may be the signal that initiates the transition from ectothermy to regional endothermy. Again, this warrants further investigation.

2.4.3. Scaling of body mass with fork length

The BM of our PBT specimens increased exponentially with increasing FL with a scaling coefficient of 3.38 ± 0.04 . Similarly, the BM of PBT specimens caught off the coast of California and reared at the Monterey Bay Aquarium (Monterey, California), for periods varying from one to nine years, increased with increasing FL with a scaling coefficient of 3.32 (Estess et al., 2014). In contrast, for PBT specimens caught from the wild off the coasts of Japan and Taiwan and analysed immediately after capture and without further rearing, BM increased with increasing FL with a scaling coefficient of 2.89 (Shimose et al., 2009). The larger scaling coefficients for our fish and the aquarium fish, compared with the wild-caught fish, could be due to more frequent feeding or reduced physical activity because of the confinement to a sea cage or an aquarium tank. Alternatively, they could be related to different body size ranges in the different studies. The fish in our study ranged in size from 18.5 to 62.5 cm FL whereas those in the aquarium study ranged in size from 65 to 209 cm FL and those that were caught from the wild and analysed without further rearing ranged in size from 47 to 260 cm FL. Thus, many of the 'wild' fish were in a somewhat larger size bracket than either our fish or the fish raised in the Monterey Bay Aquarium and perhaps larger fish have slower growth rates; this would explain the smaller scaling coefficient for the 'wild' fish compared with our fish and the fish reared in the aquarium.

2.4.4. Anatomy of the red muscle

Ectothermic fishes have their red muscle located in shallow lateral wedges just beneath the skin whereas tunas have a more medial (i.e. internal, closer to the vertebral column) location for their red muscle. Because of this, the red muscle of tunas is insulated by the overlying tissues and conductive heat loss, across the body surface, is reduced (Dickson et al., 2000, Graham and Dickson, 2000, Bernal et al., 2001b, Carey and Teal, 1969, Carey and Teal, 1966, Shadwick, 2005, Kishinouye, 1923, Dickson and Graham, 2004). In our study we observed, that regardless of the size of the fish, the red muscle had the characteristic medial location that is typical of tunas. Thus, an ontogenetic shift from shallow lateral wedges to internal cones buried deep within the body

does not explain the increasing red muscle temperature elevation we observed in our young PBT specimens.

In addition to its more medial location, tuna red muscle also has a more anterior (i.e. closer to the snout) location when compared with what is found in other teleosts (Dickson et al., 2000, Graham and Dickson, 2000, Dickson and Graham, 2004). In our study we observed that the maximum amount of red muscle was found at approximately 50% of FL from the snout of the fish and this did not differ between the smallest, intermediate sized and largest fish we studied. This compares well with previously reported values for other tuna species. For example, in frigate tuna (*Auxis thazard*), black skipjack tuna (*Euthynnus lineatus*), skipjack tuna (*Katsuwonus pelamis*), yellowfin tuna (*Thunnus albacares*) and albacore tuna (*Thunnus alalunga*), the maximum amount of red muscle was located at 41-58% of FL from the snout (Dickson et al., 2000, Graham et al., 1983, Graham and Dickson, 2000). In contrast, in close ectothermic relatives of the tunas, including Pacific mackerel (*Scomber japonicus*), Pacific bonito (*Sarda chiliensis*) and Pacific sierra (*Scomberomorus sierra*), the maximum amount of red muscle was located at 74-78% of FL from the snout. The more anterior-medial location of the red muscle in tunas is proposed to facilitate their thunniform mode of swimming (Donley et al., 2004). Unlike other modes of swimming, such as the carangiform swimming mode displayed by the bonitos and mackerels, the thunniform mode results in locomotion powered primarily by the lateral motion of the hydrofoil-like tail rather than full-body undulations (Sfakiotakis et al., 1999, Shadwick and Syme, 2008, Dowis et al., 2003).

Total red muscle mass as a percentage of total BM has been reported to be ~5%, ~12%, ~11%, ~7%, ~7% and ~4% in slender tuna (*Allothunnus fallai*), frigate tuna, black skipjack tuna, skipjack tuna, yellowfin tuna and albacore tuna (Graham et al., 1983, Graham and Dickson, 2000). Thus, total red muscle mass as a percentage of total BM varies greatly between tunas from different genera (*Thunnus*, *Auxis* and *Euthynnus*), but is relatively similar between different members of the genus *Thunnus*. In our study we found that the total red muscle mass, as a percentage of the total BM, was $5.8 \pm 1.5\%$, when we took all of the data for all of our young PBT specimens together. Thus, the

value we found for PBT was very similar to the previously reported values for yellowfin tuna and albacore tuna, both of which belong to the same genus (i.e. *Thunnus*) as PBT. Thus, our results are within the range observed for species within this genus. In contrast, in ectothermic fishes in the family Scombridae (mackerels and bonitos), the total red muscle mass as a percentage of the total BM has been reported to be ~2%, ~4%, ~6% and ~5% in dogtooth tuna (*Gymnosarda unicolor*), striped bonito (*Sarda orientalis*), Pacific mackerel and Pacific bonito (Graham et al., 1983, Graham and Dickson, 2000). These values are generally smaller than the values for the tunas. This indicates that the total red muscle mass as a percentage of the total BM is generally lower in the other fishes in the family Scombridae (mackerels and bonitos) than what is observed for most tuna species. This indicates that PBT, like other tunas may be better adapted to sustained swimming at high speeds than their closest ectothermic relatives.

Red muscle mass has been shown to increase with increasing BM with scaling coefficients of 0.82 ± 0.35 , 0.93 ± 0.09 , 0.66 ± 0.23 , 0.92 ± 0.12 and 0.96 ± 0.05 in frigate tuna (*Auxis thazard*), black skipjack tuna (*Euthynnus lineatus*), skipjack tuna (*Katsuwonus pelamis*), yellowfin tuna (*Thunnus albacares*) and albacore tuna (*Thunnus alalunga*), respectively (Graham et al., 1983). Thus, in all of these tuna species, except for skipjack tuna, the scaling of red muscle mass with increasing BM was slightly less than isometric. In our study, we found that red muscle mass increased with increasing BM with a scaling coefficient of 0.90 ± 0.24 in PBT. Thus, we also observed slightly less than isometric scaling of red muscle mass with increasing BM. This is the first time that scaling of red muscle mass with BM has been studied in young tuna specimens still in the process of transitioning from ectothermy to regional endothermy. Thus, our results provide the most convincing evidence yet that increasing red muscle mass as a proportion of total BM is not the explanation for the increasing red muscle temperature elevation observed as tunas grow larger.

In contrast to the above, red muscle mass has been shown to increase with increasing BM with scaling coefficients of 1.23 ± 0.17 and 1.72 ± 0.35 , respectively, in the close ectothermic relatives of the tunas, the Pacific

mackerel and the Pacific bonito (Graham et al., 1983). These values are greater than those observed for the tunas and they indicate greater than isometric scaling with increasing BM. It has been hypothesised that a greater than proportional increase in red muscle mass with increasing BM may be an adaptation to increase power output during swimming to overcome the increased drag associated with increasing body size (Graham et al., 1983). Thus, this may explain the greater than isometric scaling of red muscle mass with increasing BM in the ectothermic relatives of the tunas. In contrast, in tunas, it has also been hypothesised that the less than isometric scaling of red muscle mass with increasing BM may be a result of the elevated red muscle temperature enhancing the contraction efficiency and therefore power output of the red muscle as the fish grow larger (Graham et al., 1983). Thus, an increase in contraction efficiency, due to the increasing thermal excess in the red muscle with increasing body size, could be the reason why we observed a decrease in the amount of red muscle mass with increasing body size in our juvenile PBT specimens. It has also been observed, that PBT glide without beating their tails as they swim and this is presumably to save energy (Okano et al., 2006, Takagi et al., 2013). Therefore, it might also be that the less than isometric scaling of red muscle mass could be a result of increased glide swimming efficiency in tunas with increasing body size.

2.4.5. Anatomy of the red muscle retia

We observed a strong positive relationship between the magnitude of the red muscle temperature elevation (above the ambient water temperature) and the extent of the proliferation of the red muscle *retia*, in our young PBT specimens. In particular, we found that our youngest PBT specimens, at ~20 cm FL, exhibited minimal, if any, development of their red muscle *retia* and the temperature elevation in this tissue was only 1.1°C. In contrast, in our intermediate-sized and largest specimens there was increasing proliferation of the red muscle *retia* that was clearly associated with increasing red muscle temperature elevation. This is strong evidence that the development of the red muscle *retia* in our PBT specimens is essential for increasing red muscle temperature elevation with increasing body size.

There is a dearth of studies investigating the ontogenetic development of the heat exchanging blood vessels that support the development of regional endothermy in tunas, especially in individuals that are young enough to still be in the process of transitioning from ectothermy to endothermy. In fact, we know of only one study besides our own. In that study, Dickson et al. (2000) investigated the ontogenetic development of the red muscle *retia* in black skipjack tuna and found, like us, that there was a strong positive relationship between the magnitude of the red muscle temperature elevation and the extent of the proliferation of the red muscle *retia*. Specifically, Dickson et al. (2000) found that in juvenile black skipjack tuna, the proliferation of the red muscle *retia* and the red muscle temperature elevation increased linearly with increasing fish FL. This was the same as we observed in PBT.

2.4.6. Anatomy of the visceral *retia*

We observed that the cross-sectional area of the visceral rete was only approximately 0.9-2.0 mm² in our smallest PBT specimens but increased to an impressive 27-57 mm² in our largest specimens. As a result of this, the numbers of heat exchanging blood vessels in the rete also increased greatly. Thus, there would have been a greater surface area for heat exchange to occur and therefore a greater potential for heat retention. Despite this, we saw only a small elevation of the visceral temperature above the ambient water temperature. This can presumably be explained by the fact that temperature elevation requires heat production as well as heat retention. The main heat source in the viscera is specific dynamic action (SDA) (Fitzgibbon et al., 2007). Therefore, the small temperature elevations recorded in our PBT specimens were likely to be a result of the heat generated by SDA from our fish being fed to satiation once or twice a day.

In a previous study, Blank et al. (2008) measured visceral temperatures in small PBT juveniles swimming in a respirometer at water temperatures ranging from 8 to 25°C and when they did this they found visceral temperature elevations of only 1.1 to 1.8°C above the ambient water temperature. This was surprising because the fish in the study of Blank et al. were larger (70 to 84 cm FL) than the largest fish in our study (~60 cm FL) and yet we saw substantially larger visceral temperature elevations, i.e., 2.2 to 5.1°C, in our study. The

likely explanation for the discrepancy is that Blank et al. used archival tags implanted into the peritoneal cavity (i.e. the visceral cavity) that would have measured the average temperature of the viscera whereas we used a probe inserted into the warmest part of the visceral cavity. Another explanation could be that Blank et al. (2008) fasted their fish for 45–72 h prior to the commencement of the temperature measurements, whereas our fish had not been fasted and might recently have fed. Thus, there might still have been substantial heat generation in the viscera of our fish as a result of SDA.

In the same study, Blank et al. (2008) also measured visceral temperatures in free-ranging PBT. Once again they used tags implanted into the peritoneal cavity of ten PBT specimens that were a similar size to the specimens used in their swim tunnel experiments, but in this case, the mean visceral temperature was $22.9 \pm 0.9^{\circ}\text{C}$ at a mean ambient water temperature of $18.4 \pm 1.2^{\circ}\text{C}$ giving an average visceral temperature elevation of 4°C above the ambient water temperature. This was greater than the thermal excess seen in their swim tunnel experiments but similar to that seen in the largest fish in our own study. This suggests that the free-ranging fish may have just recently eaten and were still generating substantial visceral heat due to SDA.

In another study with young free-ranging PBT from the same geographical region as the fish in our study, juvenile PBT were implanted with archival tags in their peritoneal cavity and an average visceral temperature elevation of 1°C was observed in the months of August to November, corresponding to the Japanese autumn compared with nearly 3°C in December corresponding to the Japanese winter (Furukawa et al., 2017). This was consistent with our own observations.

Recently, the results of a decade (1995 – 2015) of archival tagging studies designed to clarify the migration patterns of young PBT juveniles (< 2 years of age) tagged in their two main nursery areas, the East China Sea and the coastal waters to the south of Shikoku and Honshu Islands, were compiled and published (Fujioka et al., 2018b). The tags had been inserted in the peritoneal cavity of these fish and therefore measured the average temperature of this cavity. Fish that migrated across the Pacific Ocean encountered an average T_a of $14.7 \pm 2.0^{\circ}\text{C}$ and had a substantial peritoneal cavity thermal excess value

of 6.9°C (Fujioka et al., 2018b). This was higher than we observed in our study, presumably because the fish were larger/older and the T_a was cooler.

In another example, with a different but closely related species, large (~100 cm FL) free-ranging southern bluefin tuna (SBT, *Thunnus maccoyii*) were tracked with archival tags implanted into their peritoneal cavity to record their temperature (Bestley et al., 2008). The authors identified the start of a feeding event by a sharp decrease in peritoneal cavity temperature (associated with the ingestion of cold food and/or water) followed by a steep steady increase above the initial temperature, or by a steep steady increase without the preceding decrease. For one individual, a steep steady increase from ~20°C lasted for several hours before peaking at a maximum temperature of ~25°C at an ambient water temperature of ~15°C. This was indicative that the fish had just recently fed. Thus, in SBT, and possibly other tuna species such as PBT, the maximum thermal excess value in the peritoneal cavity is observed several hours after feeding. Our PBT specimens were fed to satiation once or twice a day. This further indicates that in our intermediate-sized and largest PBT specimens it is possible that we were recording the thermal excess resulting from SDA after feeding. It is possible that the thermal excess values were lower in our fish because they only ranged from ~20 to 60 cm FL compared to the ~100 cm FL SBT in the previous study. This indicated that the visceral rete was less developed in our young PBT juveniles than in the larger SBT specimens.

Continuous monitoring of the stomach temperatures of large (~350 to ~450 kg) Atlantic bluefin tuna (ABT) specimens revealed thermal excess values for the stomach 10 to 15°C at ambient water temperatures of 12 to 17°C, 12 to 20 hours after feeding (Carey et al., 1984). In this study, the temperature measurements were made using acoustic transmitters that were fed to the fish and recorded the temperature in their stomachs. These temperature elevations were much higher than those we observed for our own specimens. It is highly likely that this is due to a difference in methods between the studies. For example, our temperature measurements were for the warmest location in the visceral cavity of the fish, whereas in the study with ABT, the temperature of the stomachs was recorded. The temperatures within the stomachs of the ABT

were likely higher because the stomach is the site of digestion, which contributes to SDA.

2.4.7. Cranial temperature elevation

We observed that the thermal excess for the cranium increased with increasing fish size and decreasing water temperature in our young PBT specimens but the increase was modest compared with what we had observed for the red muscle and the viscera. The cranial thermal excess we observed increased from 0.5°C for the ~20 cm FL fish to 1.3°C for the ~40 cm FL fish to 2.0°C for the ~60 cm FL fish. This contrasts with several previous studies, with other tuna species, in which greater cranial thermal excess values were observed. For example, a study with skipjack tuna (*Katsuwonus pelamis*) juveniles, with an average size of 44.5 cm FL, found a cranial thermal excess of 4.5°C above an ambient water temperature of 25.6°C (Stevens and Fry, 1971). These fish were approximately the same size as our intermediate-sized fish in which we saw a temperature elevation of only 1.3°C. Based on a previous study, the size of the 44.5 cm FL skipjack tuna corresponds to an age of approximately one year for this species (Tanabe et al., 2003). Thus, skipjack tuna individuals at one year of age can elevate their cranial temperature considerably above the ambient water temperature whereas PBT individuals of the same size cannot. This suggests that skipjack tuna may have a greater capacity for cranial heat generation and/or a greater capacity for cranial heat retention than PBT.

In another example, a cranial temperature elevation of ~7°C at an ambient water temperature of ~20°C was observed in large ABT individuals ranging in size from 180 to 410 kg (Linthicum and Carey, 1972). This compared with a cranial temperature elevation of ~6°C at a water temperature of ~21°C in smaller ABT individuals ranging in size from 7 to 11 kg (Linthicum and Carey, 1972). Thus, the large and small ABT specimens had similar cranial temperature elevations to one another suggesting that the capacity for cranial endothermy was already fully developed in the 7 to 11 kg fish. Both the large and the small ABT specimens in the previous study were all larger than the PBT specimens in our study suggesting that our fish had not yet fully developed the capacity for cranial endothermy. Alternatively, the differences between the different studies could be due to differences in the methods used.

For example, in our study, the temperature probe was inserted into the ocular cavity behind the eye where the ocular muscles and the optic nerve are located and while the fish were still alive. In contrast, in the previous study, the fish were euthanised with a shot to the head with a 12-gauge shotgun and their brain temperatures were taken immediately afterwards by inserting a temperature probe through the pineal window and into the brain. Therefore, it is possible that we were measuring the temperatures of different parts of the cranium in the two different studies.

2.4.8. Conclusions

In this study, we have shown that the transition from ectothermy to endothermy in the red muscle of PBT occurs at a body size of approximately 29 cm FL corresponding to an age of approximately 5.5 months. We observed a steep linear increase in red muscle thermal excess with increasing body size in our intermediate and large sized specimens, with a maximum temperature elevation of 14.2°C observed in a 61.2 cm FL individual. We have shown that red muscle mass scales slightly less than isometrically with increasing BM indicating that increasing red muscle mass as a proportion of total BM is not the explanation for the increasing red muscle thermal excess with increasing body size that we have observed. Instead, our data indicate that the increasing red muscle thermal excess is due to the corresponding increase in the proliferation of the red muscle *retia* with increasing body size. We also observed a modest increase in visceral thermal excess with increasing body size. This corresponded with major proliferation of the visceral rete resulting in increasing surface area for heat exchange to occur. In the future, it will be important to identify the endogenous and/or environmental signals that trigger the onset of the ontogenetic development of red muscle endothermy in tunas. This will be important because it could lead to a better understanding of how these species will tolerate alterations in the flow of warm ocean currents occurring and predicted as a result of climate change.

CHAPTER 3 - Regulation of the ontogenetic transition from ectothermy to regional endothermy in pacific bluefin tuna (*Thunnus orientalis*):
Biochemistry and molecular biology

Abbreviations

Pacific bluefin tuna, PBT; Fork length, FL; Body mass, BM; Citrate synthase, CS; Cytochrome c oxidase, COX; Pyruvate kinase, PK

Abstract

Early in their post-larval development, tunas undergo an ontogenetic transition from ectothermy to regional endothermy but it is unknown how this is regulated. In the bluefin tunas, it is the red ('slow-twitch, aerobic) skeletal muscle, the eye/brain and the viscera that are endothermic but the white ('fast-twitch', glycolytic) skeletal muscle and the heart are ectothermic. In Pacific bluefin tuna (PBT, *Thunnus orientalis*), young juveniles ranging in size from 20 to 60 cm fork length (FL) and in age from ~2 months to ~2 years, displayed increasing elevation of their maximum red skeletal muscle temperature (T_{RM}) above the ambient water temperature (T_a) as they grew larger (Chapter 2). Thus, we hypothesized that they would display increasing enzyme activity and gene expression for enzymes involved in aerobic metabolism in this tissue. To test this we measured enzyme activity and transcript abundance for the mitochondrial marker enzymes citrate synthase (CS) and cytochrome c oxidase (COX) as well as for the glycolytic marker enzyme pyruvate kinase (PK) in red and white muscle of these same PBT specimens. CS enzyme activity (per g tissue) was on average 7.1-fold higher in the red muscle compared with the white muscle of these fish but CS transcript abundance (expressed as copies per g tissue) was not significantly different between the two tissues. In contrast, COX enzyme activity (per g tissue) was on average 12.4-fold higher, COXI transcript abundance was on average 2.4-fold higher and COXIV transcript abundance was on average 2.6-fold higher in the red muscle compared with the white muscle. For PK, enzyme activity (per g tissue) was on average 4.3-fold higher in the white muscle compared with the red muscle and PK transcript abundance (expressed as copies per g tissue) was on average 9-fold higher in the white muscle compared with the red muscle. CS enzyme activity decreased with increasing body size in both the red muscle and the white muscle whereas CS transcript abundance remained constant with increasing body size. In contrast, COX enzyme activity remained constant with increasing body size in both muscle types but COXI transcript abundance and COXIV transcript abundance both decreased. For PK, enzyme activity (per g tissue) increased with increasing body size in the white muscle but not in the red muscle and transcript abundance (copies per g tissue) decreased with increasing body size in both muscle types. The results are discussed in

terms of the different functions of the different muscle types and in terms of the changes in aerobic and glycolytic metabolic capacity as the fish grew larger.

3.1. Introduction

3.1.1. Regional endothermy in tunas

Tunas are unique amongst regionally endothermic fishes in that they have a relatively long period of their early lives in which they function as ectotherms and it is only later during their development that they become regional endotherms (Dickson, 1994, Kubo et al., 2008). For most tuna species, it is unknown when the ontogenetic transition from ectothermy to regional endothermy occurs. Recently, we undertook a study of the anatomical and physiological changes associated with the transition from ectothermy to regional endothermy in Pacific bluefin tuna (PBT, *Thunnus orientalis*) (Chapter 2). In this study we observed significant red ('slow-twitch', aerobic) skeletal muscle temperature (T_{RM}) elevation above the ambient water temperature (T_a) at a minimum body size of 29 cm FL corresponding to a minimum age of 5.5 months. Thus, it is around about this size/age that this particular species makes the transition from ectothermy to regional endothermy.

3.1.2. The effects of muscle type on mitochondrial abundance and aerobic metabolic capacity in fishes

Fish skeletal muscle consists of clearly distinct bundles of red and white muscle fibres (Johnston et al., 2011). The red muscle fibres are used for sustained, cruise-type swimming and their metabolism is predominantly oxidative whereas the white muscle fibres are used for short, burst-type activities, such as the pursuit of prey, and their metabolism is predominantly glycolytic. Consistent with these different roles, the red muscle fibres have large numbers of mitochondria and prominent lipid droplets which they use as fuels whereas the white muscle fibres have fewer mitochondria and fewer lipid droplets. Mitochondrial abundance and a tissue's aerobic metabolic capacity can be assessed using mitochondrial marker enzymes such as citrate synthase (CS, the first enzyme in the tricarboxylic acid (TCA) cycle) and cytochrome *c* oxidase (COX, the last enzyme in the mitochondrial electron transfer chain (mETC)) (Guderley, 1990, LeMoine et al., 2008). Both enzymes can be used as indicators of mitochondrial abundance and therefore aerobic metabolic capacity but in addition, COX can also be used as an indicator of

the extent of folding of the inner mitochondrial membrane and hence the capacity of the mETC.

In bigeye tuna (*Thunnus obesus*), yellowfin tuna (*Thunnus albacares*) and skipjack tuna (*Katsuwonus pelamis*), CS enzyme activity, expressed per g tissue, has been shown to be approximately 5- to 6-fold higher in the red muscle compared with the white muscle and COX enzyme activity, expressed in the same way, has been shown to be 6- to 10-fold higher (Dalziel et al., 2005, Moyes et al., 1992). These data are indicative of the red muscle having a greater number of mitochondria and aerobic metabolic capacity than the white muscle.

3.1.3. The effects of muscle type on glycolytic capacity in fishes

In mammals, white muscle fibres are characterised by a high glycolytic capacity compared to the red muscle (Schiaffino and Reggiani, 2011). Similarly, the white muscle in fishes has a greater glycolytic capacity than red muscle (Childress and Somero, 1990). In studies with both mammals and with fishes, pyruvate kinase (PK) the last enzyme in glycolysis, has been used as an indicator of a tissue's glycolytic capacity (McClelland et al., 2006, Cordiner and Egginton, 1997, Kyprianou et al., 2010, Childress and Somero, 1990, Emmett and Hochachka, 1981). Consistent with the white muscle being more glycolytic than the red muscle, it has been shown that PK enzyme activity is approximately 7-fold greater in the white muscle than in the red muscle in skipjack tuna (Guppy and Hochachka, 1979). These data are indicative of the white muscle having a greater glycolytic capacity than the red muscle in tunas.

3.1.4. The effects of body size on mitochondrial abundance and aerobic metabolic capacity in fish skeletal muscle

In terrestrial mammals, there is a decrease in resting aerobic metabolic activity with increasing body size (Kleiber, 1947, Riek and Geiser, 2013). It is hypothesised that this decrease is a means of preventing overheating due to the decrease in the surface area-to-volume ratio with increasing body size. This hypothesis was developed for terrestrial mammals but the same appears to be true in fishes. For example, CS enzyme activity has been shown to

decrease with increasing body size in the white muscle of the ectothermic fish species including deep-sea rattail (*Coryphaenoides armatus*), largemouth bass (*Micropterus salmoides*), smallmouth bass (*Micropterus dolomieu*), pumpkinseed sunfish (*Lepomis gibbosus*) and bluegill sunfish (*Lepomis macrochirus*) (Somero and Childress, 1985, Davies and Moyes, 2007). This suggests that mitochondrial abundance and aerobic metabolic capacity of the white muscle decreases with increasing body size in these fishes.

3.1.5. The effects of body size on the glycolytic capacity of skeletal muscle fibres of fishes

Previous studies have shown that the PK enzyme activity increases with increasing body size in the white muscle of zebrafish, deep-sea rattail, kelp bass (*Paralabrax clathratus*), rainbow trout, black bass, smallmouth bass, pumpkinseed sunfish and bluegill sunfish (Goolish, 1989, Davies and Moyes, 2007, McClelland et al., 2006, Childress and Somero, 1990). The same analysis was not performed on the red muscle of these fishes. The increase in PK enzyme activity indicates that the glycolytic capacity of the white muscle increases with increasing body size in these fishes but it is unknown how body size effects the glycolytic capacity of the red muscle. In fishes, during burst swimming, anaerobic metabolism is dominant. Therefore, it has been proposed that positive scaling of glycolytic capacity with increasing body size provides increasing power for the muscles of fishes with a greater body mass to reach the same burst swimming velocities as smaller-bodied fishes (Somero and Childress, 1985).

3.1.6. The effects of decreasing water temperature on mitochondrial abundance and aerobic metabolic capacity in fish skeletal muscle

Ectothermic fishes compensate for the negative thermodynamic effects of cooler water temperatures by increasing the concentrations of metabolic enzymes, especially those involved in aerobic metabolic activity in the mitochondria of the skeletal muscle (Battersby and Moyes, 1998, McClelland et al., 2006, LeMoine et al., 2008, Cordiner and Egginton, 1997, Kyprianou et al., 2010, Orczewska et al., 2010, O'Brien, 2011). For example, rainbow trout caught at 4°C, compared with 18°C, had 4-fold higher CS enzyme activities

per g tissue in their red muscle and 2.8-fold higher CS enzyme activities per g tissue in their white muscle (Cordiner and Egginton, 1997). Similarly, rainbow trout held at 4°C, compared with 18°C, for two months, had 1.4-fold higher CS and COX enzyme activities per g tissue in their red muscle and 1.7-fold higher COX enzyme activity per g tissue in their white muscle (Battersby and Moyes, 1998). In another study, zebrafish held at 18°C, compared with 28°C, for 21 days, had 1.5-fold higher CS enzyme activity per g tissue and 1.2-fold higher COX enzyme activity per g tissue in their skeletal (presumably white) muscle (McClelland et al., 2006). In yet another study, threespine stickleback (*Gasterosteus aculeatus*) maintained at 8°C, compared with 20°C, for 9 weeks, had 1.7-fold higher CS enzyme activity per g tissue and 1.9-fold COX enzyme activity per g tissue in their oxidative pectoral adductor muscle (predominantly red muscle) (Orczewska et al., 2010). Collectively, these data indicate that the mitochondrial abundance within the red and white skeletal muscle fibres of fishes increases in response to cooler water temperatures. In contrast to the wealth of information available for ectothermic fishes on the effects of cooler water temperatures on metabolic enzyme activities in the red and white skeletal muscle, there is a lack of equivalent information for endothermic fishes.

3.1.7. The effects of decreasing water temperature on glycolytic capacity in fish muscle

Suboptimal ambient water temperature has been reported to result in both increases and decreases in glycolytic capacity in the skeletal muscle of fishes (Cordiner and Egginton, 1997, McClelland et al., 2006, Kyprianou et al., 2010). For example, zebrafish held at a suboptimal water temperature of 18°C over a period of 21 days, compared with 28°C, had ~60% higher PK enzyme activity per g tissue in their skeletal muscle (McClelland et al., 2006). The muscle fibre type was not reported in this study but due to the fact that the bulk of the muscle mass in fishes is white, it is likely it was white skeletal muscle. In contrast, Cordiner and Egginton (1997) reported that rainbow trout caught at different water temperatures at different times of the year had PK enzyme activities per g tissue in their red muscle that were not statistically significantly different between fish caught at 11°C compared to 28°C but were 82% lower in rainbow

trout caught at 4°C compared to 28°C. In contrast, in the same study, PK enzyme activity in the white muscle was ~70% greater in fish caught at 11°C compared to 28°C and 47% lower in fish caught at 4°C compared to 28°C. In another study, in which gilt-head sea bream were held at 10°C for ten days, PK activity per g tissue increased by approximately ~20% in the red muscle, compared to the control fish held at 18°C, after 5 days before decreasing back to control levels after 10 days and the same was observed in the white muscle (Kyprianou et al., 2010). Collectively, these data show that the effects of cold water temperature on the glycolytic capacity of the red and white skeletal muscle of fishes is much more variable than what is observed for aerobic metabolic capacity.

3.1.8. Aims

The aim of the present study was to investigate the effects of muscle type, body size and water temperature on CS and COX enzyme activity as indicators of aerobic capacity and PK enzyme activity as an indicator of glycolytic metabolic capacity in red and white muscle of young PBT juveniles undergoing the ontogenetic transition from ectothermy to regional endothermy. We hypothesised that the number of mitochondria, and/or their aerobic metabolic capacity, would increase with increasing body size in the red muscle. We also hypothesised that the glycolytic capacity would increase in the white muscle with increasing body size in juvenile PBT.

3.2. Materials and Methods

3.2.1. Fish specimens

Young Pacific bluefin tuna (PBT, *Thunnus orientalis*) juveniles, ranging in size from 18.5 to 62.5 cm fork length (FL) and 71 to 5,350 g body mass (BM), were used in this study. They were caught in Japanese waters on three separate occasions. For details refer to Chapter 2. The Group one fish [18.5 – 21.2 cm fork length (FL), 71 – 142 g body mass (BM), n = 21] were caught by fishermen operating offshore from the port of Kaminokae (Kochi Prefecture, Shikoku Island) on the 2nd of August 2016 (late summer) (Fig. 1). The Group two fish [33.3 – 42.6 cm FL, 750 – 1,700 g BM, n = 10] and the Group three fish [57.5 – 62.5 cm FL, 4,050 – 5,350 g BM, n = 4] were caught from a sea cage farm located approximately 1 km offshore from the town of Imazato (Nagasaki Prefecture, Tsushima Island) on the 28th of November 2016 (late autumn) and the 27th of March 2017 (early spring), respectively. The fish were subjected to the tissue temperature measurements described in Chapter 2 and following this, samples were taken for the enzyme activity and gene expression analyses described here. The samples were taken from the left side of the fish at ~40-50% of FL from the snout. For the enzyme activity analyses, two samples (~1 cm³) were taken from the red muscle and two from the white muscle whereas for the gene expression analyses, four samples (~0.5 cm³) were taken from each muscle type. The samples for the enzyme activity analyses were initially snap frozen in dry ice and then later transferred to liquid nitrogen in an Arctic Express™ Cryogenic dry shipper (Thermo Fisher Scientific). For the gene expression analyses, the samples were immersed in RNA^{later}® (Ambion®), initially on ice and then later at -20°C for longer term storage.

3.2.2. Citrate synthase enzyme activity analysis

Citrate synthase (CS) enzyme activity analysis was essentially as previously described (Gibb and Dickson, 2002). In brief, the procedure was as follows. Approximately 50 mg of frozen tissue was homogenised for 45 s at 4,000 rpm in nine volumes of ice-cold extraction buffer [50 mM imidazole (pH 6.6), 2 mM ethylenediaminetetraacetic (EDTA)] using a TOMY micro Smash™ MS-100

tissue homogeniser. The resulting homogenate was clarified by centrifugation at 12,000 g for 10 min at 4°C and then the supernatant was desalted using a Bio-Spin® P-30 Gel column (Bio-Rad), equilibrated with the extraction buffer. The desalted extract was used for the enzyme assays. To ensure that the initial rate of the reaction could be reliably measured, the red muscle extract was diluted 1:20 and the white muscle extract was diluted 1:2 before the assay. The enzyme activity was assayed using a Corona SH-9000 microplate reader (Corona Electric Co. Ltd.) in a room maintained at a constant temperature of 25°C. The reactions were performed in flat-bottomed 96-well plates and each reaction (160 µL total volume) contained 80 mM Tris buffer (pH 8.0), 2 mM MgCl₂, 0.1 mM 5,5'-dithio-bis(2-nitrobenzoic acid) (DTNB), 0.1 mM acetyl CoA, 0.5 mM oxaloacetate and 10 µL of the appropriate dilution of the tissue extract. The reactions were initiated with the addition of the oxaloacetate and the change in absorbance, due to the reduction of DTNB, was monitored at a wavelength of 412 nm. Preliminary experiments had been carried out to ensure that doubling or halving the volume of the diluted tissue extract added to the assay resulted in proportional changes in the reaction rate.

3.2.3. Cytochrome c oxidase enzyme activity analysis

Cytochrome c oxidase (COX) enzyme activity analysis was essentially as previously described (Bremer and Moyes, 2011). In brief the procedure was as follows. Approximately 25 mg of frozen tissue was homogenised for 4 min in 20 volumes of ice-cold extraction buffer [25 mM potassium phosphate buffer (pH 7.4), 1 mM EDTA, 0.6 mM n-dodecyl β-D-maltoside] using a Retsch MM40 bead mill set at a frequency of 30 Hz. The resulting homogenate was used directly for the enzyme assays. To ensure that the initial rate of the reaction could be reliably measured, the red muscle homogenate was diluted 1:50 and the white muscle homogenate was diluted 1:5. The enzyme activity was assayed using a FLUOstar Omega microplate reader (BMG LABTECH) set at 25°C. The reactions were performed in flat-bottomed 96-well plates and each reaction (200 µL total volume) contained 25 mM potassium phosphate buffer (pH 7.4), 0.6 mM n-dodecyl β-D-maltoside, 0.15 mM reduced cytochrome c and 10 µL of the appropriate dilution of the tissue homogenate. The reactions were initiated with the addition of the reduced cytochrome c and the change in

absorbance due its oxidation was monitored at a wavelength of 550 nm. The reduced cytochrome *c* had been prepared by adding an excess of sodium ascorbate to a 1 mM stock solution of cytochrome *c* dissolved in 25 mM potassium phosphate buffer (pH 7.4) and then removing the ascorbate using a PD-10 desalting column (GE Healthcare), pre-equilibrated with the same phosphate buffer. Reduction of the cytochrome *c* was confirmed by performing a wavelength scan between 350 and 700 nm to identify the characteristic absorption maximum for the reduced form of cytochrome *c* at 550 nm. Preliminary experiments had been carried out to ensure that doubling or halving the volume of the diluted tissue homogenate added to the assay resulted in proportional changes in the reaction rate.

3.2.4. Pyruvate kinase enzyme activity analysis

Pyruvate kinase (PK) enzyme activity analysis was essentially as previously described (Davies and Moyes, 2007). In brief the procedure was as follows. Approximately 25 mg of frozen tissue was homogenised for 4 min in 20 volumes of ice-cold extraction buffer [20 mM HEPES (pH 7.2), 1 mM EDTA, 0.1% (v/v) Triton X-100] using a Retsch MM40 bead mill set at a frequency of 30 Hz. The resulting homogenate was used directly for the enzyme assays. To ensure that the initial rate of the reaction could be reliably measured, the red muscle homogenate was diluted 1:20 and the white muscle homogenate was diluted 1:100. The enzyme activity was assayed using a FLUOstar Omega microplate reader (BMG LABTECH) set at 25°C. The reactions were performed in flat-bottomed 96-well plates and each reaction (200 µL total volume) contained 50 mM HEPES (pH 7.4), 5 mM ADP, 100 mM KCl, 10 mM MgCl₂, 0.15 mM NADH, 5 mM phosphoenolpyruvate (PEP), 10 mM KCN, 10 units/mL lactate dehydrogenase (LDH) and 10 µL of the appropriate dilution of the tissue homogenate. The reactions were initiated with the addition of the ADP and the change in absorbance due the oxidation of NADH was monitored at a wavelength of 340 nm. Preliminary experiments had been carried out to ensure that doubling or halving the volume of the diluted tissue homogenate added to the assay resulted in proportional changes in the reaction rate.

3.2.5. Primer design for polymerase chain reaction

At the time of this research, there were no annotated sequences for any of the genes of interest available for PBT. There was, however, an unannotated whole genome shotgun contigs database for this species (accession number BADN00000000 available at <http://www.ncbi.nlm.nih.gov/>). Therefore, the primers for polymerase chain reaction (PCR) were designed using BLAST searches of this database. First of all, cDNA sequences for CS from yellowfin tuna (*Thunnus albacares*, AY461848.1), COXI and COXIV-1 from bigeye tuna (*Thunnus obesus*, HM071005.1 and AF204870.1) and PK from Atlantic salmon (*Salmo salar*, PKM paralog, NM_001141703.1) were downloaded from the GenBank database (available at <http://www.ncbi.nlm.nih.gov/>). Then each of the downloaded sequences was used one by one to query the PBT whole genome shotgun contigs database. Several contigs were retrieved for each gene and each contig was aligned individually with the query sequence using ClustalX 2.1 (Larkin et al., 2007). Subsequently, regions of sequence conservation were chosen for primer design. The primers were designed using Primer3 (version 0.4.0) (Untergasser et al., 2012). Primer3 was set to choose a primer with a length of 20 base pairs (bp), a melting temperature of approximately 60°C and a GC content between 40 and 60%. Following this, the potential primers chosen using Primer3, were tested for their suitability using Oligo Analyzer Version 3.1 (<http://sg.idtdna.com/analyzer/Applications/OligoAnalyzer/>). Oligo Analyzer was used to check for primer-dimer formation and for the formation of secondary structures within the primer sequence which if present could reduce the amplification efficiency of the PCR reactions. Finally, the selected primers were ordered from GeneWorks Pty. Ltd. (Australia) or Integrated DNA Technologies™ (Singapore).

3.2.6. RNA extraction and cDNA synthesis

RNA was extracted from the various red and white muscle samples (see section 3.2.1) using the RNeasy® Fibrous Tissue Mini kit (QIAGEN), essentially as described by the manufacturer. In the first step, the tissue samples were removed from the RNA/later® (Ambion®) storage solution and blotted dry. Then approximately 60 mg of tissue was homogenised for 45 s at 4,000 rpm in 300 µL of RLT buffer (supplied with the kit), with 40 mM DTT added, using a TOMY

micro Smash™ MS-100 tissue homogeniser. The homogenate was applied to one of the columns supplied with the kit and whilst it was on the column, it was subjected to an on-column RNase-free DNase I digestion to remove any genomic DNA that might have been present. Following this, the RNA was eluted from the column and the concentration was determined using a NanoDrop™ 1000 spectrophotometer (Thermo Scientific). First strand cDNA was synthesized from one µg of the extracted RNA using a SuperScript® IV Reverse Transcriptase kit (Invitrogen™) as described by the manufacturer and the synthesized cDNA was stored at -20°C until it was required.

3.2.7. Conventional polymerase chain reaction

Conventional PCR was performed to amplify fragments of the genes of interest and the normalisation gene β -actin to be used as standards for gene expression analysis using quantitative real-time PCR (qRT-PCR). Each 50 µL conventional PCR reaction contained 5 µL of a 1:5 dilution of PBT red muscle cDNA, 0.2 µM of each of the relevant forward and reverse PCR primers (Table 3.1), 200 µM dNTPs (Promega), 2.5 units of *Taq* DNA Polymerase (New England Biolabs) and 5 µL of 10x ThermoPol® Buffer (New England Biolabs). The PCR cycling conditions consisted of an initial denaturation step at 95°C for 30 s followed by 30 cycles of denaturation at 95°C for 30 s, annealing at 60°C for 30 s and extension at 68°C for 1 min, followed by a final extension at 68°C for 5 min. The cycling was done in a Hybaid PX2 thermal cycler (Thermo Scientific). At the end of the cycling, the PCR reaction mixture was subjected to electrophoresis on a 1.5% (w/v) agarose gel to confirm that the PCR products were of the expected sizes. Subsequently, the products were purified from the remaining PCR reaction mixture using the Wizard® SV Gel and PCR Clean-Up System (Promega), following the manufacturer's instructions. The products were subsequently cloned in *Escherichia coli* (see below).

Table 3.1. Nucleotide sequences of the primers used for polymerase chain reaction in this study

Gene	Forward primer sequence (5' → 3')	Reverse primer sequence (5' → 3')
CS	CTGGACTGGTCCCACAACCTT	GGACAGGTAGGGGTCAGACA
COXI	GGAGCTGTATTCGCCATTGT	AGGAAGTGCTGTGGGAAGAA
COXIV	GCCCACTGGGACTATGAAAA	CCAAAATGCACAGACTGAGG
PK	CTGGGATGAACATTGCAAGA	TCCTGATTTCTGGTCCCTTG
β-actin ¹	ACCCACACAGTGCCCATCTA	TCACGCACGATTTCCCTCT

¹ Designed by Agawa et al. (2012)

All other primers were designed by the author of this thesis (refer to Section 3.2.5.)

3.2.8. Cloning of the PCR products in *E. coli*

The purified PCR products (Section 3.2.7) were cloned in *E. coli* to be used as standards for the subsequent gene expression analyses using qRT-PCR. To do this, the PCR products were first of all ligated into the pGEM[®]-T Easy vector (Promega) and then the resulting constructs were used to transform *E. coli* 5α competent cells (New England Biolabs). The transformed cells were plated onto Luria broth (LB) agar containing 100 µg/mL ampicillin and colonies that were resistant to the antibiotic were selected. The selected colonies were screened for the presence of the gene of interest using colony PCR. Colony PCR was performed using primers targeting the T7 (5'-TAATACGACTCACTATAGGG-3') and SP6 (5'-TATTTAGGTGACACTATAG-3') promoter regions of the vector, following the conventional PCR method outlined above (Section 3.2.7). Confirmed positive colonies were cultured overnight at 37°C in LB broth containing 100 µg/mL ampicillin. Following the overnight culture, plasmid DNA was extracted from the cells using the Wizard[®] Plus SV Minipreps DNA Purification System (Promega) and the inserts within the plasmids were sequenced using the Sanger sequencing method at the *Australian Genome Research Facility Ltd (AGRF)* using primers targeting the T7 and SP6 promoter regions of the vector. The resulting sequence data were used to perform BLAST searches of the GenBank database (available at <http://www.ncbi.nlm.nih.gov/>) to confirm the identity of the inserts. After the identity of the inserts had been confirmed, a 10-fold dilution series was produced using the remaining plasmid construct for each gene and these dilutions were used as standards for qRT-PCR. The standards were made into single use aliquots and stored at -20°C until required. To calculate the copy number for each plasmid construct, the DNA concentration was determined using a NanoDrop[™] 1000 spectrophotometer (Thermo Scientific) and the following equation was used to calculate the number of DNA copies per microliter of sample.

$$\begin{aligned} & \text{Copies per } \mu\text{l} \\ &= \frac{(\text{amount of plasmid DNA construct (ng)} \times 6.022 \times 10^{23})}{(\text{length of plasmid DNA construct (bp)} \times 1 \times 10^9 \times 650 \text{ Daltons})} \end{aligned}$$

This calculation is based on the assumption that the average molecular weight of a bp is 650 Daltons.

3.2.9. Gene expression analysis using qRT-PCR

RNA was extracted and first-strand cDNA was synthesised as described above (Section 3.2.6), using the various red and white muscle samples (Section 3.2.1) as the source of the RNA. Subsequently, the first-strand cDNAs or the standards (plasmid constructs) (Section 2.8) were used as templates for qRT-PCR. Various dilutions of the cDNAs from the various tissue samples were tested for each gene of interest to determine the optimal amount of cDNA to be added to each qRT-PCR reaction. The optimal amount of cDNA was the amount that produced fluorescence curves within the middle of the range of the fluorescence curves produced for the standards, i.e., the 10-fold dilutions of the plasmid constructs. Once the optimal cDNA concentration had been determined, qRT-PCR analyses were performed with the standards and the appropriately diluted cDNAs side by side in the same run. Each run included all of the cDNAs from the smallest (~20 cm FL), intermediate-sized (~40 cm FL) and largest fish (~60 cm FL) for one of the genes of interest from either the red muscle or the white muscle, a no template control and a no reverse-transcriptase control. For these analyses, each 20 μ L qRT-PCR reaction contained 5 μ L of the appropriately diluted first-strand cDNA or plasmid construct plus 10 μ L of the KAPA SYBR[®] FAST qPCR Master Mix (2X) Universal (KAPA Biosystems) and 0.4 μ L each of the relevant forward and reverse qRT-PCR primers (Table 3.1) to give a final primer concentration of 200 nM each. Thermal cycling was performed using a Rotor-Gene Q thermal cycler (QIAGEN) fitted with fluorescence detection. The thermal cycling conditions were an initial denaturation step at 95°C for 3 min followed by 40 cycles of denaturation at 95°C for 3 s, annealing at 60°C for 20 s and extension at 72°C for 20 s. At the end of each amplification run, melt curve analysis was performed to ensure that only one product was produced for each set of primers. This was done by raising the temperature from 60 to 95°C in 0.5°C increments and observing the change in fluorescence as the DNA strands separated. Amplification of only one product was confirmed by analysing the amplicons using agarose gel electrophoresis. For all primer pairs, the amplification efficiency was between 90 and 105% and each primer pair gave

only one product. Primer efficiency was calculated by plotting \log_{10} transcript copy number against C_t values for each standard and then determining the linear regression. By using the slope of the regression and the following equation the efficiency could be calculated: *Primer efficiency (%)* = $\left(10^{\left(\frac{-1}{\text{slope}}\right)} - 1\right) \times 100$. The transcript copy number for each gene of interest for each tissue sample was calculated by comparing the C_t values for the red muscle and white muscle cDNAs with the C_t values for the standards and multiplying the copy number per microgram of RNA by the total RNA extracted per mg tissue. All of the cDNA samples were analysed in duplicate (technical replication) and the average values for the duplicates were used to calculate the copy numbers. In addition to calculating the transcript abundance per g tissue, the relative transcript abundance for the genes of interest was calculated by dividing the transcript abundance for the gene of interest by the transcript abundance for the normalisation gene β -actin.

3.2.10. Statistical analyses

All statistical analyses were performed using the IBM® SPSS Statistics version 22.0 software package (IBM, New York, USA). Independent-samples t-tests were performed to test for significant differences in the enzyme activity or transcript abundance between the red and the white muscle. This comparison between tissues was made independently for the smallest, intermediate-sized and largest fish. Scaling coefficients were calculated through linear regression analysis of the \log_{10} of the variable of interest and the \log_{10} of BM. Pearson correlation analyses were used to determine whether the relationship between transcript abundance and enzyme activity was significant. For all of the statistical tests applied in this study, values were considered to be statistically significantly different when $P < 0.05$.

3.3 Results

3.3.1. *The effects of muscle type and body size on citrate synthase enzyme activity*

Citrate synthase (CS) enzyme activity is a marker for mitochondrial abundance and aerobic metabolic capacity. Fig. 3.1 shows the effects of muscle type and body size on CS enzyme activity in young PBT juveniles in the process of transitioning from ectothermy to regional endothermy. When expressed per g tissue, the mean \pm SE CS enzyme activities for the smallest (~20 cm FL), intermediate-sized (~40 cm FL) and largest (~60 cm FL) fish were 46.9 ± 3.1 , 43.0 ± 2.1 and 26.4 ± 2.2 U/g tissue, respectively, in the red muscle compared with 7.2 ± 0.7 , 5.9 ± 0.4 and 2.5 ± 0.5 U/g tissue, respectively, in the white muscle. This resulted in statistically significant differences ($P < 0.05$) between the two different muscle types of 7-, 10- and 10-fold, respectively. Similarly, when expressed per mg protein, the mean \pm SE CS enzyme activities for the smallest, intermediate-sized and largest fish were 2.46 ± 0.14 , 2.38 ± 0.07 and 1.27 ± 0.04 U/mg protein, respectively, in the red muscle compared with 0.26 ± 0.02 , 0.20 ± 0.01 and 0.10 ± 0.02 U/mg protein, respectively, in the white muscle. This resulted in statistically significant differences ($P < 0.05$) between the two different muscle types of 9-, 12- and 13-fold, respectively. Thus, the CS enzyme activity in the red muscle was approximately an order of magnitude greater than that in the white muscle and this was regardless of whether the activity was expressed per g tissue or per mg protein. This result indicates that mitochondrial abundance and aerobic metabolic capacity were also approximately an order of magnitude greater in the red muscle than they were in the white muscle.

CS enzyme activity decreased with increasing fish size in both muscle types. For the red muscle, the BM-dependent scaling coefficient was -0.12 ± 0.04 whereas for the white muscle it was -0.21 ± 0.06 . This was true regardless of whether the data were expressed per g tissue or per mg protein. Taken together, these data indicate that mitochondrial abundance and aerobic metabolic capacity were decreasing with increasing body size in both muscle types but the decrease was proportionally greater in the white muscle.

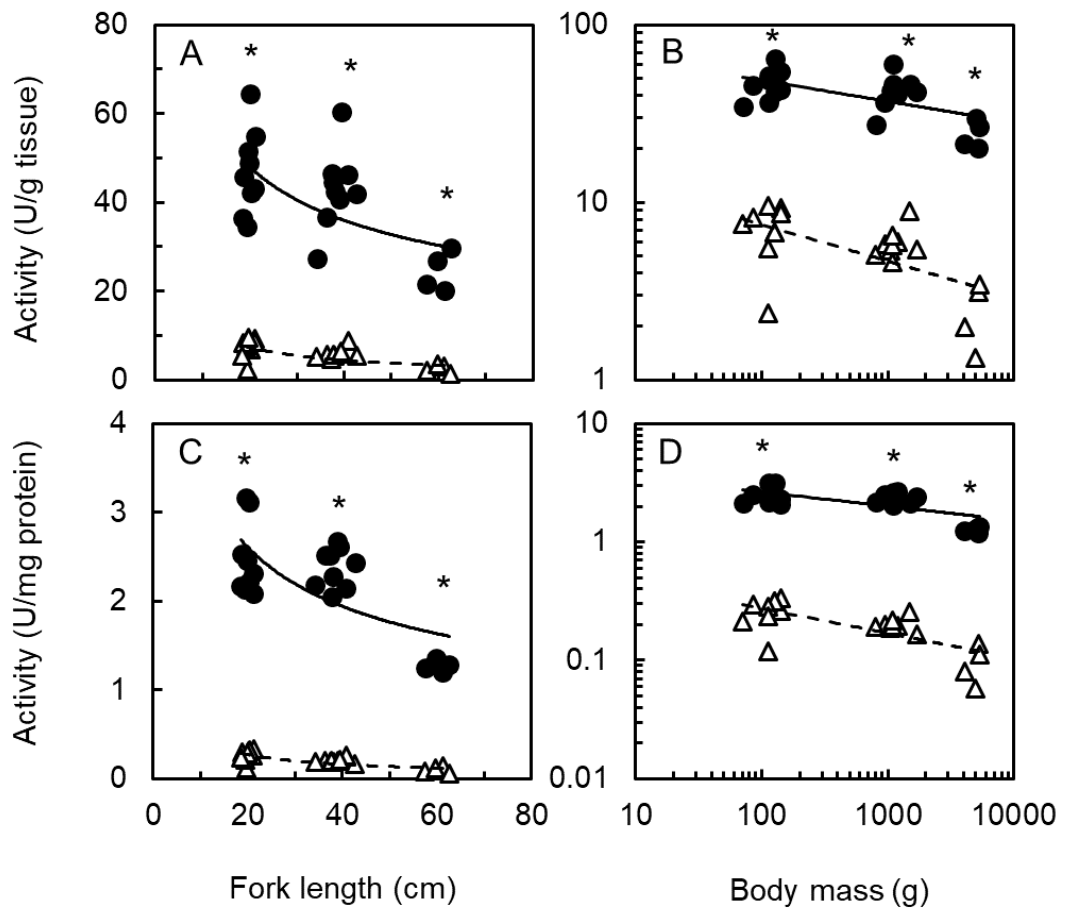


Fig. 3.1. The effects of increasing FL and BM on CS enzyme activity per g tissue and per mg protein in red and white muscle of young PBT juveniles of different sizes. The data for the red and white muscle are represented by ● with solid lines and Δ with dashed lines, respectively. The best-fitting power functions for the data in the various panels are as follows: (A) red muscle, $y = 168.61FL^{-0.42}$, $R^2 = 0.36$; white muscle, $y = 63.86FL^{-0.72}$, $R^2 = 0.37$; (B) red muscle, $y = 84.14BM^{-0.12}$, $R^2 = 0.34$; white muscle, $y = 19.45BM^{-0.21}$, $R^2 = 0.36$; (C) red muscle, $y = 9.34FL^{-0.43}$, $R^2 = 0.45$; white muscle, $y = 2.49FL^{-0.74}$, $R^2 = 0.52$; (D) red muscle, $y = 4.59BM^{-0.12}$, $R^2 = 0.43$; white muscle $y = 0.72BM^{-0.21}$, $R^2 = 0.49$ ($n = 22$). Significant differences in enzyme activity between the red and the white muscle for fish of a particular size (i.e. ~20 cm FL, ~40 cm FL or ~60 cm FL) are indicated by *.

3.3.2. The effects of muscle type and body size on cytochrome c oxidase enzyme activity

Cytochrome c oxidase (COX) enzyme activity, like CS enzyme activity, is a marker for mitochondrial abundance and aerobic metabolic capacity but it is also a marker for the extent of folding of the inner mitochondrial membrane and therefore the capacity of the mitochondrial electron transfer chain (mETC). Fig. 3.2 shows the effects of muscle type and body size on COX enzyme activity in young PBT juveniles in the process of transitioning from ectothermy to regional endothermy. When expressed per g tissue, the mean \pm SE COX enzyme activities for the smallest, intermediate-sized and largest fish we were 207 ± 14.9 , 205 ± 7.3 and 226 ± 11.2 U/g tissue, respectively, in the red muscle compared with 15.9 ± 2.2 , 17.9 ± 1.2 and 17.3 ± 2.5 U/g tissue, respectively, in the white muscle. This resulted in statistically significant differences ($P < 0.05$) between the two different muscle types of 13-, 11- and 13-fold, respectively. Similarly, when expressed per mg protein, the mean \pm SE COX enzyme activities for the smallest, intermediate-sized and largest fish were 0.94 ± 0.07 , 0.75 ± 0.04 and 0.63 ± 0.07 U/mg protein, respectively, in the red muscle compared with 0.07 ± 0.01 , 0.05 ± 0.01 and 0.04 ± 0.01 U/mg protein, respectively, in the white muscle. This resulted in statistically significant differences ($P < 0.05$) between the two different muscle types of 14-, 16- and 17-fold, respectively. Thus, the COX enzyme activity in the red muscle was more than an order of magnitude greater than that in the white muscle and this was regardless of whether the activity was expressed per g tissue or per mg protein. This confirms the results obtained with CS and it supports the conclusion that mitochondrial abundance and aerobic metabolic capacity were approximately an order of magnitude greater in the red muscle than they were in the white muscle.

In contrast to what was observed for CS, COX enzyme activity, expressed per g tissue, remained constant with increasing fish size in both the red and the white muscle. However, when expressed per mg protein, the COX enzyme activity decreased significantly ($P < 0.001$) in the red muscle but remained constant in the white muscle with increasing body size. For the red muscle, the BM-dependent scaling coefficient was -0.09 ± 0.03 (Fig. 3.2D). This was

slightly smaller than the equivalent scaling coefficient for CS which was -0.12 ± 0.04 . Thus, there was either no change or only a very small change in COX enzyme activity with increasing body size. The constant COX enzyme activity per g tissue paired with the decrease in CS enzyme activity, per g tissue, in response to increasing body size, suggests that increasing folding of the inner mitochondrial membrane could have been compensating for decreasing mitochondrial abundance (indicated by the decrease in CS enzyme activity) as the fish grew larger. If this were the case, then the aerobic metabolic capacity of the two different muscle types would have remained constant with increasing fish size.

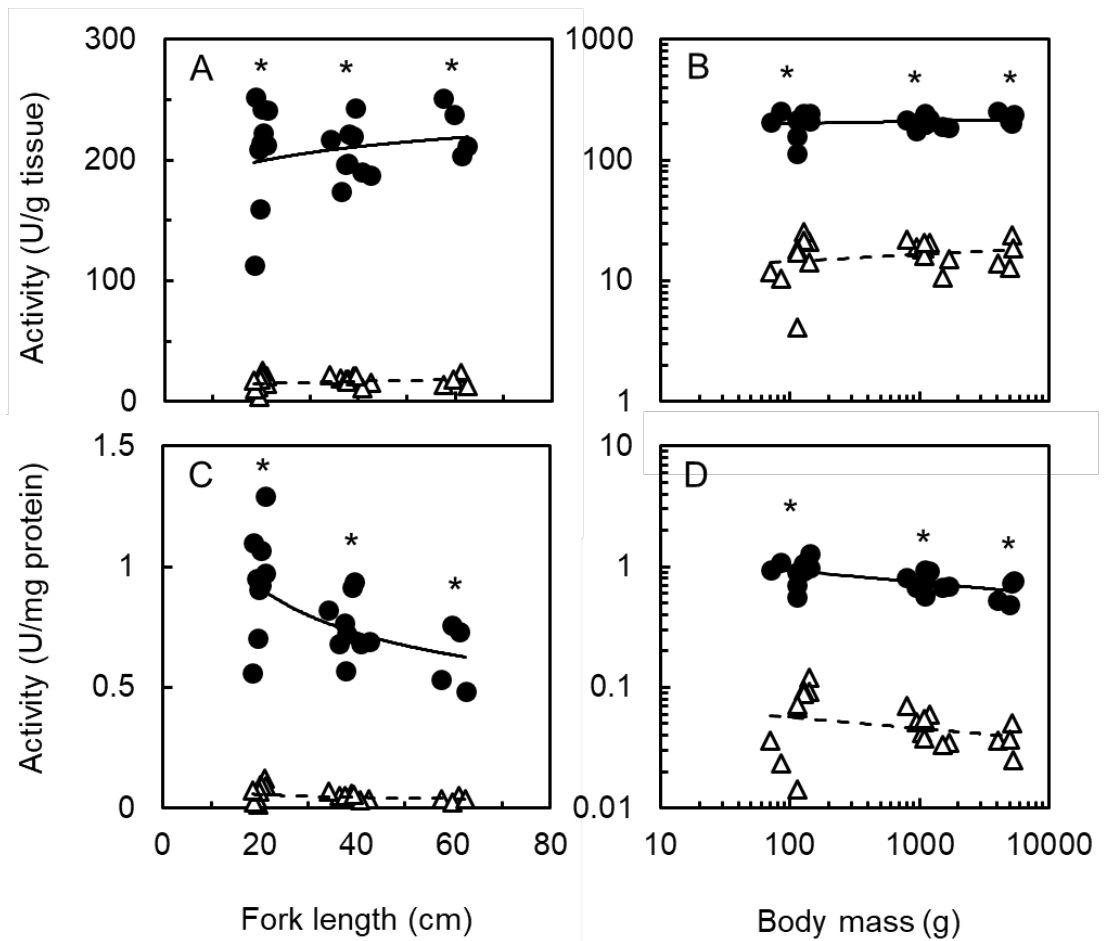


Fig. 3.2. The effects of increasing FL and BM on COX enzyme activity per g tissue and per mg protein in red muscle and white muscle of young PBT juveniles of different sizes. The data for the red muscle and white muscle are represented by ● with solid lines and Δ with dashed lines, respectively. The best-fitting power functions for the data in the various panels are as follows: (A) red muscle $y = 155.42FL^{0.08}$, $R^2 = 0.04$; white muscle $y = 8.35FL^{0.19}$, $R^2 = 0.04$; (B) red muscle $y = 209.75BM^{0.02}$, $R^2 = 0.04$; white muscle $y = 16.50BM^{0.06}$, $R^2 = 0.05$; (C) red muscle $y = 2.48FL^{-0.33}$, $R^2 = 0.33$; white muscle $y = 0.15FL^{-0.34}$, $R^2 = 0.08$ (D) red muscle $y = 1.43BM^{-0.09}$, $R^2 = 0.33$; white muscle $y = 0.09BM^{-0.09}$, $R^2 = 0.08$ ($n = 22$). Significant differences in enzyme activity between the red and the white muscle for fish of a particular size (i.e. ~20 cm FL, ~40 cm FL or ~60 cm FL) are indicated by *.

3.3.3. The effects of muscle type and body size on pyruvate kinase enzyme activity

PK enzyme activity is a marker for glycolytic metabolic capacity. In contrast to what was observed for CS and COX, PK enzyme activity was greater in the white muscle than it was in the red muscle (Fig. 3.3). This was regardless of whether the activity was expressed per g tissue or per mg protein, and also regardless of the fish size. When expressed per g tissue, the mean \pm SE PK enzyme activities for the smallest, intermediate-sized and largest fish were 219 ± 14.3 , 213 ± 20.3 and 287 ± 47.2 U/g tissue, respectively, in the red muscle compared with 857 ± 53.4 , 961 ± 37.1 and $1,267 \pm 98.1$ U/g tissue, respectively, in the white muscle. This resulted in statistically significant differences ($P < 0.05$) between the two tissues of 4-, 5- and 4-fold, respectively, with the white muscle activities being higher than the red. Similarly, when expressed per mg protein, the mean \pm SE PK enzyme activities for the smallest, intermediate-sized and largest fish were 0.9 ± 0.1 , 0.9 ± 0.1 and 0.9 ± 0.2 U/mg protein, respectively, in the red muscle compared with 3.1 ± 0.1 , 3.5 ± 0.2 and 3.5 ± 0.3 U/mg protein, respectively, in the white muscle. This resulted in statistically significant differences ($P < 0.05$) between the two tissues of 3-, 4- and 4-fold, respectively. Thus, overall PK enzyme activity was \sim 4-fold greater in the white muscle compared with the red muscle and this was regardless of the fish size (Fig. 3.3). The greater PK enzyme activity in the white muscle compared to the red muscle indicated that the glycolytic capacity of the white muscle was greater than that of the red muscle.

In the red muscle, PK enzyme activity remained constant with increasing body size regardless of how it was expressed. In the white muscle, on the other hand, it remained constant with increasing body size when it was expressed per mg protein, but it increased with increasing body size when it was expressed per g tissue ($P < 0.001$). The BM-dependent scaling coefficient for PK enzyme activity expressed per g tissue in the white muscle was 0.09 ± 0.02 . Overall there was no evidence for a change in PK enzyme activity, and therefore glycolytic capacity, in the red muscle but there was an increase in the white muscle with increasing body size in our young juvenile PBT.

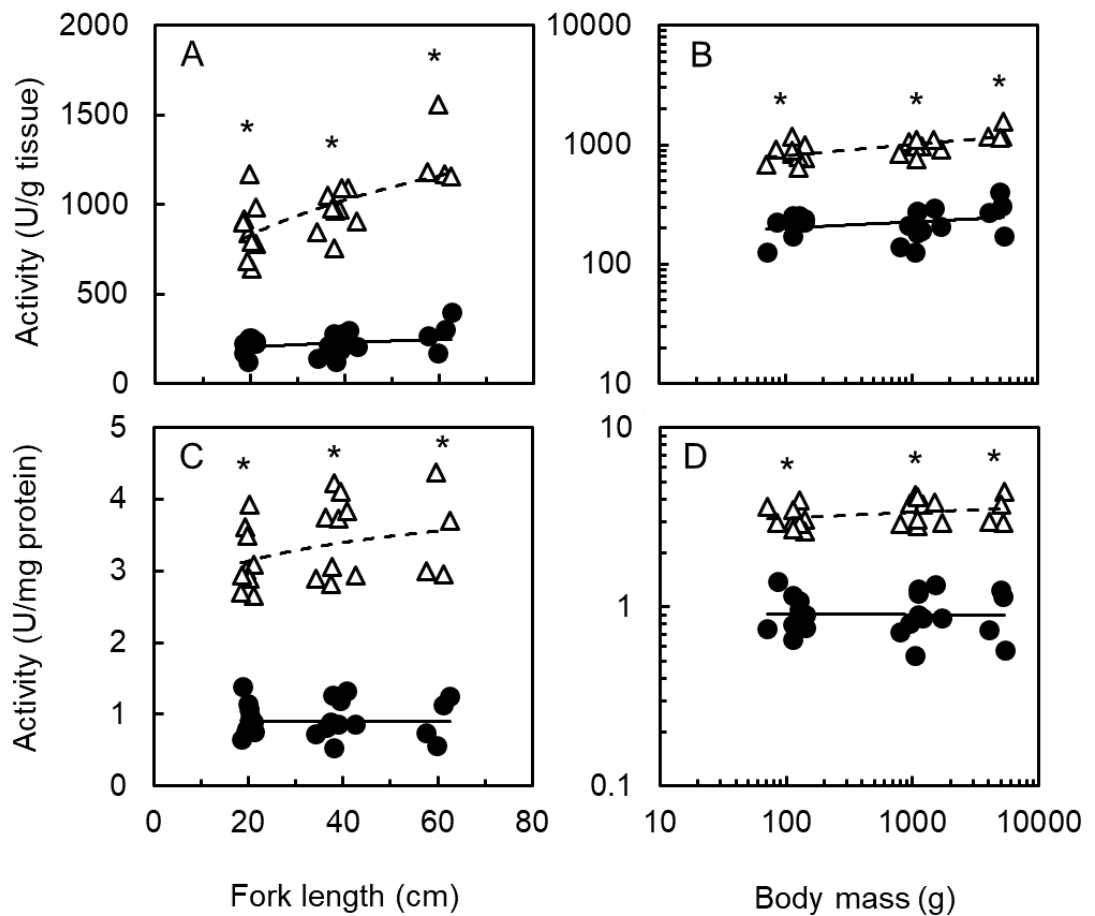


Fig. 3.3. The effects of increasing FL and BM on PK enzyme activity per g tissue and per mg protein in red muscle and white muscle of young PBT juveniles of different sizes. The data for the red and white muscle are represented by ● with solid lines and Δ with dashed lines, respectively. The best-fitting power functions for the data in the various panels are as follows: (A) red muscle $y = 119.61FL^{0.18}$, $R^2 = 0.07$; white muscle $y = 329.04FL^{0.31}$, $R^2 = 0.43$; (B) red muscle $y = 158.79BM^{0.05}$, $R^2 = 0.07$; white muscle $y = 543.77BM^{0.09}$, $R^2 = 0.43$; (C) red muscle $y = 0.93FL^{-0.01}$, $R^2 = 1.64 \times 10^{-4}$; white muscle $y = 2.23FL^{0.11}$, $R^2 = 0.10$; (D) red muscle $y = 0.91 \times BM^{-2.31 \times 10^{-3}}$, $R^2 = 1.67 \times 10^{-4}$; white muscle $y = 3.37 \times BM^{0.03}$, $R^2 = 0.09$ ($n = 22$). Significant differences in enzyme activity between the red and the white muscle for fish of a particular size (i.e. ~20 cm FL, ~40 cm FL or ~60 cm FL) are indicated by *.

3.3.4. The effects of muscle type and body size on the amount of protein extracted per g tissue

Differences in the enzyme activity results depending upon whether the data were expressed per g tissue or per mg protein, could be due to differences in the amount of protein extracted per g tissue for the different enzymes or for the different individual fish. Thus, we analysed the amount of protein extracted per g tissue for the various samples and Fig. 3.4 shows the results of this analysis. The overall mean \pm SE amount of protein extracted per g tissue for the CS enzyme assays was 18.8 ± 0.62 mg protein/g tissue for the red muscle whereas it was 27.9 ± 1.03 mg protein/g tissue for the white muscle and this did not vary with varying fish size (Figs. 3.4A and B). Thus, the overall mean amount of protein extracted per g tissue for the CS enzyme assays was 47% greater for the white muscle than it was for the red muscle ($P < 0.05$). This shows that the difference in CS enzyme activity between the two different muscle types and between the fish of different sizes cannot be explained by a difference in the amount of protein extracted.

For the COX enzyme assays, the amounts of protein extracted per g tissue \pm SE for the smallest, intermediate-sized and largest fish were 232 ± 9 , 276 ± 11 and 376 ± 41 mg/g tissue, respectively, in the red muscle compared with 281 ± 30 , 377 ± 21 and 485 ± 89 mg/g tissue, respectively, in the white muscle (Figs. 3.4C and D). Thus, the overall mean amount of protein extracted per g tissue for the COX assays was 29% greater for the white muscle than it was for the red muscle but this was not significant for the smallest and largest fish, it was only statistically significant for the intermediate-sized fish ($P < 0.05$). Overall the amount of protein extracted per g tissue for the COX enzyme assays increased with increasing FL and with increasing BM for both the red ($P < 0.005$) and the white muscle ($P < 0.005$). Therefore, it is possible that the decreasing COX enzyme activity per mg protein with increasing body size in the red muscle was due to the increasing amount of protein extracted per g tissue as the fish grew larger.

Comparing the CS and COX enzyme assay extracts, the amount of protein extracted for the COX assays was 15-fold greater for the red muscle and 13-fold greater for the white muscle compared with the amount extracted for the

CS assays. This can be explained by the different extraction methods. The extraction buffer for the COX assays contained the detergent n-dodecyl β -D-maltoside which would have dissolved membrane proteins. Thus, the total amount of protein in the COX assay extracts would have been greater because it would have included membrane proteins as well as water soluble cytosolic proteins. In addition, the COX assay extracts were not centrifuged. Thus, proteins that had not been solubilised by the detergent in the extraction buffer would have been detected in the protein assay which uses sodium hydroxide to solubilise proteins.

For the PK enzyme assays, the amounts of protein extracted per g tissue \pm SE for the smallest, intermediate-sized and largest fish were 238 ± 16 , 222 ± 8 and 314 ± 20 mg/g tissue, respectively, in the red muscle compared with 290 ± 20 , 282 ± 12 and 365 ± 20 mg/g tissue, respectively, in the white muscle. Thus, the overall mean amount of protein extracted per g tissue for the PK assays was 21% greater for the white muscle than it was for the red muscle, but this was only statistically significant for the intermediate-sized fish ($P < 0.05$). Overall the amount of protein extracted per g tissue for the PK enzyme assays increased with increasing FL and with increasing BM for both the red ($P < 0.05$) and the white muscle ($P < 0.05$). Therefore, the significant increase in PK enzyme activity per g tissue may have been due to the increasing amount of protein extracted per g tissue as the fish grew larger.

The amounts of protein extracted for the PK assays were similar to the amounts extracted for the COX assays but much greater than the amounts extracted for the CS assays. The explanation is similar to the one given above. In other words, the extraction buffer for the PK assays contained the detergent Triton X-100. Thus, membrane proteins as well as soluble cytosolic proteins would have been present in the extract. As with the extracts for the COX assays, the PK enzyme assay extracts were not centrifuged. Together, the presence of a detergent in the extraction buffer and the lack of centrifugation most likely explain why the amount of protein extracted for the PK assays was similar to the amount extracted for the COX assays but much greater than the amount extracted for the CS assays.

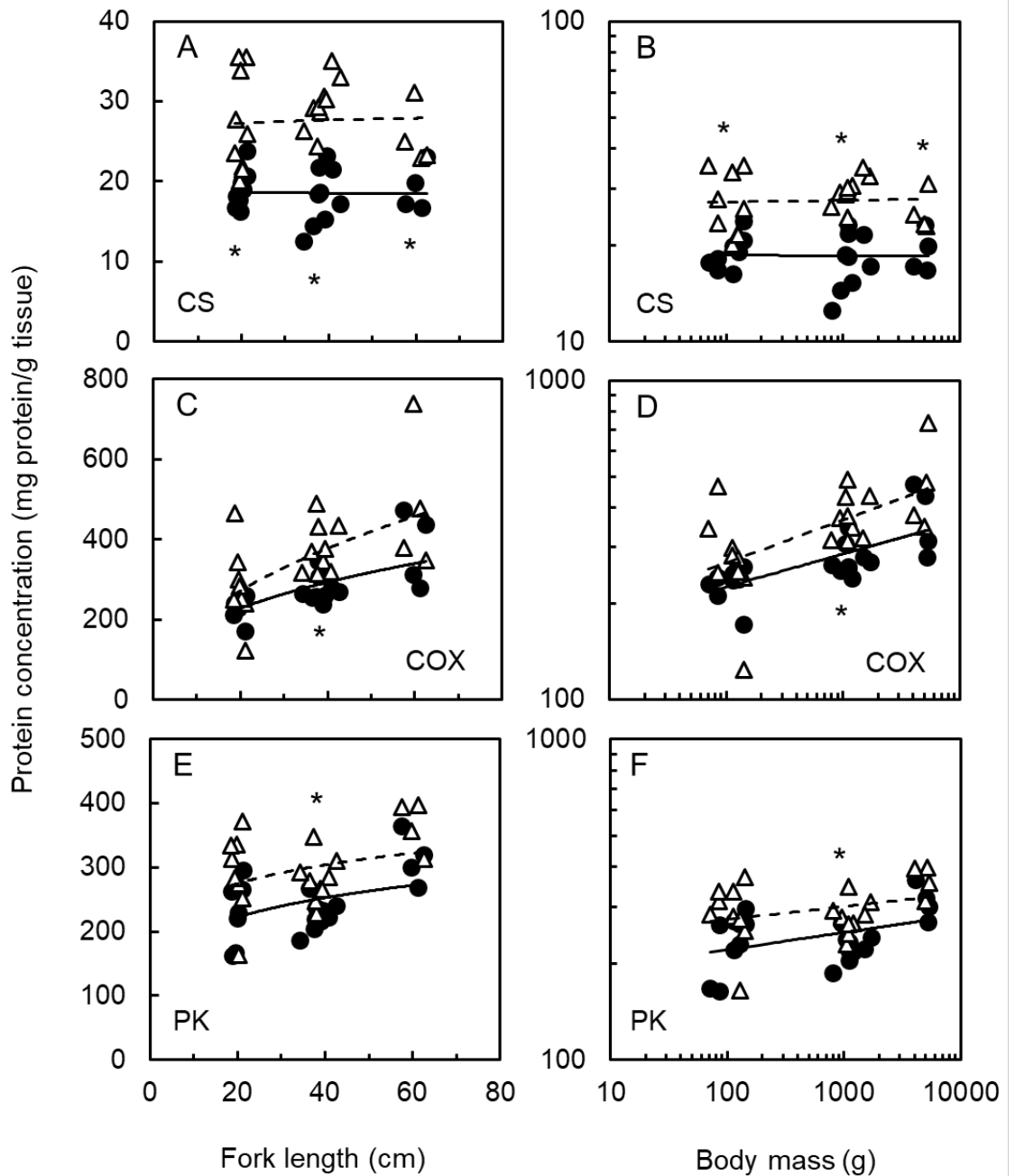


Fig. 3.4. The effects of increasing FL and BM on the amount of protein extracted per g tissue from the red muscle and white muscle of young PBT juveniles of different sizes. (AB, CS), (CD, COX), (EF, PK). The data for the red and white muscle are represented by ● with solid lines and Δ with dashed lines, respectively. The best-fitting power functions for the data in the various panels are as follows: (A) red muscle $y = 18.81FL^{-3.80 \times 10^{-3}}$, $R^2 = 1.06 \times 10^{-4}$; white muscle $y = 25.62FL^{0.02}$, $R^2 = 2.72 \times 10^{-3}$; (B) red muscle $y = 18.79BM^{-1.91 \times 10^{-3}}$, $R^2 = 3.23 \times 10^{-4}$; white muscle $y = 26.68BM^{-4.96 \times 10^{-3}}$, $R^2 = 1.87 \times 10^{-3}$; (C) red muscle $y = 76.49FL^{0.36}$, $R^2 = 0.52$; white muscle $y = 65.76FL^{0.47}$, $R^2 = 0.35$; (D) red muscle $y = 140.63BM^{0.10}$, $R^2 = 0.50$; white muscle $y = 144.21BM^{0.13}$, $R^2 = 0.35$; (E) red muscle $y = 128.66FL^{0.18}$, $R^2 = 0.16$; white muscle $y = 177.97FL^{0.15}$, $R^2 = 0.10$; (F) red muscle $y = 172.77BM^{0.05}$, $R^2 = 0.17$; white muscle $y = 227.93BM^{0.04}$, $R^2 = 0.09$ ($n = 22$). Significant differences in protein content between the red and the white muscle for fish of a particular size (i.e. ~20 cm FL, ~40 cm FL or ~60 cm FL) are indicated by *.

3.3.5. The effects of muscle type and body size on the citrate synthase transcript abundance, expressed as copies per g tissue

There was no significant difference in the number of CS transcripts, per g tissue, between the red and the white muscle (Figs. 3.5A and B). This was surprising because we had observed that the CS enzyme activity, per g tissue, was on average an order of magnitude higher in the red muscle compared with the white muscle (Fig. 3.1). Consistent with this discrepancy, there was no significant correlation between CS transcript abundance and CS enzyme activity (Fig. 3.6A). This indicates that the higher level of CS enzyme activity in the red muscle compared with the white muscle in these fish is not the result of a higher level of CS gene expression.

Transcript abundance (copies/g tissue)

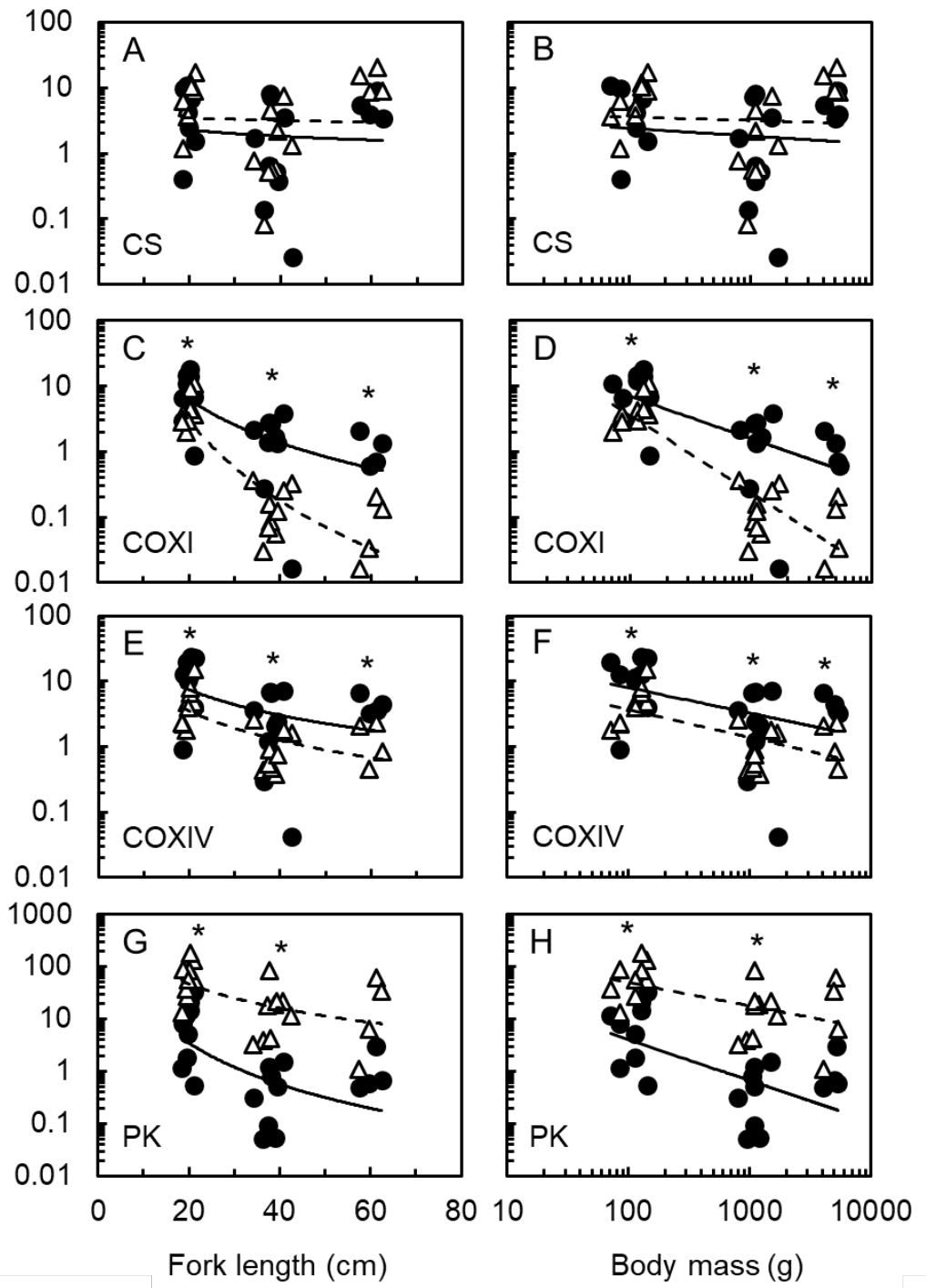


Fig. 3.5. The effects of increasing FL and BM on the number of transcripts per g tissue for CS (AB, values are $\times 10^{10}$), COXI (CD, values are $\times 10^{13}$), COXIV (EF, values are $\times 10^{11}$) and PK (GH, values are $\times 10^{11}$) in red and white muscle of young PBT juveniles of different sizes. The data for the red and white muscle are represented by ● with solid lines and Δ with dashed lines, respectively. The best-fitting power functions for the data in the various panels are as follows.: (A) red muscle $y = 6.01FL^{-0.32}$, $R^2 = 0.01$; white muscle $y = 5.33FL^{-0.14}$, $R^2=1.48 \times 10^{-3}$; (B) red muscle $y = 1.83BM^{-0.12}$, $R^2 = 0.01$; white muscle $y = 2.88BM^{0.05}$, $R^2=2.57 \times 10^{-3}$; (C) red muscle $y = 4.65 \times 10^3 FL^{-2.20}$, $R^2 = 0.37$; white muscle $y = 6.89 \times 10^5 FL^{-4.11}$, $R^2 = 0.76$; (D) red muscle $y = 134.64BM^{-0.64}$, $R^2 = 0.38$; white muscle $y = 814.91BM^{-1.18}$, $R^2 = 0.76$; (E) red muscle $y = 360.81FL^{-1.30}$, $R^2 = 0.15$; white muscle $y = 310.85FL^{-1.50}$, $R^2 = 0.40$; (F) red muscle $y = 3.26BM^{-0.39}$, $R^2 = 0.16$; white muscle $y = 1.38x^{-0.43}$, $R^2 = 0.39$; (G) red muscle $y = 8.80 \times 10^5 FL^{-2.61}$, $R^2 = 0.30$; white muscle $y = 4.74 \times 10^3 FL^{-1.54}$, $R^2 = 0.26$; (H) red muscle $y = 143.30x^{-0.78}$, $R^2 = 0.32$; white muscle $y = 381.79x^{-0.44}$, $R^2 = 0.26$ ($n = 22$). Significant differences in transcript abundance between the red and the white muscle for fish of a particular size (i.e. ~20 cm FL, ~40 cm FL or ~60 cm FL) are indicated by *.

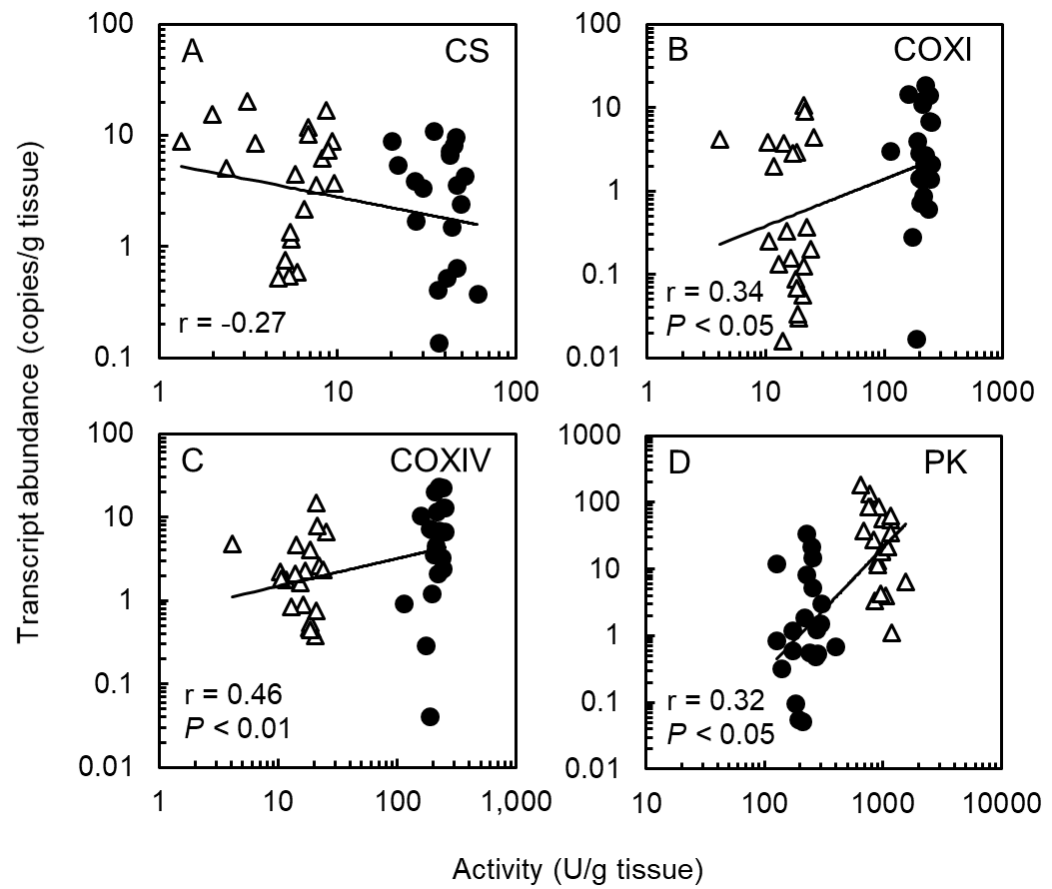


Fig. 3.6. Correlations between enzyme activity and transcript abundance for CS, COXI, COXIV and PK. Transcript abundance values are $\times 10^{10}$, $\times 10^{13}$, $\times 10^{11}$ and $\times 10^{11}$ for CS, COXI, COXIV and PK, respectively. The data for the RM and WM are represented by ● and Δ, respectively. The r and P values were determined using a Pearson correlation analysis in IBM® SPSS Statistics version 22.0.

3.3.6. The effects of muscle type and body size on the cytochrome c oxidase subunits I and IV-1 transcript abundances, expressed as copies per g tissue

The COX enzyme is made up of thirteen different subunits, ten encoded in the nucleus and three in the mitochondria (Tsukihara et al., 1996). We investigated the expression of COXI and COXIV as examples of mitochondrial and nuclear encoded COX subunits, respectively. COXI transcript abundance was greater in the red muscle than it was in the white muscle, but the magnitude of the difference varied depending upon the size of the fish. In the smallest, intermediate-sized and largest fish, COXI transcript abundance, expressed per g tissue, was 2-, 11- and 12-fold greater in the red muscle compared with the white muscle and the differences between the tissues were statistically significant ($P < 0.05$). This was in contrast to the 13-, 11- and 13-fold greater COX enzyme activity per g tissue in the red muscle compared to the white muscle in the same fish, respectively. Thus, in the intermediate-sized and largest fish, there was a good correlation between transcript abundance and enzyme activity in terms of the differences between the two different muscle types but in the smallest fish, this was not the case. In the smallest fish, the difference between the two different muscle types was only 2-fold for the COXI transcript abundance whereas it was 13-fold for the COX enzyme activity. This suggests that the greater COX enzyme activity in the red muscle compared with the white muscle could have been due to greater COXI transcript abundance in the red muscle of the intermediate-sized and largest fish but not in the smallest fish.

COXI transcript abundance showed a decrease with increasing FL and with increasing BM in both muscle types ($P < 0.01$) (Fig. 3.5C and D). For the red muscle, the BM-dependent scaling coefficient was -0.64 ± 0.13 whereas for the white muscle it was -1.18 ± 0.15 . Thus, the relative decrease in COXI transcript abundance with increasing body size was approximately twice as great in the white muscle as it was in the red muscle. In contrast, the COX enzyme activity, per g tissue, remained constant with increasing body size in both the red muscle and the white muscle. This suggests that the transcript translation efficiency for COXI may be greater in the white muscle compared

to the red muscle in larger PBT. When all of the data, for both tissues and all of the fish were taken together, COXI transcript abundance showed a small but significant positive correlation with COX enzyme activity (Fig 3.6B). This suggests that the greater COX enzyme activity in the red muscle compared to the white muscle could at least to some extent be explained by the greater COXI transcript abundance in the red muscle compared with the white muscle.

In the smallest, intermediate-sized and largest fish we sampled, COXIV transcript abundance, expressed as copies per g tissue, was 2-, 3- and 3-fold greater, respectively, in the red muscle compared with the white muscle and the differences between the tissues were statistically significant ($P < 0.05$) (Fig. 3.5 E and F). This differed from the 11 to 13-fold greater COX enzyme activity per g tissue in the red muscle compared with the white muscle that we had observed (Fig. 3.2). This suggests that the greater COX enzyme activity in the red muscle compared with the white muscle, is not due to a greater COXIV transcript abundance in this tissue. In addition, COXIV transcript abundance showed a decrease with increasing FL and BM in both the red muscle and the white muscle, with BM-dependent scaling coefficients of -0.39 ± 0.20 and -0.43 ± 0.12 , respectively ($P < 0.05$) (Fig. 3.5E and F). As was true for COXI transcript abundance, this was in contrast to the COX enzyme activity, per g tissue, which remained constant with increasing body size in both the red muscle and the white muscle. Thus, the relative decrease in COXIV transcript abundance with increasing body size was approximately the same for the two different muscle types. When all of the data, for both tissues and all of the fish were taken together, COXIV transcript abundance showed a small but significant positive correlation with COX enzyme activity (Fig 3.6C). The correlation of COX enzyme activity with COXIV transcript abundance was stronger than the correlation with COXI transcript abundance. This suggests that although the COX enzyme activity showed only a small positive correlation with COXIV transcript abundance, the greater COX enzyme activity in the red muscle compared to the white muscle could at least to some extent be explained by the greater COXIV transcript abundance in the same tissue. This was similar to what was observed for COXI transcript abundance.

3.3.7. The effects of muscle type and body size on the pyruvate kinase transcript abundance, expressed as copies per g tissue

PK transcript abundance, expressed as copies per g tissue, was greater in the white muscle than it was in the red muscle, but the magnitude of the difference varied depending upon the size of the fish. In the smallest, intermediate-sized and largest fish, the transcript abundance was 7-, 40- and 22-fold higher in the white muscle compared with the red muscle and the differences between the two different muscle types were statistically significant ($P < 0.05$) (Fig. 3.5 G and H). This was much more variable than the 4.3-fold higher PK enzyme activity per g tissue observed in the white muscle compared with the red muscle (Fig. 3.3). Although the fold differences between PK transcript abundance and PK enzyme activity were dissimilar, both were greater in the white muscle than in the red muscle. This suggested that greater PK transcript abundance may directly result in greater PK protein abundance and in-turn greater PK enzyme activity in the white muscle compared with the red muscle. Thus, unlike CS and COX, PK appears to be regulated at the level of transcription. Additionally, PK transcript abundance showed a decrease with increasing FL and with increasing BM in both muscle types ($P < 0.01$) (Fig. 3.5G and H). For the red muscle, the BM-dependent scaling coefficient was -0.78 ± 0.26 whereas for the white muscle it was -0.44 ± 0.17 . This was in contrast to what we had observed for PK enzyme activity, which, when expressed per g tissue, had remained constant in the red muscle but increased significantly in the white muscle with increasing body size. This suggests that either there is a greater amount of the PK protein translated from less mRNA or the PK protein stability increases with increasing body size. When all of the data, for both muscle types and all fish sizes were taken together, PK transcript abundance showed a small but significant positive correlation with PK enzyme activity (Fig. 3.6D). This indicated that PK enzyme activity may be regulated at the transcriptional level. However, the discrepancy in the changes occurring in PK enzyme activity and PK transcript abundance with increasing body size suggest that PK may also be regulated at the post-transcriptional and/or post-translational levels.

3.3.8. The effects of muscle type and body size on β -actin transcript abundance, expressed as copies per g tissue

A trivial explanation for the poor correlations we observed between enzyme activity and transcript abundance could be differences in cDNA synthesis efficiency between the red and the white muscle samples. To test for this, we investigated the transcript abundance for β -actin, a frequently used normalization gene in quantitative PCR analyses (Hendriks-Balk et al., 2007). β -actin transcript abundance per g tissue was greater in the red muscle than it was in the white muscle, but the magnitude of the difference differed depending upon the size of the fish. In the smallest fish, it was 4-fold greater whereas in the intermediate-sized fish it was 8-fold greater and in the largest fish, it was 3-fold greater (Fig. 3.7 A and B). Thus, it is possible that cDNA synthesis efficiency could have been greater in the red muscle than in the white muscle. If this were the case, however, we would have expected that the differences in transcript abundance for our genes of interest would have been greater than the differences in enzyme activity when in fact it was the opposite, i.e., the difference in transcript abundance was less than the difference in enzyme activity. Thus, greater efficiency of cDNA synthesis in the red muscle compared with the white muscle cannot explain the differences we observed between transcript abundance and enzyme activity.

To visualise this more clearly, the transcript abundances for each of the genes of interest were divided by the transcript abundance for β -actin. When this was done, the difference in CS transcript abundance between the red and white muscle increased from no difference between the two different tissue types to an average of 8.6-fold greater in the white muscle compared with the red muscle, but this apparent difference was not statistically significant (Figs. 3.8A and B). The greater relative CS transcript abundance in the white muscle compared with the red was the opposite of what we had observed for CS enzyme activity, where the activity per g tissue on average 7.1-fold greater in the red muscle compared with the white muscle. When the COXI transcript abundance was expressed relative to the β -actin transcript abundance, there was a decrease from an average of ~2.4-fold higher in the red muscle compared with the white muscle to no difference between the two different

tissue types (Figs. 3.8C and D). When COXIV transcript abundance was expressed relative to the β -actin transcript abundance there was a decrease from an average of ~2.6-fold higher in the red muscle compared with white muscle to no difference between the two different tissue types (Figs. 3.8E and F). Thus, it can be concluded that the difference in COXIV transcript abundance the difference in enzyme activity between muscle types is not explained by a difference in transcript abundance. Finally, when the PK transcript abundance was expressed relative to the β -actin transcript abundance, the difference in PK transcript abundance increased from an average of ~9-fold higher to an average of 25.6-fold higher in the white muscle compared with the red muscle (Figs. 3.8G and H). Thus, it can be concluded that there was a greater PK transcript abundance in the white muscle compared with the red muscle regardless of whether the data were expressed as copies per g tissue or relative to β -actin transcript abundance. However, the difference between the two different muscle types was much greater when expressed relative to β -actin transcript abundance than when expressed as copies per g tissue. These findings are consistent with PK being regulated at the transcriptional level.

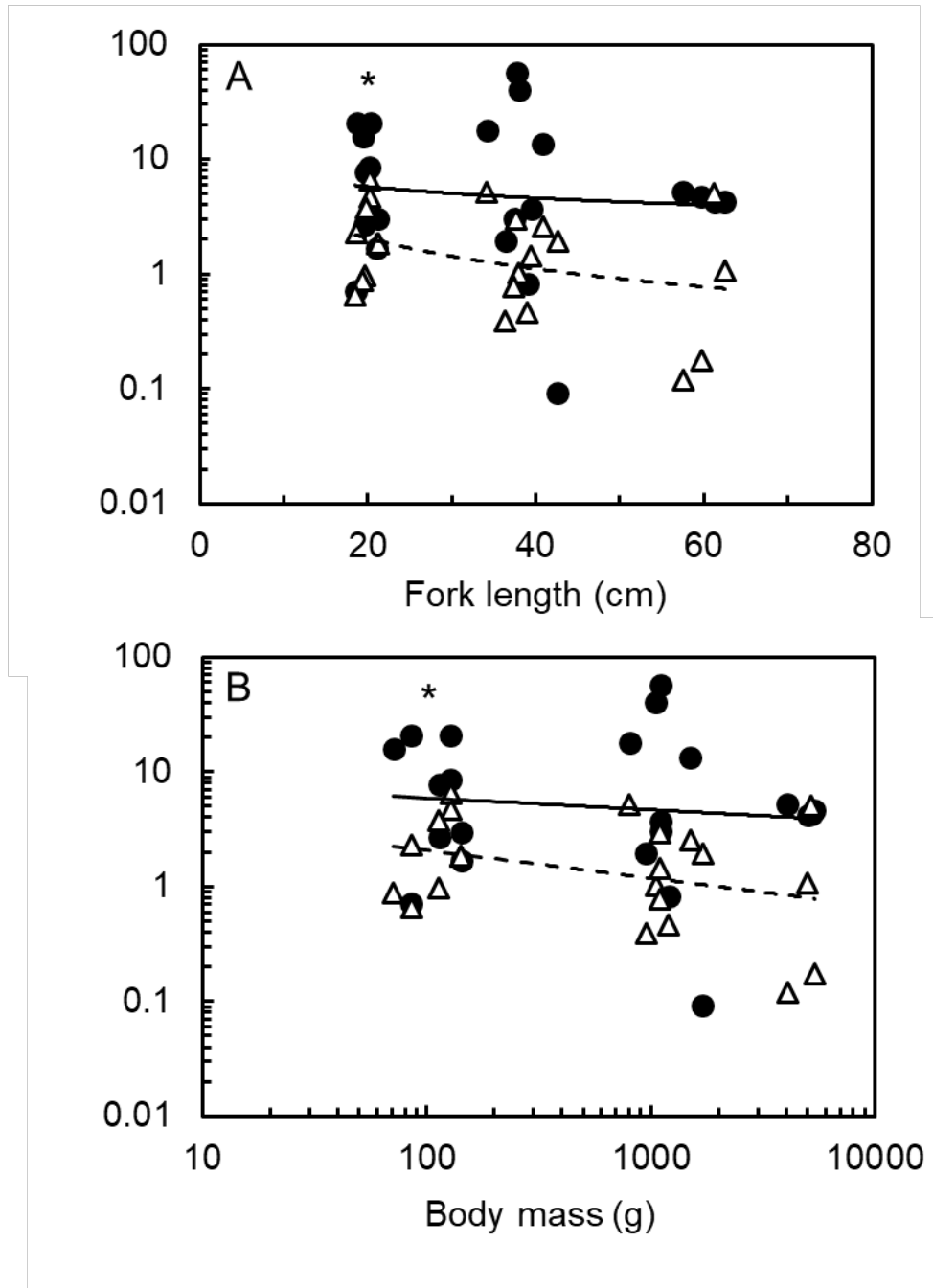


Fig. 3.7. The effects of increasing FL and BM on the number of β -actin transcripts per g tissue in red and white muscle of young PBT juveniles of different sizes (values are $\times 10^{11}$). The data for the red muscle and white muscle are represented by \bullet with solid lines and Δ with dashed lines, respectively. The best-fitting power functions for the data in the various panels are as follows: (A) red muscle $y = 274.35FL^{-0.52}$, $R^2 = 0.02$; white muscle $y = 187.59FL^{-0.74}$, $R^2 = 0.09$; (B) red muscle $y = 42.27BM^{-0.16}$, $R^2 = 0.03$; white muscle $y = 12.75BM^{-0.20}$, $R^2 = 0.08$ ($n = 22$). Significant differences in transcript abundance between the red and the white muscle for fish of a particular size (i.e. ~ 20 cm FL, ~ 40 cm FL or ~ 60 cm FL) are indicated by *.

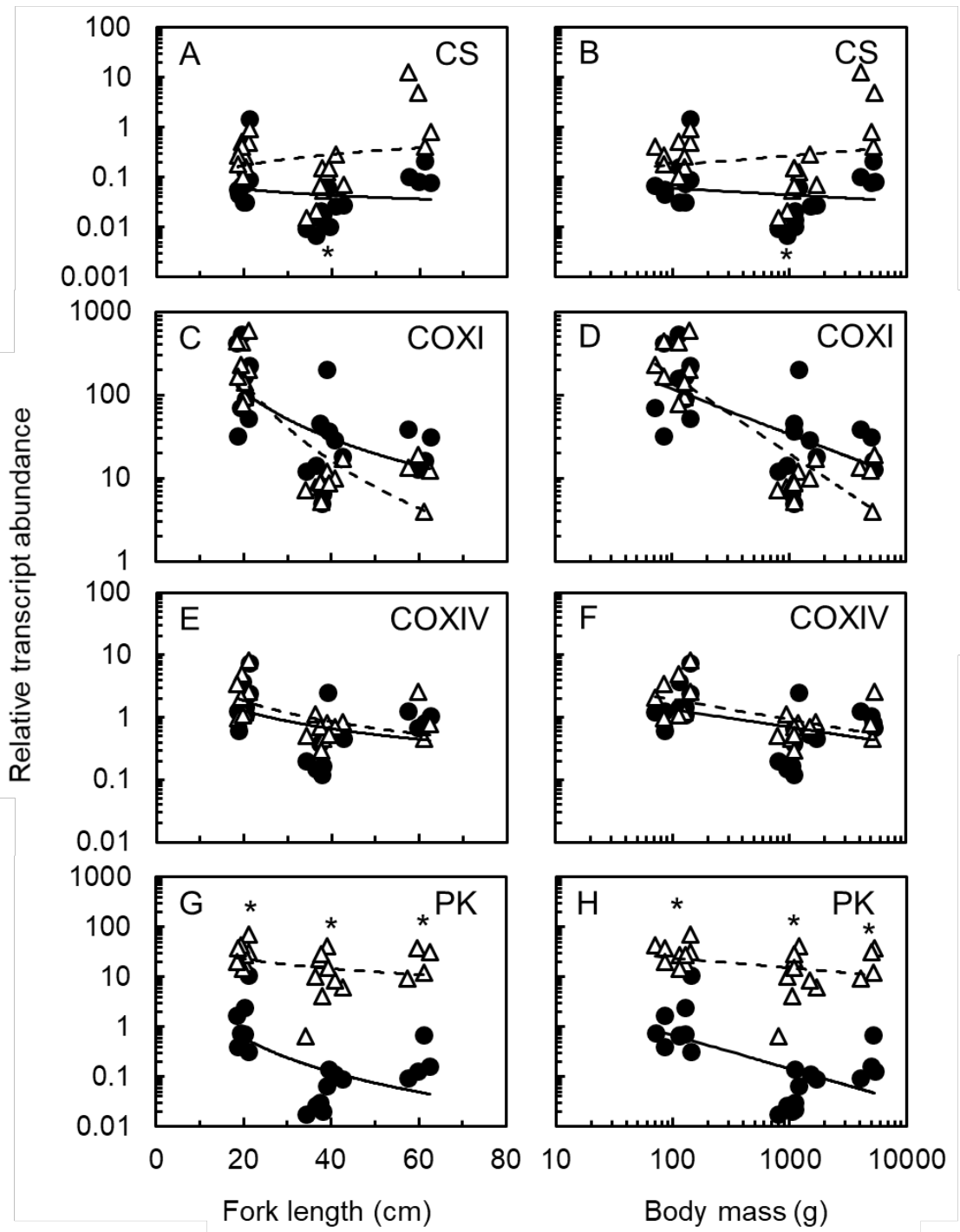


Fig. 3.8. The effects of increasing FL and BM on the relative gene expression for CS (AB), COXI (CD), COXIV (EF) and PK (GH) normalised to β -actin in red muscle and white muscle of young PBT juveniles of different sizes. The data for the red muscle and white muscle are represented by \bullet with solid lines and Δ with dashed lines, respectively. The best-fitting power functions for the data in the different panels are as follows: (A) red muscle $y = 0.20FL^{-0.42}$, $R^2 = 0.02$; white muscle $y = 0.02FL^{0.75}$, $R^2 = 0.04$; (B) red muscle $y = 0.11BM^{-0.13}$, $R^2 = 0.03$; white muscle $y = 0.07BM^{0.19}$, $R^2 = 0.03$; (C) red muscle $y = 3.01 \times 10^4 FL^{-1.87}$, $R^2 = 0.40$; white muscle $y = 2.36 \times 10^6 FL^{-3.23}$, $R^2 = 0.72$; (D) red muscle $y = 1.41 \times 10^3 BM^{-0.54}$, $R^2 = 0.40$; white muscle $y = 1.29 \times 10^4 BM^{-0.94}$, $R^2 = 0.74$; (E) red muscle $y = 23.35 FL^{-0.97}$, $R^2 = 0.16$, white muscle $y = 52.53x^{-1.12}$, $R^2 = 0.31$; (F) red muscle $y = 8.43x^{-0.32}$, $R^2 = 0.31$; white muscle $y = 5.04x^{-0.29}$, $R^2 = 0.17$; (G) red muscle $y = 5.69 \times 10^2 FL^{-2.29}$, $R^2 = 0.34$; white muscle $y = 1.62 \times 10^2 FL^{-0.65}$, $R^2 = 0.08$; (n = 22). (H) red muscle $y = 15.00 BM^{-0.67}$, $R^2 = 0.35$; white muscle $y = 60.34 BM^{-0.20}$, $R^2 = 0.09$. Significant differences in transcript abundance between the red and the white muscle for fish of a particular size (i.e. ~20 cm FL, ~40 cm FL or ~60 cm FL) are indicated by *.

3.3.9. The effects of muscle type and body size on total RNA extracted per g tissue

The total amount of RNA extracted per g tissue did not differ significantly between the different muscle types but it decreased both with increasing FL and with increasing BM in both the red and the white muscle (Fig. 3.8). The decrease with increasing BM in the total amount of RNA extracted per g tissue resulted in scaling coefficients of -0.91 ± 0.25 for the red muscle and -0.27 ± 0.07 for the white muscle. Thus, the decrease in the total amount of RNA was more pronounced in the red muscle than it was in the white muscle. This was consistent with the decrease we observed in PK transcript abundance in the white muscle as the fish grew larger but it was in contrast to the increase we observed in PK enzyme activity. This could indicate that the larger fish could produce more protein from a relatively smaller quantity of RNA. Alternatively, it could indicate that protein stability was greater in our largest fish.

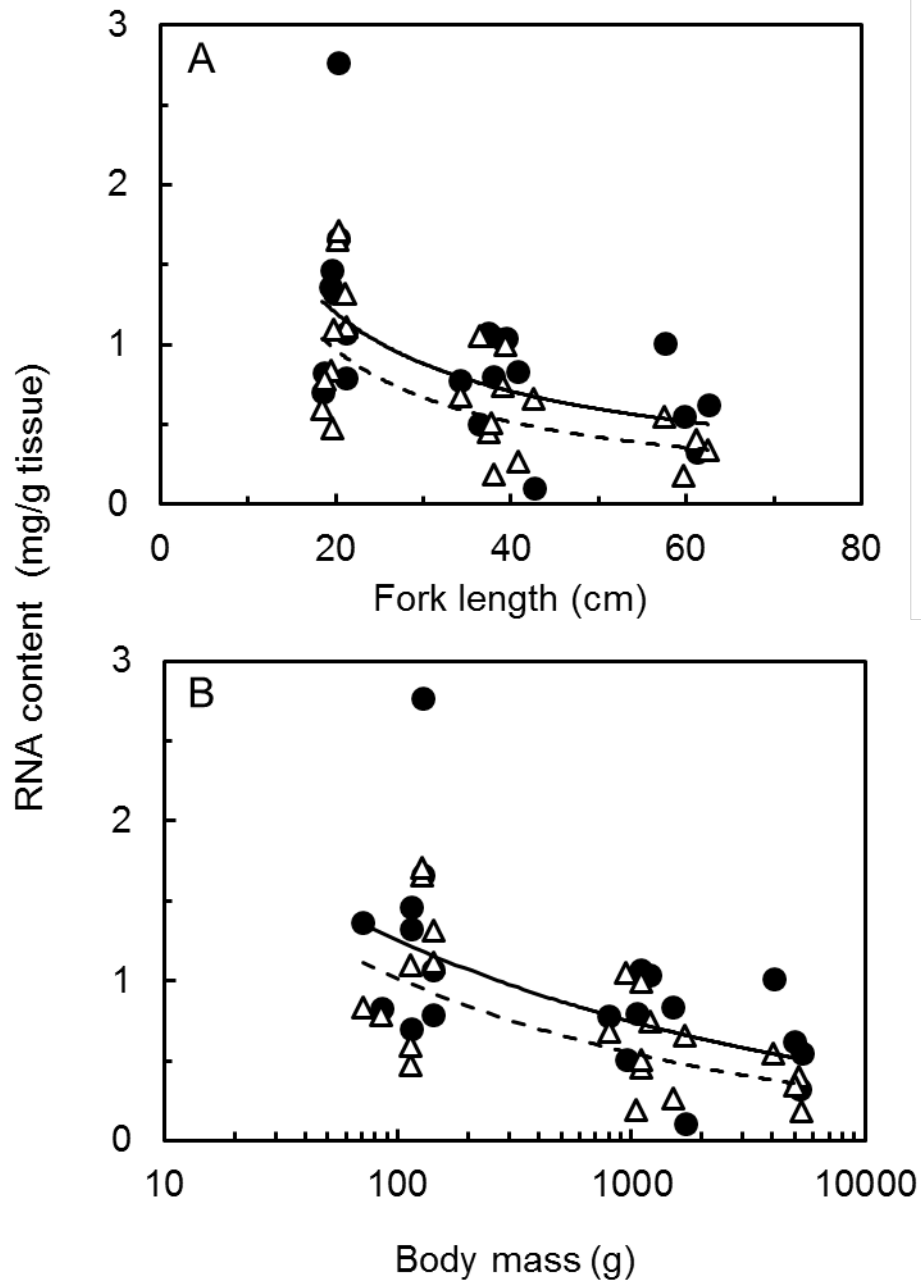


Fig. 3.9. The effects of increasing FL and BM on the total amount of RNA extracted per g tissue from red and white muscle of young PBT juveniles of different sizes. The data for the red and white muscle are represented by ● with solid lines and Δ with dashed lines, respectively. The best-fitting power functions for the data in the various panels are as follows: (A) red muscle $y = 11.72FL-0.76$, $R^2 = 0.27$; (white muscle) $y = 14.79x-0.91$, $R^2 = 0.40$; (B) red muscle $y = 3.54x-0.23$, $R^2 = 0.28$; white muscle $y = 3.47x-0.27$, $R^2 = 0.41$, $P < 0.001$. ($n = 22$).

3.4. Discussion

3.4.1. The effect of muscle type on citrate synthase enzyme activity

Citrate synthase (CS) enzyme activity, expressed per g tissue, was on average 7.1-fold higher in the red muscle than in the white muscle in the young PBT juveniles we analysed in this study. This indicated that mitochondrial abundance and aerobic metabolic capacity were almost an order of magnitude greater in the red muscle compared with the white muscle in these fish. This difference between the two different muscle types was similar to differences reported previously for other tuna species. For example, CS enzyme activity, expressed per g tissue, was approximately 6 to 10-fold higher in the red muscle compared to the white muscle in bigeye tuna (*Thunnus obesus*), yellowfin tuna (*Thunnus albacares*), and skipjack tuna (*Katsuwonus pelamis*) (Dalziel et al., 2005, Moyes et al., 1992). Interestingly, similar fold differences between red and white muscle have also been seen in other highly active fishes. For example, CS enzyme activity per g tissue was approximately 6-fold higher in the red muscle compared with the white muscle in swordfish (*Xiphias gladius*) and striped marlin (*Tetrapturus audax*) (Dalziel et al., 2005).

The CS enzyme activities we observed were similar to those reported previously for other tuna species. In our study, the mean \pm SE CS enzyme activities was 41.3 ± 2.5 U/g tissue in the red muscle and 5.8 ± 1.2 U/g tissue in the white muscle, in our smallest (~20 cm FL), intermediate-sized (~40 cm FL) and largest (~60 cm FL) PBT specimens, respectively. This compared well with CS enzyme activities ranging from 21 to 80 U/g tissue in the red muscle and 2 to 16 U/g tissue in the white muscle of bigeye tuna (*Thunnus obesus*), yellowfin tuna, (*Thunnus albacares*) and skipjack tuna (Guppy et al., 1979, Moyes et al., 1992, Dalziel et al., 2005). In contrast, red muscle CS enzyme activities in non-tunas have been shown to be lower than to those in tunas. For example, CS enzyme activities ranging from ~16 to 20 U/g tissue in the red muscle of Atlantic salmon (*Salmo salar*), rainbow trout (*Oncorhynchus mykiss*), swordfish and striped marlin have been reported (Dalziel et al., 2005, Morash et al., 2014, Zhang et al., 2016). Similarly, CS enzyme activities of only 1 to 4 U/g tissue have been reported for the white muscle of these species. These data indicate that the mitochondrial abundance and therefore aerobic

metabolic capacity in the red muscle and white muscle of tunas is greater than in non-tuna species. The red muscle in tunas is endothermic. Therefore, in the red muscle, the greater mitochondrial abundance could be due to a greater energy requirement in tunas to maintain an elevated muscle temperature. It has been proposed that the greater aerobic metabolic capacity of the white muscle of tunas could be due to the fibres being recruited at sustainable speeds or it may be related to rapid lactate turnover or growth rates (Dickson, 1996).

3.4.2. The effect of fish body size on citrate synthase enzyme activity

CS is an indicator of mitochondrial abundance and aerobic metabolic capacity. We hypothesised that the number of mitochondria, and/or their aerobic metabolic capacity, would increase with increasing body size in the red muscle and that this increase in metabolic capacity would contribute to the temperature elevation we observed in the red muscle of our juvenile PBT specimens with increasing body size (Chapter 2). However, here we found that CS enzyme activity decreased with increasing body size in both the red muscle and the white muscle in our young PBT juveniles and this was regardless of whether the data were expressed per g tissue or per mg protein. This suggested that mitochondrial abundance, and therefore aerobic metabolic capacity, were decreasing with increasing fish size and in both muscle types. However, the BM-specific scaling coefficient for CS enzyme activity per g tissue was greater in the white muscle (-0.21 ± 0.06) than it was in the red muscle (-0.12 ± 0.04). Thus, the decrease in mitochondrial abundance and aerobic metabolic capacity was proportionally greater in the white muscle than it was in the red muscle.

In contrast, Dickson et al. (2000) reported an increase in BM-dependent red muscle CS enzyme activity per g tissue with increasing body size. Specifically, they found a BM-specific scaling coefficient of 0.24 ± 0.21 for the red muscle of small (8 to 18 cm FL) juveniles of black skipjack tuna (*Euthynnus lineatus*) but this was not investigated in the white muscle. The positive scaling coefficient for red muscle indicated that mitochondrial abundance and aerobic metabolic capacity in the red muscle of this species increased with increasing body size as opposed to the decrease we had observed. One possible reason

for the difference between our results and those of the previous study could be that the fish in the previous study were smaller than those in our own study. Thus, it is possible that aerobic metabolic capacity increases with increasing body size up to a certain maximum size and then it decreases thereafter as the fish grow larger. This could be a means of generating sufficient heat in small fish to avoid hypothermia but avoiding overheating as the body grows larger and the surface area to volume ratio decreases.

The BM-dependent scaling coefficient of -0.21 ± 0.06 we observed for CS enzyme activity per g tissue in the white muscle of PBT was consistent with previous findings. For example, Childress and Somero (1990) determined the scaling coefficients for CS enzyme activity in the white muscle but not in the red muscle in a number of different fish species from a range of different habitats. It was observed that the BM-dependent scaling coefficients for CS enzyme activity per g tissue in the white muscle ranged from -0.06 to -0.37 in oceanic pelagic species, -0.06 to -0.22 in near-bottom pelagic species and -0.16 to -0.68 in benthic species. From this it can be concluded that regardless of the habitat these fishes were from, their aerobic metabolic rate decreased with increasing BM. Similarly, Davies and Moyes (2007) observed scaling coefficients of -0.15 to -0.19 in the white muscle of freshwater species of fish but the same analysis was not performed for the red muscle. Thus, both of these studies indicate that the aerobic metabolic capacity of fishes, from a wide variety of different habitats, decreases with increasing body size in the white muscle.

In terrestrial vertebrates, the BM-specific aerobic metabolic rate, determined by measuring the rate of oxygen consumption, is inversely related to body size with a scaling coefficient of approximately -0.25 (Peters, 1986, Savage et al., 2004, Savage et al., 2007). It is hypothesised that this decrease in the BM specific aerobic metabolic rate with increasing body size prevents overheating because as an animal becomes larger it loses less heat to the environment due to its decreasing surface area-to-volume ratio (Kleiber, 1947, Riek and Geiser, 2013). Interestingly, the scaling coefficient of -0.25 determined for terrestrial vertebrates for BM-specific aerobic metabolic rate, determined by the rate of oxygen consumption, was not significantly different from the scaling

coefficient of -0.21 ± 0.62 we observed for the decrease in CS enzyme activity in the white muscle with increasing BM. This suggests that the aerobic metabolic rate decreases in the white muscle of PBT with increasing body size and this may be a means of avoiding overheating, as is true in terrestrial mammals. In contrast, the BM-dependent scaling coefficient of -0.12 ± 0.04 that we observed in the red muscle was proportionally lower than the observed scaling coefficient of -0.25 for aerobic metabolic rate in terrestrial mammals (Peters, 1986, Savage et al., 2004, Savage et al., 2007). Therefore, the slower decrease in metabolic rate in the red muscle could be an indication of the high abundance of mitochondria in this tissue.

In terrestrial mammals differing in body size by almost six orders of magnitude, CS enzyme activity in the gastrocnemius muscle (composed of ~50% red and ~50% white muscle fibres) has been shown to decrease with increasing BM with a scaling coefficient of -0.106 (Emmett and Hochachka, 1981). This value was lower than we observed in the red muscle and the white muscle of PBT. This could possibly be because, unlike the white muscle of fishes, the gastrocnemius muscle in mammals is a combination of both red muscle and white muscle fibres.

3.4.3. The effect of muscle type on cytochrome c oxidase enzyme activity

We found that cytochrome c oxidase (COX) enzyme activity, expressed per g tissue was, on average, 12.4-fold higher in the red muscle than it was in the white muscle in the three different size classes of young PBT juveniles we studied. This indicated that the mitochondrial abundance was much greater in the red muscle compared with the white muscle. Additionally, the higher COX enzyme activity could indicate that the folding of the mitochondrial inner membrane could also be greater in the red muscle than in the white muscle. The higher COX enzyme activity in the red muscle compared to the white muscle corresponded with what we observed for CS enzyme activity. The fold difference in COX enzyme activity we observed between the red muscle and the white muscle was greater than what has been observed previously for other tuna species. For example, in the only other published study comparing COX enzyme activity in the red and white muscle of tunas, it was 6 to 10-fold

higher in the red muscle compared with the white muscle in bigeye tuna, yellowfin tuna and skipjack tuna (Dalziel et al., 2005). Similarly, the fold differences in COX enzyme activity between the red and white muscle observed for highly active pelagic non-tuna fish species were comparable to that of tunas. For example, COX enzyme activity per g tissue was approximately 6-fold higher in the red muscle compared with the white muscle in swordfish and striped marlin (Dalziel et al., 2005). Overall the difference observed in COX enzyme activity between the red muscle and white muscle of both tunas and non-tunas was lower in the previous study than in our own.

The COX enzyme activities we observed in this study were greater than those observed in previous studies both in tunas and in other highly active pelagic fish species. In our study, when all PBT specimens were considered, the mean \pm SE COX enzyme activities were 210 ± 7 U/g tissue in the red muscle and 17.0 ± 3.6 , U/g tissue in the white muscle. In contrast, Dalziel et al. (2005) reported lower COX enzyme activities of approximately 55 to 65 U/g tissue in the red muscle and 5 to 10 U/g tissue in the white muscle of skipjack tuna, bigeye tuna and yellowfin tuna. In this same study, they also reported activities of approximately 20 U/g tissue in the red muscle and < 5 U/g tissue in the white muscle in non-tuna species (swordfish and striped marlin). The greater activities we observed compared to other tuna species could be due different protein extraction and/or enzyme assay methods. Alternatively, it could be due to the fact that we investigated the activity in a different species of fish. Although both the study by Dalziel et al. (2005) and our own study investigated COX enzyme activity in tuna species, the habitats of the species are different. PBT are found in temperate waters whereas bigeye tuna, yellowfin tuna and skipjack tunas are found in more tropical waters. Bluefin tunas, such as PBT, have higher aerobic metabolic rates, muscle temperatures, heart rates, and cardiac outputs than tropical tuna species (Blank et al., 2007). Thus, higher aerobic metabolic rates in PBT could be the reason why we observed greater COX enzyme activities in PBT than had previously been reported for bigeye tuna, yellowfin tuna and skipjack tuna. The estimated minimum amount of oxygen needed by a fish to support its aerobic metabolism (standard metabolic rate (SMR)) for tunas is 2 to 5 times greater than it is for even highly active non-tuna fish species, such as salmonids (Korsmeyer and Dewar, 2001).

Thus, the high SMR of tunas could explain why the COX enzyme activity reported by Dalziel et al. (2005) and by us for tropical tunas and PBT, respectively, was greater when compared with swordfish and striped marlin, as reported by Dalziel et al. (2005).

3.4.4. The effect of fish body size on cytochrome c oxidase enzyme activity

When expressed per g tissue, there was no change in COX enzyme activity with increasing body size in either the red muscle or the white muscle in our young PBT specimens. These results were different from those observed for CS where the activity per g tissue decreased with increasing body size. COX is located in the inner mitochondrial membrane as the terminal electron acceptor in the mitochondrial electron transfer chain (mETC). This means that COX enzyme activity can be both an indicator of mitochondrial abundance and an indicator of mitochondrial inner membrane folding. Increasing mitochondrial inner membrane folding could lead to increasing activity of the mitochondrial electron transfer chain as a result of increasing abundance of the enzymes involved, including COX. Thus, the constant COX enzyme activity, coupled with the decreasing CS enzyme activity we observed, could indicate increasing folding of the inner mitochondrial membrane to compensate for a decreasing number of mitochondria as the fish grew larger.

In contrast to what we observed, Nyack et al. (2007), reported that COX enzyme activity per g tissue decreased with increasing BM in the white muscle of black sea bass (*Centropristis striata*), with a scaling coefficient of -0.1. Thus, mitochondrial abundance and aerobic metabolic capacity scaled negatively with increasing BM in black sea bass. Similarly, it has previously been shown, using electron micrographs, that the surface area of the inner mitochondrial membrane is significantly greater in the skeletal muscle of small mammals compared with the skeletal muscle of large mammals (Else and Hulbert, 1985). From this, the authors concluded that there was less inner membrane surface area and therefore fewer copies of the proteins in the mETC in large mammals. This suggested that there was decreasing respiratory capacity per g tissue with increasing body size. This would have been consistent with the theory that in mammals the resting aerobic metabolic rate decreases with increasing body

size in order to avoid overheating (Kleiber, 1947). The unchanged COX enzyme activity per g tissue with increasing body size we observed for PBT is not consistent with this theory. Instead the constant COX activity with increasing body size supports our theory that there is increased folding of the inner mitochondrial membrane to compensate for a decreasing number of mitochondria as the fish grew larger. Further investigation is required to determine if this theory is correct.

3.4.5. The effects of temperature on citrate synthase and cytochrome c oxidase enzyme activities

It has frequently been observed, that ectothermic fishes respond to declining water temperatures by increasing the activities of mitochondrial enzymes such as CS and COX (Guderley, 2004). This has been taken to indicate that these fishes are increasing their mitochondrial abundance and/or folding of the inner mitochondrial membrane in order to compensate for the decreasing enzyme activity that occurs at lower temperatures due to the laws of thermodynamics (Guderley, 2004). Interestingly, we observed that CS enzyme activity in the red and white muscle of our young PBT specimens decreased with increasing body size and that this decrease was coincident with a decrease in the ambient water temperature, from 29.4°C to 15.8°C. At first this seems counterintuitive when we consider what is known for ectothermic fishes but we must remember that the muscle temperature in our young PBT specimens did not follow the ambient water temperature. Instead the temperature in the red muscle remained at a relatively constant 30.5°C to 26.9°C. This relatively constant tissue temperature would obviate the need to increase the amounts of the various mitochondrial enzymes in order to compensate for the cooling water temperature. Alternatively, the decrease in CS enzyme activity per g tissue, regardless of decreasing water temperatures, could indicate that body size has a greater influence on the aerobic metabolic capacity of the red and white skeletal muscle of juvenile PBT than water temperature.

3.4.6. The effect of muscle type on pyruvate kinase enzyme activity

In fishes, as in other vertebrates, white muscle is used for short, unsustainable bursts of activity such as the pursuit of prey and its metabolism, under these

circumstances, is predominantly glycolytic (Love, 1970, Johnston, 1977, Somero and Childress, 1980, Norton et al., 2000). As a result, white muscle has a greater glycolytic capacity than red muscle in fishes and in other vertebrates (Peter et al., 1972, Childress and Somero, 1990). In our study we observed that PK enzyme activity, expressed per g tissue, was 4.3-fold higher in the white muscle than it was in the red muscle. This is consistent with white muscle having a greater reliance on glycolytic metabolism than red muscle, as has been observed for other fish species and for other vertebrates. Guppy et al. (1979) found the PK enzyme activity per g tissue in skipjack tuna was approximately 7-fold greater in the white muscle than it was in the red muscle. This difference is greater than the difference that we observed but our findings are broadly consistent with those of Guppy et al. (1979). Similarly, Johnston (1977) has reported that, in rainbow trout, PK enzyme activity per g tissue was approximately only 3-fold greater in the white muscle than it was in the red muscle. However, the same study also showed PK enzyme activity per g tissue was the same in both red and white muscle tissue of carp. The 4.3-fold higher PK enzyme activity we observed in the white muscle of PBT compared with the red muscle was consistent with what had been reported for skipjack tuna and rainbow trout.

Taking all of our PBT specimens all together, the mean PK enzyme activity expressed per g tissue was ~230 U/g tissue in the red muscle and ~970 U/g tissue in the white muscle. Similar PK enzyme activities have been reported for other tuna species such as skipjack tuna. In this species, the average PK enzyme activity was ~195 U/g tissue in the red muscle and ~1,300 U/g tissue in the white muscle of fish that were of similar size to our intermediate-sized PBT (1,000 to 2,000 g BM) (Guppy et al., 1979). In contrast, it has been shown that PK enzyme activity, was approximately 400 U/g tissue in the red muscle and 1,200 U/g tissue in the white muscle of rainbow trout (Johnston, 1977). These values are much higher than the values we observed for PBT. In contrast, in carp, a relatively sluggish fish species, it has been shown that PK enzyme activity was approximately 200 U/g tissue in both the red muscle and the white muscle. (Moyes et al., 1992, Bushnell and Jones, 1994, Kottelat and Freyhof, 2007). This is consistent with more active fish species having a greater glycolytic capacity in their white muscle compared to their red muscle,

whereas it is approximately the same in both muscle types in more sluggish fishes.

3.4.7. The effect of fish body size on pyruvate kinase enzyme activity

In the young PBT specimens we studied, PK enzyme activity, expressed per g tissue, remained constant with increasing body size in the red muscle but it increased with increasing body size in the white muscle, with a scaling coefficient of 0.09 ± 0.02 . A wide range of BM-specific scaling coefficients (0.08 – 0.23) has been reported for PK enzyme activity in the white muscle of various fish species including rainbow trout, largemouth bass, smallmouth bass, pumpkinseed sunfish and bluegill sunfish (Goolish, 1989, Davies and Moyes, 2007). The scaling coefficient of 0.09 ± 0.02 we observed for PBT was within the range of scaling coefficients reported for the other fish species but towards the lower end of that range. It has been hypothesised that positive scaling of anaerobic metabolic enzyme activity with increasing BM provides increasing power for the muscles of larger-bodied fishes to be able reach the same burst swimming velocities as smaller-bodied fishes (Somero and Childress, 1985). Thus, we conclude that the increase in PK enzyme activity with increasing body size in the white muscle of the fishes in our study may have the same explanation.

3.4.8. The effect of muscle type on citrate synthase transcript abundance

CS transcript abundance, expressed as copies per g tissue, showed no significant difference between the red and the white muscle in our young PBT specimens. This was surprising given that CS enzyme activity, expressed on the same basis, was approximately an order of magnitude greater in the red muscle compared with the white muscle in these same fish. The lack of correlation we observed between CS enzyme activity and CS transcript abundance could have several different explanations. One could be that CS is regulated not at the transcriptional level but at the post-transcriptional level. For example, a greater transcript translation efficiency could explain why we observed a 7 to 10-fold greater CS enzyme activity per g tissue in the red muscle compared to the white muscle of PBT despite there being no difference

in the CS transcript abundance between the different tissues. Other authors have found a similar lack of correspondence between CS enzyme activity and CS transcript abundance (O'Brien, 2011, Dalziel et al., 2005). For example, when goldfish were cold treated at a suboptimal water temperature of 4°C for 6 weeks, CS enzyme activity, per g tissue, was approximately 2- and 2.3-fold greater in the red and white muscle of the control fish maintained at 20°C, respectively, but there was no change in CS transcript abundance (LeMoine et al., 2008). Similarly, when zebrafish (*Danio rerio*) were maintained at a suboptimal water temperature of 18°C for 3 weeks, there was 50% greater CS enzyme activity in the skeletal muscle (presumably white muscle) compared with the control fish maintained at 28°C, but there was no change in CS transcript abundance (McClelland et al., 2006). In contrast, when threespine stickleback (*Gasterosteus aculeatus*) were maintained at a suboptimal water temperature of 8°C for 9 weeks, it was found that the red muscle had ~2-fold greater CS transcript abundance and ~70% greater enzyme activity per g tissue compared to control fish maintained at the optimal temperature of 20°C (Orczewska et al., 2010).

Some caution is necessary when analysing transcript abundance as an indicator of the transcriptional regulation of proteins. For example, the process of transcription itself may not result in a change transcript abundance due to process of RNA degradation. Similarly, an increase in protein abundance may not affect protein activity. This has previously been well documented in a study where cold acclimation in goldfish resulted in a significant reduction of 60% and 30% to thyroid hormone receptor α -1 (TR α -1) transcript abundance in the white muscle when expressed relative to RNA and per g tissue, respectively, without there being a similar decrease in TR α nuclear protein (Bremer et al., 2012).

CS enzyme activity, expressed per g tissue, has been shown to be 6 to 10-fold higher in the red muscle compared with the white muscle of skipjack tuna, bigeye tuna and yellowfin tuna but CS transcript abundance expressed per mg of DNA ranged from no difference to 1.5-fold higher in the red muscle than in the white muscle in these fishes (Dalziel et al., 2005). The red muscle of these fishes has been shown to have a 2.5-fold greater DNA content than the white

muscle (Dalziel et al., 2005). From this, the authors concluded that having more DNA per g tissue, red muscle would be expected to have a greater capacity to synthesise more CS mRNA than an equivalent mass of white muscle (Dalziel et al., 2005). Therefore, if protein translation efficiency is equal between the red and the white muscle in these fishes then a greater amount of CS protein should be synthesised in the red muscle than in the white muscle. However, when exploring this further, Dalziel et al. (2005) found that the amount of CS enzyme activity produced per femtomole of CS mRNA was 2 to 3-fold greater in the red muscle than in the white muscle of the tunas they studied. This indicated that CS mRNA translation efficiency was greater in the red muscle than in the white muscle. From this they concluded that the greater translation efficiency in the red muscle could account for the greater CS enzyme content per mg of DNA (Dalziel et al., 2005). This was consistent with our observations in PBT of no difference in CS transcript abundance between the red and white muscle but CS enzyme activity per g tissue being approximately an order of magnitude higher in the red muscle compared to the white.

In a recent study with human HAP1 cells, it was discovered that CS enzyme activity was inhibited through methylation catalysed by methyltransferase-like protein 12 (METTL12) (Małeckı et al., 2017). It was determined that methylation of a lysine (Lys-395) residue located in the active site was catalysed by a METTL12 and this inhibited CS enzyme activity. This suggests that CS enzyme activity is down-regulated at the post-translational level by methylation. Therefore, the 7-fold higher CS enzyme activity in the red muscle compared to the white muscle in our PBT specimens could suggest that the CS protein is more highly methylated in the white muscle than in the red muscle. By investigating the methylation status of CS in the red and white muscle of PBT it would be possible to determine if CS enzyme activity is inhibited by methylation in this fish as it is in humans.

3.4.9. The effect of body size on citrate synthase transcript abundance

There was no effect of body size on CS transcript abundance in either the red or the white muscle in our young PBT specimens. This was in contrast to what we had observed for CS enzyme activity which decreased with increasing body

size in both muscle types both when the activity was expressed per g tissue and when it was expressed per mg protein. The lack of correlation between CS enzyme activity and CS transcript abundance we observed here could possibly be because CS is not regulated at the transcriptional level.

3.4.10. The effects of muscle type on the transcript abundances for cytochrome c oxidase subunits I and IV-1

COX is a large enzyme complex composed of 13 different subunits (Tsukihara et al., 1996). Three of these subunits (subunits I, II, III) are encoded by mitochondrial DNA and form the catalytic core of the enzyme whereas the remaining ten subunits are encoded by nuclear DNA. This includes COXIV. In mice, COXIV is essential for the correct assembly and function of the COX holoenzyme (Li et al., 2006). Thus, it has been proposed that COXIV gene expression may be rate-limiting for the assembly of the COX enzyme complex. However, it should be noted that the assembly of the COX enzyme complex is an intricate process and some caution needs to be taken when measuring the levels of a single subunit to make an argument about control of synthesis of the COX holoenzyme. We investigated the transcript abundance of the nuclear encoded COXIV and mitochondrially encoded COXI subunits to determine whether there was a correlation between transcript abundance and the enzyme activity of COX in PBT. In the young PBT specimens we studied, COXI transcript abundance, expressed as copies per g tissue, ranged from 2- to 12-fold higher in the red muscle compared with the white muscle depending upon the size of the fish. In contrast, COXIV transcript abundance, also expressed as copies per g tissue, ranged from 2- to 3-fold higher in the red muscle compared with the white muscle depending upon the size of the fish. These results were surprising given that COX enzyme activity, expressed per g tissue, was, on average, 12.5-fold higher in the red muscle compared with the white muscle in all of our PBT specimens, regardless of their body size.

Several previous studies have explored the relationship between COX transcript abundance and COX enzyme activity in fishes. For example, in goldfish exposed to a suboptimal water temperature of 4°C for 6 weeks, it was found that COX enzyme activity expressed per g tissue was ~2-fold higher in the white muscle but not statistically significantly different in the red muscle

when compared to the control fish maintained at 20°C (LeMoine et al., 2008). Similarly, the COXIV transcript abundance was ~2-fold higher in both the red and the white muscle compared to the control fish, resulting in a strong correlation between the two variables. In the same fish, COXI transcript abundance was ~1.5-fold higher in the red muscle but not significantly higher in the white muscle when compared to the control fish. There was a weaker correlation between COX enzyme activity and COXI transcript abundance compared to the correlation between COX enzyme activity and COXIV transcript abundance. Therefore, the fold differences between the red muscle and white muscle were very similar for both COX enzyme activity and the transcript abundance of the COX subunits in goldfish. However, the overall the differences in the transcript abundance of the COX subunits were much less than the difference in COX enzyme activity in PBT. This suggests that COX enzyme activity may not be regulated at the transcriptional level in PBT. However, the small but significant correlations between COXI and COXIV are likely to be driven by the differences between tissues rather than a common pattern among tissues.

3.4.11. The effects of body size on the transcript abundances for cytochrome c oxidase subunits I and IV-1

COXI and COXIV transcript abundances, expressed as copies per g tissue, both decreased with increasing body size in both the red and the white muscle in our young PBT specimens. In contrast, we had seen that COX enzyme activity per g tissue remained constant with increasing body size. In addition, we observed a poor correlation between COX enzyme activity and COXI transcript abundance in specimens of different body sizes. The same was true for COXIV transcript abundance but the correlation between COXIV transcript abundance and COX enzyme activity was stronger than with COXI transcript abundance and COX enzyme activity. The constant COX enzyme activity per g tissue despite decreases in the transcript abundance of both the COXI and COXIV subunits with increasing body size suggests that larger sized PBT may have a better translation efficiency or perhaps there is greater protein stability in the larger fish. As far as we can ascertain, there are no other studies on the

relationship between COX transcript abundance and fish body size reported in the literature.

3.4.12. The effect of muscle type on pyruvate kinase transcript abundance

PK transcript abundance, expressed as copies per g tissue, was 7, 40 and 22-fold greater in the white muscle than it was in the red muscle, in the smallest, intermediate-size and largest PBT specimens we studied. In contrast, PK enzyme activity, also expressed per g tissue, ranged from 4 to 5-fold greater in the white muscle compared with red muscle in these fish. This suggests that greater transcript abundance may lead directly to increasing protein abundance and therefore greater enzyme activity in the case of PK. This indicates that PK protein abundance is regulated at the transcriptional level in the red and white muscle of PBT. However, the difference in PK enzyme activity between the two different muscle types was not directly proportional to the difference in PK transcript abundance. In fact, the difference between the red and white muscle was smaller for PK enzyme activity than it was for PK transcript abundance. This suggests that PK may be regulated at the post-transcriptional level as well as at the transcriptional level in PBT.

3.4.13. The effect of body size on pyruvate kinase transcript abundance

In the red muscle of our young PBT specimens, increasing body size resulted in a decrease in PK transcript abundance but no change in PK enzyme activity. In contrast, in the white muscle there was a decrease in PK transcript abundance with increasing body size but this paralleled an increase in PK enzyme activity. There could be at least two possible explanations for the difference observed in the white muscle. One reason why we observed the highest PK enzyme activities but the lowest PK transcript abundances in the largest fish could be greater PK protein stability with increasing body size and the other could be better translation efficiency with increasing body size in our PBT specimens. Similar to our study, PK enzyme activity in rainbow trout ranging in size from approximately 20 to 2,600 g, has been observed to increase steeply with increasing body size in the white muscle (Burness et al., 1999). From this, the authors concluded that the glycolytic capacity of the white

muscle in rainbow trout increases with increasing body size. In contrast to our own study, there was also a steep increase in PK transcript abundance reported in rainbow trout between 20 to 380 g. However, the transcript abundance decreased considerably when larger, approximately 900 to 2,600 g, rainbow trout were introduced into the dataset. From this the authors concluded that larger fish were able to produce more protein from less mRNA. Consistent with this conclusion, we observed that there was a significant decrease in total RNA content and PK transcript abundance, with increasing body size, in both the red and the white muscle of our young PBT specimens but that there was a significant increase in PK enzyme activity, per g tissue, in the white muscle. This suggested that the significant increase in PK enzyme activity per g tissue in the white muscle of our PBT specimens with increasing body size may have been due to larger fish producing more protein from less mRNA.

3.4.14. Conclusions

This study has found that: (a) CS and COX enzyme activity was approximately an order of magnitude greater in the red muscle compared with the white muscle in our young PBT specimens and this was regardless of whether the activity was expressed per g tissue or per mg protein; (b) CS enzyme activity decreased with increasing body size in both the red muscle and the white muscle (c) There was no difference in CS transcript abundance between the muscle types and the transcript abundance remaining constant with increasing body size; (d) COX enzyme activity was also approximately an order of magnitude higher in the red muscle compared to the white muscle, regardless of whether expressed per g tissue or per mg protein; (e) COX enzyme activity remained constant with increasing body size when expressed per g tissue but decreased significantly when expressed per mg protein; (f) The transcript abundance of the COX subunits were more variable than the COX enzyme activity but were also significantly higher in the red muscle than in the white muscle but in contrast to the enzyme activity the transcript abundance of the COX subunits decreased significantly with increasing body size in both muscle types.

We hypothesised that the number of mitochondria, and/or their aerobic metabolic capacity, would increase with increasing body size in the red muscle during the development of regional endothermy in PBT. These findings of this Chapter indicate that this was not true. Instead, the decrease in CS enzyme activity per g tissue suggested that mitochondrial abundance decreases in these tissues with increasing body size but the constant COX enzyme activity suggested that the folding of the mitochondrial inner membrane increases to compensate for the decrease in mitochondrial abundance. Previously we showed that red muscle temperature elevation increases linearly in juvenile PBT ranging in size from ~20 cm to ~60 cm FL and ~2 months to ~2 years of age (Chapter 2). Thus, overall the results of this Chapter suggest that aerobic metabolic capacity may remain constant with increasing fish size. Thus, the increase in red muscle temperature elevation did not coincide with an increase in aerobic capacity.

CHAPTER 4 - Roles of the PGC-1 transcriptional co-activators in red muscle endothermy in Pacific bluefin tuna (*Thunnus orientalis*)

Abstract

Tunas are unusual fishes because they are regionally endothermic. In bluefin tunas, the red ('slow-twitch', predominantly oxidative) skeletal muscle, the eye/brain and the viscera are the tissues that are warm whereas the white ('fast-twitch', predominantly glycolytic) skeletal muscle and the heart are cool (i.e. at approximately the ambient water temperature). Previously we reported that citrate synthase (CS) and cytochrome *c* oxidase (COX) enzyme activities were approximately an order of magnitude greater in the red muscle than they were in the white muscle of Pacific bluefin tuna (PBT, *Thunnus orientalis*). In mammals, the peroxisome proliferator-activated receptor γ co-activator-1 (PGC-1) transcriptional co-activators are master regulators of mitochondrial biogenesis and function. Thus, we predicted that they and their transcription factor targets would be more highly expressed in the red muscle compared with the white muscle in our tuna specimens. To assess this, we cloned and sequenced a PGC-1 α cDNA from PBT and investigated its expression as well as investigating the expression of PGC-1 β , peroxisome proliferator-activated receptor α (PPAR α), one of the transcription factor targets of PGC-1 α , and medium-chain acyl-Coenzyme A dehydrogenase (MCAD), a target gene of PPAR α , in the red and the white muscle. Here we found that PGC-1 α and PGC-1 β transcript abundances were greater in the red muscle compared to the white muscle and this corresponded with greater PPAR α and MCAD transcript abundances in the red muscle compared to the white muscle. This suggested that the PGC-1 transcriptional coactivators were involved in the upregulation of MCAD transcript abundance in the red muscle through their interactions with PPAR α .

Abbreviations

Pacific bluefin tuna, PBT, Fork length, FL; Body mass, BM; peroxisome proliferator-activated receptor γ co-activator-1, PGC-1; Medium-chain acyl-Coenzyme A dehydrogenase, MCAD; peroxisome proliferator-activated receptor α , PPAR α ; Cytochrome c oxidase subunit, COX; Citrate synthase, CS

2.1. Introduction

4.1.1. The PGC-1 transcriptional coactivator family in mammals

Transcriptional coactivators are proteins that bind to transcription factors and increase the rate of transcription of their target genes without binding to DNA themselves (Puigserver et al., 1999). In mammals, there are three different transcriptional co-activators belonging to the peroxisome proliferator-activated receptor γ co-activator-1 (PGC-1) family and they are PGC-1 α , PGC-1 β and PGC-related coactivator (PRC) (Andersson and Scarpulla, 2001, Kressler et al., 2002, Lin et al., 2002a). PGC-1 α and PGC-1 β are considered to be master regulators of mitochondrial biogenesis because they interact with certain transcription factors to upregulate the expression of mitochondrial genes. PRC may play a similar role, but it has not been as intensively investigated. PGC-1 α was the first in this family to be discovered (Puigserver et al., 1998).

4.1.2. PGC-1 α in mammals

In mammals, PGC-1 α was first identified as an activator of the transcription factor peroxisome proliferator-activated receptor-gamma (PPAR γ), hence its name (Puigserver et al., 1998). Since its initial discovery, PGC-1 α has been shown to be an important transcriptional coactivator that coordinates the up-regulation of mitochondrial biogenesis and function in response to stimuli such as cold temperature treatment and endurance-type exercise training (Lin et al., 2005a, Arany, 2008, Liu and Lin, 2011). It has been shown to interact with many different transcription factors. These include, PPAR α , estrogen related receptor- α (ERR α), nuclear respiratory factors (NRF) 1 and 2 and myocyte-specific enhancer factor 2 (MEF2). When PGC-1 α interacts with PPAR α , it upregulates fatty acid β -oxidation by increasing the transcription of genes that encode enzymes involved in β -oxidation, which occurs predominantly in mitochondria. The genes upregulated by PPAR α include the acyl-CoA dehydrogenase (ACADM) gene which encodes the medium chain acyl-CoA dehydrogenase (MCAD) enzyme which catalyses the initial step in the β -oxidation of medium-chain fatty acids (i.e. fatty acids with chain lengths between 6 and 12 carbon atoms) in mitochondria (Vega et al., 2000, Lehman and Kelly, 2002). Long-chain fatty acids (LCFAs, chain lengths >12 carbon

atoms) and very long-chain fatty acids (VLCFAs, chain lengths >22 carbon atoms) are partially broken down by long-chain acyl-CoA dehydrogenase (LCAD) and very long-chain acyl-CoA dehydrogenase (VLCAD) in the peroxisomes but cannot be degraded to completion. The chain-shortened fatty acids are subsequently exported to mitochondria where they can be further broken down by enzymes such as MCAD and short-chain acyl-CoA dehydrogenase (SCAD) which oxidise medium-chain and short-chain fatty acids (SCFAs, chain lengths <6 carbon atoms), respectively (Camões et al., 2009, Schrader et al., 2015). When PGC-1 α interacts with ERR α , it upregulates genes involved in mitochondrial biogenesis, oxidative phosphorylation and β -oxidation, including MCAD. When PGC-1 α interacts with NRF-1 and 2 it directly or indirectly upregulates the transcription of genes that encode enzymes in the mitochondrial electron transfer chain (mETC) (Collu-Marchese et al., 2015). Examples of these are the genes that encode the subunits that constitute cytochrome c oxidase (COX), the last enzyme in the mETC. COX is made up of 13 subunits encoded by both the nuclear and mitochondrial genomes. PGC-1 α is directly involved in upregulating the transcription of the nuclear encoded COX subunits, such as COXIV and it does this through its interaction with NRF-1 (Scarpulla, 2002, Dhar et al., 2008, Collu-Marchese et al., 2015). PGC-1 α is also indirectly involved in upregulating the transcription of the mitochondrially encoded COX subunits, such as COXI and it does this by upregulating the expression of the mitochondrial transcription factor A (TFAM), by interacting with NRF-1 and NRF-2 (Jornayvaz and Shulman, 2010). PGC-1 α also interacts with MEF2. When it does this, it promotes a switch from white ('fast-twitch', predominantly glycolytic) to red ('slow-twitch', predominantly oxidative) muscle fibres (Lin et al., 2002b).

4.1.3. Muscle fibre types in mammals

In vertebrates, in general, there are three main types of muscle fibres, the Type I fibres, (red, 'slow twitch', predominantly oxidative), the Type IIa fibres, (red, 'fast twitch', predominantly aerobic) and the Type IIb fibres, (white, 'fast twitch', predominantly glycolytic). The Type I muscle fibres are used for endurance type activities and they have large numbers of mitochondria. In contrast, the

Type IIb muscle fibres are used for burst type activities and they have fewer mitochondria. The Type IIa muscle fibres are an intermediate type between the Type I and the Type IIb muscle fibres (Karp, 2001, Spangenburg and Booth, 2003). The difference in mitochondrial abundance between the fibre types is consistent with the different functions of the different muscle types. In contrast to the red muscle fibres, which are used for endurance type activity and are resistant to fatigue, the white muscle fibres are used for short powerful, burst-type activities, such as the pursuit of prey, but they fatigue quickly. The large number of mitochondria in the red muscle fibres produces energy aerobically to support sustained endurance type exercise (Glancy and Balaban, 2011).

4.1.4. Regulation of PGC-1 α in mammals

In mammals, PGC-1 α gene and protein expression is upregulated in response to stimuli such as endurance-type exercise and cold acclimation (Lin et al., 2005a, Liu and Lin, 2011). For example, it has been observed in a study with biopsies taken from the predominantly 'fast twitch' human vastus lateralis muscle, that there are transient increases in PGC-1 α gene and protein expression, reaching a maximum increase within 2 h after exercise and sustained for 3 h (Pilegaard et al., 2003). In a different study PGC-1 α protein content in the Type IIa fibres of the quadriceps gradually increased when rats were endurance trained for a period of 60 min, twice per day and 5 days per week for 4, 11, 25, or 53 days (Taylor et al., 2005).

The effects of external stimuli have also been shown in a study where rats were maintained at a suboptimal temperature of 4°C for 45 days (Stancic et al., 2013). During this study there was a gradual increase in PGC-1 α transcript abundance in the gastrocnemius muscle (contains predominantly Type I muscle fibres) of the rats maintained at 4°C compared to the control rats that were maintained at approximately 22°C.

4.1.5. PGC-1 β in mammals

PGC-1 β was first identified due to nucleotide sequence similarities with PGC-1 α (Lin et al., 2002a). Due to the similarities between PGC-1 α and PGC-1 β , it has been proposed that PGC-1 β also interacts with the transcription factors

mentioned above, meaning that PGC-1 β and these transcription factors have similar effects in terms of promoting the expression of genes involved in muscle mitochondrial biogenesis and function and differentiating red muscle fibres from white (Lin et al., 2005a, Arany et al., 2007). In addition, PGC-1 β , but not PGC-1 α , has been shown to interact with sterol regulatory element-binding protein (SREBP) transcription factors to activate the expression of genes involved in lipogenesis (Lin et al., 2005b). While endurance-type exercise has been shown to result in increased PGC-1 α transcript abundance in skeletal muscle, the opposite has been observed for PGC-1 β . For example, in a study where the effects of 10 weeks of endurance training on human vastus lateralis muscle (40–56% Type I fibers) were investigated, it was found that PGC-1 β transcript abundance decreased by approximately 35% (Mortensen et al., 2007).

4.1.6. PGC-1 α and PGC-1 β in fishes

The PGC-1 α amino acid sequence is highly conserved between all members of the subphylum vertebrata except for the ray-finned fishes, a subclass of the bony fishes (LeMoine et al., 2010a). This conservation includes the leucine rich motifs that facilitate binding between PGC-1 α and transcription factors from the family of nuclear receptors such as PPAR α and ERR α but not the recognition site for AMP-activated protein kinase (AMPK) or the NRF-1, PPAR γ and MEF2c transcription factor binding domains (LeMoine et al., 2010a, Bremer et al., 2016). In the ray-finned fishes, the transcription factor binding domains are interrupted by various insertions including serine (S)-rich and glutamine (Q)-rich insertions (Wu et al., 1999, Michael et al., 2001, LeMoine et al., 2010a). Thus, it is proposed that PGC-1 α may have a different role in ray-finned fishes (LeMoine et al., 2010a).

Compared with the wealth of information available for mammals, comparatively little is known about the role of PGC-1 α fishes. However in fishes, as in mammals, the expression of PGC-1 α is influenced by suboptimal temperatures (LeMoine et al., 2008, McClelland et al., 2006). For example, LeMoine et al. (2008) reported that PGC-1 α transcript abundance was reduced by more than 50% in the red muscle and white muscle of goldfish held at a suboptimal temperature of 4°C for six weeks compared to control fish

maintained at 20°C. In contrast, the transcript abundance of PGC-1 β did not differ between the fish maintained at 4°C and 20°C. This suggests that unlike PGC-1 α , PGC-1 β transcript abundance remains constant with decreasing temperature in the red muscle of goldfish. The same trend was observed for white muscle, but this was not statistically significant. In the same study, LeMoine et al. (2008) found that PPAR α transcript abundance decreased by approximately 80% in the red muscle and the white muscle of the fish maintained at 4°C compared with the control fish. Similar to what was observed for PGC-1 α , this indicated that there was a strong negative correlation between decreasing water temperature and PPAR α transcript abundance. In a different study, this time with zebrafish, McClelland et al. (2006) found that there was no statistically significant difference in PGC-1 α transcript abundance in the skeletal muscle (presumably white muscle) between zebrafish maintained either at 18 or 28°C. In contrast, PPAR α transcript abundance was significantly lower in the fish maintained at 18°C compared with the fish maintained at 28°C.

In fishes, as in mammals, the expression of PGC-1 α has also been shown to be influenced by endurance exercise. For example, LeMoine et al. (2010b), reported that when zebrafish were endurance trained over a period of 8 weeks, it was found that PGC-1 α transcript abundance increased approximately 3-fold in the red and 4-fold in the white muscle after one week of this training, but returned to the pre-training levels after 8 weeks. In the same study, there was an approximately 3-fold increase in PGC-1 β transcript abundance in the red muscle of the trained fish after one week but this also returned to pre-training levels after 8 weeks. In contrast, the endurance training had no significant effect on PGC-1 β transcript abundance in the white muscle.

4.1.7. The role of the PGC-1 family of transcriptional co-activators in regionally endothermic fishes.

The role of the PGC-1 family of transcriptional co-activators in regionally endothermic fishes has not been investigated. Regionally endothermic fishes are unusual because they can produce and retain sufficient metabolic heat to warm certain regions of their bodies (Dickson and Graham, 2004). As a result, these tissues are maintained at temperatures significantly in excess of the

ambient water temperature. This is in contrast to ectothermic fishes, whose body temperatures are typically the same or only slightly warmer than the ambient water temperature. Fishes that are regional endothermic include tunas (Family Scombridae), billfishes (Family Istiophoridae), lamnid sharks (Family Lamnidae), the common thresher shark (*Alopias vulpinus*, Family Alopiidae) and the opah (*Lampris guttatus*, Family Lampridae) (Dickson and Graham, 2004, Sepulveda et al., 2005, Wegner et al., 2015). In most tunas, the red ('slow-twitch', predominantly oxidative) skeletal muscle that is used for sustained cruise-type swimming and the eye/brain are endothermic but in the bluefin tunas, in addition to these tissues, the viscera are also endothermic (Dickson and Graham, 2004). Atlantic bluefin tuna (ABT, *Thunnus thynnus*), Pacific bluefin tuna (PBT, *Thunnus orientalis*) and southern bluefin tuna (SBT, *Thunnus maccoyii*) belong to the bluefin group. The lamnid sharks are also regionally endothermic and maintain elevated temperatures in their red skeletal muscle, eye/brain and viscera. An important difference though is that lamnid sharks give birth to pups which are miniature versions of their parents and most likely begin life as endotherms whereas tunas that hatch from eggs have a larval stage and begin life as ectotherms but later transition to become regional endotherms (Dickson, 1994). Recently we demonstrated that PBT can significantly elevate their red skeletal muscle temperature above the ambient water temperature at a minimum body size of ~29 cm fork length (FL), corresponding to a minimum age of ~5.5 months. In addition, we also showed that in the same fish, the activities of the mitochondrial marker enzymes citrate synthase (CS) and COX were approximately an order of magnitude greater in the red muscle than in the white muscle. Furthermore, CS enzyme activity decreased with increasing body size in both the red muscle and the white muscle. This suggested that mitochondrial abundance was decreasing with increasing body size. Having observed that the mitochondrial marker enzyme activities were greater in the red muscle than in the white muscle, it can be concluded that mitochondrial abundance/aerobic metabolic capacity was also greater in the red muscle compared to the white muscle. Due to the role of the PGC-1 transcriptional coactivators in mitochondrial biogenesis and function in mammals it is possible that PGC-1 α , and possibly also PGC-1 β , expression could also be greater in the red muscle than in the white muscle of fishes. However, the lack of conservation in the NRF-1, PPAR γ and MEF2c

transcription factor binding domains between mammals and ray-finned fishes could indicate that this may not be the case (Wu et al., 1999, Michael et al., 2001, LeMoine et al., 2010a).

4.1.8. Aims

The overall aim of the present study was to determine whether PGC-1 α is involved in the development of regional endothermy in PBT by investigating the effect of fish body size/age on PGC-1 α transcript abundance in red muscle and white muscle during the development of regional endothermy in PBT. We also investigated the expression of PGC-1 β and the transcription factor PPAR α , which is known to interact with PGC-1 α , and its target gene MCAD. We hypothesised that the transcript abundance of all of the genes of interest would be greater in the red muscle compared with the white muscle due to their role in fatty acid β -oxidation. An additional aim of this study was to further clarify the differences between mammals and ray-finned fishes, especially regionally endothermic ray-finned fishes, in terms of the roles of the PGC-1 transcription factors.

4.2. Materials and Methods

4.2.1. Fish sampling

Three groups of young PBT juveniles, ranging in size from 18.5 to 62.5 cm fork length (FL) and 71 to 5,350 g body mass (BM), were caught in Japanese waters and used for this study. The Group one fish [18.5 – 21.2 cm fork length (FL), 71 – 142 g body mass (BM), $n = 21$] were caught by fishermen operating offshore from the port of Kaminokae (Kochi Prefecture, Shikoku Island) on the 2nd of August 2016 (late summer, $T_a = 29.4^\circ\text{C}$) (Fig. 1). The Group two fish [33.3 – 42.6 cm FL, 750 – 1,700 g BM, $n = 10$] and the Group three fish [57.5 – 62.5 cm FL, 4,050 – 5,350 g BM, $n = 4$] were caught from a sea cage farm approximately 1 km offshore from the town of Imazato (Nagasaki Prefecture, Tsushima Island) on the 28th of November 2016 (late autumn, $T_a = 20.4$) and the 27th of March 2017 (early spring, $T_a = 15.8^\circ\text{C}$), respectively. The fish were subjected to the temperature measurements described in Chapter 2 and then immediately afterwards samples of the red and white skeletal muscle were taken for the gene expression analyses described here. Four samples ($\sim 0.5\text{ cm}^3$) of each muscle type were taken, at $\sim 40\text{-}50\%$ of FL from the snout, from the left side of the fish. Initially, the samples were immersed in RNA $later^{\text{®}}$ (Ambion $^{\text{®}}$) on ice and then later they were transferred, in this same solution, to a refrigerator at -20°C for longer-term storage. The samples used in this chapter were the same as those used for the gene expression analyses in Chapter 3.

4.2.2. RNA extraction and cDNA synthesis

RNA was extracted, essentially as described by the manufacturer, using an RNeasy $^{\text{®}}$ Fibrous Tissue Mini Kit (QIAGEN). To do this, the tissue samples described above (Section 4.2.1) were removed from the RNA $later^{\text{®}}$ storage solution and gently blotted and then approximately 60 mg of tissue was disrupted in 300 μL of the RLT buffer, supplied with the kit, with 40 mM dithiothreitol (DTT) added. The tissue disruption was performed using a TOMY micro Smash $^{\text{TM}}$ MS-100 tissue homogeniser set at 4,000 rpm for 45 s. The extraction method included an optional on-column RNase-free DNase I digestion to remove any genomic DNA that might have been contaminating

the RNA. The RNA concentration was quantified using a NanoDrop™ 1000 spectrophotometer (Thermo Scientific) and one µg of the extracted RNA was used as the template to synthesise first strand cDNA. The first strand cDNA was synthesized using a SuperScript® IV Reverse Transcriptase Kit (Invitrogen™) and the synthesized cDNA was subsequently stored at -20°C until it was required.

4.2.3. Primer design for cloning a PGC-1α cDNA from PBT red muscle using conventional polymerase chain reaction

Primers were designed to clone a large fragment of the open reading frame (ORF) of a PGC-1α cDNA from PBT red muscle using conventional polymerase chain reaction (PCR). At the time of this research, there were no publicly available PGC-1α cDNA sequences for PBT, or any other tuna species. Therefore, the primers were designed using the unannotated whole genome shotgun contigs database for PBT (accession number BADN000000000 available at <http://www.ncbi.nlm.nih.gov/>). The primers were designed in several steps as follows. Firstly, a yellowtail kingfish (YTK, *Seriola lalandi*) PGC-1α cDNA sequence (accession number KU869768.1) was used to perform a Basic Local Alignment Search Tool (BLAST) search of the unannotated PBT whole genome shotgun contigs database. This resulted in multiple different contigs being retrieved from the database. Each contig was aligned individually with the YTK PGC-1α query sequence using ClustalX 2.1 (Larkin et al., 2007) and then regions of conservation adjacent to the 5' and 3' ends of the ORF were chosen for primer design. Initially, the primers were designed using Primer3 (version 0.4.0) (Untergasser et al., 2012). Primer3 was set to choose primers with a length of 20 bp, a melting temperature of approximately 60°C and a GC content between 40 and 60%. Subsequently the primers designed using Primer3 were tested for their suitability for PCR using Oligo Analyzer Version 3.1 (<http://sg.idtdna.com/analyzer/Applications/OligoAnalyzer/>). Oligo Analyzer was used to check for primer-dimer formation and for the formation of secondary structures within the primers which if present could reduce the amplification efficiency of the PCR amplification. Finally, the selected primers were ordered from GeneWorks Pty. Ltd. (Australia).

Table 4.1. PCR primer sequences

Primer	Sequence (5' → 3')	Usage
PGC-1 α qRT F	CTGCCTTGGTTGGTGAAGAC	cDNA cloning/qRT-PCR
PGC-1 α R1	GTTTGCTGCCTGGTTCTCTC	cDNA cloning
PGC-1 α R2	CTGCTTAGCCAAAGGACCAG	cDNA Sequencing
T7 ¹	TAATACGACTCACTATAGGG	cDNA sequencing
SP6 ¹	TATTTAGGTGACACTATAG	cDNA sequencing
β -actin F ²	ACCCACACAGTGCCCATCTA	qRT-PCR
β -actin R ²	TCACGCACGATTTCCCTCT	qRT-PCR
PGC-1 α qRT R	CAACGAAGCAGCCAATCTTT	qRT-PCR
PPAR α F	GATTTTCCACTGCTGCCAAT	qRT-PCR
PPAR α R	CGCCTCATACACGCCATA	qRT-PCR
MCAD F	GAGGAAGACGTTTGGCAGAG	qRT-PCR
MCAD R	GCAATGGAGGCAAAGTAGGT	qRT-PCR
PGC-1 β F	GTATGGGGAGGAGGAGGTGT	qRT-PCR
PGC-1 β R	CAGCTCGCTGAGACAGTTGA	qRT-PCR

¹ Promega T7 (Q5021) and SP6 (Q5011) primers

² Designed by Agawa et al. (2012)

All of the remaining primers were designed by the author (Section 4.2.6)

4.2.4. Conventional polymerase chain reaction for cloning a PGC-1 α cDNA from PBT red muscle

Total RNA was extracted, and first-strand cDNA was synthesised as described in Section 4.2.2. Primers were designed for conventional PCR as described in Section 4.2.3. Conventional PCR was performed as follows. Each 50 μ L reaction contained 5 μ L of a 1:5 dilution of PBT red muscle cDNA, 0.2 μ M each of the relevant forward and reverse primers (Table 4.1), 200 μ M dNTPs (Promega), 2.5 units of *Taq* DNA Polymerase (New England Biolabs) and 5 μ L of 10x ThermoPol[®] Buffer (New England Biolabs). The PCR cycling conditions consisted of an initial denaturation step at 95°C for 30 s followed by 30 cycles of denaturation at 95°C for 30 s, annealing at 60°C for 30 s and extension at 68°C for 4 min. At the end of the cycling, there was a final extension step at 68°C for 5 min. The cycling was done in a Hybaid PX2 thermal cycler (Thermo Scientific) and when it was complete, the PCR reaction mixture was subjected to electrophoresis on a 1.5% (w/v) agarose gel containing 1 \times SYBR[®] Safe DNA Gel Stain (Invitrogen[™]) to determine whether the products were of the expected size. The PCR products in the agarose gel were visualised using a Gel Doc[™] EZ System (Bio-Rad) and a digital image was obtained using Image Lab software (version 4.0) (Bio-Rad). Products close to the expected size were purified from the gel using the Wizard[®] SV Gel and PCR Clean-Up System (Promega) according to the manufacturer's instructions.

4.2.5. Cloning of the PGC-1 α PCR product in *Escherichia coli*

The gel purified PGC-1 α PCR products obtained in Section 4.2.4 were ligated into the pGEM[®]-T Easy vector (Promega) and the resulting constructs were used to transform *Escherichia coli* 5 α competent cells (New England Biolabs). To test for successful transformation, the cells were plated onto Luria broth (LB) agar containing 100 μ g/mL ampicillin and colonies that were resistant to the antibiotic were selected. The selected colonies were screened for the presence of the PGC-1 α insert using colony PCR. Colony PCR was performed using primers targeting the T7 and SP6 promoter regions of the vector (Table 4.1). Confirmed positive colonies were cultured overnight at 37°C in LB broth containing 100 μ g/mL ampicillin. Following the overnight culture, plasmid DNA was extracted from the cells using the Wizard[®] Plus SV Minipreps DNA

Purification System (Promega) and the insert DNA was sequenced in both directions using primers that targeted the T7 and SP6 promotor regions in the vector. This produced sequence data for approximately 770 bp at the 5'- and approximately 620 bp at the 3'-end of the PGC-1 α cDNA but no data for the central region between these ends. Thus, a new primer was designed to obtain the sequence of the central region. The procedure followed was essentially as described in Section 4.2.3 except that the now known sequence of the newly cloned PBT PGC-1 α cDNA was used as the template to design the new primer. The cDNA sequence obtained in this way overlapped with the cDNA sequences obtained from the 5' and 3' ends. Using this approach, sequence data were obtained from 8 independent colonies and all colonies yielded the same sequence. The resulting sequence data were used to perform BLAST searches of the GenBank database (available at <http://www.ncbi.nlm.nih.gov/>) to confirm the identity of the PCR products.

4.2.6. Quantitative real time polymerase chain reaction

The expression of PGC-1 α , PGC-1 β , PPAR α , MCAD and the normalization gene β -actin, in the red and white muscle of the PBT specimens sampled for this study, was investigated using quantitative real time polymerase chain reaction (qRT-PCR). The primers for this procedure were designed essentially as described above for the primers for conventional PCR (Section 4.2.3), but with some modifications. The sequence of the newly cloned PGC-1 α cDNA from PBT red muscle (Section 4.2.5) was used directly to design the primers for this gene but for the other genes, the indirect approach described in Section 4.2.3 was used. Specifically, cDNA sequences for large yellow croaker (*Larimichthys crocea*) PGC-1 β (accession no. XM_019255239.1), Atlantic bluefin tuna (*Thunnus thynnus*) PPAR α (accession no. KU900605.1) and greater amberjack (*Seriola dumerili*) MCAD (accession no. XM_022758058) were used to query the unannotated whole genome shotgun contigs database for PBT and then the contigs thus retrieved were used for primer design as described in Section 4.2.3. Each qRT-PCR reaction (total volume 20 μ L) contained 5 μ L of the relevant cDNA, 10 μ L of the KAPA SYBR[®] FAST qPCR Master Mix (2X) Universal (KAPA Biosystems), 200 nM each of the relevant forward and reverse primers (Table 4.1) and the appropriate volume of autoclaved deionized water. Amplification was performed using a Rotor-Gene

Q thermal cycler (QIAGEN) fitted with fluorescence detection. The cycling conditions consisted of an initial denaturation step at 95°C for 3 min followed by 40 cycles of denaturation at 95°C for 3 s, annealing at 60°C for 20 s and extension at 72°C for 20 s. At the end of each amplification run, melt curve analysis was performed to ensure that only one product was produced for each set of primers. This was done by raising the temperature from 60 to 95°C in 0.5°C increments and observing the fluorescence change as the DNA strands separated. Amplification of only one product was confirmed by analysing the products using agarose gel electrophoresis.

4.2.7. Preparation of the standards for qRT-PCR

Transcript abundance for the genes of interest was determined using absolute quantification. Thus, it was necessary first to prepare standards for each of the genes interest. The standards were prepared using conventional PCR and cloning in *E. coli* as described in Sections 4.2.4 and 4.2.5, respectively, but with some modifications. In particular, the extension time during the PCR cycling was reduced to 1 min and the products produced were purified directly from the reaction mixture, rather than first being subjected to gel electrophoresis. Once the standards had been prepared and their identity had been confirmed, using sequencing, the copy number for each standard was determined using the equation:

$$\begin{aligned} & \text{Copies per } \mu\text{L} \\ &= \frac{(\text{amount of plasmid DNA construct (ng)} \times 6.022 \times 10^{23})}{(\text{length of plasmid DNA construct (bp)} \times 1 \times 10^9 \times 650 \text{ Daltons})} \end{aligned}$$

Following this, a series of 10-fold dilutions was prepared for each of the standards and these dilutions were stored as single use aliquots at -20°C until they were required.

4.2.8. Preparation of the samples for qRT-PCR

To quantify the expression of the genes of interest in the red and white muscle of the PBT specimens sampled for this study, RNA was extracted, and first-strand cDNA was synthesised as described in Section 4.2.2 and then qRT-PCR was performed as described in Section 4.2.6. Prior to these analyses, various dilutions of the cDNAs from the various tissues were tested for each of

the genes of interest to determine the optimal amount of cDNA to be added to each reaction. The optimal amount of cDNA was the amount that produced fluorescence curves within the middle of the range of the fluorescence curves produced for the standards, i.e., the 10-fold dilutions of the plasmid constructs. Once the optimal cDNA concentrations had been determined, qRT-PCR analyses of the standards and the appropriately diluted cDNAs were performed side by side in the same run. Each run included all of the cDNAs from both the red and the white muscle from either the Group one (smallest, ~20 cm FL), Group two (intermediate-sized, ~40 cm FL) or Group three (largest, ~60 cm FL) fish for one of the genes of interest plus a no template control and a no reverse-transcriptase control. Preliminary analyses had shown that each primer pair gave only one product and for all primer pairs, the amplification efficiency was between 90 and 105%. The amplification efficiency was calculated by plotting the \log_{10} of the DNA copy number against the corresponding C_t value for each standard. The slope of this plot was then used in the following equation to determine the amplification efficiency for each primer: $Amplification\ efficiency\ (\%) = \left(10^{\left(\frac{-1}{slope}\right)} - 1\right) \times 100$. The transcript copy number for each of the genes of interest was then calculated by comparing the C_t values for the cDNAs with the C_t values for the standards and multiplying the copy number per microgram of RNA by the total RNA extracted per mg tissue in order to obtain the copy number per mg tissue. All of the cDNA samples were analysed in duplicate (technical replication) and the average values for the duplicates were used in the calculations. In addition to calculating the transcript abundance per g tissue, the relative transcript abundance for the genes of interest was calculated by dividing the transcript abundance for the gene of interest by the transcript abundance for the housekeeping gene β -actin.

4.2.9 Statistical analyses

All statistical analyses were performed using the IBM® SPSS Statistics version 22.0 software package (IBM, New York, USA). Independent-samples t-tests were performed to test for significant differences in the transcript abundance between the red and the white muscle. This comparison between tissues was made independently for the smallest, intermediate-sized and largest fish.

Scaling coefficients were calculated through linear regression analysis of the \log_{10} of the variable of interest and the \log_{10} of BM. Pearson correlation analyses were used to determine whether the relationship between the transcript abundances of the PGC-1 transcriptional coactivators and either PPAR α or MCAD were significant. For all of the statistical tests applied in this study, values were considered to be statistically significantly different when $P < 0.05$.

4.3. Results

4.3.1. Sequence analysis of a PGC-1 α cDNA from PBT red muscle

We have cloned approximately two-thirds of the open reading frame (ORF) of a PGC-1 α gene from PBT red muscle. The cDNA was deposited in the NCBI nucleotide database with the accession no. MF737438.1 and the corresponding protein has the accession no. ASX95437.1. When the translated protein sequence was aligned with other PGC-1 α proteins, the protein from PBT appeared to be missing ~18 amino acids at the N-terminus and ~336 amino acids at the C-terminus of the ORF (Fig. 4.1). Nevertheless, the remainder of the protein still contained the canonical motifs that are characteristic of PGC-1 α proteins from vertebrates in general. Specifically, it contained the transcriptional activation domains, AD1, with the sequence DLPELDLSELD and AD2, with the sequence NEANLLAVLTETLD, at residues 30 – 40 and 82 – 95, respectively, relative to the brown rat sequence (Sadana and Park, 2007b). It contained the three leucine-rich motifs L1, with the sequence LLAVL, L2, with the sequence LKKLL, and L3, with the sequence LLKYL, at residues 86 – 90, 142 – 146 and 208 – 212, respectively, relative to the brown rat sequence (Knutti et al., 2001). In mammals, the L2 motif facilitates binding between the PGC-1 α protein and transcription factors from the nuclear receptor family, including PPAR α (Vega et al., 2000). In mammals, the L3 motif facilitates binding between the PGC-1 α and ERR α proteins, another member of the nuclear receptor family (Huss et al., 2002). Furthermore, it also contained the tri-lysine motif (KKK) typical of the NRF-1 interaction domain at residues 237 – 239, relative to the brown rat sequence.

In contrast to the above, there were certain regions that were not so well conserved. Specifically, this refers to the recognition site for AMP-activated protein kinase (AMPK) and the binding sites for certain of the transcription factors. In the brown rat sequence, there is a recognition site for AMPK between residues 165 and 186 (numbered according to the brown rat sequence). In mammals, AMPK has been shown to activate PGC-1 α by phosphorylating a threonine residue (Thr₁₇₇) within the AMPK recognition site (Jager et al., 2007). This residue is highly conserved between chicken (representing birds), the Chinese alligator (representing reptiles) and the African clawed frog (representing amphibians) but not in PBT or any of the

other fish sequences from the classes of bony fishes (both ray-finned and lobe-finned fishes) or cartilaginous fishes. In the PBT sequence, the AMPK binding site is highly conserved but the Thr₁₇₇ residue that is phosphorylated by AMPK is absent. Instead, a proline residue can be found at this site in PBT.

In the brown rat sequence (representing mammals), there is a binding site for NRF-1 at residues 180 – 403 (Wu et al., 1999). This is well conserved in the chicken (representing birds), the Chinese alligator (representing reptiles), the African clawed frog (representing amphibians), the spiny dogfish (representing cartilaginous fishes) and the West African lungfish (representing bony fishes in the subclass of the lobe-finned fishes) (Fig. 4.1). However, it is not well-conserved in either the swordfish or PBT, both of which are bony fishes in the subclass of the ray-finned fishes (Fig. 4.1). In these ray-finned fishes, the canonical NRF-1 binding site is interrupted by a serine (S)-rich insertion, a glutamine (Q)-rich insertion and multiple mixed amino acid residue insertions. Similarly, in the brown rat sequence there is a binding site for PPAR γ at residues 338 – 403 (Puigserver et al., 1998). Again this is well conserved in the representatives of the birds, reptiles, amphibians, cartilaginous fishes and lobe-finned fishes but not in the ray-finned fishes, including PBT. In the ray-finned fishes (PBT and swordfish), this transcription factor binding site is interrupted by mixed amino acid residue insertions. Finally, in the brown rat sequence, there is a binding site for MEF2 at residues 403 – 570 that is well conserved in all of the other vertebrates except the ray-finned fishes (Michael et al., 2001). In PBT, this region was not cloned but it is interrupted by a large mixed amino acid residue insertion in the swordfish sequence.

Fig. 4.1. A multiple sequence alignment of PGC-1 α amino acid sequences from representatives of six of the seven classes that make up the subphylum vertebrata. The GenBank accession numbers are as follows: PBT (bony fishes/ray-finned fishes), ASX95437.1; swordfish (bony fishes/ray-finned fishes), ACY24361.1; West African lungfish (bony fishes/lobe-finned fishes), FJ710608.1; spiny dogfish (cartilaginous fishes), ACY24363.1; African clawed frog (amphibians), ACY24354.1; Chinese alligator (reptiles), XP_025061364.1; chicken (birds), NP_001006457.1; brown rat (mammals), NP_112637.1. The alignment was performed using ClustalX2 software (Larkin et al., 2007) and the shading was done using GeneDoc software (Nicholas et al., 1997). The degree of amino acid conservation is indicated by 3 levels of shading with black, dark grey and light grey indicating 100, 80 and 60% conservation, respectively. The transcription activation domains are indicated by DLPELDLSELD (AD1) and NEANLLAVLTETLD (AD2) above the sequences. The leucine-rich motifs (L1, L2 and L3) are indicated by grey text and the tri-lysine motif is indicated by KKK. The AMPK recognition site is indicated by light grey shading above the sequences and Thr₁₇₇ is indicated by dark grey shading and 'T'. The NRF-1, PPAR γ and MEF2C transcription factor binding sites are indicated by black solid, grey solid and black dotted lines, respectively, above the sequences. The RNA recognition motif is indicated by a dashed line above the sequences.

4.3.2. Phylogenetic analysis of the PBT PGC-1 α amino acid sequence

Fig. 4.2 shows the results of a phylogenetic analysis with the PBT PGC-1 α amino acid sequence compared with PGC-1 α amino acid sequences from six of the seven classes that make up the subphylum vertebrata. No data were available for the seventh class, the jawless fishes (class Agnatha). From the figure it is clear that there are two major clades, one containing bony fishes from the subclass of the ray-finned fishes (class Osteichthyes, subclass Actinopterygii) and the other containing all of the other vertebrates, including bony fishes from the subclass of the lobe-finned fishes (class Osteichthyes, subclass Sarcopterygii). This separation is most likely due to the insertions in the transcription factor binding sites in the PGC-1 α sequences from the ray-finned fishes. This applies to PBT as well as to the other ray-finned fishes in the phylogenetic analysis.

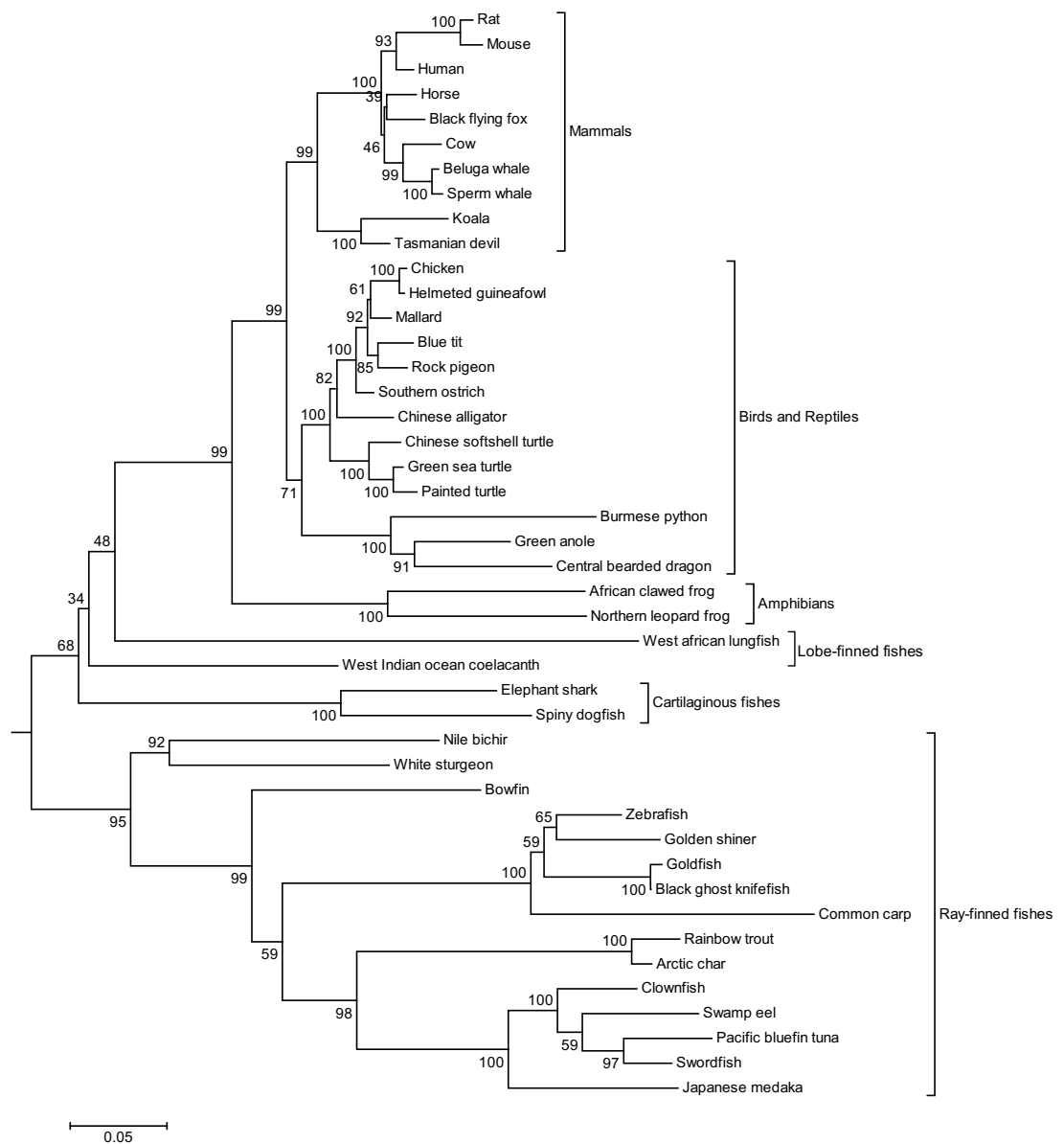


Fig. 4.2. A phylogenetic tree representing the evolutionary relationships between PGC-1 α amino acid sequences from six of the seven classes that make up the subphylum vertebrata. An invertebrate (oriental fruit fly) amino acid sequence was used as the outgroup to root the tree (sequence collapsed). The amino acid sequences were aligned using ClustalX2 software (Larkin et al., 2007) and the tree was constructed using the Neighbor-Joining method (Saitou and Nei, 1987) with Mega 6 software (Tamura et al., 2013). The scale bar indicates the estimated number of amino acid substitutions per site. Evaluation of statistical confidence was based on 1,000 bootstrap replicates. The species names and corresponding GenBank or Uniprot accession numbers can be found in Table 4.2.

Table 4.2. Species names and GenBank or Uniprot accession numbers for the amino acid sequences used to construct the phylogenetic tree in Fig. 4.2.

Class/Subclass	Taxon	Accession number
Mammalia (mammals)	Rat (<i>Rattus norvegicus</i>)	NP_112637.1
	Mouse (<i>Mus musculus</i>)	NP_032930.1
	Human (<i>Homo sapiens</i>)	NP_037393.1
	Horse (<i>Equus caballus</i>)	XP_023494058.1
	Black flying fox (<i>Pteropus alecto</i>)	ELK06450.1
	Cow (<i>Bos taurus</i>)	AAQ82595.1
	Beluga whale (<i>Delphinapterus leucas</i>)	XP_022422385.1
	Sperm whale (<i>Physeter catodon</i>)	XP_007130825.1
	Koala (<i>Phascolarctos cinereus</i>)	XP_020848134.1
	Tasmanian devil (<i>Sarcophilus harrisii</i>)	XP_003773396.1
Aves (birds)	Chicken (<i>Gallus gallus</i>)	NP_001006457.1
	Helmeted guineafowl (<i>Numida meleagris</i>)	XP_021251408.1
	Mallard (<i>Anas platyrhynchos</i>)	XP_005031720.1
	Blue tit (<i>Cyanistes caeruleus</i>)	XP_023781190.1
	Rock pigeon (<i>Columba livia</i>)	ACY24353.1
	Southern ostrich (<i>Struthio camelus australis</i>)	KFV80390.1
Reptilia (reptiles)	Chinese alligator (<i>Alligator sinensis</i>)	XP_025061364.1
	Chinese softshell turtle (<i>Pelodiscus sinensis</i>)	XP_006138222.1
	Green sea turtle (<i>Chelonia mydas</i>)	XP_007058167.1
	Painted turtle (<i>Chrysemys picta</i>)	ACY24356.1
	Burmese python (<i>Python bivittatus</i>)	XP_007429584.1
	Green anole (<i>Anolis carolinensis</i>)	ACY24355.1
	Central bearded dragon (<i>Pogona vitticeps</i>)	XP_020636089.1

Amphibia (amphibians)	African clawed frog (<i>Xenopus laevis</i>)	ACY24354.1
	Northern leopard frog (<i>Rana pipiens</i>)	ACY24357.1
Chondrichthyes (cartilaginous fishes)	Elephant shark (<i>Callorhynchus milii</i>) (PREDICTED)	XP_007887233.1
	Spiny dogfish (<i>Squalus acanthias</i>)	ACY24363.1
Osteichthyes (bony fishes)		
Sarcopterygii (lobe-finned fishes)	West African lungfish (<i>Protopterus annectens</i>)	FJ710608.1
	West Indian ocean coelacanth (<i>Latimeria chalumnae</i>)	H3B241
Actinopterygii (ray-finned fishes)	Nile bichir (<i>Polypterus bichir</i>)	ACY24364.1
	White sturgeon (<i>Acipenser transmontanus</i>)	ACY24367.1
	Bowfin (<i>Amia calva</i>)	ACY24368.1
	Common carp (<i>Cyprinus carpio</i>)	XP_018964173.1
	Zebrafish (<i>Danio rerio</i>)	ACY24358.1
	Golden shiner (<i>Notemigonus crysoleucas</i>)	ACY24360.1
	Goldfish (<i>Carassius auratus</i>)	ACY24365.1
	Black ghost knifefish (<i>Apteronotus albifrons</i>)	ACY24366.1
	Rainbow trout (<i>Oncorhynchus mykiss</i>)	ACY24359.1
	Arctic char (<i>Salvelinus alpinus</i>)	XP_023838104.1
	Japanese medaka (<i>Oryzias latipes</i>)	XP_023821574.1
	Clownfish (<i>Amphiprion ocellaris</i>)	XP_023133583.1
	Pacific bluefin tuna (<i>Thunnus orientalis</i>)	ASX95437.1
	Swordfish (<i>Xiphias gladius</i>)	ACY24361.1
	Swamp eel (<i>Monopterus albus</i>)	XP_020467108.1
Insecta (insects)	Oriental fruit fly (<i>Bactrocera dorsalis</i>)	JAC44983.1

4.3.3. The effects of tissue type and fish size on PGC-1 α transcript abundance

PGC-1 α transcript abundance was compared between the red and the white muscle and also between individuals of different sizes/ages. When expressed per g tissue, PGC-1 α transcript abundance was ~20-, ~100- and ~50-fold higher in the red muscle compared with white muscle in the smallest (~20 cm FL), intermediate-sized (~40 cm FL) and largest (~60 cm FL) PBT specimens, respectively, and the differences between the tissues were statistically significant ($P < 0.05$) (Figs. 4.3A and B). When comparing individuals of different sizes, we observed that the number of PGC-1 α transcripts per g tissue remained constant regardless of the fish size and regardless of the muscle type. Thus, increasing body size had no effect on PGC-1 α transcript abundance in either the red or the white muscle in the young PBT specimens we sampled.

4.3.4. The effects of tissue type and fish size on PGC-1 β transcript abundance

PGC-1 β transcript abundance, expressed per g tissue, was ~9-, ~6- and ~5-fold higher in the red muscle compared with white muscle in the smallest, intermediate-sized and largest PBT specimens, respectively, but the difference between the tissues was statistically significant only for the smallest fish. ($P < 0.05$) (Figs. 4.3C and D). In addition, the number of PGC-1 β transcripts per g tissue decreased significantly with increasing FL ($P < 0.05$, Fig. 4.3C) in the red muscle but not in the white muscle. The same was true for PGC-1 β transcript abundance with increasing BM in the red muscle, with a BM scaling coefficient of -0.42 ± 0.18 but there was no significant difference in the white muscle (Fig. 4.3D). Thus, the increase in body size had a significant effect on PGC-1 β transcript abundance in the red muscle but not in the white muscle. Compared with PGC-1 α transcript abundance, PGC-1 β transcript abundance was approximately an order of magnitude greater in the red muscle and approximately two orders of magnitude greater in the white muscle.

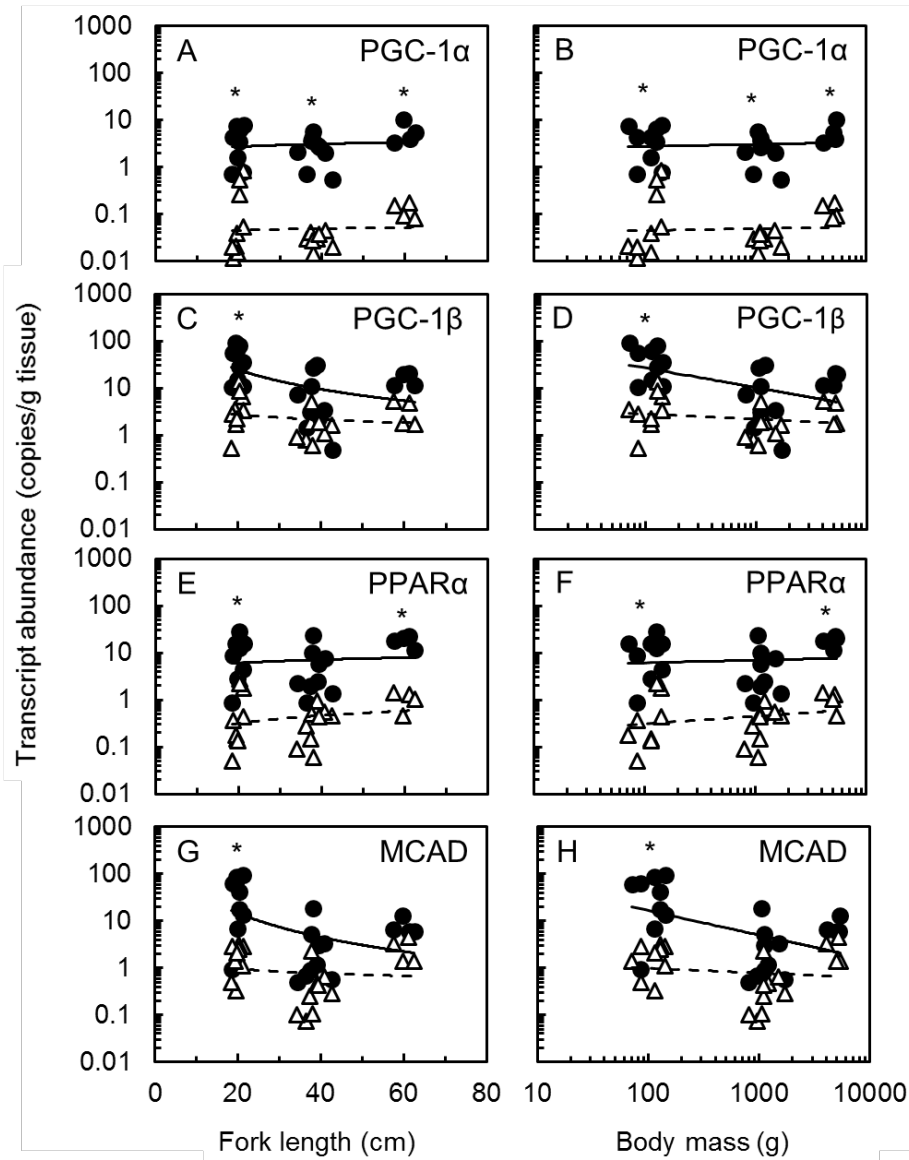


Fig. 4.3. The effects of muscle tissue type and body size on the number of transcripts per g tissue for PGC-1 α (A, B, values are $\times 10^9$), PGC-1 β (C, D, values are $\times 10^{10}$), PPAR α (E, F, values are $\times 10^7$) and MCAD (G, H, values are $\times 10^9$) in the red and white muscle of young PBT juveniles caught in Japanese waters. The data for the red muscle and the white muscle are represented by \bullet with solid lines and Δ with dashed lines, respectively. The best-fitting power functions for the data in the different panels are as follows: (A) red muscle $y = 1.50FL^{0.20}$, $R^2 = 0.01$; white muscle $y = 0.03FL^{0.13}$, $R^2 = 2.10 \times 10^{-3}$; (B) red muscle $y = 2.23BM^{0.05}$, $R^2 = 0.01$; white muscle $y = 0.04BM^{0.04}$, $R^2 = 2.59 \times 10^{-3}$; (C) red muscle $y = 1.58 \times 10^3 FL^{-1.39}$, $R^2 = 0.20$; white muscle $y = 8.14 FL^{-0.37}$, $R^2 = 0.03$; (D) red muscle $y = 184.71 BM^{-0.42}$, $R^2 = 0.22$; white muscle $y = 4.56 BM^{-0.11}$, $R^2 = 0.04$; (E) red muscle $y = 2.93 FL^{0.24}$, $R^2 = 0.01$; white muscle $y = 0.06 FL^{0.56}$, $R^2 = 0.04$; (F) $y = 4.79 BM^{0.05}$, $R^2 = 0.01$; white muscle $y = 0.15 BM^{0.16}$, $R^2 = 0.05$; (G) $y = 2.61 \times 10^3 FL^{-1.72}$, $R^2 = 0.20$; white muscle $y = 2.44 FL^{-0.31}$, $R^2 = 0.01$; (H) red muscle $y = 180.74 BM^{-0.52}$, $R^2 = 0.22$; white muscle $y = 1.61 BM^{-0.11}$, $R^2 = 0.02$. Significant differences in transcript abundance between the red and the white muscle are indicated by *.

4.3.5. The effect of tissue type and fish size on PPAR α transcript abundance

PPAR α transcript abundance, expressed per g tissue, was ~13-, ~16- and ~17-fold higher in the red muscle compared with white muscle in the smallest, intermediate-sized and largest PBT specimens, respectively. The differences between the tissues in the smallest and largest fish, but not in the intermediate-sized fish, were statistically significant ($P < 0.05$) (Figs. 4.3E and F). PPAR α transcript abundance showed no significant change either with increasing FL or with increasing BM in either the red muscle or the white muscle. Thus, increasing body size had no effect on PPAR α transcript abundance in either the red or the white muscle in our juvenile PBT specimens.

4.3.6. The effect of tissue type and fish size on MCAD transcript abundance

MCAD transcript abundance, expressed per g tissue, was ~23-, ~7- and ~3-fold higher in the red muscle compared with white muscle in the smallest, intermediate-sized and largest PBT specimens, respectively, however, the apparent difference between the tissues was statistically significant only in the smallest fish ($P < 0.05$) (Figs. 4.3G and H). There was a significant decrease in MCAD transcript abundance in the red muscle with increasing FL and also with increasing BM, with a BM-dependent scaling coefficient of -0.52 ± 0.22 . In contrast, there was no significant change in MCAD transcript abundance either with increasing FL or with increasing BM in the white muscle. Thus, the increase in body size had influenced MCAD transcript abundance in the red muscle but not in the white muscle

4.3.7. The effect of tissue type and fish size on β -actin transcript abundance

β -actin is a frequently used normalization gene in qRT-PCR analyses (Hendriks-Balk et al., 2007). Normalization genes are used in qRT-PCR to correct for differences in cDNA synthesis efficiency between different samples. To test for such differences, we analysed β -actin transcript abundance in all of our samples. β -actin transcript abundance, expressed per g tissue, was ~23-, ~17- and ~9-fold higher in the red muscle compared with white muscle in the

smallest, intermediate-sized and largest of our PBT specimens, respectively, but the apparent difference between the tissues was statistically significant only for the smallest fish ($P < 0.05$) (Figs. 4.4A and B). In addition to the above, regression analyses showed that there was a significant decrease with increasing FL (Fig. 4.4A) and with increasing BM (Fig. 4.4B) in the red muscle but not the white muscle in the β -actin transcript abundance. The decrease in β -actin transcript abundance in the red muscle corresponded to a BM scaling coefficient of -0.33 ± 0.14 . The greater β -actin transcript abundance in the red muscle compared to the white muscle indicates either that cDNA synthesis efficiency was greater in the red muscle samples compared with the white muscle samples or that β -actin transcript abundance was just simply higher in the red muscle than in the white muscle. If the first of these explanations is correct then the absolute transcript abundances for our genes of interest are overestimated in the red muscle. Alternatively, if the second of these explanations is correct then it is possible that our findings are as they should be.

To correct for potential differences in cDNA synthesis efficiency, we divided the absolute transcript abundances for PGC-1 α , PGC-1 β , PPAR α and MCAD by those for β -actin. When this was done, the difference in PGC-1 α transcript abundance between the red and the white muscle decreased from ~20-fold to no difference in the smallest fish, ~100-fold to ~10-fold in the intermediate-sized fish and ~50-fold to 4-fold in the largest fish, but the difference between the tissues was statistically significant only for the largest fish. ($P < 0.05$) (Figs. 4.5A and B). In addition, there was a statistically significant increase in the relative PGC-1 α transcript abundance with increasing FL and with increasing BM in the red muscle but not in the white muscle. The BM-specific scaling coefficient was 0.38 ± 0.11 .

When the PGC-1 β transcript abundance was expressed relative to the β -actin transcript abundance, the difference between the red and the white muscle decreased from ~6-fold to ~2-fold in the smallest fish, ~6-fold to no difference in the intermediate-sized fish and ~5-fold to ~2-fold in the largest fish, but these differences were not statistically significant ($P < 0.05$) (Figs. 4.5C and D). In addition, there was no change in PGC-1 β transcript abundance with increasing FL or BM in the red muscle or the white muscle.

When the PPAR α transcript abundance was expressed relative to the β -actin transcript abundance there was a decrease from ~13-fold to no difference in the smallest fish, ~16-fold to no difference in the intermediate-sized fish and ~17-fold to no difference in the largest fish (Figs. 4.5E and F). In addition, there was a statistically significant increase in the relative PPAR α transcript abundance with increasing FL and BM in the red muscle but not in the white muscle. The increase in the relative PPAR α transcript abundance corresponded to a BM scaling coefficient to 0.38 ± 0.11 . Interestingly this was the same scaling coefficient observed for the increase in the relative PGC-1 α transcript abundance with increasing BM. This suggests that there may be a connection between the two.

Finally, when MCAD transcript abundance was expressed relative to the β -actin transcript abundance there was no significant difference between the red muscle and the white muscle in the small and intermediate-sized PBT specimens. This was in contrast to the ~23 and ~7-fold and greater transcript abundance in the red muscle compared with white muscle in the same fish. However, surprisingly, there was a change from ~3-fold greater MCAD transcript abundance in the red muscle compared to the white to ~3-fold greater MCAD transcript abundance in the white muscle compared to the red in the largest fish and this was statistically significant. In addition, there was no change in MCAD transcript abundance with increasing FL or BM in the red muscle or the white muscle.

Overall, when expressed relative to the β -actin transcript abundance, the difference in transcript abundances of our genes of interest between the red and white muscle decreased or disappeared completely. The transcript abundances for all of our genes of interest were greater in the red muscle compared to the white muscle before normalisation but these differences either decreased or disappeared completely after normalisation.

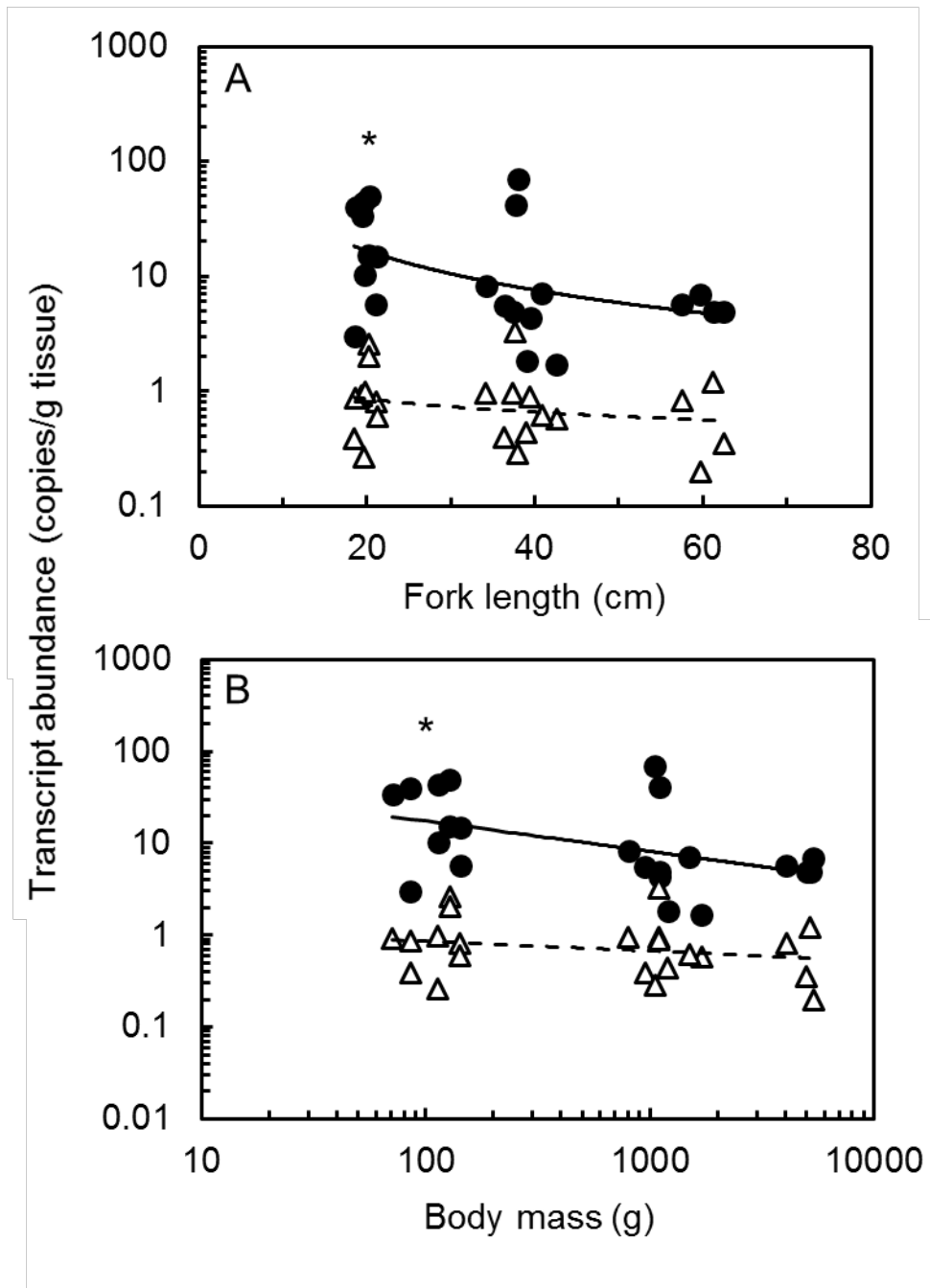


Fig. 4.4. The effects of muscle tissue type and body size on the number of β -actin transcripts per g tissue in the red and white muscle of young PBT juveniles caught in Japanese waters (values are $\times 10^{11}$). The data for the red muscle and the white muscle are represented by \bullet with solid lines and Δ with dashed lines, respectively. The best-fitting power functions for the data in the various panels are as follows: (A) red muscle $y = 497.40FL^{-1.13}$, $R^2 = 0.20$; white muscle $y = 2.66FL^{-0.38}$, $R^2 = 0.05$; (B) red muscle $y = 80.25BM^{0.33}$, $R^2 = 0.21$; white muscle $y = 1.41BM^{-0.11}$, $R^2 = 0.05$. Significant differences in transcript abundance between the red and the white muscle are indicated by *.

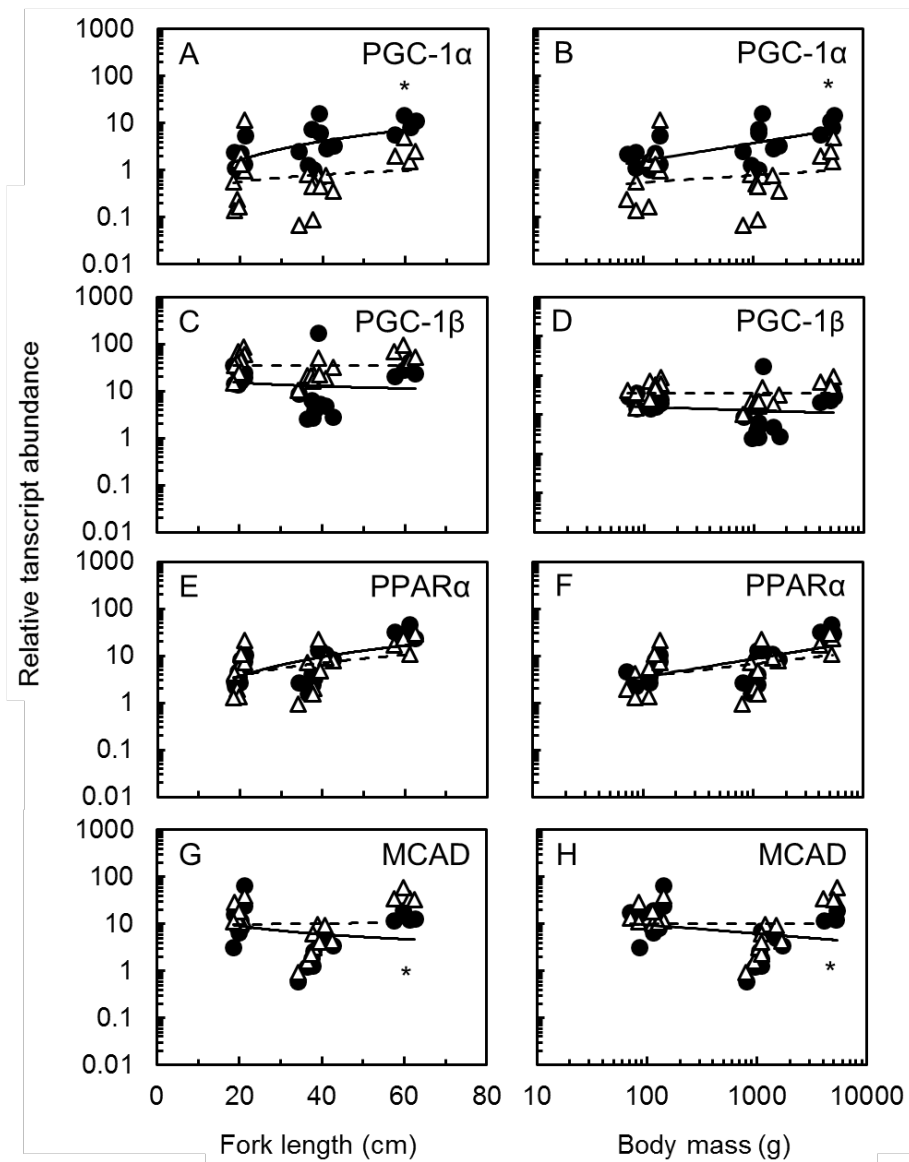


Fig.4.5. The effects of muscle tissue type and body size on the relative gene expression for PGC-1 α (A, B), PGC-1 β (C, D), PPAR α (E, F) and MCAD (G, H) normalised to β -actin in the red muscle and white muscle of young juvenile specimens of PBT. The data for the red muscle and white muscle are represented by \bullet with solid lines and Δ with dashed lines, respectively. Transcript abundance values are $\times 10^{-3}$, $\times 10^{-5}$ and $\times 10^{-3}$ for PGC-1 α , PPAR α and MCAD, respectively. The best-fitting power functions for the data in the different panels are as follows: (A) red muscle $y = 0.03FL^{1.33}$, $R^2 = 0.39$; white muscle $y = 0.12FL^{0.51}$, $R^2 = 0.03$; (B) red muscle $y = 0.28BM^{0.38}$, $R^2 = 0.38$, white muscle $y = 0.28BM^{0.15}$, $R^2 = 0.03$; (C) red muscle $y = 32.63FL^{-0.26}$, $R^2 = 0.01$, white muscle $y = 32.85x^{0.01}$, $R^2 = 0.01$; (D) red muscle $y = 23.50BM^{-0.09}$, $R^2 = 0.02$, white muscle $y = 34.69BM^{-9.86 \times 10^{-2}}$, $R^2 = 5.87 \times 10^{-6}$; (E) red muscle $y = 0.06FL^{1.38}$, $R^2 = 0.39$, white muscle $y = 0.22FL^{0.94}$, $R^2 = 0.14$; (F) red muscle $y = 0.60BM^{0.39}$, $R^2 = 0.37$, white muscle $y = 1.04BM^{0.27}$, $R^2 = 0.14$; (G) red muscle $y = 53.78FL^{-0.59}$, $R^2 = 0.05$, white muscle $y = 7.43FL^{0.09}$, $R^2 = 0.01$; (H) red muscle $y = 22.99BM^{-0.19}$, $R^2 = 0.06$, white muscle $y = 9.58BM^{0.01}$, 9.14×10^{-5} . Significant differences in transcript abundance between the red and the white muscle are indicated by *.

4.3.8. Correlation analyses between PPAR α , MCAD, PGC-1 α and PGC-1 β transcript abundances

Correlation analyses were performed to determine whether the transcript abundances for PPAR α and MCAD correlated better with the transcript abundance for PGC-1 α or with the transcript abundance for PGC-1 β . For these analyses, the data for the red and white muscle were combined and the absolute transcript abundances were used, i.e., not relative to β -actin. PPAR α transcript abundance was strongly and significantly correlated with PGC-1 α transcript abundance ($r = 0.86$) and also with PGC-1 β transcript abundance ($r = 0.70$) (Figs. 4.6A and B). Similarly, MCAD transcript abundance was highly and significantly correlated with PGC-1 α transcript abundance ($r = 0.63$) and also with PGC-1 β transcript abundance ($r = 0.80$) (Figs. 4.6C and D). Interestingly, the correlation between the transcript abundances of PPAR α and PGC-1 α was stronger than the correlation between the transcript abundances of PPAR α and PGC-1 β . In contrast the correlation between the transcript abundances of MCAD and PGC-1 β was stronger than it was between the transcript abundances of MCAD and PGC-1 α . However, the correlations are likely to be driven by the differences between tissues rather than a common pattern among tissues.

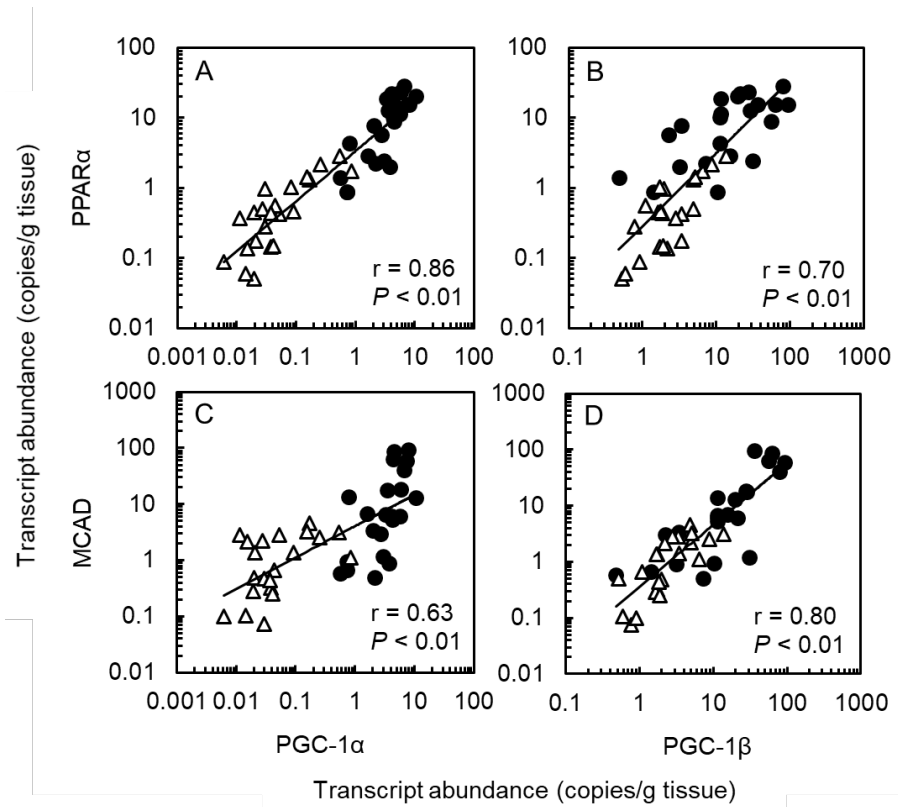


Fig. 4.6. Correlation analysis of the transcript abundance values for PGC-1α, PGC-1β, PPARα and MCAD. Transcript abundance values are $\times 10^9$, $\times 10^{10}$, $\times 10^7$ and $\times 10^9$ for PGC-1α, PGC-1β, PPARα and MCAD, respectively. The data for the red muscle and the white muscle are represented by ● and Δ, respectively. The r values were determined using a Pearson correlation analysis in IBM® SPSS Statistics version 22.0.

4.3.9. Correlation analyses between CS, COXI, COXIV, PGC-1 α and PGC-1 β transcript abundances

Citrate synthase (CS) is the first enzyme of the tricarboxylic acid (TCA) cycle and cytochrome *c* oxidase (COX) is the last enzyme in the mitochondrial electron transfer chain (mETC). Both enzymes can be investigated as indicators of mitochondrial abundance and therefore aerobic metabolic capacity (Guderley, 1990, LeMoine et al., 2008). In addition, COX has also been used as an indicator of the extent of folding of the inner mitochondrial membrane and hence the capacity of the mETC. (Guderley, 1990, LeMoine et al., 2008). Thus, a correlation might be expected between the transcript abundances for CS, COX, PGC-1 α and PGC-1 β due to the role of the PGC-1 transcriptional coactivators in mitochondrial biogenesis in mammals (Lin et al., 2005a). Correlation analyses were performed to determine whether the transcript abundances for CS, COXI and COXIV-1 correlated better with the transcript abundance for PGC-1 α or with the transcript abundance for PGC-1 β . For these analyses, the data from the previous chapter (Section 3.2.5.) were used and the data for the red and white muscle were combined. Interestingly, we observed no statistically significant correlation between the number of CS transcripts and the number of either PGC-1 α ($r = 0.05$) or PGC-1 β ($r = 0.23$) transcripts (Figs. 4.7A and B). In contrast, there was a weak, yet statistically significant, correlation between COXI transcript abundance and PGC-1 α transcript abundance ($r = 0.39$) and there was a strong statistically significant correlation between COXI transcript abundance and PGC-1 β transcript abundance ($r = 0.71$) (Figs. 4.7C and D). Similarly, there was a strong statistically significant correlation between COXIV-1 transcript abundance and PGC-1 α transcript abundance ($r = 0.60$) but there was a stronger statistically significant correlation between COXIV-1 transcript abundance and PGC-1 β transcript abundance ($r = 0.78$) (Figs. 4.7E and F). From this we conclude that PGC-1 β may have the role as the master regulator of mitochondrial biogenesis in PBT and not PGC-1 α , as is true in mammals. However, the correlations may also be driven by the differences between tissues rather than a common pattern among tissues.

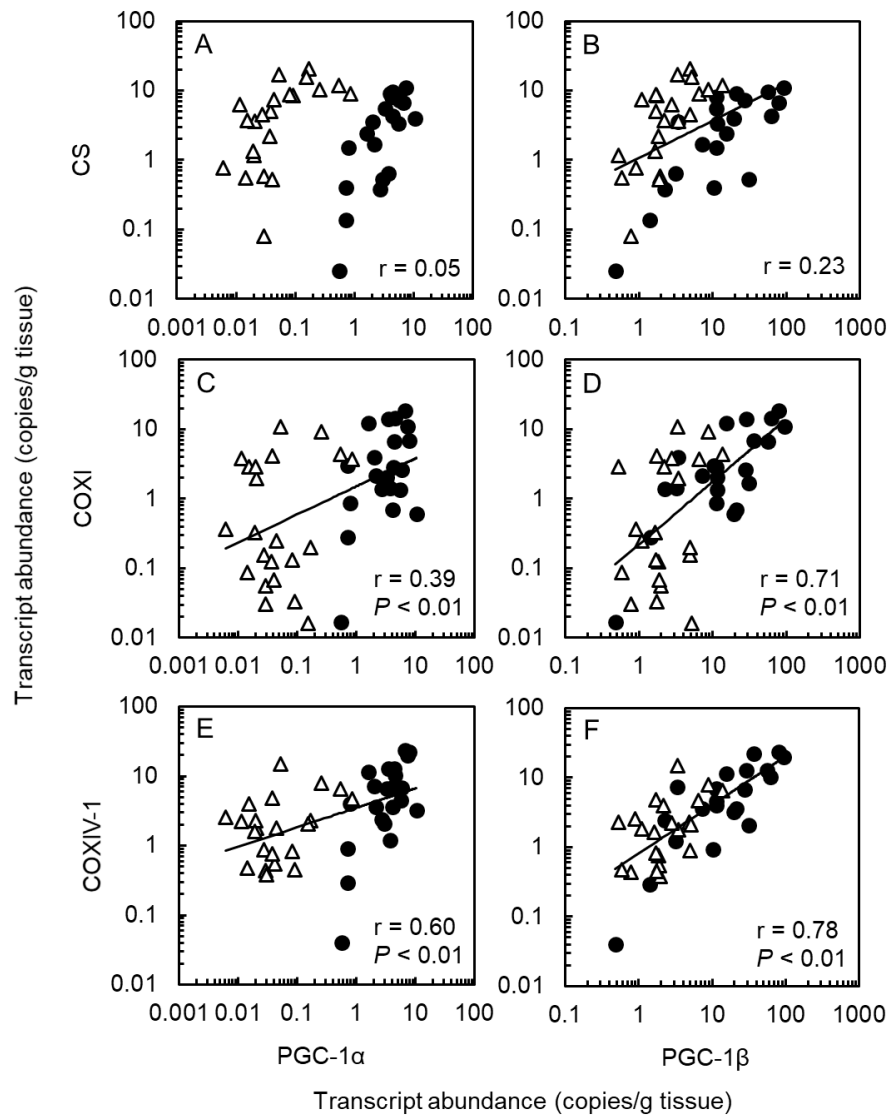


Fig. 4.7. Correlation analysis of the transcript abundance values for PGC-1 α , PGC-1 β , CS, COXI and COXIV-1. Transcript abundance values are $\times 10^9$, $\times 10^{10}$, $\times 10^{10}$, $\times 10^{13}$, and $\times 10^{11}$ for PGC-1 α , PGC-1 β , CS, COXI and COXIV-1, respectively. The data for the red muscle and white muscle are represented by ● and △, respectively. The r values were determined using a Pearson correlation analysis in IBM® SPSS Statistics version 22.0.

4.4. Discussion

4.3.1. Sequence analysis of a PGC-1 α cDNA from PBT red muscle

We have cloned and sequenced a PGC-1 α cDNA from PBT red muscle. The cDNA encodes approximately two-thirds of a PGC-1 α protein with a high degree of similarity to other PGC-1 α proteins. In particular, the PBT protein's amino acid sequence contains the two transcriptional activation domains AD1 and AD2, the three leucine-rich motifs L1, L2 and L3 and the tri-lysine motif that are characteristic of all PGC-1 α proteins from all vertebrates (Sadana and Park, 2007a, Knutti et al., 2001, LeMoine et al., 2010a). In mammals, it has been hypothesised that the AD1 and AD2 domains increase transcriptional activation of PGC-1 target genes by interacting with the basal transcription machinery (Sadana and Park, 2007a). The L1 motif is within the AD2 domain and therefore may have a role in binding to the basal transcription machinery. The L2 motif facilitates binding between PGC-1 α and transcription factors from the nuclear receptor family, including PPAR α (Vega et al., 2000). However, not all nuclear receptors interact with the L2 motif. In mammals, the L3 motif facilitates binding between PGC-1 α and ERR α , another member of the nuclear receptor family (Huss et al., 2002). The tri-lysine motif is typical of the NRF-1 interaction domain of vertebrate PGC-1 proteins (LeMoine et al., 2010a).

In contrast to the above, other regions in the PBT PGC-1 α protein are not so well conserved. The recognition site for AMPK is one of the regions lacking in conservation. When investigating the relationship between AMPK and PGC-1 α , it was revealed that a human PGC-1 α peptide corresponding to the AMPK phosphorylation site could be phosphorylated *in vitro* by human AMPK but zebrafish and goldfish PGC-1 α peptides could not be phosphorylated by human AMPK. PGC-1 α amino acid sequence alignments of organisms from the different classes of vertebrates have shown that in fishes, including goldfish and zebrafish, the essential Thr177 targeted by AMPK to phosphorylate the PGC-1 α protein, is not present (Bremer et al., 2016). This was consistent with our finding that this residue was not conserved in PBT or any fishes from the classes of bony fishes or the cartilaginous fishes. This suggests that AMPK does not activate the PGC-1 α protein in fishes by phosphorylating the essential Thr177 residue.

Other regions in the PBT PGC-1 α protein that are not so well conserved are the binding sites for the transcription factors NRF-1 and PPAR γ . The NRF-1 binding site is interrupted by a serine (S)-rich insertion, a glutamine (Q)-rich insertion and several other insertions. Similarly, the PPAR γ binding site is interrupted by several insertions. The swordfish PGC-1 α sequence had inserts within the same domains as the PBT sequence. Additionally, in the swordfish sequence, the MEF2C binding domain has quite a different amino acid sequence to the corresponding domain of most of the other PGC-1 α proteins. PBT and swordfish are both bony fishes from the subclass of ray-finned fishes. This indicates that the inserts found within the NRF-1, PPAR γ and MEF2C binding domains of the PGC-1 α protein might be a characteristic of ray-finned fishes. The presence of insertions in the MEF2C binding domain of PBT will need to be further explored because this domain was not included in the large cDNA we cloned here. Previously, similar insertions have been found within the NRF-1, PPAR γ and MEF2C binding domains in bichir (*Polypterus bichir*), sturgeon (*Acipenser transmontanus*), bowfin (*Amia calva*), zebrafish (*Danio rerio*), golden shiner (*Notemigonus crysoleucas*), black ghost knifefish (*Apteronotus albifrons*), goldfish (*Carassius auratus*), rainbow trout (*Oncorhynchus mykiss*), stickleback (*Gasterosteus aculeatus*), medaka (*Oryzias latipes*) and swordfish, all of which are ray-finned fishes (LeMoine et al., 2010a). This is consistent with our proposal that the insertions in the NRF-1, PPAR γ and MEF2C regions of the PGC-1 α protein are characteristic of ray-finned fishes. In other words, they are not found in other vertebrates and that includes the lobe-finned fishes and the cartilaginous fishes. LeMoine et al. (2010a) proposed that these insertions could prevent interactions between PGC-1 α and the NRF-1 transcription factor. To test this, Bremer et al. (2016) investigated the binding of a recombinantly expressed NRF-1 protein from zebrafish to recombinantly expressed PGC-1 α proteins from either goldfish or rat. Interestingly, the zebrafish NRF-1 protein bound to the PGC-1 α protein from rat but not from goldfish. Based on this result, the authors proposed that the NRF-1 transcription factor does not bind to the PGC-1 α transcriptional co-activator in ray-finned fishes as it does in other vertebrates. Alternatively, they proposed that the recombinantly expressed protein may have been folded incorrectly compared to the native protein. Similar research has not been undertaken to determine whether the PGC-1 α protein of ray-finned fishes can

still interact with the PPAR γ and MEF2C transcription factors. Therefore, to investigate this interaction, the same procedure undertaken by Bremer et al. (2016) could be performed with recombinantly expressed fish or mammalian PPAR γ and MEF2C proteins.

4.3.2. The effects of tissue type and body size on PGC-1 α transcript abundance

In the smallest (~20 cm FL), intermediate-sized (~40 cm FL) and largest (~60 cm FL) PBT specimens we studied, PGC-1 α transcript abundance, expressed as copies per g tissue, was ~20-, ~100- and ~50-fold higher in the red muscle than it was in the white muscle and the differences between the tissues were statistically significant. In contrast, there was no effect of fish body size on this parameter. The many fold greater expression of PGC-1 α in the red muscle compared with the white muscle suggests an important role for this transcriptional co-activator in the development and maintenance of these 'slow-twitch', predominantly oxidative, muscle fibres which are rich in mitochondria. As far as we are aware, this is the first time that PGC-1 α transcript abundance has been compared between red and white skeletal muscle tissues in any fish species. The large difference between the two different muscle types in PBT is in stark contrast to the much smaller differences between similar muscle types in mammals. In mice, for example, PGC-1 α transcript abundance was approximately 2-fold greater in the soleus muscle, composed predominantly of 'slow-twitch' muscle fibres, than it was in the extensor digitorum longus (EDL) muscle, composed predominantly of 'fast-twitch' muscle fibres (Quinn et al., 2013). One explanation as to why the difference in PGC-1 α transcript abundance was less in mice than in PBT could be that fish skeletal muscle types are very distinct being made up almost exclusively of only one fibre type, i.e., red or white, whereas mammalian muscle types are much less distinct being made up of more of a mixture of different fibre types (Greek-Walker and Pull, 1975, Shadwick, 2005). Thus, any white muscle fibres in the soleus muscle of the mice would have contributed to lower the relative abundance of red muscle fibres and could therefore, explain the smaller difference in PGC-1 α transcript abundance between the different muscle types in the mice compared with PBT.

4.3.3. The effects of tissue type and body size on PGC-1 β gene expression

In mammals, PGC-1 β , like PGC-1 α , is expressed in tissues where mitochondria are abundant and oxidative metabolism is active, such as the red skeletal muscle (Liang and Ward, 2006). The greater PGC-1 β transcript abundance in the red muscle may contribute to the greater mitochondrial abundance in this tissue compared to the white muscle (Scarpulla, 2011). In the smallest, intermediate-sized and largest PBT specimens we studied, PGC-1 β transcript abundance, expressed as copies per g tissue, was ~9-, ~6- and ~5-fold higher in the red muscle than it was in the white muscle but the difference between the tissues was only statistically significant for the smallest fish. It is likely that this was only significant in the smallest fish because the number of biological replicates was greatest for the smallest fish and the size variation between fish was less than for the intermediate-sized and largest fish. We also observed a significant decrease in PGC-1 β transcript abundance in the red muscle but not in the white muscle with increasing fish size. As far as we are aware this is the first time the effects of fish size on PGC-1 β transcript abundance have been investigated.

The difference between the red and the white muscle in the abundance of the PGC-1 β transcript which we observed in PBT, is similar to the difference between similar muscle types in mammals. For example, both PGC-1 β transcript abundance and protein expression have previously been shown to be greater (2-fold and 6-fold, respectively) in the soleus muscle (predominantly consisting of 'slow-twitch' muscle fibres) compared to the EDL muscle (predominantly consisting of 'fast-twitch' muscle fibres) in mice (Quinn et al., 2013).

Interestingly, the transcript abundance for PGC-1 β was an order of magnitude greater than that for PGC-1 α in the red muscle and two orders of magnitude greater in the white muscle in the young PBT specimens we studied. This could indicate that PGC-1 β may have a greater importance in regulating mitochondrial abundance and function in the skeletal muscle of PBT compared with PGC-1 α . In contrast to what we observed for PBT, it has previously been observed that PGC-1 α transcript abundance is ~3-fold greater in the soleus

muscle and ~2.5-fold greater in the EDL muscle than PGC-1 β transcript abundance in the respective muscle types in mice (Quinn et al., 2013). This suggests that PGC-1 β may be more important in mitochondrial biogenesis and function than PGC-1 α in PBT whereas the opposite may be the case in mammals.

4.3.4. The effects of tissue type and body size on PPAR α gene expression

When PGC-1 α interacts with PPAR α , it upregulates fatty acid β -oxidation by increasing the transcription of genes that encode enzymes involved in β -oxidation, which occurs predominantly in mitochondria (Vega et al., 2000, Lehman and Kelly, 2002). PPAR α transcript abundance was ~13-, ~16- and ~17-fold higher in the red muscle compared with white muscle in our smallest, intermediate-sized and largest PBT specimens, respectively. However, this apparent difference was only statistically significant for the smallest (~20 cm FL) and the largest (~60 cm FL) fish. The PPAR α transcript abundance showed no significant change with increasing body size in either the red or the white muscle of our young PBT specimens. In plaice (*Pleuronectes platessa*) and gilthead sea bream (*Sparus aurata*), the PPAR α transcript abundance, relative to the expression of the housekeeping gene (α -tubulin) has been shown to be high in tissues with high rates of mitochondrial fatty acid β -oxidation, such as the liver, heart and red muscle (Leaver et al., 2005). In particular, it was 9-fold greater in red muscle than in white muscle in gilthead sea bream. A similar pattern of expression has been observed in mammals. For example, PPAR α protein abundance has been shown to be ~4-fold greater in soleus muscle (predominantly consisting of 'slow-twitch' fibres) than it is in EDL muscle (predominantly consisting of 'fast-twitch' fibres) in mice (Long et al., 2007). The difference in PPAR α transcript abundance between tissues was much greater in PBT than it was in the mice. It is possible that this is because unlike the soleus muscle of mammals which consists of both red and white muscle fibres (mostly red), the red muscle of tunas is comprised of entirely red muscle fibres.

4.3.5. The effects of tissue type and body size on MCAD gene expression

We found that MCAD transcript abundance was ~23-, ~7- and ~3-fold greater in the red muscle compared with white muscle in our smallest, intermediate-sized and largest PBT specimens, respectively, but this difference was only statistically significant in the smallest fish. This can possibly be explained by the number of biological replicates being greatest for the smallest fish and the size variation between fish was less than for the intermediate-sized and largest fish. MCAD is the enzyme that catalyses the initial step in mitochondrial fatty acid β -oxidation of medium-chain fatty acids (fatty acids with chain lengths between 6 and 12 carbon atoms). PGC-1 α interacts with PPAR α to increase the transcription of the MCAD gene in the skeletal muscle of mammals (Vega et al., 2000, Lehman and Kelly, 2002). Thus, a high transcript abundance of MCAD, could also suggest a high capacity for the translation of the MCAD protein. As far as we are aware this is the first study that has compared the transcript abundance of MCAD in the red muscle and white muscle of fishes. In mice, the MCAD transcript abundance, relative to the expression of the housekeeping gene ribosomal coding gene L-19, is ~2-fold greater in the highly aerobic soleus muscle compared to the highly glycolytic gastrocnemius muscle (Seth et al., 2007). As was true for the other genes of interest, the difference in MCAD transcript abundance between tissues was much greater in PBT than it was in the mice, possibly due to the soleus muscle of mammals consisting of both red muscle fibres and white muscle fibres.

MCAD transcript abundance showed a significant decrease with increasing FL and with increasing BM in the red muscle but not in the white muscle in our juvenile PBT specimens. This suggests that there were fewer MCAD transcripts to translate and therefore probably less MCAD protein in the red muscle with increasing body size. It has been previously shown that small (20–25 cm FL) PBT juveniles prey upon small squid and zooplankton and as they grow larger (25–40 cm FL) their diet gradually shifts to epipelagic and mesopelagic fishes (Shimose et al., 2013). Previous studies have shown that both marine fish and squid contain a high abundance of LCFAs and VLCFAs (Chedoloh et al., 2011, Mehta and Nayak, 2017, Meynier et al., 2008). This suggests that as the diet of juvenile PBT changes as they grow larger LCFAs

and VLCFAs remain plentiful. This suggests that the fatty acid profile of PBT prey items may not change drastically as they grow larger. Thus, the decrease in MCAD transcript abundance with increasing body size may not be due to a change in the fatty acid type. Instead it could possibly be due to the changes in energy requirements or fatty acid storage with increasing body size. To further our understanding of this, analysis of the fatty acid profiles of the prey items of PBT should be investigated. This would confirm whether or not the fatty acid profile of PBT prey items remains unchanged with increasing PBT body size. Additionally, investigating the MCAD protein abundance or enzyme activity would show if MCAD transcript abundance can be used to give an accurate prediction of enzyme activity.

4.3.6. The effects of tissue type and body size on transcript abundance of β -actin

In our juvenile PBT specimens, we found that β -actin transcript abundance was 23-fold greater in the smallest fish (~20 cm FL), 17-fold greater in the intermediate-sized fish (~40 cm FL) and 9-fold greater in the largest fish (~60 cm FL) in the red muscle compared to the white muscle. This difference was only statistically significant for the smallest fish but there was a general trend for β -actin transcript abundance to be greater in red muscle than in the white muscle. It is likely that the difference was only significant in the smallest fish because the number of biological replicates was greatest for the smallest fish and the size variation between fish was less than for the intermediate-sized and largest fish. Evidence to support the observation that β -actin transcript abundance is greater in the red muscle compared to the white muscle comes from a study in which Northern blotting was used to analyse β -actin transcript abundance in the highly oxidative soleus muscle compared to the more glycolytic EDL muscle in rats (Sketelj et al., 1998). Therefore, it is possible that the difference in β -actin transcript abundance between the red and white muscle of PBT is due to β -actin being more abundant in red muscle than white muscle and not due to greater cDNA synthesis efficiency in the red muscle compared with the white muscle. This indicates that when we observed greater transcript abundances for our genes of interest in the red muscle compared to the white muscle it was not due to a greater cDNA synthesis efficiency in the red muscle. We also observed that β -actin transcript abundance decreased

significantly with increasing body size in the red muscle but not in the white muscle of our PBT specimens.

4.3.7. Transcript abundances for PPAR α and MCAD are strongly correlated with transcript abundances for the PGC-1 transcriptional coactivators

We found that PPAR α transcript abundance was strongly positively correlated with PGC-1 α and with PGC-1 β transcript abundance, but the correlation was stronger for PGC-1 α . Similarly, there were strong positive correlations between the transcript abundance of MCAD and both PGC-1 α and PGC-1 β transcript abundance, but the correlation was stronger PGC-1 α transcript abundance. PPAR α is a transcription factor that activates the transcription of genes involved in fatty acid β -oxidation (Vega et al., 2000). Therefore, the strong correlation between PPAR α and PGC-1 α transcript abundance may be due to their interaction to upregulate the transcription of genes that encode enzymes involved in β -oxidation. The existence of a protein–protein interaction between the L2 leucine-rich motif of PGC1 α and PPAR α was confirmed using co-immunoprecipitation assays in a mammalian cell protein system (Vega et al., 2000). The L2 leucine-rich motif was intact in our PBT PGC-1 α amino acid sequence. Therefore, this suggests that the interaction between PGC-1 α and PPAR α is conserved in PBT. When Northern blot analyses were performed on RNA that was isolated from mouse 3T3-L1 pre-adipocytes that were overexpressing either the PPAR α protein or the PGC-1 α protein alone, it was found that there was a modest increase in the transcript abundance of genes involved in fatty acid β -oxidation (Vega et al., 2000). However, when both PPAR α and PGC-1 α were overexpressed together in the preadipocytes there was a large increase in the transcripts encoding the fatty acid β -oxidation genes (Vega et al., 2000). This included genes encoding MCAD, long-chain acyl-CoA dehydrogenase (LCAD), and carnitine palmitoyltransferase I (CPT I). This indicated that PGC-1 α enhanced the PPAR α -dependent transcriptional activation of the fatty acid β -oxidation genes. If this is also true for fish and both of these genes (PPAR α and PGC-1 α) are highly expressed, then their downstream target genes should also be highly expressed. This would indicate that the capacity for fatty acid β -oxidation should be high. Thus, the greater PGC1 α and PPAR α transcript abundance in the red muscle compared to the

white muscle that we observed for PBT could possibly be due to the role of the interaction between PPAR α and PGC1 α in the upregulation of genes that encode enzymes involved in β -oxidation in this highly oxidative tissue. This interaction will need to be further explored by analysing the PPAR α and PGC-1 α protein content in the tissue samples collected from our PBT specimens.

In mammals, when PPAR α interacts with PGC-1 α , it upregulates fatty acid β -oxidation by increasing the transcription of genes that encode enzymes involved in β -oxidation, such as MCAD (Lehman and Kelly, 2002). However, the interaction between estrogen-related receptor alpha (ERR α) and PGC-1 β , also upregulates the transcription of the gene that encodes MCAD (Kamei et al., 2003, Rodriguez-Calvo et al., 2006). The strong correlation we observed between MCAD and PGC-1 β transcript abundance in our juvenile PBT specimens could possibly indicate that the upregulation of MCAD may be more dependent on an interaction between ERR α and PGC-1 β rather than an interaction between PPAR α and PGC-1 α in our juvenile PBT specimens. In contrast to our own observations in PBT, there was only a weak positive correlation of MCAD transcript abundance with either PGC-1 α or PGC-1 β transcript abundance in goldfish (LeMoine et al., 2008). Therefore, more work needs to be done to better determine which of the PGC-1 coactivators is more important for the upregulation of MCAD. This could include the deletion (knockout) of the PGC-1 α or PGC-1 β gene *in vitro* in a bluefin tuna cell line. A suitable cell line that could be used for such assays has already been established from southern bluefin tuna (*Thunnus maccoyii*) (Bain et al., 2013). Knockout assays with this cell line could indicate which, if any, of these transcriptional coactivators is more important for the upregulation of MCAD.

4.3.8. Correlations of the PGC-1 transcriptional co-activators with the genes that encode the mitochondrial marker enzymes citrate synthase and cytochrome c oxidase

Mitochondrial abundance and a tissue's aerobic metabolic capacity can be assessed using mitochondrial marker enzymes such as citrate synthase (CS, the first enzyme in the TCA cycle and cytochrome c oxidase (COX, the last enzyme in the mitochondrial electron transfer chain (mETC)) (Guderley, 1990, LeMoine et al., 2008). Previously, we observed that CS and COX enzyme

activities were approximately an order of magnitude greater in the red muscle compared with the white muscle in PBT (Chapter 3). This indicated that mitochondrial abundance was approximately an order magnitude greater in the red muscle than in the white muscle in PBT. However, surprisingly, the transcript abundances for the genes that encode these enzymes did not follow the same pattern. Specifically, there was no statistically significant difference in CS transcript abundance between the red and white muscle. In contrast to the COX enzyme activity, the transcript abundances of COXI and COXIV were much more variable being 2- to 12-fold and 2- to 3-fold greater in the red muscle compared to the white muscle, respectively. This suggested that post-transcriptional and/or post-translational modification of these enzymes may explain the differences between the different muscle types. Here we show that there was no significant correlation of CS transcript abundance either with PGC-1 α or with PGC-1 β transcript abundance. This could indicate that neither PGC-1 transcriptional coactivator is involved in the regulation of CS in the red and white muscle of PBT. This is not entirely surprising because unlike the COX subunits, which have been shown to be transcriptionally upregulated by PGC-1 α through the interaction of PGC-1 α with NRF1/NRF2, CS is not among the list of PGC1, NRF1/NRF2 sensitive genes. Instead, if there were a correlation between PGC-1 and CS transcript abundance it would likely be due to the involvement of CS in the general mitochondrial biogenesis network. In contrast to our own study, CS transcript abundance showed a poor yet significant correlation with PGC-1 α transcript abundance and a very strong and significant correlation with PGC-1 β transcript abundance in data pooled from the red muscle, white muscle, heart and liver of goldfish subjected to three different temperature treatments (4, 20 and 35°C) and to three different dietary treatments (food deprivation, low fat and high fat) (LeMoine et al., 2008).

In mice, rats and humans, there is evidence that PGC-1 α is directly involved in upregulating the transcription of nuclear encoded COX subunits, such as COXIV, through its interaction with NRF-1 (Scarpulla, 2002, Dhar et al., 2008). In mice myoblasts, PGC-1 α is also indirectly involved in regulating the expression of mitochondrially encoded COX subunits, such as COXI. This occurs by PGC-1 α upregulating the expression of the mitochondrial transcription factor A (TFAM), by interacting with NRF-1 and NRF-2, which

then upregulates the expression of the mitochondrial subunits of COX (Collu-Marchese et al., 2015). We found strong significant correlations between the transcript abundances of COXI and COXIV with both PGC-1 α and PGC-1 β for our PBT specimens and the correlations we observed were much stronger with PGC-1 β for both COX subunits. This suggests that if the PGC-1 transcriptional coactivators are involved in the upregulation of the transcription of genes associated with mitochondrial biogenesis in fishes, including the COX subunits, then PGC-1 β may be more important than PGC-1 α . LeMoine et al. (2008) also observed a stronger correlation between the transcript abundance of COXIV and PGC-1 β compared to PGC-1 α . In fact, no correlation was observed between the transcript abundances of COXIV and PGC-1 α . However, it is important to note that these patterns of transcript abundance may not necessarily reflect a direct interaction between the different factors because transcript abundance may not parallel protein abundance due to post-translational regulation. Therefore, much more research must be conducted before a definitive conclusion can be reached.

4.3.9. Conclusions

Previously we reported that CS and COX enzyme activities were both approximately an order of magnitude greater in the red muscle than in the white muscle of young PBT juveniles ranging in size from 18.5 to 62.5 cm FL and in age from ~2 months to ~2 years (Chapter 3). From this we concluded that mitochondrial abundance was approximately an order of magnitude greater in the red muscle compared with the white muscle in these fish. Because of this, we predicted that PGC-1 α and PGC-1 β transcript abundances would also be approximately an order of magnitude greater in the red muscle compared with the white muscle. Here we have confirmed that this prediction was true for PGC-1 β and the transcript abundance for PGC-1 α ranged between one to two orders of magnitude greater in the red muscle compared to the white muscle. This suggests that although the role of PGC-1 α in mitochondrial biogenesis is disputed in fishes, it may still be involved in mitochondrial function, specifically β -oxidation. We also observed greater PPAR α and MCAD transcript abundances in the red muscle compared to the white muscle. This suggested that the rate of β -oxidation is also greater in the red muscle compared to the white muscle. Finally, there were strong positive

correlations between the transcript abundance of PPAR α and the PGC-1 α and PGC-1 β transcriptional coactivators and the same was true between the transcript abundance of MCAD and the PGC-1 α and PGC-1 β transcriptional coactivators, which provides further evidence that the PGC-1 transcriptional coactivators are involved in the upregulation of the capacity for β -oxidation in these tissues.

CHAPTER 5 - The effects of feed restriction on aerobic and glycolytic metabolic capacity in yellowtail kingfish (*Seriola lalandi*) farmed at suboptimal water temperatures

Abstract

Yellowtail kingfish (YTK, *Seriola lalandi*) is an important aquaculture species in South Australia but in winter it suffers from impaired feed digestion due to suboptimal water temperatures. Here we have investigated the combined effects of feed restriction and suboptimal water temperatures on the mitochondrial abundance/aerobic metabolic capacity and the glycolytic capacity in the red muscle, white muscle and liver of this important aquaculture species. We hypothesized that there would be a decrease in the enzyme activity and gene expression for the enzymes involved in aerobic metabolism and glycolytic metabolism in these tissues in response to feed restriction. To test this we measured enzyme activity and transcript abundance for the mitochondrial marker enzymes citrate synthase (CS) and cytochrome c oxidase (COX) as well as for the glycolytic marker enzyme pyruvate kinase (PK) in red muscle, white muscle and liver of juvenile YTK specimens. Feed restriction increased CS enzyme activity by 57% in the liver but it had no significant effect on the activity in the red muscle or the white muscle. In contrast, feed restriction resulted in COX enzyme activity decreasing by 29% in the red muscle and increasing by 20% in the liver, but it had no significant effect in the white muscle. Finally, feed restriction resulted in a 33% decrease in PK enzyme activity in the red muscle but had no effect in the white muscle or liver. In mammals, proliferator-activated receptor-gamma coactivator 1-alpha (PGC-1 α) is considered to be a master regulator of mitochondrial biogenesis and function. Due to its regulatory role in these processes, we cloned a YTK PGC-1 α cDNA and investigated its transcript abundance in the different tissues and in response to feed restriction. We found that PGC-1 α transcript abundance increased by 3- and 7-fold in the red muscle and the white muscle, respectively, in response to feed restriction but we observed no difference in the liver. Lastly, we investigated the effects of tissue type and feed restriction on the transcript abundance of the transcription factor peroxisome proliferator-activated receptor-alpha (PPAR α) which interacts with PGC-1 α to upregulate the transcription of genes involved in mitochondrial β -oxidation, such as medium-chain acyl-coenzyme A dehydrogenase (MCAD). We found that feed restriction had no statistically significant effect on the transcript abundance of PPAR α or MCAD in the red muscle, white muscle or

liver. However, there was an apparent 96% decrease in PPAR α transcript abundance in the liver but due to the large fish to fish variation, this apparent decrease was not statistically significant.

Abbreviations

Yellowtail kingfish, YTK, Fork length, FL; Body mass, BM; peroxisome proliferator-activated receptor γ co-activator-1, PGC-1; Medium-chain acyl-Coenzyme A dehydrogenase, MCAD; peroxisome proliferator-activated receptor α , PPAR α ; Cytochrome c oxidase subunit, COX; Citrate synthase, CS; Pyruvate kinase, PK

5.1. Introduction

5.1.1. Yellowtail kingfish distribution and aquaculture

Yellowtail kingfish (YTK, *Seriola lalandi*) is a large, carnivorous, marine fish that can have a lifespan of up to 21 years and grow to a size of up to ~250 cm total length and ~100 kg total body mass (Stewart et al., 2004, Fielder, 2013). It is a member of the genus *Seriola* which consists of nine species. Most of these species are found in coastal or oceanic waters in tropical or warm temperate regions of the world (Benetti et al., 2005). Similar to other *Seriola* species, YTK prefers water temperatures ranging from 18 to 24°C (Fielder and Heasman, 2011). Several *Seriola* species, including YTK, are farmed, predominantly in sea-cages. For example, Japanese yellowtail (*Seriola quinqueradiata*) is farmed in Japan, Almaco jack (*Seriola rivoliana*) near Hawaii and greater amberjack (*Seriola dumerili*) in Japan, the Mediterranean and Vietnam (Webster and Lim, 2002, Benetti et al., 2005, Naomasa et al., 2013, Sicuro and Luzzana, 2016).

YTK, the subject of the research described here, is farmed in sea cages in Australia, New Zealand, Mexico, Chile and Hawaii as well as in indoor facilities in the Netherlands (Premachandra et al., 2017, Kolkovski and Sakakura, 2004, CST, 2016, Norwood, 2017, Benetti et al., 2005, Kingfish-Zeeland, 2018). The culture of YTK in countries such as Australia, New Zealand and Chile depends on the rearing of larvae/fingerlings produced in a hatchery from captive brood stock (Kolkovski and Sakakura, 2004, Orellana et al., 2014, CST, 2016). In contrast, the culture of Japanese yellowtail and greater amberjack in Japan is reliant, mainly, on the on-growing of readily available wild-caught juveniles (Kolkovski and Sakakura, 2004). In Australia, YTK aquaculture takes place predominantly in South Australia but there has been some expansion into New South Wales and Western Australia as well (Norwood, 2017). In South Australia, YTK aquaculture is carried out by Clean Seas Seafoods Ltd. which is the largest commercial producer of farmed kingfish outside of Japan (CST, 2016). This company has a hatchery at Arno Bay on the Eyre Peninsula of South Australia where it maintains its broodstock and raises its larvae and fingerlings. Approximately 75 days after hatching, the fingerlings are transferred to sea cages near Port Lincoln, South Australia, where they are on-grown to a marketable size.

5.1.2. The effects of water temperature on YTK physiology

The water temperature in the sea cages where YTK juveniles are cultured in South Australia ranges from a low of 10°C in the winter to a high of 24°C in the summer (Miegel et al., 2010). Reportedly, the optimal water temperature for the growth of YTK juveniles is 22.8°C (Pirozzi and Booth, 2009). Thus, the low winter water temperatures experienced in South Australia are sub-optimal for YTK growth. Sub-optimal water temperatures have been shown to increase gut transit times, and decrease digestion rates, in farmed YTK (Miegel et al., 2010, Bowyer et al., 2013). For example, when the water temperature was decreased from ~21°C to ~13°C, YTK juveniles took approximately three times as long to digest their feed (Miegel et al., 2010). Increasing gut transit times, as a result of sub-optimal water temperatures, can lead to a condition known as winter syndrome (Sheppard, 2004). The main symptom of winter syndrome is inflammation of the intestine (Sheppard, 2004). This inflammation can lead to ulceration and necrosis of the intestine and even the death of the fish (Sheppard, 2004).

5.1.3. Diet of cultured YTK

The most important macronutrients in the diets of carnivorous marine fishes are lipids and proteins; these fishes make poor use of carbohydrates as macronutrients (Tocher, 2003). Lipids provide both essential and non-essential fatty acids. In fishes, as in other vertebrates, fatty acids are catabolised via the process of β -oxidation in the mitochondria of the cell. Thus, it is important to understand how mitochondrial abundance and metabolic activity are affected by the quantity and quality (i.e. fatty acid composition) of the lipid in the diet. The omega-3 long-chain polyunsaturated fatty acids (n-3 LC-PUFA), eicosapentaenoic acid (EPA) and docosahexaenoic acid, are considered essential for carnivorous marine fishes, i.e., they cannot be synthesized *de novo* (Tocher, 2010). In the natural environment, EPA and DHA are ultimately derived from phytoplankton and algae at the bottom of the marine food web. These fatty acids accumulate to high levels in the flesh of large carnivorous marine fish species such as YTK due to the phenomenon known as bioaccumulation (Huynh and Kitts, 2009). Thus, feeds for farmed carnivorous marine fishes generally contain high concentrations of EPA and DHA.

Historically, these fatty acids have been provided by the fish oils added to fish feeds but in recent decades the supply of fish oils has stagnated and these oils have become increasingly more expensive (Turchini et al., 2009). Consequently, fish farmers have increasingly been replacing fish oils with terrestrial plant and animal oils e.g. canola oil and poultry oil in the feeds for their fish (Norambuena et al., 2013). Unfortunately, however, these oils are lacking in the essential fatty acids EPA and DHA. This has two important potential consequences. One is reduced growth of the fish and the other is a reduction in the health benefits ascribed to the consumption of fish for the human consumer (Swanson et al., 2012).

Previous research with farmed YTK in South Australia has focussed on the effects of fish oil replacement, at both optimal and sub-optimal water temperatures, on the growth of the fish (Higgs et al., 2006, Bowyer et al., 2012b, Bowyer et al., 2012a). For example, in one study, YTK were fed diets containing 20% (w/w) lipid in the form of fish oil (FO), canola oil (CO), poultry oil (PO), a mixture of fish oil with canola oil (1:1) (FO/CO) or a mixture of fish oil with poultry oil (1:1) (FO/PO) at two different water temperatures, i.e., either 18°C or 22°C (Bowyer et al., 2012b). The fish were fed twice a day to apparent satiation over a period of 34 days and the results showed that the weight gain was greater when the water temperature was 22°C (optimal) compared to when it was 18°C (sub-optimal) and this was regardless of the composition of the diet. Weight gain appeared to be lower (by 19%) for the fish fed the CO diet compared to the fish fed the FO control diet when the fish were maintained at 22°C but the apparent difference was not statistically different. In contrast, when the fish were maintained at 18°C the weight gain was statistically indistinguishable for the fish fed the FO, PO, FO/CO and FO/PO diets but it was statistically significantly lower (by 58%) for the fish fed the CO diet. Thus, complete replacement of FO with CO significantly reduced the growth of the fish at the suboptimal water temperature of 18°C but not at the optimal water temperature of 22°C.

In a more recent study, the effects of various degrees of feed restriction on the growth of YTK that were fed diets containing FO instead of PO or CO were investigated at the suboptimal water temperatures of winter to develop better feed management practices for YTK during winter (Bansemer et al., 2018). To

achieve this aim, the fish were fed diets containing 9% (w/w) lipid in the form of fish oil but with different degrees of restricted feeding and this was done over a period 84 days during the Australian winter at suboptimal water temperatures for YTK growth of between 11.5°C and 16.0°C. The fish were fed to apparent satiation either six days per week (Treatment 1), two days per week (Treatment 2) or one day per week (Treatment 3) or at 0.65% (w/w) body mass (BM) two days per week (Treatment 4), 0.35% (w/w) BM two days per week (Treatment 5), 0.12% (w/w) BM six days per week (Treatment 6) or 0.1% (w/w) BM one day per week (Treatment 7). The fish fed to apparent satiation six days per week (Treatment 1) gained weight and the fish fed to apparent satiation two days per week neither lost nor gained weight and the fish fed the other treatments lost increasingly more weight with the decreasing amount of feed. Thus, the reduction in feed supplied to the fish resulted in reduced growth and even weight loss. The results of this study suggested that feeding YTK to apparent satiation 2 days per week was the minimum requirement to avoid weight loss at winter water temperatures. Additionally, feeding them to apparent satiation 6 days per week was the minimum amount of feed required to maximise growth at winter water temperatures.

5.1.4. Fish skeletal muscle structure and metabolism

The mitochondria are the site of aerobic metabolic activity in fishes just as they are in other vertebrates (Johnston et al., 2011). Fish have two main skeletal muscle types generally referred to as red muscle and white muscle (Johnston et al., 2011). The red muscle consists predominantly of red muscle fibres and the white muscle predominantly of white muscle fibres. The red muscle fibres have large numbers of mitochondria and their metabolism is predominantly aerobic. They are used for sustained, cruise-type swimming and their main fuel sources are fatty acids which are metabolized aerobically via the process of β -oxidation in the abundant mitochondria. The white muscle fibres, on the other hand, have fewer mitochondria and their metabolism is predominantly glycolytic. They are used for short duration, burst-type activities, such as the pursuit of prey, and their main fuel source is glucose which is metabolized via the process of glycolysis. Previous studies have used citrate synthase (CS), the first enzyme in the tricarboxylic acid (TCA) cycle in the mitochondria and cytochrome c oxidase, the last enzyme in the mitochondrial electron transfer

chain (mETC) as indicators of mitochondrial abundance and aerobic metabolic capacity in fishes (Dalziel et al., 2005, LeMoine et al., 2008). Similarly, previous studies have used pyruvate kinase (PK), the last enzyme in glycolysis, as an indicator of glycolytic/anaerobic metabolic capacity in fishes (McClelland et al., 2006, Cordiner and Egginton, 1997, Kyprianou et al., 2010).

5.1.5. Effects of fasting and feed restriction on mitochondrial abundance and aerobic metabolic capacity in fishes

Fasting in fishes has been shown to decrease mitochondrial abundance and therefore aerobic metabolic capacity in the skeletal muscle. For example, shortspine thornyhead (*Sebastolobus alascanus*) juveniles fasted for a period of approximately 102 days, displayed a ~35% decrease in their red muscle and a ~52% decrease in their white muscle in their CS enzyme activity expressed per g tissue (Yang and Somero, 1993). Similarly, in the same study, CS enzyme activity (expressed per g tissue) decreased by ~14% in the red muscle and ~25% in the white muscle of spotted scorpionfish (*Scorpaena guttata*) juveniles fasted for a period of approximately 98 days. Both of these results indicate that mitochondrial metabolic capacity decreases in response to fasting. In another study, freshwater catfish (*Clarias batrachus*) were fasted for 7, 14, 21, 28 or 35 days and it was shown that there was a decrease in CS enzyme activity (expressed per g tissue) in both the white muscle and the liver, with a maximum decrease of approximately 46% observed in both tissues at the end of the experiment (Tripathi and Verma, 2003). In contrast, when goldfish (*Carassius auratus* L.) were fasted for 21 days, CS enzyme activity per g tissue decreased by 50% in the liver but remain unchanged in the red and white muscle (LeMoine et al., 2008). Thus, fish frequently respond to fasting by decreasing the aerobic metabolic capacity in their red muscle, white muscle and liver but there is species to species variation (Yang and Somero, 1993, Tripathi and Verma, 2003, LeMoine et al., 2008).

Although there have been multiple studies investigating the effects of fasting on mitochondrial abundance and aerobic metabolic capacity in fishes, the effects of feed restriction on the same variables have not been as extensively explored. Instead, studies that investigate feed restriction in fishes mostly explore the effects of feed restriction on growth performance (Tian and Qin,

2004, Sæther and Jobling, 1999, Pirhonen and Forsman, 1998, Bansemer et al., 2018). However, it has been shown, using a microarray analysis, that when rainbow trout (*Oncorhynchus mykiss*) were fed *ad libitum* once a week, the expression of genes involved in β -oxidation were mostly upregulated in the skeletal muscle (presumably white skeletal muscle) compared to control fish that had been fed *ad libitum* twice per day (Kondo et al., 2012). This could suggest that the aerobic metabolic capacity actually increased in response to feed restriction.

5.1.6. Effects of fasting on glycolytic metabolic capacity in fishes

Fasting in fishes has been shown to result in a decrease in the glycolytic capacity in the skeletal muscle. For example, in shortspine thornyhead juveniles fasted for approximately 102 days, PK enzyme activity (expressed per g tissue) decreased by ~23% in the red muscle and by ~62% in the white muscle (Yang and Somero, 1993). In the same study, PK enzyme activity (expressed per g tissue) decreased by ~33% in the red muscle and ~44% in the white muscle of spotted scorpionfish juveniles fasted for approximately 98 days. Together these findings indicate that there is a decrease in the glycolytic metabolic capacity in the red muscle and the white muscle of fishes in response to fasting.

5.1.7. Peroxisome proliferator-activated receptor-gamma coactivator 1-alpha in mammals

In mammals, peroxisome proliferator-activated receptor-gamma coactivator 1-alpha (PGC-1 α) is a transcriptional co-activator that upregulates the transcription of genes involved in mitochondrial biogenesis and β -oxidation by interacting with an assortment of different transcription factors (Lin et al., 2005a, Liu and Lin, 2011). PGC-1 α is highly expressed in mitochondria-rich tissues with high energy demands, including red muscle (Puigserver et al., 1998). It was first discovered in the brown fat tissue of mice where it was shown to interact with the transcription factor peroxisome proliferator-activated receptor-gamma (PPAR γ), hence its name. Later, PGC-1 α was found to interact with several other transcription factors including PPAR α , estrogen related receptor-alpha (ERR α), nuclear respiratory factors (NRF) 1 and 2 and

myocyte-specific enhancer factor 2 (MEF2) (Lin et al., 2005a). These transcription factors upregulate mitochondrial biogenesis and function. Specifically, PPAR α activates the transcription of genes that encode enzymes involved in fatty acid β -oxidation, a process that occurs predominantly in the mitochondria of the cell. One of the genes transcriptionally activated by PPAR α is acyl-CoA dehydrogenase (ACADM), which encodes medium chain acyl-CoA dehydrogenase (MCAD). MCAD is the enzyme that catalyses the first step in the mitochondrial β -oxidation of medium-chain fatty acids (i.e. fatty acids with chain lengths between 6 and 12 carbon atoms) (Vega et al., 2000, Gulick et al., 1994). PGC-1 α also interacts with ERR α to upregulate the transcription of genes involved in mitochondrial biogenesis, oxidative phosphorylation and β -oxidation, including MCAD (Ikeda et al., 1986, Sladek et al., 1997). In addition, when PGC-1 α interacts with NRF-1 and 2 together they directly or indirectly upregulate the transcription of genes that encode enzymes in the mitochondrial electron transfer chain (mETC) (Collu-Marchese et al., 2015). Examples of these genes are those that encode the subunits that constitute cytochrome *c* oxidase (COX), the last enzyme in the mETC. PGC-1 α upregulates the transcription of nuclear encoded COX subunits, such as COXIV by interacting with NRF-1, while mitochondrially encoded COX subunits, such as COXI, are upregulated through increased expression of the mitochondrial transcription factor A (TFAM), which is also upregulated by PGC-1 α by interacting with NRF-1 (Scarpulla, 2002, Dhar et al., 2008, Collu-Marchese et al., 2015). PGC-1 α also interacts with MEF2 to promote a switch from white ('fast-twitch', predominantly glycolytic) to red ('slow-twitch', predominantly oxidative) skeletal muscle fibres (Lin et al., 2002b).

5.1.8. The effects of fasting on PGC-1 α gene and protein expression in the skeletal muscle and liver of fishes

In fine flounder (*Paralichthys adspersus*) and goldfish, PGC-1 α transcript and protein abundance have been reported to increase in response to fasting (LeMoine et al., 2008, Fuentes et al., 2013). Specifically, in fine flounder that were fasted for a period of three weeks, the protein content of PGC-1 α was elevated by ~60% and the abundance of the mitochondrial electron transport chain (mETC) complexes, succinate dehydrogenase (Complex II), cytochrome *c* oxidase (Complex IV) and ATP synthase (Complex V) was 50 to 100% higher

within the white muscle. The authors concluded that increasing expression of these proteins indicated an increase in mitochondrial biogenesis in the white skeletal muscle of these fish (Fuentes et al., 2013). In a different study, when goldfish were fasted for three weeks, there was an apparent ~50% increase in PGC-1 α transcript abundance in the red muscle and an apparent ~100% increase in the white muscle, but these were not statistically significant (LeMoine et al., 2008). In the same study, there was a small statistically significant increase in PPAR α transcript abundance in the liver but there was no change in the red muscle or the white muscle in response to fasting. This could indicate that there was increased β -oxidation of fatty acids in the liver in response to fasting but not in the red or white skeletal muscle.

5.1.8. Aims

The aims of this study were to investigate the effects of feed restriction on the aerobic and glycolytic metabolic capacity in the red muscle, white muscle and liver of farmed YTK cultured at suboptimal water temperatures. Specifically, we measured the effects of feed restriction on the activities of the mitochondrial marker enzymes CS and COX and the glycolytic marker enzyme PK in the red muscle, white muscle and liver of YTK. In addition, we also cloned a PGC-1 α cDNA from YTK red muscle and we investigated the effects of feed restriction on the expression of the genes that encode CS, COX, PK, PGC-1 α , PPAR α and MCAD.

5.2. Materials and Methods

5.2.1. Fish culture

Our research was part of a larger study aimed at investigating the effects of feed restriction on the growth of juvenile yellowtail kingfish (YTK, *Seriola lalandi*) exposed to sub-optimal water temperatures (Bansemer et al. (2018)). YTK juveniles with an initial fork length (FL) of 46.1 ± 1.5 cm (mean \pm standard error of the mean, SE) and an initial body mass (BM) of 1.44 ± 0.13 kg (mean \pm SE) were obtained from the Clean Seas Aquaculture Hatchery at Arno Bay, South Australia and cultured at the South Australian Aquatic Sciences Centre at West Beach, Adelaide, South Australia. The full details of the culture conditions can be found in Bansemer et al. (2018) but the most important details are as follows. Twenty-one fish were stocked into each of twenty one 5,000 L tanks. The tanks were connected to a water recirculation/flow-through system which drew seawater from the beach nearby. The system gave 100% water exchange per day and the water temperature fluctuated naturally between 11.5°C and 16.0°C. Over the course of the experiment, the mean \pm SE water temperature was 12.8 ± 0.8 °C. All of the fish were fed the same feed but with varying degrees of feed restriction. Only the control fish and the most severely feed-restricted fish were sampled for the work reported here. The control fish were fed to apparent satiation six days per week whereas the most severely feed-restricted fish were fed at 0.1% (w/w) of their BM only once per week. There were three replicate tanks for the control fish and three for the feed-restricted fish. Three fish were sampled from each tank for the work reported here. The feed was a commercially formulated pellet (Ridley Clean Seas Pelagica) containing 30% (w/v) fish meal and 9% (w/w) fish oil and it was manufactured by Ridley Aquafeeds (Narangba, Queensland, Australia). The full details of the composition of the feed can be found in Bansemer et al. (2018).

5.2.2. Fish tissue sampling

The fish were fed the experimental diets for a total of 84 d and at the end of this time, three fish were randomly sampled from each of the three tanks per treatment. The control fish were last fed one day before sampling whereas the feed-restricted fish were last fed three days before sampling. Once the fish had

been caught, their FL and BM were recorded and then they were euthanized. Following this, samples were taken of the red muscle, white muscle and liver. The samples for the enzyme activity analyses were initially snap frozen in liquid nitrogen and then later transferred to a freezer at -150°C whereas those for the gene expression analyses were initially immersed in ice-cold RNeasy[®] (Ambion[™]) and then later transferred, in this same solution, to a freezer at -20°C . Fulton's condition factor (K) was calculated using the equation $K = (\text{BM}/\text{FL}^3) \times 100$. For all animal handling procedures, animal ethics approval was obtained from the Flinders University of South Australia Animal Welfare Committee (Project No. E424/15) and all procedures were carried out in accordance with the South Australian Animal Welfare Act 1985 and the Australian Code for the Care and Use of Animals for Scientific Purposes, 8th Edition, 2013.

5.2.3. Citrate synthase enzyme activity analysis

Citrate synthase (CS) enzyme activity analysis was essentially as previously described (Gibb and Dickson, 2002). In brief, the procedure was as follows. Approximately 50 mg of frozen tissue was homogenised for 45 s at 4,000 rpm in nine volumes of ice-cold extraction buffer [50 mM imidazole (pH 6.6), 2 mM ethylenediaminetetraacetic (EDTA)] using a TOMY micro Smash[™] MS-100 tissue homogeniser. The resulting homogenate was clarified by centrifugation at 12,000 *g* for 10 min at 4°C and then the supernatant was desalted using a Bio-Spin[®] P-30 Gel column (Bio-Rad), equilibrated with the extraction buffer. The desalted extract was used for the enzyme assays. Prior to performing the assays, the red muscle extract was diluted 1:20, the white muscle extract 1:2 and the liver extract 1:4. This was to ensure that the initial rate of the reaction could be reliably measured. Enzyme activity was assayed using a Corona SH-9000 microplate reader (Corona Electric Co. Ltd.) in a room maintained at a constant temperature of 25°C . The reactions were performed in flat-bottomed 96-well plates and each reaction (final total volume 160 μL) contained 80 mM Tris buffer (pH 8.0), 2 mM MgCl_2 , 0.1 mM 5,5'-dithio-bis(2-nitrobenzoic acid) (DTNB), 0.1 mM acetyl CoA, 0.5 mM oxaloacetate and 10 μL of the appropriate dilution of the tissue extract. The reactions were initiated with the addition of the oxaloacetate and the change in absorbance due to the reduction of DTNB was monitored at a wavelength of 412 nm. Preliminary experiments had been

carried out to ensure that doubling or halving the volume of the diluted tissue extract added to the assay resulted in proportional changes in the reaction rate.

5.2.4. Cytochrome *c* oxidase enzyme activity analysis

Cytochrome *c* oxidase (COX) enzyme activity analysis was essentially as previously described (Bremer and Moyes, 2011). In brief, the procedure was as follows. Approximately 25 mg of frozen tissue was homogenised for 4 min in 20 volumes of ice-cold extraction buffer [25 mM potassium phosphate buffer (pH 7.4), 1 mM EDTA, 0.6 mM n-dodecyl β -D-maltoside] using a Retsch MM40 bead mill set at a frequency of 30 Hz. The resulting homogenate was used directly for the enzyme assays. Prior to performing the assays, the red muscle extract was diluted 1:25, the white muscle extract 1:5 and the liver extract 1:5. This was to ensure that the initial rate of the reaction could be reliably measured. Enzyme activity was assayed using a FLUOstar Omega microplate reader (BMG LABTECH) set at 25°C. The reactions were performed in flat-bottomed 96-well plates and each reaction (final total volume 200 μ L) contained 25 mM potassium phosphate buffer (pH 7.4), 0.6 mM n-dodecyl β -D-maltoside, 0.15 mM reduced cytochrome *c* and 10 μ L of the appropriate dilution of the tissue homogenate. The reactions were initiated with the addition of the reduced cytochrome *c* and the change in absorbance due its oxidation was monitored at a wavelength of 550 nm. The reduced cytochrome *c* had been prepared by adding an excess of sodium ascorbate to a 1 mM stock solution of cytochrome *c* dissolved in 25 mM potassium phosphate buffer (pH 7.4) and then removing the ascorbate using a PD-10 desalting column (GE Healthcare), pre-equilibrated with the same phosphate buffer. Reduction of the cytochrome *c* was confirmed by performing a wavelength scan between 350 and 700 nm to identify the characteristic absorption maximum for the reduced form of cytochrome *c* at 550 nm. Preliminary experiments had been carried out to ensure that doubling or halving the volume of the diluted tissue extract added to the assay resulted in proportional changes in the reaction rate.

5.2.5. Pyruvate kinase enzyme activity analysis

Pyruvate kinase (PK) enzyme activity analysis was essentially as previously described (Davies and Moyes, 2007). In brief the procedure was as follows.

Approximately 25 mg of frozen tissue was homogenised for 4 min in 20 volumes of ice-cold extraction buffer [20 mM HEPES (pH 7.2), 1 mM EDTA, 0.1% (v/v) Triton X-100] using a Retsch MM40 bead mill set at a frequency of 30 Hz. The resulting homogenate was used directly for the enzyme assays. Prior to performing the assays, the red muscle extract was diluted 1:20, the white muscle extract 1:100 and the liver extract 1:10. This was to ensure that the initial rate of the reaction could be reliably measured. Enzyme activity was assayed using a FLUOstar Omega microplate reader (BMG LABTECH) set at 25°C. The reactions were performed in flat-bottomed 96-well plates and each reaction (final total volume 200 µL) contained 50 mM HEPES (pH 7.4), 5 mM ADP, 100 mM KCl, 10 mM MgCl₂, 0.15 mM NADH, 5 mM phosphoenolpyruvate (PEP), 10 mM KCN, 10 units/mL lactate dehydrogenase (LDH) and 10 µL of the appropriate dilution of the tissue homogenate. The reactions were initiated with the addition of the ADP and the change in absorbance due to the oxidation of NADH was monitored at a wavelength of 340 nm. Preliminary experiments had been carried out to ensure that doubling or halving the volume of the diluted tissue extract added to the assay resulted in proportional changes in the reaction rate.

5.2.6. RNA extraction and cDNA synthesis

Total RNA was extracted using an RNeasy® Fibrous Tissue Mini Kit (QIAGEN) following the manufacturer's instructions but with some modifications. The tissue samples (Section 5.2.2) that had been stored in RNAlater® were gently blotted dry and then 60 mg of the tissue was disrupted in 300 µL of buffer RLT, containing 40 mM dithiothreitol (DTT), supplied with the kit. Tissue disruption was performed using a motorised Kimble Chase® cordless pellet pestle. The extraction method included an optional on-column RNase-free DNase I digestion to remove any DNA that might have been contaminating the RNA. The RNA concentration was quantified using a NanoDrop™ 1000 spectrophotometer (Thermo Scientific) and one µg of the extracted RNA was used as the template to synthesise first strand cDNA. The first strand cDNA was synthesized using a SuperScript® IV Reverse Transcriptase Kit (Invitrogen™) and the synthesized cDNA was subsequently stored at -20°C until it was required.

5.2.7. Primer design for cloning a PGC-1 α cDNA from YTK red muscle using conventional polymerase chain reaction

A large fragment of the open reading frame (ORF) of a YTK PGC-1 α cDNA was cloned using conventional polymerase chain reaction (PCR). The forward PCR primer (PGC-1 α F1, Table 4.1) was designed by LeMoine et al. (2008) and the reverse (PGC-1 α R1) as follows. Firstly, PGC-1 α cDNA sequences from swordfish (*Xiphias gladius*, GenBank accession no. FJ710607.1), large yellow croaker (*Larimichthys crocea*, GenBank accession no. XM_010733812.1) and rainbow trout (*Oncorhynchus mykiss*, Genbank accession no. FJ710605.1) were aligned using ClustalX 2.1 (Larkin et al., 2007). Then a region of conservation adjacent to the 3' end of the ORF was chosen for primer design. Initially, the primer was designed using Primer3 (version 0.4.0) (Untergasser et al., 2012). Primer3 was set to choose a primer with a length of 20 bp, a melting temperature of approximately 60°C and a GC content between 40 and 60%. Subsequently, the potential primer chosen by Primer3, was tested for its suitability for PCR using Oligo Analyzer Version 3.1 (<http://sg.idtdna.com/analyzer/Applications/OligoAnalyzer/>). Oligo Analyzer was used to check for primer-dimer formation and for the formation of secondary structures within the primer sequence which if present could reduce the amplification efficiency of the PCR reactions. Finally, the selected primers were ordered from GeneWorks Pty. Ltd. (Australia).

5.2.8. Conventional polymerase chain reaction for cloning a PGC-1 α cDNA from YTK red muscle

Total RNA was extracted from YTK red muscle and first-strand cDNA was synthesised from 1 μ g of this RNA as described in Section 5.2.6. Conventional PCR was performed as follows. Each 50 μ L PCR reaction contained 5 μ L of a 1:5 dilution of YTK red muscle cDNA, 0.2 μ M each of the PGC-1 α F1 and PGC-1 α R1 PCR primers (Table 5.1), 200 μ M dNTPs (Promega), 2.5 units of *Taq* DNA Polymerase (New England Biolabs) and 5 μ L of 10x ThermoPol[®] Buffer (New England Biolabs). The PCR cycling conditions consisted of an initial denaturation step at 95°C for 30 s followed by 30 cycles of denaturation at 95°C for 30 s, annealing at 60°C for 30 s and extension at 68°C for 4 min. At the end of the cycling, there was a final extension step at 68°C for 5 min. The

cycling was done in a Hybaid PX2 thermal cycler (Thermo Scientific) and when it was complete, the PCR reaction mixture was subjected to electrophoresis on a 1.5% (w/v) agarose gel containing 1 × SYBR[®] Safe DNA Gel Stain (Invitrogen[™]). The DNA in the agarose gel was visualised using a Gel Doc[™] EZ System (Bio-Rad) and a digital image was obtained using Image Lab software (version 4.0) (Bio-Rad). PCR products close to the expected size were purified from the gel using the Wizard[®] SV Gel and PCR Clean-Up System (Promega), according to the manufacturer's instructions.

Table 5.1. PCR primer sequences

Primer	Sequence (5' → 3')	Usage
T7 ^b	TAATACGACTCACTATAGGG	cDNA sequencing
SP6 ^b	TATTTAGGTGACACTATAG	cDNA sequencing
PGC-1α F1 ^a	ATGGCGTGGGACAGGTGTA	cDNA cloning/qRT-PCR
PGC-1α R1	GTGGAGGCTGGATCAAAGTC	cDNA cloning
PGC-1α F2	CTCGTTCTCCTCCCTCTCCT	cDNA sequencing
PGC-1α R2	GCCTTCGGTAGTGTGAGGAG	cDNA sequencing
PGC-1α qRT R	TGATTGGTCACTGTACCATTTGAG	qRT-PCR
PPARα F	CACCACTTTGCCATTGATTG	qRT-PCR
PPARα R	GCAGTCATGTCCGGGTATCT	qRT-PCR
MCAD F	CGGAACAGCAGAAGGAGTTC	qRT-PCR
MCAD R	TGAGGCAGTTGTCGAAGATG	qRT-PCR
CS F ^d	CTGGACTGGTCCCACA ACTT	qRT-PCR
CS R ^d	GGACAGGTAGGGGTCAGACA	qRT-PCR
PK F ^d	CTGGGATGAACATTGCAAGA	qRT-PCR
PK R ^d	TCCTGATTTCTGGTCCCTTG	qRT-PCR
COXI F	TGAACAGTCTACCCGCCTCT	qRT-PCR
COXI R	CGGCTAGA ACTGGGAGTGAC	qRT-PCR
β-actin F ^c	ACCCACACAGTGCCCATCTA	qRT-PCR
β-actin R ^c	TCACGCACGATTTCCCTCT	qRT-PCR

^a Designed by LeMoine et al. (2008)

^b Promega T7 (Q5021) and SP6 (Q5011) primers

^c Designed by Agawa et al. (2012)

^d Designed by the author of this thesis (refer to Chapter 3)

5.2.9. Cloning of the PGC-1 α PCR product in *Escherichia coli*

The gel purified PGC-1 α PCR product (Section 5.2.8) was ligated into the pGEM[®]-T Easy vector (Promega) and the resulting construct was used to transform *E. coli* 5 α competent cells (New England Biolabs), following the manufacturers' instructions. Subsequently, the transformed cells were plated onto Luria broth (LB) agar containing 100 μ g/mL ampicillin and colonies that were resistant to the antibiotic were selected. The selected colonies were screened for the presence of the PGC-1 α insert using colony PCR. Colony PCR was performed using primers targeting the T7 and SP6 promoter regions of the vector. Confirmed positive colonies were cultured overnight at 37°C in LB broth containing 100 μ g/mL ampicillin. Following the overnight culture, plasmid DNA was extracted from the cells using the Wizard[®] Plus SV Minipreps DNA Purification System (Promega) and the insert DNA was sequenced commencing from both the 5' and 3' ends, using the Sanger sequencing method, with primers targeting the T7 and SP6 promoter regions of the vector. Using these primers, approximately 1,000 bp of sequence was obtained at the 5'-end of the PGC-1 α cDNA and approximately 700 bp at the 3'-end but no sequence data were obtained for the central region between these two ends. Thus, two new primers were designed to obtain the sequence of the central region. The procedure followed was essentially as described in Section 5.2.7 except that the now known sequence of the newly cloned YTK PGC-1 α cDNA was used as the template to design the PGC-1 α F2 and PGC-1 α R2 primers (Table 5.1). The PGC-1 α F2 and PGC-1 α R2 primers were used for sequencing in the forward and reverse directions, respectively. The cDNA sequences obtained in this way overlapped with the cDNA sequences obtained for the 5' and 3' ends. The cDNA sequences obtained from the second round of sequencing also overlapped with each other in the middle of the PGC-1 α cDNA. Using this approach, sequence was obtained from 11 independent colonies and all colonies yielded the same sequence. The resulting sequence data were used to perform a BLAST search of the GenBank database (available at <http://www.ncbi.nlm.nih.gov/>) to confirm the identity of the PCR product.

5.2.10. Quantitative Real Time-Polymerase Chain Reaction

Quantitative real time-polymerase chain reaction (qRT-PCR) was used to analyse the expression of the CS, COXI, PK, PGC-1 α , PPAR α and MCAD genes and the normalization gene β -actin in the red muscle, white muscle and liver of the YTK specimens sampled for this study. The forward primer for PGC-1 α (PGC-1 α F1) was designed by LeMoine et al. (2008). The reverse primer for PGC-1 α (PGC-1 α qRT R) was designed by the author of this thesis using the sequence of the newly cloned YTK PGC-1 α cDNA as the template (Section 5.2.9). The β -actin primers were designed by Agawa et al. (2012) and the CS and PK primers were designed by the author of this thesis (refer to Section 3.2.5.). The PPAR α and MCAD primers were designed based on cDNA sequences from YTK (GenBank accession nos. XM_023402034.1 and XM_023424498.1, respectively). The COXI primers were designed based on the mitochondrial DNA sequence from YTK (GenBank accession no. NC_016869.1). Each qRT-PCR run included the cDNAs from all of the control fish and all of the feed-restricted fish for one tissue type for one of the genes of interest and for the normalisation gene β -actin. The samples were analysed in duplicate (technical replication) and the average values for the duplicates were used in the calculations. The mean value for the three fish from each tank was used as the unit of biological replication. Each qRT-PCR reaction (total volume 20 μ L) contained 5 μ L of the relevant cDNA, 10 μ L of the KAPA SYBR[®] FAST qPCR Master Mix (2X) Universal (KAPA Biosystems), 0.4 μ L each of the relevant forward and reverse primers (Table 5.1) to give a final primer concentration of 200 nM plus the appropriate volume of autoclaved deionized water. Amplification was performed using a Rotor-Gene Q thermal cycler (QIAGEN) fitted with fluorescence detection. The cycling conditions consisted of an initial denaturation step at 95°C for 3 min followed by 40 cycles of denaturation at 95°C for 3 s, annealing at 60°C for 20 s and extension at 72°C for 20 s. At the end of each amplification run, melt curve analysis was performed to ensure that only one product was produced for each set of primers. This was done by raising the temperature from 60 to 95°C in 0.5°C increments and observing the fluorescence change as the DNA strands separated. Amplification of only one product was re-confirmed by analysing the products using agarose gel electrophoresis. The transcript abundances for the genes of interest were normalised to the transcript abundance for the

housekeeping gene β -actin using the $2^{-\Delta C_t}$ method, where $\Delta C_t = C_t(\text{gene of interest}) - C_t(\beta - \text{actin})$ (Livak and Schmittgen, 2001).

5.2.11. Determining the amplification efficiency for the qPCR primers

The amplification efficiency for each pair of qPCR primers was between 90 and 105% and it was determined as follows. Conventional PCR was performed as described in Section 5.2.8 but with some modifications. The primers used were those designated as being for qRT-PCR in Table 5.1, the extension time during the PCR cycling was reduced to 1 min and the PCR products were purified directly from the PCR reaction mixture using the Wizard[®] SV Gel and PCR Clean-Up System (Promega) rather than being gel purified. The purified PCR products were cloned in *E. coli* and the plasmid DNA was extracted from the cells as described in Section 5.2.9. Subsequently, the insert DNA was sequenced using the Sanger sequencing method, at the Australian Genome Research Facility Ltd (AGRF), using the primers targeting the T7 and SP6 promoter regions of the vector. The resulting sequence data were used to perform BLAST searches of the GenBank database (available at <http://www.ncbi.nlm.nih.gov/>) to confirm the identity of the products. After the identity of the PCR products had been confirmed, a 10-fold dilution series was produced using the remaining plasmid construct for each gene of interest. The 10-fold dilution series was then used as the DNA template for qRT-PCR following the procedure above (Section 5.2.10). The amplification efficiency for each primer pair was then calculated by plotting the \log_{10} transcript copy number and the resulting C_t values for each dilution and fitting a linear regression. The slope of the resulting linear regression was then used in the following equation; $\text{Primer efficiency (\%)} = \left(10^{\left(\frac{-1}{\text{slope}}\right)} - 1\right) \times 100$.

5.2.12. Statistical analyses

Statistical analyses were performed using the IBM[®] SPSS Statistics version 22.0 software package (IBM, New York, USA). The FL, BM and K values were statistically analysed using Independent-samples *t*-tests to determine whether there were significant differences between the control and the feed-restricted fish. The enzyme activity and transcript abundance values were statistically analysed using One-way Analysis of variance (ANOVA), with *post hoc*

comparisons performed using Tukey's test, to determine whether or not there were significant differences between the different tissue types and also between the control and the feed-restricted fish. Pearson Correlation analysis was used to identify significant correlations between enzyme activities and transcript abundances. Values were considered to be statistically significantly different when $P < 0.05$.

5.3. Results

5.3.1. Fish growth

The final fork length (FL), body mass (BM) and condition factor (K) values for the control and feed-restricted fish can be seen in Table 5.2. Compared with the control fish, the feed-restricted fish exhibited a significant 14% reduction in their final BM ($P < 0.005$) and a significant 9% reduction in their final condition factor ($P < 0.005$) but no change in their final FL. Thus, feed restriction significantly reduced the growth of the fish. As stated in the Materials and Methods section, the fish we sampled were taken from a larger pool of individuals as part of a larger study. Thus, we know the initial FL, BM and K values for this larger pool of individuals but not for the particular fish we sampled. The initial mean \pm SE FL, BM and K values for the larger pool of individuals were 46.7 ± 1.5 cm, 1.44 ± 0.13 kg and 1.46 ± 0.10 , respectively. Thus, although we cannot perform any statistical analyses, it is apparent that the control fish in our study increased in BM and body condition whereas the severely feed-restricted fish actually lost weight and decreased in body condition.

Table 5.2. The effects of restricted feeding over a period of 84 days on the growth of juvenile YTK at winter water temperatures.

	Control	Feed restricted
Final fork length (cm)	46.2±0.5	47.2±0.3
Final body mass (kg)	1.52±0.03 ^a	1.31±0.03 ^b
Final condition factor (K)	1.45±0.03 ^a	1.32±0.03 ^b

Values are the mean ± the standard error of the mean (n = 3). There were three replicate tanks for the control fish and three for the feed-restricted fish. Three fish were harvested from each tank. For the statistical analyses, the unit of replication was the tank. Statistically significant differences within a row are indicated by different superscript letters ($P < 0.05$).

5.3.2. Effects of tissue type and feed restriction on CS enzyme activity

CS enzyme activity was assayed as an indicator of mitochondrial abundance and aerobic metabolic capacity. In the control fish, the mean CS enzyme activities were 19.9 ± 2.1 , 2.6 ± 0.3 and 1.8 ± 0.1 U/g tissue in the red muscle, the white muscle and the liver, respectively (Fig. 5.1). Thus, the CS enzyme activity per g tissue was approximately 8-fold greater in the red muscle than in the white muscle and approximately 11-fold greater in the red muscle than in the liver. This is consistent with the red muscle having a greater number of mitochondria and a greater aerobic metabolic capacity than either the white muscle or the liver. A similar pattern was observed when the CS enzyme activity was expressed per mg protein (Fig. 5.2). Specifically, CS enzyme activity per mg protein was 15-fold greater in the red muscle compared with the white muscle and 42-fold greater in the red muscle compared with the liver.

There was no statistically significant effect of feed restriction on CS enzyme activity expressed either per g tissue or per mg protein in either the red muscle or the white muscle but there was a statistically significant effect in the liver (Figs. 5.1 and 5.2). In the liver, the feed-restricted fish exhibited a significant 57% increase in CS enzyme activity when expressed per g tissue and a significant 45% increase in CS enzyme activity when expressed per mg protein, relative to the control. Thus, there was a substantial increase in CS enzyme activity in the liver in response to feed restriction. This suggests that feed restriction results in an increase in mitochondrial abundance and aerobic metabolic capacity in the liver of YTK.

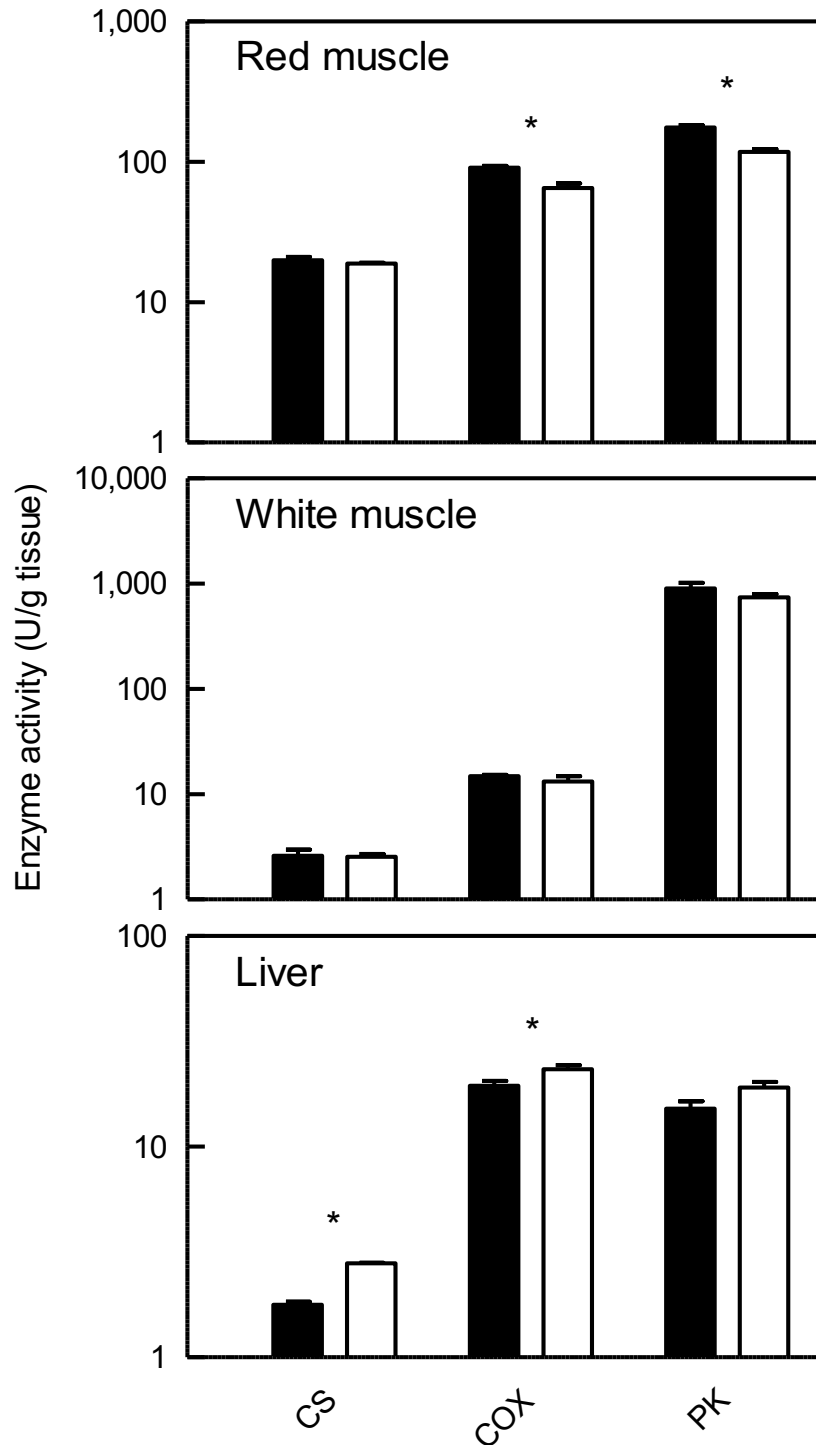


Fig. 5.1. The effects of restricted feeding on CS, COX and PK enzyme activities expressed per g tissue in the red muscle, white muscle and liver of juvenile YTK. The control fish were fed to apparent satiation six days per week (black columns) whereas the feed restricted fish were fed at 0.1% (w/w) BM once per week (white columns). The data are the mean \pm the standard error of the mean (n = 3). One-way ANOVA was performed to identify statistically significant differences between the control and the treated fish ($P < 0.05$). Statistically significant differences are indicated by *.

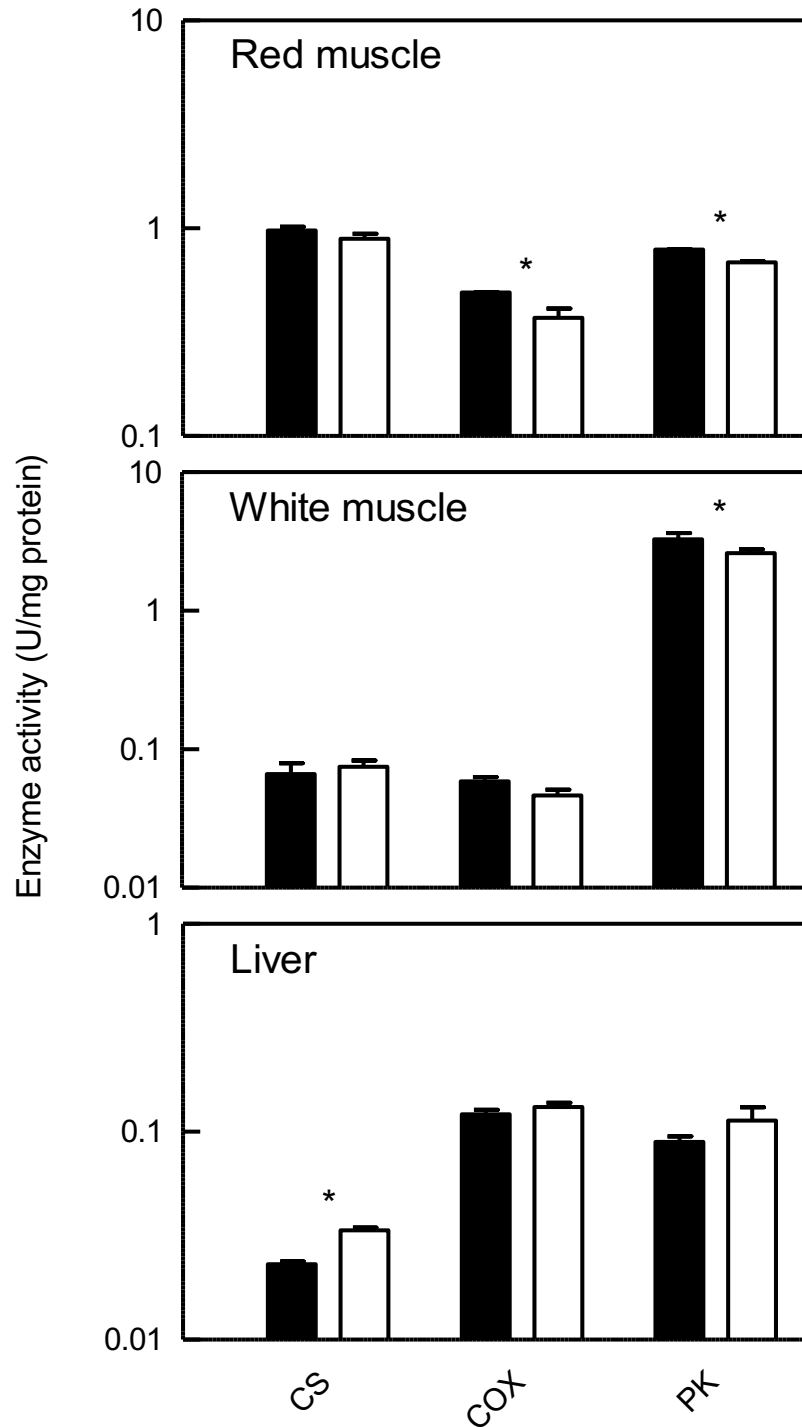


Fig. 5.2. The effects of restricted feeding on CS, COX and PK enzyme activities expressed per mg protein in the red muscle, white muscle and liver of juvenile YTK. The control fish were fed to apparent satiation six days per week (black columns) whereas the feed restricted fish were fed at 0.1% (w/w) BM once per week (white columns). The data are the mean \pm the standard error of the mean (n = 3). One-way ANOVA was performed to identify statistically significant differences between the control and the treated fish ($P < 0.05$). Statistically significant differences are indicated by *.

5.3.3. Effects of tissue type and feed restriction on COX enzyme activity

COX enzyme activity was assayed as an alternative indicator of mitochondrial abundance and also as an indicator of the extent of folding of the inner mitochondrial membrane. In the control fish, the mean COX enzyme activities were 91.1 ± 2.5 , 14.9 ± 0.8 and 19.5 ± 0.6 U/g tissue in the red muscle, the white muscle and the liver, respectively (Fig. 5.1). Thus, the COX enzyme activity per g tissue was approximately 6-fold greater in the red muscle compared with the white muscle and approximately 5-fold greater in the red muscle compared with the liver. Again, this is consistent with the red muscle having a greater number of mitochondria and a greater aerobic metabolic capacity than either the white muscle or the liver. Similarly, when expressed per mg protein, the COX enzyme activity was 8-fold greater in the red muscle compared with the white muscle and 4-fold greater in the red muscle compared with the liver.

There were no statistically significant effects of feed restriction on COX enzyme activity either per g tissue or per mg protein in the white muscle but there were significant effects in the red muscle and the liver (Figs. 5.1 and 5.2). In the red muscle, COX enzyme activity was 29% lower when it was expressed per g tissue ($P < 0.05$) and 24% lower when it was expressed per mg protein ($P < 0.05$), in the feed-restricted fish compared with the activity in the control fish. In the liver, on the other hand, COX enzyme activity was 20% higher in the feed-restricted fish compared with the control fish when it was expressed per g tissue ($P < 0.05$) but there was no significant difference when the activity was expressed per mg protein. In summary, feed restriction appeared to decrease mitochondrial abundance and/or folding of the mitochondrial inner membrane in the red muscle, have no effect on these parameters in the white muscle but increase these parameters in the liver.

5.3.4. Effects of tissue type and feed restriction on PK enzyme activity

PK enzyme activity was assayed as an indicator of glycolytic capacity. In the control fish, the mean PK enzyme activities were 176.0 ± 8.7 , 903.2 ± 74.9 and 15.2 ± 1.4 U/g tissue in the red muscle, the white muscle and the liver, respectively (Fig. 5.1). Thus, the PK enzyme activity per g tissue was approximately 5-fold greater in the white muscle compared with the red muscle

and approximately 60-fold greater in the white muscle compared with the liver. This is consistent with white muscle metabolism being predominantly glycolytic. Similarly, when expressed per mg protein, PK enzyme activity was 4-fold greater in the white muscle compared with the red muscle and approximately 37-fold greater in the white muscle compared with the liver.

In the red muscle, PK enzyme activity of the feed-restricted fish was 33% lower than that of the control fish when it was expressed per g tissue ($P < 0.05$) and 13% lower than that of the control fish when it was expressed per mg protein ($P < 0.05$). In contrast, in the white muscle, PK enzyme activity of the feed-restricted fish did not differ significantly from that of the control fish when it was expressed per g tissue but was 20% lower than that of the control fish when it was expressed per mg protein ($P < 0.05$). Regardless of how the enzyme activity was expressed, feed restriction had no effect on PK enzyme activity in the liver. Taken together, these data indicate that feed restriction decreases glycolytic capacity in the red and white muscle of YTK but not in the liver.

5.3.5. Effects of tissue type and feed restriction on the amount of protein extracted per g tissue

The mean amounts of protein extracted for the CS enzyme assays were 20.6 ± 0.1 , 40.4 ± 2.1 and 77.1 ± 4.6 mg per g tissue for the red muscle, white muscle and liver respectively (Fig. 5.3) Thus, the amount of protein extracted per g tissue was approximately 2-fold greater in the white muscle and approximately 4-fold greater in the liver compared to the red muscle and these differences were statistically significant ($P = 0.05$). There were no statistically significant effects of feed restriction on the amount of protein extracted per g tissue for the CS enzyme assays from the red muscle, white muscle or liver (Fig. 5.3).

The mean amounts of protein extracted for the COX enzyme assays were 186.8 ± 4.9 , 258.8 ± 25.1 and 161.3 ± 4.7 mg per g tissue for the red muscle, white muscle and liver respectively (Fig. 5.3). Thus, the amount of protein extracted per g tissue was approximately 39% greater in the white muscle compared to the red muscle and this was statistically significant ($P = 0.05$). In contrast, there was no significant difference in the amount of protein extracted

per g tissue between the red muscle and the liver. There were no statistically significant effects of feed restriction on the amount of protein extracted per g tissue for the COX enzyme assays in the red muscle or the white muscle but there was a 10% greater amount of protein extracted from the liver ($P < 0.05$). Although this effect was statistically significant, the small difference makes it unlikely to be biologically relevant.

The mean amounts of protein extracted for the PK enzyme assays were 224.0 ± 10.0 , 274.08 ± 5.1 and 170.0 ± 8.1 mg per g tissue for the red muscle, white muscle and liver respectively (Fig. 5.3). Thus, the amount of protein extracted per g tissue was approximately 22% greater in the white muscle and approximately 24% lower in the liver compared to the red muscle and these differences were statistically significant ($P = 0.05$). The amount of protein extracted per g tissue for the PK enzyme assays did not differ significantly between the feed-restricted fish and the control fish in either the white muscle or the liver but it was 23% lower in the red muscle of the feed-restricted fish compared with the control fish ($P < 0.05$) (Fig. 5.3).

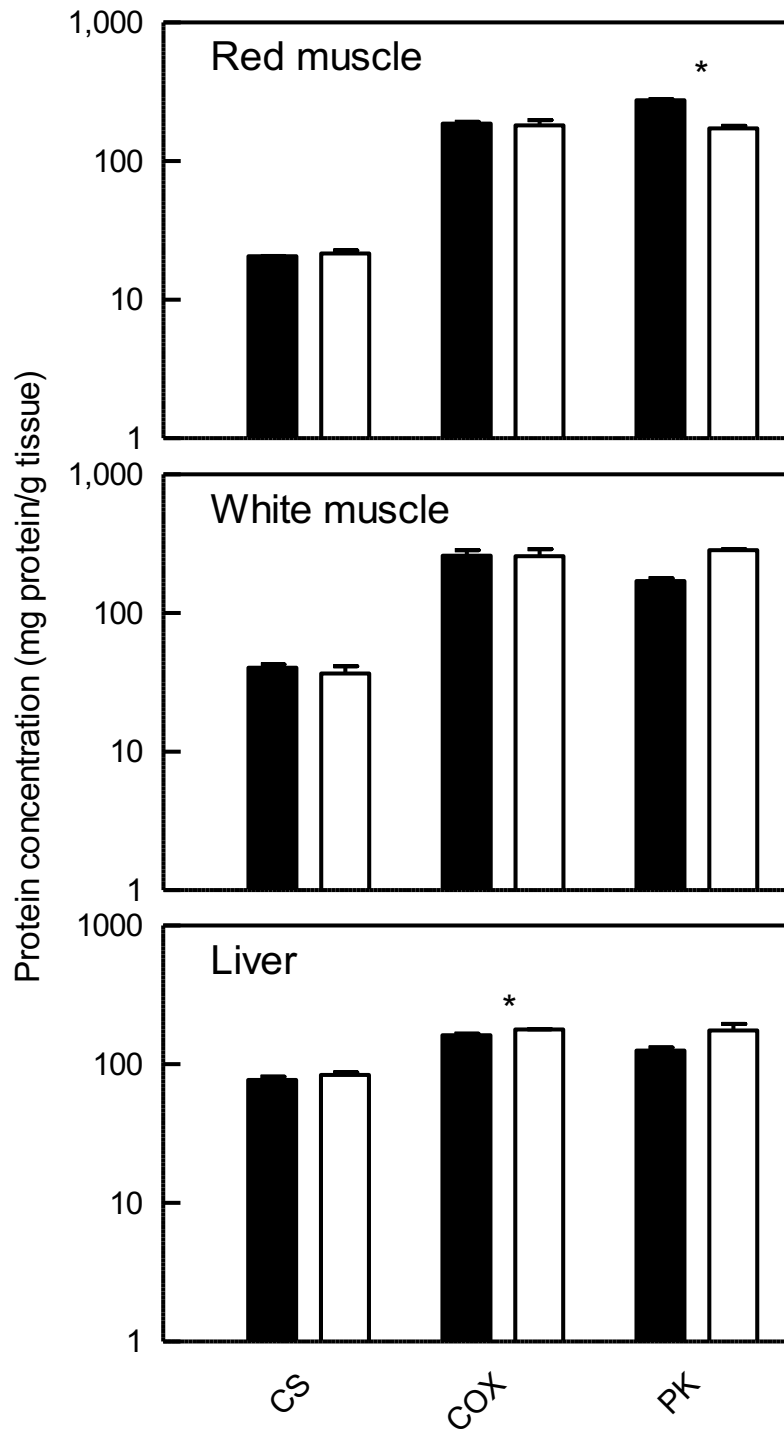


Fig. 5.3. The effects of restricted feeding on the amount of protein extracted per g tissue from the red muscle, white muscle and liver of juvenile YTK for the CS, COX and PK enzyme assays (Fig. 1 and Fig 2). The control fish were fed to apparent satiation six days per week (black columns) whereas the feed restricted fish were fed at 0.1% (w/w) BM once per week (white columns). The data are the mean \pm the standard error of the mean ($n = 3$). One-way ANOVA was performed to identify statistically significant differences between the control and the treated fish ($P < 0.05$). Statistically significant differences are indicated by *.

5.3.6. Effects of tissue type and feed restriction on CS transcript abundance

The effects of tissue type and feed restriction on the relative abundance of the CS transcript are shown in Fig. 5.4. Interestingly, there was no statistically significant difference in CS transcript abundance between the red and the white muscle (Fig 5.4). This was surprising because when we examined CS enzyme activity it was approximately an order of magnitude greater in the red muscle compared with the white muscle (Fig. 5.1). This lack of correlation between CS transcript abundance and CS enzyme activity suggests that CS enzyme activity is regulated at the post-transcriptional or post-translational level rather than at the transcriptional level. We observed a 9-fold greater CS transcript abundance in the red muscle compared with the liver but this apparent difference was not statistically significant. The lack of statistical significance is most likely due to the large amount of fish to fish variation in the CS transcript abundance.

There was no significant effect of feed restriction on CS transcript abundance in either the red muscle, the white muscle or the liver (Fig. 5.4). Similarly, we had seen no significant effect of feed restriction on CS enzyme activity in either the red muscle or white muscle, but we had seen a significant effect in the liver. From this we conclude that restricted feeding increases CS enzyme activity and therefore mitochondrial abundance and aerobic metabolic capacity in the liver of YTK without increasing the transcript abundance. Again, this suggests that CS enzyme activity is regulated at the post-transcriptional or post-translational level and not at the transcriptional level. When the CS transcript abundance was plotted against the CS enzyme activity (expressed as U/g tissue) there was no significant correlation between these two parameters (Fig. 5.5). This further supports our conclusion that CS enzyme activity is regulated at the post-transcriptional or post-translational level rather than the transcriptional level.

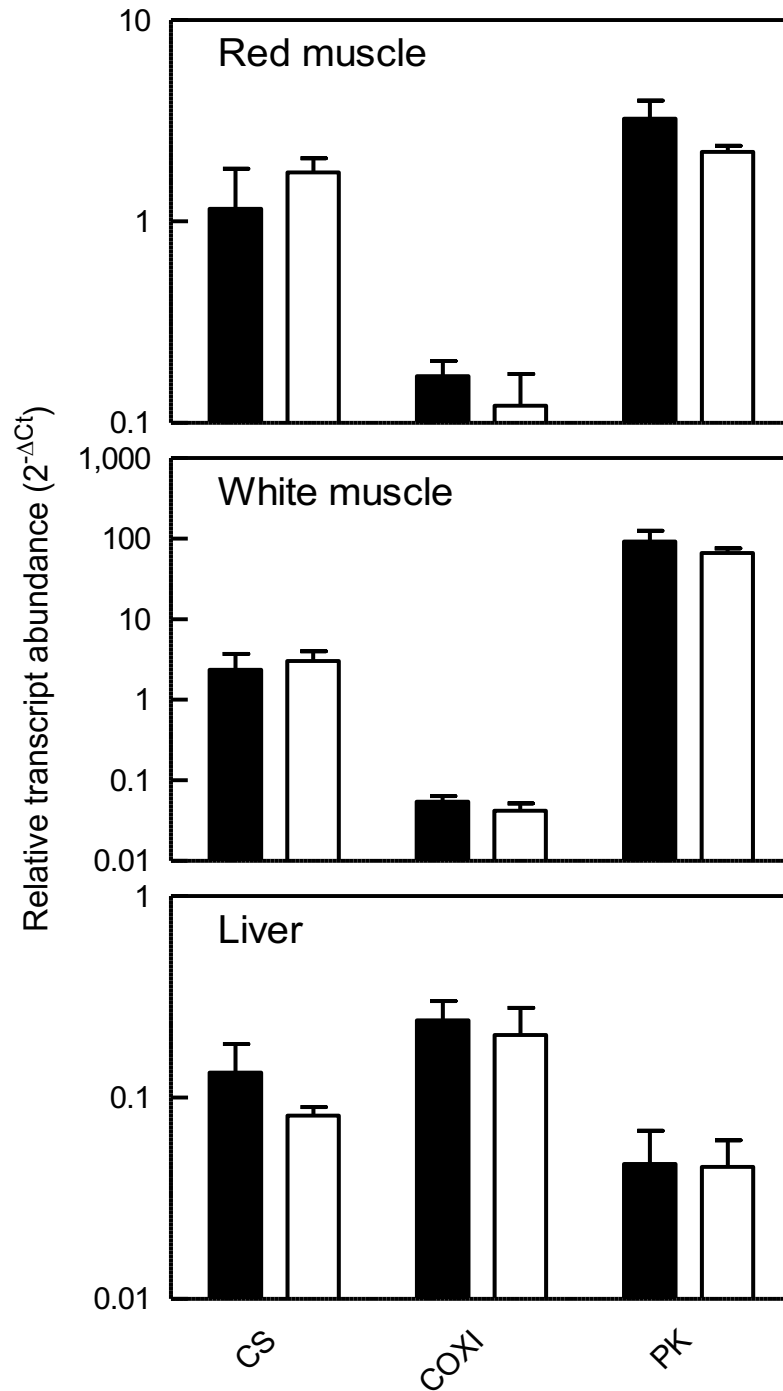


Fig. 5.4. The effects of restricted feeding on the relative transcript abundances for CS, COXI and PK in the red muscle, white muscle and liver of juvenile YTK. The control fish were fed to apparent satiation six days week (black columns) whereas the feed restricted fish were fed at 0.1% (w/w) BM once per week (white columns). The transcript abundances for the genes of interest were normalised to the transcript abundance for the housekeeping gene β -actin using the $2^{-\Delta C_t}$ method (Livak and Schmittgen, 2001). The data are the mean \pm the standard error of the mean (n = 3). One-way ANOVA was performed to identify statistically significant differences between the control and the treated fish ($P < 0.05$). Statistically significant differences are indicated by *.

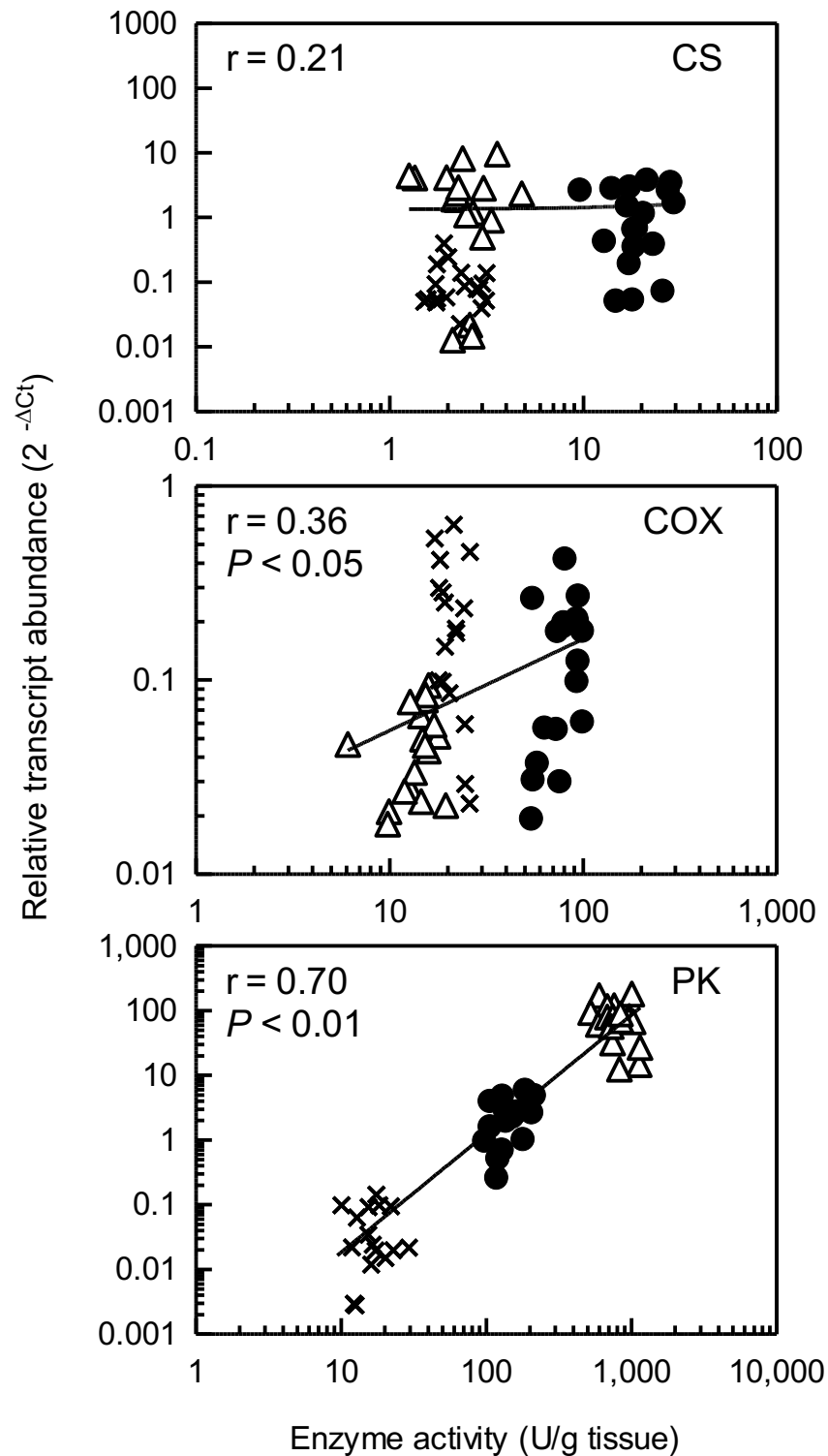


Fig 5.5. Correlation analysis of enzyme activity with transcript abundance for citrate synthase (CS), cytochrome c oxidase (COX) and pyruvate kinase (PK) in the red muscle (●), white muscle (Δ) and liver (×) of YTK. The data were combined for the control and the feed restricted fish (n = 18 for each tissue type).

5.3.7. Effects of tissue type and feed restriction on COXI transcript abundance

In the control fish, the highest COXI transcript abundance was observed in the liver and it was 40% greater than in the red muscle and was approximately 3-fold higher in the red muscle compared with the white muscle. The apparently higher COXI transcript abundance in the red muscle compared to the white was not statistically significant but the higher transcript abundance in the liver compared to the white muscle was statistically significant ($P < 0.05$) (Fig 5.4). The lack of any significant difference in COXI transcript abundance between the red muscle and the white muscle was in stark contrast the 6-fold difference in COX enzyme activity with the red muscle having a much higher activity than the white (Fig. 5.1). As explained above for CS, our data suggest that COX enzyme activity is regulated at the post-transcriptional or post-translational level rather than at the transcriptional level in these tissues.

There was no significant effect of feed restriction on COXI transcript abundance in either the red muscle, the white muscle or the liver (Fig. 5.4). In contrast, feed restriction had resulted in a significant decrease in COX enzyme activity in the red muscle and a significant increase in this parameter in the liver (Fig. 5.1). Due to the difference we observed between COX enzyme activity and COXI transcript abundance, we conclude that COX enzyme activity may be regulated not at the transcriptional level but at the post-transcriptional or post-translational level. When COXI transcript abundance was plotted against COX enzyme activity (expressed as U/g tissue) there was a weak but significant correlation between these two parameters ($r = 0.36$, $P < 0.05$) (Fig. 5.5). The weakness of this correlation is further evidence that COX enzyme activity is not regulated at the transcriptional level.

5.3.8. Effects of tissue type and feed restriction on PK transcript abundance

In the control fish, PK transcript abundance was greater in the white muscle than it was in either the red muscle or the liver (Fig. 5.4). Specifically, PK transcript abundance was approximately 29-fold greater in the white muscle compared with the red muscle ($P < 0.05$) and approximately 2000-fold greater

in the white muscle compared with the liver ($P < 0.05$). This was to some extent consistent with what we had observed for PK enzyme activity except that the fold differences were not of the same magnitude. Specifically, PK enzyme activity per g tissue was 5-fold greater in the white muscle compared with the red muscle and 60-fold greater in the white muscle compared with the liver. Overall, these data suggest that, unlike CS enzyme activity and COX enzyme activity, PK enzyme activity is regulated at the transcriptional level. When PK transcript abundance was plotted against PK enzyme activity, expressed per g tissue, there was a strong positive correlation between these two parameters ($r = 0.70$, $P < 0.01$) (Fig. 5.5). This adds weight to our hypothesis that PK enzyme activity/protein abundance is regulated at the transcriptional level.

In contrast to the stark differences observed between the different tissue types, feed restriction had no statistically significant effect on PK transcript abundance in any of the tissues we examined. This was surprising because although PK enzyme activity per g tissue remained unchanged in the white muscle and the liver in response to feed restriction, it was 33% lower in the red muscle of the feed restricted fish compared with the control fish.

5.3.9. Cloning and sequence analysis of a PGC-1 α cDNA from YTK red muscle

We have cloned 2,789 base pair (bp) of the open reading frame (ORF) of a PGC-1 α gene from YTK red muscle. The cDNA was deposited in the NCBI nucleotide database with the accession no. KU869768.1 and the corresponding protein has the accession no. AMQ10352.1. According to a multiple sequence alignment, the YTK PGC-1 α ORF was missing approximately ~22 amino acids at the C-terminus but no amino acids at the N-terminus (Fig. 5.6). Despite the missing amino acids, the predicted protein still contained the canonical motifs that are characteristic of PGC-1 α proteins from fish and vertebrates in general. Specifically, the YTK sequence contained the transcriptional activation domains, AD1, with the sequence DLPELDLSELD and AD2, with the sequence NEANLLAVLTETLD, at residues 30 – 40 and 82 – 95, respectively (Sadana and Park, 2007b). It also contained the tri-lysine motif (KKK) which is part of the NRF-1 interaction domain at residues 278 – 281. Furthermore, it contained the three leucine-rich motifs L1, with the

sequence LLAVL, L2, with the sequence LKKLL, and L3, with the sequence LLKYL, at residues 86 – 90, 142 – 146 and 210 – 214 (Knutti et al., 2001). In mammals, the L2 motif facilitates binding between PGC-1 α and transcription factors from the nuclear receptor family, including PPAR α (Vega et al., 2000). In mammals, the L3 motif facilitates binding between PGC-1 α and ERR α , another member of the nuclear receptor family (Huss et al., 2002).

In contrast to the above, there were certain regions that were not so well conserved. Specifically, this refers to the recognition site for AMP-activated protein kinase (AMPK) and the binding sites for certain other transcription factors. In the brown rat sequence, there is a recognition site for AMPK between residues 165 and 186 (numbered according to the brown rat sequence). In mammals, AMPK has been shown to activate PGC-1 α by phosphorylating a threonine residue (Thr₁₇₇) within the AMPK recognition site (Jager et al., 2007). This residue is highly conserved between chicken (representing birds), the Chinese alligator (representing reptiles) and the African clawed frog (representing amphibians) but not in YTK or any of the other fish sequences.

In the brown rat sequence, there is a binding site for the NRF-1 transcription factor at residues 180 – 403 (Wu et al., 1999). This is well conserved in the chicken, the Chinese alligator, the African clawed frog, the spiny dogfish and the West African lungfish but not in either YTK or the swordfish (Fig. 5.6). YTK and the swordfish are members of the subclass Actinopterygii (ray-finned fishes). In the YTK sequence, the canonical NRF-1 binding site is interrupted by a serine (S)-rich insertion (residues 231 – 269 of the YTK sequence), a glutamine (Q)-rich insertion (residues 289 – 300 of the YTK sequence) and multiple mixed amino acid residue insertions (residues 386 – 392, 422 – 431, 443 – 446 of the YTK sequence). In the brown rat sequence, there is a binding site for PPAR γ at residues 338 – 403 (Puigserver et al., 1998). Again, this is well conserved in the representatives of the birds, reptiles, amphibians, cartilaginous fishes and lobe-finned fishes but not in the ray-finned fishes, including YTK. In YTK, this transcription factor binding site is interrupted by mixed amino acid residue insertions (residues 422 – 431, 443 – 446 of the YTK sequence). Finally, in the brown rat sequence, there is a binding site for MEF2 at residues 403 – 570 that is well conserved in all of the other vertebrates

except the ray-finned fishes (Michael et al., 2001). In YTK, this region of the PGC-1 α protein is interrupted by various amino acid insertions at residues 485 – 502, 510 – 513, 527 – 549, 564 – 575 and 619 – 628 in the YTK sequence.


```

                    500      *      520      *      540      *      560
Yellowtail kingfish : VTSGATAAMPMTACTGVEDRHVQCKDSAMPSSSSSSSSCSPSSASSGGLAKQNFASVDGEAVRVQGLGK : 554
Swordfish          : VTSGAPAAPMPMTACTGVDRHVQCKDSAMPSSLSSSSSCSPSSAPSGGLAKQNFASVDGEAVRVQGLGK : 551
West African lungfish : R-----QSHGKYN-----VHGHLHLHLPVQT-----DRSGK : 396
Spiny dogfish      : KL-----QDHPCDE-----PLSGTHKQNFLSANED-----CGYKK : 410
African clawed frog : -----RHPECDE-----PLPGKELQVCSNFDQE-----CCQ-K : 417
Chinese alligator  : -----RQEFKDE-----SSPAWQCCICSSLEQD-----OYKKK : 432
Chicken            : -----RQEFKDE-----SSPGWQCCICSSLEQD-----OYFKK : 432
Rat                : -----RQDEFKDE-----ASCDWQGHICSSIDSS-----CYLK : 433

                    *      580      *      600      *      620      *
Yellowtail kingfish : QTTTQTTTIPSEATDRDQEHPSATSRKLLQDQIRAE LNKHFGHPLOALYSQGGQEREFGSKPNKSA : 624
Swordfish          : QTTTQTTTIPSQEATIDRDQHPHSATSRKLLQDQIRAE LNKHFGHPLOALYSQGGQEREFGSKPNKLA : 621
West African lungfish : ETQQLNRHP-----DQLTNRKHLQDQIRAE LNKHFGHPNOAFDQKSIATFSESQD----- : 448
Spiny dogfish      : ESQQLDTQIP-----IYSNTRIQDQDQIRAE LNKHFGHPQAEYDEVEDQARHQR----- : 462
African clawed frog : DSTPVTMP-----SSQNSHRKPLQDQIRAE LNKHFGHPQAVYNNETQISELVD----- : 467
Chinese alligator  : ETLQTNKQ-----GSHCNRRKQLQDQIRAE LNKHFGHPQAVFEEADQISELVD----- : 483
Chicken            : ETLQTSKQ-----GSGQNNRKLQDQIRAE LNKHFGHPQAVFEEADQISELVD----- : 483
Rat                : ETLQASKQ-----VSPCSTRKQLQDQIRAE LNKHFGHPQAVFDDKVDQISELVD----- : 484

                    640      *      660      *      680      *      700
Yellowtail kingfish : PQSLKEGDEYLSQKLPGSTVTHPCITPFHDELELGGRESRFLYFWEGLPLDLLEFCPPCSSSCSPSS : 694
Swordfish          : PQSLEGAADDYSSQRLPGSSVTHPCITPFHDELELGGRESRFLYFWEGLPLDLLEFCPPCSSSCSPSS : 691
West African lungfish : ---NDASANEYS-KLP--LCINAC-MPANGIFDESDDGDGKLLMSWDCEQADVLEFEEC---NSSPYS- : 506
Spiny dogfish      : ---KDFYHEYS-KLP--TILSAC-MSDDGVEDSDDETEKFLYWDGCPDG-PLERP---CSRSLSS- : 519
African clawed frog : ---SKYSDEQLS-RLP--LELTAC-LGIDSLEFDDSEDENDKLCYTWDEQSYSLFDES---SRSTFN- : 525
Chinese alligator  : ---SDYSNEQES-KLP--MEINSG-LAMDGLFDDSEDESDKLCYTWGQVAYSLEFVS---SSSFFN- : 541
Chicken            : ---SDYSNEQES-KLP--MEINSG-LAMDGLFDDSEDESDKLCYTWGQVAYSLEFVS---SSSFFN- : 541
Rat                : ---GNFSNEQES-KLP--VEINSG-LAMDGLFDDSEDENDKLSYFWDGQVAYSLEFVS---SSSFFN- : 542

                    *      720      *      740      *      760      *
Yellowtail kingfish : CSPSRGCVSPSSSLLSPGRPYCWTGCGSRSRSRSHGCSRSSSSHYRRLSLSPPDRPSSSRHN---T : 761
Swordfish          : CSPSRGCVSPSSSLLSPGRPFCWTSWRSRSRSHGCSRSSSSHYRRLSLSPPDRPSSSRHN---T : 758
West African lungfish : SPFRGCVSPPKS-LFLKTT--CRGRSRSRSRSHRCSRSSSYSHSRSRSPHSRSSRSCYCDSDNLSR : 572
Spiny dogfish      : SPFRGCVSPPKS-LFLKTT--CRGRSRSRSRSHRCSRSSSYSHSRSRSPHSRSSRSCYCDSDNLSR : 572
African clawed frog : SPFRGCVSPPKS-LFLKTT--CRGRSRSRSRSHRCSRSSSYSHSRSRSPHSRSSRSCYCDSDNLSR : 572
Chinese alligator  : SPFRGCVSPPKS-LFLKTT--CRGRSRSRSRSHRCSRSSSYSHSRSRSPHSRSSRSCYCDSDNLSR : 572
Chicken            : SPFRGCVSPPKS-LFLKTT--CRGRSRSRSRSHRCSRSSSYSHSRSRSPHSRSSRSCYCDSDNLSR : 572
Rat                : SPFRGCVSPPKS-LFLKTT--CRGRSRSRSRSHRCSRSSSYSHSRSRSPHSRSSRSCYCDSDNLSR : 572

                    780      *      800      *      820      *      840
Yellowtail kingfish : DSSTFRSRVYKSPHPOSRSPLSR--PRYDSYEEYQERLKRREYRDRYKREPERAQERORQKALIEE : 829
Swordfish          : ESSTFRSRVYKSPHPOSRSPLSR--PRYDSYEEYQERLKRREYRDRYKREPERAQERORQKALIEE : 826
West African lungfish : SSTSVPVTHVLDPGHHTGEOGMTAMRNDYSEYQERLKRREYRDRYKREPERAQERORQKALIEE : 642
Spiny dogfish      : VQHRSRGSPCSYSRSRSPSYRYNRDYDSYEEYQERLKRREYRDRYKREPERAQERORQKALIEE : 655
African clawed frog : CRE---KSPMYARSRS--PRGR--PRYDSYEEYQERLKRREYRDRYKREPERAQERORQKALIEE : 650
Chinese alligator  : CRHRAYSPLHARSRSRSPGNRR--PRYDSYEEYQERLKRREYRDRYKREPERAQERORQKALIEE : 672
Chicken            : CRHRAYSPLHARSRSRSPGNRR--PRYDSYEEYQERLKRREYRDRYKREPERAQERORQKALIEE : 672
Rat                : YRHRTHRNSPLYVRSRSPSYR--PRYDSYEEYQERLKRREYRDRYKREPERAQERORQKALIEE : 673

                    *      860      *      880      *      900      *
Yellowtail kingfish : RRVVYVGRLRNCRTRTELRRRFEVFGIEECCAVNLRDDGDNFGFITRYTCDAPFAALENGHTLRRSNEPQ : 899
Swordfish          : RRVVYVGRLRNCRTRTELRRRFEVFGIEECCAVNLRDDGDNFGFITRYTCDAPFAALENGHTLRRSNEPQ : 896
West African lungfish : RRVVYVGRLRNCRTRTELRRRFEVFGIEECCAVNLRDDGDNFGFITRYTCDAPFAALENGHTLRRSNEPQ : 712
Spiny dogfish      : RRVVYVGRLRNCRTRTELRRRFEVFGIEECCAVNLRDDGDNFGFITRYTCDAPFAALENGHTLRRSNEPQ : 725
African clawed frog : HRVYVGRKIRPDTTRTELRRRFEVFGIEECCAVNLRDDGDNFGFITRYTCDAPFAALENGHTLRRSNEPQ : 720
Chinese alligator  : RRVVYVGRKIRPDTTRTELRRRFEVFGIEECCAVNLRDDGDNFGFITRYTCDAPFAALENGHTLRRSNEPQ : 742
Chicken            : RRVVYVGRKIRPDTTRTELRRRFEVFGIEECCAVNLRDDGDNFGFITRYTCDAPFAALENGHTLRRSNEPQ : 742
Rat                : RRVVYVGRKIRPDTTRTELRRRFEVFGIEECCAVNLRDDGDNFGFITRYTCDAPFAALENGHTLRRSNEPQ : 743

                    920      *      940      *      960
Yellowtail kingfish : FELCFCKQKQFCKSHYTDLDSHSDDFDPAST----- : 930
Swordfish          : FELCFCKQKQFCKSHYTDLDSHSDDFDPAST----- : 927
West African lungfish : FEMCFCKRQKQFCKSEYTDLDCNLDDDFDPAST----- : 743
Spiny dogfish      : FELCFCKRQKQFCKSEYTDLDCNLDDDFDPAST----- : 737
African clawed frog : FEVCFCKRQKQFCKSNADLDSNSDDDFDPASTESKYDSMDFDSSLKEA----- : 767
Chinese alligator  : FEVYCFCKRQKQFCKSNADLDSNSDDDFDPASTESKYDSMDFDSSLKEAQRSRLLR : 795
Chicken            : FEVYCFCKRQKQFCKSNADLDSNSDDDFDPASTESKYDSMDFDSSLKEAQRSRLLR : 795
Rat                : FEVYCFCKRQKQFCKSNADLDSNSDDDFDPASTESKYDSLDFDSSLKEAQRSRLLR : 796

```

Fig. 5.6. A multiple sequence alignment of PGC-1 α amino acid sequences from representatives of six of the seven classes that make up the subphylum vertebrata. The protein accession numbers are as follows: YTK (bony fishes/ray-finned fishes) AMQ10352.1; swordfish (bony fishes/ray-finned fishes), ACY24361.1; West African lungfish (bony fishes/lobe-finned fishes) FJ710608; spiny dogfish (cartilaginous fishes) ACY24363.1; African clawed frog (amphibians) ACY24354.1; Chinese alligator (reptiles) XP_025061364.1; chicken (birds) NP_001006457.1; rat (mammals) NP_112637.1. The alignment was performed using ClustalX2 software (Larkin et al., 2007) and the shading was done using GeneDoc software (Nicholas et al., 1997). The degree of amino acid conservation is indicated by 3 levels of shading with black, dark grey and light grey indicating 100, 80 and 60% conservation, respectively. The transcription activation domains are indicated by DLPELDLSELD (AD1) and NEANLLAVLTETLD (AD2), the leucine-rich motifs (L1, L2 and L3) are indicated by grey text and the tri-lysine motif is indicated by KKK. The AMPK recognition site is indicated by grey shading above the text and Thr₁₇₇ is indicated by dark grey shading and 'T' within the shaded region. The NRF-1, PPAR γ and MEF2C transcription factor binding domains are indicated by black solid, grey solid and black dotted lines, respectively. The RNA recognition motif is indicated by a dashed line above the sequence.

Table 5.3. Species names and accession numbers used to construct the phylogenetic tree shown in Fig. 5.7

Class/subclass	Taxon	Accession number
Mammalia (mammals)	Rat (<i>Rattus norvegicus</i>)	NP_112637.1
	Mouse (<i>Mus musculus</i>)	NP_032930.1
	Cow (<i>Bos taurus</i>)	AAQ82595.1
Aves (birds)	Chicken (<i>Gallus gallus</i>)	NP_001006457.1
	Southern ostrich (<i>Struthio camelus australis</i>)	KFV80390.1
Reptilia (reptiles)	Chinese alligator (<i>Alligator sinensis</i>)	XP_025061364.1
	Green sea turtle (<i>Chelonia mydas</i>)	XP_007058167.1
	Burmese python (<i>Python bivittatus</i>)	XP_007429584.1
	Central bearded dragon (<i>Pogona vitticeps</i>)	XP_020636089.1
Amphibia (amphibians)	African clawed frog (<i>Xenopus laevis</i>)	ACY24354.1
Chondrichthyes (cartilaginous fishes)	Spiny dogfish (<i>Squalus acanthias</i>)	ACY24363.1
Osteichthyes (bony fishes)		
Sarcopterygii (lobe-finned fishes)	African lungfish (<i>Protopterus annectens</i>)	FJ710608
Actinopterygii (ray-finned fishes)	Nile bichir (<i>Polypterus bichir</i>)	ACY24364.1
	White sturgeon (<i>Acipenser transmontanus</i>)	ACY24367.1
	Bowfin (<i>Amia calva</i>)	ACY24368.1
	Zebrafish (<i>Danio rerio</i>)	ACY24358.1
	Golden shiner (<i>Notemigonus crysoleucas</i>)	ACY24360.1
	Goldfish (<i>Carassius auratus</i>)	ACY24365.1
	Black ghost knifefish (<i>Apteronotus albifrons</i>)	ACY24366.1
	Rainbow trout (<i>Oncorhynchus mykiss</i>)	ACY24359.1
	Arctic char (<i>Salvelinus alpinus</i>)	XP_023838104.1
	Pacific bluefin tuna (<i>Thunnus orientalis</i>)	ASX95437.1
	Yellowtail kingfish (<i>Seriola lalandi</i>)	AMQ10352.1
	Swordfish (<i>Xiphias gladius</i>)	ACY24361.1
	Clownfish (<i>Amphiprion ocellaris</i>)	XP_023133583.1
	Japanese medaka (<i>Oryzias latipes</i>)	XP_023821574.1
Insecta (insects)	Oriental fruit fly (<i>Bactrocera dorsalis</i>)	JAC44983.1

5.3.10. Phylogenetic analysis

Fig. 5.7 shows a phylogenetic analysis the YTK PGC-1 α amino acid sequence compared with PGC-1 α amino acid sequences from six of the seven classes that make up the subphylum vertebrata. No data were available for the seventh class, the jawless fishes (class Agnatha). In the figure, there are two major clades, one containing YTK and various other ray-finned fishes (class Osteichthyes, subclass Actinopterygii) and the other containing all of the other vertebrates, including the lobe-finned fishes (class Osteichthyes, subclass Sarcopterygii) and the cartilagenous fishes (class Chondrichthyes). The separation of YTK and the other ray-finned fishes from the rest of the vertebrates indicates major differences in their PGC-1 α amino acid sequences. Some of these differences we have identified above. We will discuss this in more detail in the Discussion section.

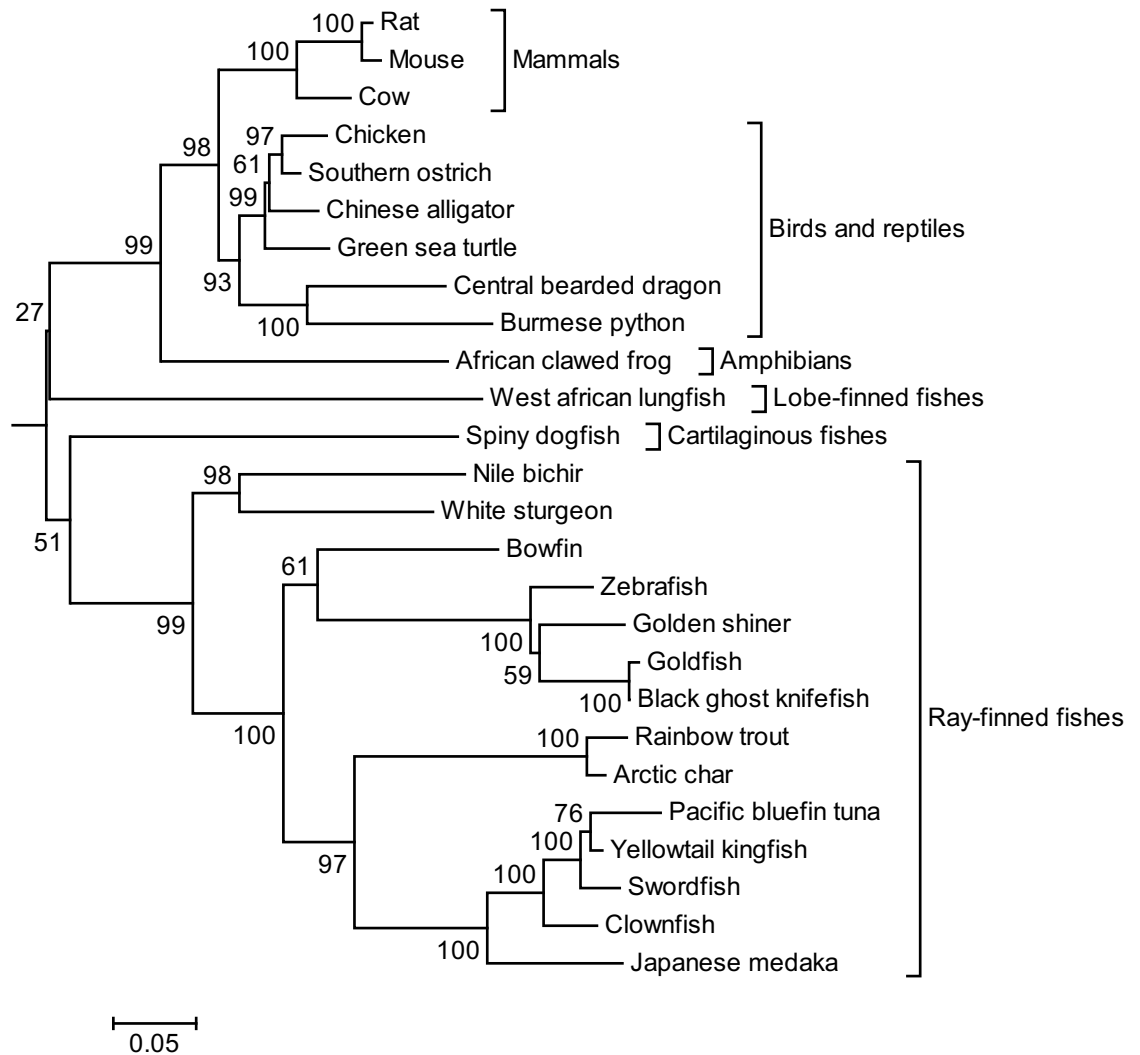


Fig. 5.7. A phylogenetic tree representing the evolutionary relationships between PGC-1 α amino acid sequences from six of the seven classes that make up the subphylum vertebrata. An invertebrate (oriental fruit fly) amino acid sequence was used as the outgroup to root the tree (sequence collapsed). The amino acid sequences were aligned using ClustalX2 software (Larkin et al., 2007) and the tree was constructed using the Neighbor-Joining method (Saitou and Nei, 1987) employing the Mega 6 software (Tamura et al., 2013). The scale indicates the estimated number of amino acid substitutions per site. Evaluation of statistical confidence was based on 1,000 bootstrap replicates. The species names and corresponding protein accession numbers can be found in Table 3.

5.3.11. Effects of tissue type and feed restriction on PGC-1 α transcript abundance

In mammals, PGC-1 α upregulates mitochondrial biogenesis and function (e.g. β -oxidation) (Lin et al., 2005a, Liu and Lin, 2011). Thus, we predicted that PGC-1 α transcript abundance would be greater in the red muscle than in either the white muscle or the liver. In the control fish, PGC-1 α transcript abundance was approximately 4-fold greater in the red muscle compared with the white muscle and approximately 14-fold greater in the liver compared with the red muscle (Fig. 5.8). However, due to the large fish to fish variation, these apparent differences were not statistically significant. Nevertheless, as we predicted, there was a trend towards higher PGC-1 α transcript abundance in the red muscle compared with the white muscle. The apparently very high level of expression of PGC-1 α in the liver is also noteworthy.

Feed restriction significantly increased PGC-1 α transcript abundance in the red muscle and also in the white muscle but not in the liver. Specifically, PGC-1 α transcript abundance was 3-fold greater in the red muscle ($P < 0.01$) and 7-fold greater in the white muscle ($P < 0.05$) of the feed restricted fish compared with the control fish (Fig. 5.8).

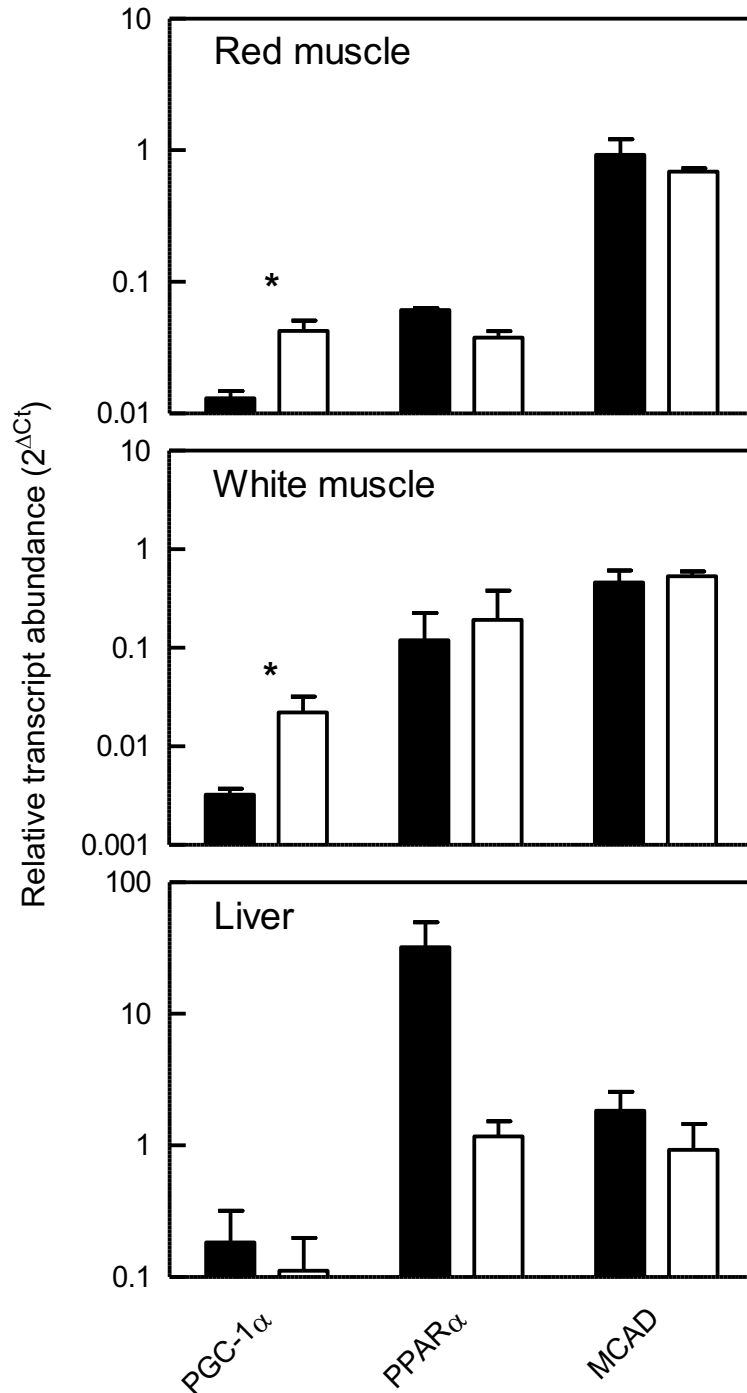


Fig. 5.8. The effects of restricted feeding on the transcript abundance for PGC-1 α , PPAR α and MCAD in the red muscle, white muscle and liver of juvenile YTK. The control fish were fed to apparent satiation six days week (black columns) whereas the feed restricted fish were fed at 0.1% (w/w) BM once per week (white columns). The transcript abundances for the genes of interest were normalised to the transcript abundance for the housekeeping gene β -actin using the 2- Δ Ct method (Livak and Schmittgen, 2001). The data are the mean \pm the standard error of the mean (n = 3). One-way ANOVA was performed to identify statistically significant differences between the control and the treated fish ($P < 0.05$). Statistically significant differences are indicated by *.

5.3.12. Effects of tissue type and feed restriction on PPAR α transcript abundance

In mammals, PPAR α upregulates the transcription of genes that encode enzymes involved in fatty acid β -oxidation, a process that occurs predominantly in the mitochondria of the cell (Vega et al., 2000). PPAR α transcript abundance was approximately 2-fold greater in the white muscle compared with the red muscle and approximately 500-fold greater in liver compared with the red muscle but the differences between the tissues were not statistically significant. This lack of statistical significance is presumably due to the large fish to fish variation.

Feed restriction decreased PPAR α transcript abundance in the red muscle and the liver but not in the white muscle. Specifically, PPAR α transcript abundance was 38% lower in the red muscle and 96% lower in the liver of the feed-restricted fish compared with the control fish but again, due to the large fish to fish variation, these apparently large differences were not statistically significant. Since PPAR α is involved in β -oxidation in mammals, this decrease in PPAR α transcript abundance could indicate that there was a decrease in the transcription of PPAR α target genes that encode enzymes involved in β -oxidation in the red muscle and liver of YTK in response to feed restriction.

5.3.13. Effects of tissue type and feed restriction on MCAD transcript abundance

In mammals, the transcription factor PPAR α activates the transcription of the gene that encodes MCAD (Vega et al., 2000). MCAD is the enzyme that catalyses the first step in the mitochondrial β -oxidation of medium-chain fatty acids (i.e. fatty acids with chain lengths between 6 and 12 carbon atoms) (Vega et al., 2000, Gulick et al., 1994). MCAD transcript abundance was approximately 2-fold greater in the red muscle compared with the white muscle and approximately 4-fold greater in the liver compared with the white muscle but these differences were not statistically significant. Restricted feeding had no effect on MCAD transcript abundance in either the red muscle or the white muscle. However, there was an apparent 50% decrease in MCAD transcript abundance in response to feed restriction in the liver but this was not

statistically significant. Thus, the decrease in MCAD transcript abundance could suggest a decrease in the abundance of the MCAD protein, therefore resulting in a decrease in the capacity for β -oxidation in the liver of the feed restricted fish.

5.4. Discussion

5.4.1. Fish growth

In this study, juvenile YTK were fed either to apparent satiation six days per week (control fish) or at 0.1% (w/w) of their body mass (BM) only once per week (feed-restricted fish) and this was over a period of 84 days at an average ambient water temperature of $12.8 \pm 0.8^{\circ}\text{C}$ (mean \pm SE). Under these conditions, there was a statistically significantly lower final BM and condition factor for the feed restricted fish compared to the control fish but the differences were only small. Specifically, the final BM and condition factor were only 14% and 9% lower, respectively, in the feed-restricted fish compared with the control fish. When comparing the mean initial BM (1.44 kg) of all of the fish in the larger study of which this study was a part with the mean final BM of our feed-restricted fish, we observed a weight loss of approximately 9%. Although we cannot perform any statistical analyses, it is apparent that the control fish in our study increased in BM and body condition whereas the severely feed-restricted fish actually lost weight and decreased in body condition. It is possible that the suboptimal water temperature used in this study was the major factor limiting the growth of the fish. In other words, because of the low ambient water temperature, the fish were unable to respond to the availability of additional nutrients by increasing their growth rate. In contrast to our own findings, juvenile YTK that were either fasted or fed to apparent satiation (control) at an optimal water temperature of $22.8 \pm 1^{\circ}\text{C}$ for 35 days both gained weight but there was a $25.9 \pm 9.0\%$ reduction in BM of the fasted fish, relative to the control (Barreto-Curiel et al., 2017). The lower amount of weight loss in our feed restricted YTK compared to the fasted YTK in the previous study suggests that there was more scope for a response to diet at the optimal water temperature of the previous study compared to the suboptimal temperature in our own.

5.4.2. Effects of tissue type and restricted feeding on CS enzyme activity

CS enzyme activity per g tissue was approximately 8-fold greater in the red muscle compared with the white muscle. This is consistent with the red muscle having a greater number of mitochondria and a greater aerobic metabolic

capacity than the white muscle. A similar pattern was observed when the CS enzyme activity was expressed per mg protein. Similar results have been found for a broad range of other fish species. For example, CS enzyme activity per g tissue ranged from 6 to 14-fold greater in the red muscle compared with the white muscle in fish species including Pacific bluefin tuna (*Thunnus orientalis*, PBT), bigeye tuna (*Thunnus obesus*), yellowfin tuna, (*Thunnus albacares*), skipjack tuna (*Katsuwonus pelamis*), swordfish (*Xiphias gladius*), striped marlin (*Tetrapturus audax*) and carp (*Cyprinus carpio*) (Chapter 3, Dalziel et al., 2005, Moyes et al., 1989). Tunas, swordfish and striped marlin are large, highly active pelagic fish whereas carps are more sluggish fishes (Carey and Teal, 1966, Carey, 1982, Holts, 1990). Thus, similar differences between the red and the white muscle were seen both in highly active predators such as YTK and tunas as well as a less active fish such as the carp.

We observed a 57% increase in CS enzyme activity per g tissue in the liver of our YTK specimens in response to feed restriction but no statistically significant effect was observed in the red muscle or the white muscle. Therefore, the increase in CS enzyme activity we observed in response to feed restriction in the liver could indicate increased mitochondrial abundance in the liver whereas mitochondrial abundance was unaffected by feed restriction in the red muscle and the white muscle. This could indicate that the capacity for fatty acid β -oxidation increases in the liver in response to feed restriction.

Consistent with our own findings, it has been shown that when goldfish (*Carassius auratus* L.) were fasted for three weeks there was no change in CS enzyme activity per g tissue in the red muscle or the white muscle of the feed restricted fish compared to the control fish (LeMoine et al., 2008). However, in contrast to what we found, the same study showed that there was an approximately 50% decrease in CS enzyme activity in the liver of the fasted goldfish. Together with our findings this could suggest that the acclimation to long-term feed restriction in our study may have resulted in the liver of YTK becoming adapted to take advantage of dietary fatty acids when they become available by increasing mitochondrial abundance in the liver whereas in the previous study, the goldfish had adapted to a complete absence of supplied dietary fatty acids, meaning that the capacity for β -oxidation of fatty acids may have decreased to conserve the fuel reserves in the body.

5.4.3. Effects of tissue type and restricted feeding on COX enzyme activity

COX enzyme activity per g tissue was approximately 6-fold greater in the red muscle compared with the white muscle in the juvenile YTK we studied. This is consistent with red muscle having a larger number of mitochondria and a greater aerobic metabolic capacity than either the white muscle or the liver. A similar pattern was observed when the COX enzyme activity was expressed per mg protein. Similar results have been found for other fish species. For example, COX enzyme activity ranged from 6- to 12.5-fold higher in red muscle than in white muscle in PBT (Chapter 3), bigeye tuna, yellowfin tuna, skipjack tuna, swordfish and striped marlin (Dalziel et al., 2005). This indicates that the red muscle of YTK, as with other active predatory fishes, has approximately one order of magnitude greater mitochondrial abundance than the white muscle.

Feed restriction resulted in significant changes in COX enzyme activity in YTK. Specifically we observed a 29% reduction in activity per g tissue in the red muscle, a 20% increase in the liver and no change in the white muscle in our juvenile YTK specimens. This suggested that feed restriction decreased mitochondrial abundance and/or folding of the inner mitochondrial membrane of the red muscle whereas it increased these parameters in the liver while at the same time having no effect in the white muscle. However, considering the results we obtained for CS, it is more likely that the decrease in COX enzyme activity was indicative of a decrease in folding of the mitochondrial inner membrane rather than a decrease in mitochondrial abundance because feed restriction had no statistically significant effect on CS enzyme activity in the red muscle. Martínez et al. (2003) investigated the effects of fasting, suboptimal ambient water temperature and the combination of the two on muscle metabolic capacity in Atlantic cod (*Gadus morhua*). The fish were maintained in tanks for 16 weeks at ambient water temperatures that were low (<4°C) for most of the time but gradually rose to 8.8°C towards the end of the study. At the end of the study, there was an approximately 20% decrease in the COX enzyme activity in the red muscle of the fasted fish compared with the control fish. This suggested that fasting decreased mitochondrial abundance and/or folding of the inner mitochondrial membrane in the red muscle of Atlantic cod.

This was consistent with the decrease we observed in COX activity per g tissue in the red muscle of our feed restricted fish and with our conclusion that feed restriction results in a decrease in red muscle mitochondrial abundance or the folding of the inner mitochondrial membrane in fishes. In contrast, Martínez et al. (2003) observed an approximately 45% decrease in the mitochondrial COX enzyme activity in the white muscle of the fasted Atlantic cod, whereas we observed no change in COX enzyme activity in the white muscle of our feed restricted YTK specimens. This indicated that, in fishes, mitochondrial abundance or the folding of the inner mitochondrial membrane may decrease in the white muscle in response to fasting but not in response to feed restriction, as was implemented in our own study. Again, this could indicate that feed restriction in fishes could result in an adaptation to take advantage of dietary fatty acids when they become available whereas fasting could result in a decrease in fatty acid β -oxidation to conserve the fuel reserves in the body. However, LeMoine et al. (2008) observed that goldfish fasted for 3 weeks, exhibited a significant ~30% increase in COX activity per g tissue in their white muscle but not in their red muscle. In contrast to the findings of Martínez et al. (2003), the increase in COX activity in the white muscle suggests that mitochondrial abundance or the folding of the inner mitochondrial membrane actually increased in response to fasting in the white muscle of fishes. This was in contrast to the lack of change observed for both COX and CS enzyme activity per g tissue in the white muscle of YTK in response to feed restriction in our study.

5.4.4. Effects of tissue type and restricted feeding on PK enzyme activity

PK enzyme activity per g tissue was approximately 5-fold greater in the white muscle compared with the red muscle in the juvenile YTK specimens we studied. Similar differences between these two tissues have also been found in other fish species. For example, PK enzyme activity, per g tissue, ranged from 3- to 7-fold higher in the white muscle compared with the red muscle in PBT, skipjack tuna and rainbow trout (*Oncorhynchus mykiss*) (Chapter 3, Guppy et al., 1979, Johnston, 1977). These results are consistent with the glycolytic metabolic capacity of the white muscle being substantially greater than that of the red muscle in all of these fish species, including YTK.

In our YTK specimens, feed restriction reduced PK enzyme activity per g tissue by 33% in the red muscle but it had no effect in the white muscle. It has previously been reported that Atlantic cod fasted for 16 weeks exhibited a ~30% decrease in the PK enzyme activity per g tissue in their red muscle and ~70% decrease in the white muscle (Martínez et al., 2003). This was interesting because this suggests that the effects of fasting were greater in the white muscle than the red muscle of Atlantic cod but the opposite seems to be true in YTK. This could possibly be a result of feed being totally withheld from the fish in the previous study whereas the fish in our study were still supplied with some feed, only at a restricted quantity.

We also observed that feed restriction had no effect on the PK enzyme activity in the liver of our YTK specimens. This was interesting because PK activity is known to decrease in the liver of fishes in response to fasting (Foster and Moon, 1991). This decrease in PK enzyme activity was well illustrated in a study where yellow perch (*Perca flavescens*) were fasted for a period of seven weeks and at the end of the experiment PK enzyme activity per g tissue was ~20% lower in the liver of the fasted fish compared to the control fish that were fed daily (Foster and Moon, 1991). Similar effects have been observed in mammals. For example, when mice were fed a calorie restricted diet (50% of the amount of feed supplied to the control mice), there was ~60% lower PK enzyme activity and transcript abundance in the liver of the calorie restricted mice compared to the control mice (Dhahbi et al., 1999). Our findings together with the findings of the previous studies could suggest that although feed restriction is sufficient to decrease PK enzyme activity in the liver of mammals, feed restriction may not be sufficient to cause a decrease in PK enzyme activity in fishes, as we observed for YTK, and instead fasting may be necessary, as was observed for yellow perch.

5.4.5. Effects of tissue type and restricted feeding on CS transcript abundance

In our YTK specimens, there was no significant difference in CS transcript abundance between the red and the white muscle. This was surprising because we had observed an 8-fold greater CS enzyme activity in the red muscle compared to the white muscle. The lack of correlation between CS

enzyme activity (per g tissue) and CS transcript abundance was evident when the two variables were plotted against each other, as there was no significant correlation between these two parameters. This suggested that CS enzyme activity is not regulated at the transcriptional level and that instead it might be regulated at the post-transcriptional or post-translational level. This lack of correlation between CS enzyme activity and CS transcript abundance was also shown in Chapter 3 in our work with PBT. Thus, it is not unique to just one species and it begs the question why is this so? Other authors have found a similar lack of correspondence between CS enzyme activity and CS transcript abundance (O'Brien, 2011, Dalziel et al., 2005). For example, when zebrafish (*Danio rerio*) were maintained at a suboptimal water temperature of 18°C for 3 weeks, there was 50% greater CS enzyme activity in the skeletal muscle (presumably white muscle) of the cold treated fish compared with the control fish maintained at 28°C, but there was no difference in CS transcript abundance (McClelland et al., 2006). This is consistent with our theory that the regulation of CS enzyme activity is most likely not at the transcriptional level. Instead, it might be at the post-transcriptional or post-translational level.

Restricted feeding had no significant effect on CS transcript abundance in either the red muscle, the white muscle or the liver in our juvenile YTK specimens. This mirrored what we observed for CS enzyme activity per g tissue in the red muscle and the white muscle but in the liver we observed a 30% increase in CS enzyme activity in response to restricted feeding. This is similar to what has been observed for other fish species. For example, LeMoine et al. (2008) observed that in goldfish fasted for 3 weeks, both CS enzyme activity per g tissue and CS transcript abundance remained unchanged. However CS enzyme activity per g tissue decreased by approximately 50% without there being a change in CS transcript abundance in the liver. This is also consistent with our theory that the regulation of CS enzyme activity is most likely not at the transcriptional level.

5.4.6. Effects of tissue type and restricted feeding on COXI transcript abundance

COX is a large enzyme made up of 13 different subunits, 10 of which are nuclear encoded and 3 of which are mitochondrially encoded (Ludwig et al.,

2001, Duggan et al., 2011). This makes it challenging to understand how COX enzyme activity is regulated as this regulation may occur at different levels. The catalytic core of COX is comprised of the 3 mitochondrially encoded subunits (COXI, COXII and COXIII) (Soto et al., 2012). Therefore, we investigated the transcript abundance of COXI due to its essential role for the functioning of the enzyme. COXI transcript abundance was approximately 3-fold greater in the red muscle compared with the white muscle. This was surprising because COX enzyme activity per g tissue was 6-fold greater in the red muscle compared with the white muscle. Although the apparent difference between the red muscle and the white muscle was large, it was not statistically significant. There could be several possible explanations for this. One explanation could be that the availability of the COXI subunit is not rate limiting during the assembly of the COX enzyme complex. Another explanation could be that the regulation of COX is at the post-transcriptional or post-translational level, rather than the transcriptional level. Similarly, we have previously observed that COXI transcript abundance per g tissue was 2 to 12-fold greater in the red muscle, compared with the white muscle of juvenile PBT but COX enzyme activity per g tissue was consistently 12.5-fold greater in the red muscle compared with the white muscle (Chapter 3). In contrast to our findings with YTK and PBT, Leary et al. (2003) observed that the COXI transcript abundance was approximately 3-fold greater in the red muscle compared to the white muscle of rainbow trout. This was very similar to the approximately 4-fold greater COX enzyme activity in the red muscle compared with the white muscle that they observed for the same fish. The lack of consistency between different studies suggests that further investigation is required to fully understanding how COX protein expression/enzyme activity is regulated in YTK and in fishes in general.

Feed restriction decreased COX enzyme activity by 29% in the red muscle whereas it increased this activity in the liver by 20% and did not affect the activity in the white muscle in the juvenile YTK we studied. In contrast, there was no statistically significant effect of this treatment on transcript abundance for the COXI subunit in any of the tissues in response to restricted feeding. These data suggest that restricted feeding had no impact on the transcription of the COXI gene. In contrast, LeMoine et al. (2008) observed that there was

an approximately 6-fold increase in COXI transcript abundance in the white muscle and an approximately 50% decrease in COXI transcript abundance in the liver, while it remained unchanged in the red muscle of goldfish fasted for three weeks. The reason why our findings differed from those of this previous study could be due to the difference in the feeding treatment. Unlike in our study where YTK were fed 0.1% (w/w) once per week, the fish were fasted in the previous study. This could suggest that rapid changes in COX enzyme activity can occur at the post-transcriptional or post-translational level when feed is restricted but under fasting conditions changes in the transcription of the COX subunits are required. We did however observe a small yet significant correlation between COX enzyme activity and COXI transcript abundance when all tissues were considered. LeMoine et al. (2008) observed that there were stronger correlations between COX enzyme activity and the transcript abundance of the nuclear encoded COX IV subunit compared with the mitochondrial COXI subunit. This suggests that COXIV transcript abundance may be a better indicator of COX enzyme activity than COXI transcript abundance.

5.4.7. Effects of tissue type and restricted feeding on PK transcript abundance

PK transcript abundance was approximately 29-fold greater in the white muscle compared with the red muscle and approximately 2000-fold greater in the white muscle compared with the liver and the differences were statistically significant. The pattern in PK transcript abundance was to some extent consistent with what we had observed for PK enzyme activity except that the fold changes were not of the same magnitude. Specifically, PK enzyme activity per g tissue was approximately 5-fold greater in the white muscle compared with the red muscle and approximately 60-fold greater in the white muscle compared with the liver. Similar results have previously been found in PBT (Chapter 3). The difference in PK transcript abundance per g tissue ranged from 7 to 40-fold greater in the red muscle, compared with the white muscle but PK enzyme activity per g tissue was approximately 4.3-fold higher in the white muscle than it was in the red muscle (Chapter 3). As far as we are aware, this is the first time that the transcript abundance of PK has been compared between the red and white muscle in fish. Together these data suggest that

the large differences in transcript abundance result in much smaller differences in enzyme activity but that there is an overall similar pattern in terms of the differences in enzyme activity and the differences in transcript abundance between the red and the white muscle for PK. In other words, PK enzyme activity is substantially greater in the white muscle than in the red muscle and the same is true for PK transcript abundance.

We observed that feed restriction had no significant effect on PK transcript abundance in red muscle, white muscle or liver of our juvenile YTK. This was not what we observed for PK enzyme activity per g tissue. Feed restriction decreased PK enzyme activity by 33% in the red muscle whereas it did not affect this activity in the white muscle or the liver of the YTK juveniles we studied. In contrast, it has previously been reported that there was an approximately 4-fold increase in PK transcript abundance in the white muscle of rainbow trout that had been fasted for 30 days (Johansen and Overturf, 2006). As with COX enzyme activity, the reason we might not have observed such a finding could be due to the difference in the feeding treatments between the previous study and our own. Unlike in our own study where feed was supplied at a restricted quantity, the feed was totally withheld from the fish in the previous study.

5.4.8. Sequence analysis of a PGC-1 α cDNA cloned from YTK red muscle

The 2,789 bp PGC-1 α cDNA we cloned from YTK red muscle encoded a near-complete PGC-1 α protein with strong similarity to other PGC-1 α proteins, especially from the ray-finned fishes. The two transcriptional activation domains in the N-terminus region, as well as the tri-lysine motif and the three leucine-rich motifs were highly conserved between the YTK PGC-1 α protein and the PGC-1 α proteins of the other classes of vertebrates (Sadana and Park, 2007a, Knutti et al., 2001, LeMoine et al., 2010a). In mammals, it has been hypothesised that the AD1 and AD2 domains increase transcriptional activation of PGC-1 target genes by interacting with the basal transcription machinery (Sadana and Park, 2007a). The L1 motif is within the AD2 domain, which is responsible for binding to the basal transcription machinery. The L2 motif facilitates binding between PGC-1 α and transcription factors from the

nuclear receptor family, including PPAR α (Vega et al., 2000). However, not all nuclear receptors interact with the L2 motif. In mammals, the L3 motif facilitates binding between PGC-1 α and ERR α , another member of the nuclear receptor family (Huss et al., 2002). The tri-lysine motif is typical of the NRF-1 interaction domain of vertebrate PGC-1 proteins (LeMoine et al., 2010a).

The canonical NRF-1, PPAR γ and MEF2 transcription factor binding domains that are found in most vertebrates, were interrupted by a serine (S)-rich insertion, a glutamine (Q)-rich insertion and several mixed amino acid residue insertions in the YTK PGC-1 α amino acid sequence. These insertions were only found in the YTK and swordfish sequences, both of which are bony-fishes in the subclass of ray-finned fish. This suggests that the insertions are characteristic of the ray-finned fishes and not any other vertebrates, including the cartilaginous fishes and the lobe-finned fishes, the latter of which are also in the subclass of bony-fishes. The same has previously been observed by LeMoine et al. (2010a), who investigated the evolution of PGC-1 α in vertebrates by comparing the PGC-1 α amino acid sequences of other classes of vertebrates with several other ray-finned fishes. From this, LeMoine et al. (2010) concluded that these insertions had potential to prevent interactions between PGC-1 α and NRF-1, thereby hindering the capacity of PGC-1 α to coactivate the NRF-1 induced upregulation of the transcription of genes that encode enzymes in the mETC. To investigate this possibility, Bremer et al. (2016) performed a series of co-immunoprecipitation experiments between recombinantly expressed proteins from zebrafish, goldfish and rat. The NRF-1 protein interaction domain was from zebrafish and the truncated PGC-1 α protein, containing the transcription activation domain and the NRF-1 binding domain in the N-terminal region was from either rat or goldfish. They observed that the zebrafish NRF-1 protein bound to the NRF-1 interaction domain for the rat but not the goldfish PGC-1 α protein. This could indicate that the amino acid inserts within the NRF-1 interaction domain of our YTK PGC-1 α amino acid sequence could also prevent binding between the NRF-1 and PGC-1 α proteins in YTK. However, Bremer et al. (2016) advised caution when interpreting their findings, as only truncated PGC-1 α proteins were utilised for their study. In other words, when in its native structure, the complete PGC-1 α protein may respond differently.

The MEF2 binding domain in the YTK PGC-1 α protein was also interrupted by amino acid insertions. The same was true for swordfish, the other representative species of the ray-finned fishes but not for any of the other organisms we aligned our YTK PGC-1 α amino acid sequence with. The interruptions in the MEF2 binding domain have also been observed for many other ray-finned fishes (LeMoine et al., 2010a). Interestingly, the MEF2 domain has been reported to be the least conserved region of the PGC-1 α protein domains in all classes of vertebrates (LeMoine et al., 2010a). All other vertebrate PGC-1 α sequences, including those from lobe-finned fishes and cartilaginous fishes, have been shown to have no disruption of their MEF2 binding domains. Thus, the inserts in the PGC-1 α sequence are unique to the ray-finned fishes. The insertions found in the MEF2 binding domain of ray-finned fishes suggest that either the interaction between PGC-1 α and MEF2 may not occur in ray-finned fishes as it does in other vertebrates or the MEF2 binding domain may differ between ray-finned fishes and other vertebrates and that the folding of the PGC-1 α protein may be different but binding still occurs. It has not previously been shown whether the MEF2 protein from any source can bind to ray-finned fish PGC-1 α . To investigate this possibility, co-immunoprecipitation experiments between recombinant fish MEF2 and PGC-1 α proteins could be performed, similar to the ones performed by Bremer et al. (2016) between the PGC-1 α protein and the NRF-1 protein.

5.4.9. Effect of tissue type and feed restriction on PGC-1 α transcript abundance

We observed that PGC-1 α transcript abundance was 4-fold greater in the red muscle compared with the white muscle in our juvenile YTK specimens but this apparent difference was not statistically significant. The lack of statistical significance was most likely due to the large fish to fish variation in PGC-1 α transcript abundance we observed. However, CS and COX enzyme activities, per g tissue, indicated that the mitochondrial abundance was higher in the red muscle compared to the white muscle of our YTK specimens. Even if PGC-1 α does not have a similar role in the upregulation of mitochondrial biogenesis in fishes as it does in mammals, it is possible that it is still involved in the upregulation of genes that encode enzymes involved in fatty acid β -oxidation. Fatty acid β -oxidation occurs in the mitochondria. Therefore, it was expected

that PGC-1 α transcript abundance would still be higher in the red muscle than in the white muscle. We also observed 14-fold greater PGC-1 α transcript abundance in the liver compared with the red muscle in our juvenile YTK specimens but this apparent difference was not statistically significant. Similarly in mice, PGC-1 α transcript abundance has been shown to be approximately the same in the soleus muscle (composed predominantly of red muscle fibres) and liver (Reynolds et al., 2015).

We observed that PGC-1 α transcript abundance was 3-fold higher in the red muscle and 7-fold higher in the white muscle of our feed restricted fish compared with the control fish and the differences were statistically significant, whereas, there was no difference between the feed restricted and the control fish in the liver. In contrast, goldfish fasted for three weeks exhibited an apparent 50% increase in the PGC-1 α transcript abundance in their liver but the effect was not statistically significant (LeMoine et al., 2008). Similarly, an increase in PGC-1 α transcript abundance in response to calorie restriction has also been observed in mammals. Specifically, it has previously been reported that calorie restriction (feed provided on alternate days for 3 months) results in an approximately 3-fold higher PGC-1 α transcript abundance in the liver of calorie-restricted mice compared with control mice (*fed ad libitum*) (Nisoli et al., 2005). Similarly, it has been observed in calorie restricted mice, fed *ad libitum* on alternate days for 3 months, that PGC-1 α protein expression was ~3-fold higher in the liver and soleus muscle compared to what it was in the control mice that were fed *ad libitum* every day for the duration of the experiment (Ranhotra, 2010). Fasting for 24 h has been reported to stimulate a statistically significant 3.7-fold higher PGC-1 α transcript abundance in the liver of fasted mice compared with control mice (allowed free access to food) (Yoon et al., 2001). This suggests that neither feed restriction nor fasting stimulate an increase in PGC-1 α transcript abundance in fishes, as they do in mammals.

The response to feed-restriction and fasting is different depending on the species and the treatment in both mammals and fishes. In the study by Nisoli et al. (2005), where mice were feed restricted (feed provided to mice on alternate days for 3 months), the expression of genes (PGC-1 α , NRF-1 and mitochondrial transcription factor A (Tfam)) and proteins (cytochrome c

oxidase (COXIV) and cytochrome *c* (cyt *c*) involved in mitochondrial biogenesis and function was significantly higher in the feed-restricted mice compared with mice fed to satiation. In contrast, Hancock et al. (2011) observed that when rats were either fed to satiation (control) or fed 70% of the average amount of food eaten by the control group (calorie restricted) for 14 weeks, there was no difference in either the transcript abundance or protein expression of PGC-1 α in the liver, brain, adipose tissue, skeletal muscle or heart between the control and the calorie-restricted rats. Similarly, Miller et al. (2012) found that in lifelong 40% calorie-restricted mice there were significant increases in PGC-1 α transcript abundance in the skeletal muscle and liver which did not correspond to changes in PGC-1 α protein abundance. Miller et al. (2012) also found that mitochondrial protein synthesis, calculated as the change in the enrichment of deuterium-labelled alanine using gas chromatography–mass spectrometry (GC-MS) did not correspond to the increases in PGC-1 α transcript abundance. This was consistent with the increase in mitochondrial capacity, as indicated by an increase in CS and COX enzyme activity per g tissue in the liver of our feed restricted YTK but there being no corresponding increase in PGC-1 α transcript abundance in the same tissue. From this it is apparent that further investigation is needed to fully understand the relationship between feed restriction and mitochondrial biogenesis in both mammals and fishes.

In mammals, higher PGC-1 α transcript abundance is associated with higher transcript abundances for the gluconeogenic enzymes phosphoenolpyruvate carboxykinase (PEPCK) and glucose 6-phosphatase (G6Pase) (Yoon et al., 2001, Lin et al., 2003). The genes that encode these enzymes are upregulated by hepatocyte nuclear factor 4 α (HNF-4 α), a transcription factor known to interact with PGC-1 α (Finck and Kelly, 2006, Rhee et al., 2006, Yoon et al., 2001). Increases in PGC-1 α transcript abundance have been reported to coincide with increases in the expression of PPAR α target genes involved in hepatic fatty acid β -oxidation (Koo et al., 2004, Finck and Kelly, 2006). This suggests that PGC-1 α stimulates the activation of gluconeogenesis to maintain blood glucose levels by utilising fatty acids as a fuel source to fuel anabolic processes during fasting. However, we observed no statistically significant change in PGC-1 α transcript abundance in response to feed restriction in the

liver of YTK. This could suggest that PGC-1 α does stimulate the activation of gluconeogenesis in fishes as it does in mammals. Alternatively, the lack of upregulation in response to feed restriction could indicate that, in fishes, increases in PGC-1 α transcript abundance only occur in response to fasting, not feed restriction.

Fuentes et al. (2013) observed that in fine flounder (*Paralichthys adspersus*) fasted for a period of three weeks there was a 1.6-fold greater amount of PGC-1 α protein in the white muscle of the fasted fish compared with the control fish. This coincided with a 1.5- to 2-fold greater succinate dehydrogenase (Complex II), cytochrome c oxidase (Complex IV) and ATP synthase (Complex V) protein content in the same tissue. These complexes are the major constituents of the mETC. Therefore, fasting appeared to increase mitochondrial biogenesis in this fish species. In addition, it was observed that there was an approximately 1.6-fold increase in the amount of the phosphorylated (active) form of the AMP-activated protein kinase (AMPK) protein at the end of the 3 weeks of fasting. AMPK is known to activate the PGC-1 α protein in mouse skeletal muscle cells by phosphorylating the PGC-1 α protein at Thr₁₇₇ and Ser₅₃₈ (Jager et al., 2007). Therefore, Fuentes et al. (2013) proposed that the increase in mitochondrial biogenesis was caused by the activation of the PGC-1 α protein via phosphorylation by AMPK.

However, 5-aminoimidazole-4-carboxamide-1- β -D-ribofuranosyl 5'-monophosphate (AICAR, an analog of AMP that is capable of stimulating AMPK) treatment of zebrafish blastula cells to increase the phosphorylation of AMPK did not result in an increase in the transcript abundance of the PGC-1 α , NRF-1 or downstream target genes that are stimulated by the interaction between PGC-1 α and NRF-1 (Bremer et al., 2016). As mentioned above, this could be due to a lack of interaction occurring between the PGC-1 α and NRF-1 proteins in fishes. When investigating the relationship between AMPK and PGC-1 α further, it was revealed that a human PGC-1 α peptide corresponding to the AMPK phosphorylation site could be phosphorylated *in vitro* by human AMPK but zebrafish and goldfish PGC-1 α peptides could not be phosphorylated by human AMPK (Bremer et al., 2016). PGC-1 α amino acid sequence alignments of organisms from the different classes of vertebrates have shown that in fishes, including goldfish and zebrafish, the essential Thr₁₇₇

targeted by AMPK to phosphorylate the PGC-1 α protein, is not present (Bremer et al., 2016). This was consistent with our finding that this residue was not conserved in YTK or any fishes from the classes of bony fishes or the cartilaginous fishes. This suggests that AMPK does not activate the PGC-1 α protein in fishes by phosphorylating the essential Thr₁₇₇ residue because this residue is not present in fishes.

5.4.10. Effects of tissue type and feed restriction on PPAR α transcript abundance

In mammals such as mice, rats and humans, PPAR α transcript abundance is high in tissues with high mitochondrial β -oxidation activity such as the liver and the skeletal muscle (Braissant et al., 1996, Desvergne and Wahli, 1999). Specifically, the transcript abundance of PPAR α has been shown to be approximately 5-fold greater in the liver than in the skeletal muscle of rats (does not specify what type of muscle) (Lemberger et al., 1996). We observed that PPAR α transcript abundance was approximately 2-fold higher in the white muscle compared with the red muscle and 500-fold greater in liver compared with the red muscle in our YTK specimens. Due to the large fish to fish variation, however, these apparent differences were not statistically significant. Nevertheless, the large apparent difference between the liver and the red muscle (500-fold higher transcript abundance in the liver compared with the red muscle) suggests that PPAR α may have an important role to play in regulating hepatic fatty acid β -oxidation. This requires further investigation.

We observed that feed restriction in YTK led to a 38% decrease in PPAR α transcript abundance in the red muscle and a 96% decrease in the liver compared with the control fish. However, due to the large fish to fish variation, these apparently large differences were not statistically significant. In contrast, it has previously been shown that when zebrafish were fasted for 70 days, PPAR α transcript abundance was approximately 1.7-fold higher in the liver of the fasted fish compared to the liver of the control fish that were fed *ad libitum* (Olmez et al., 2015). The increase in PPAR α transcript abundance may upregulate the expression of genes encoding enzymes involved in fatty acid β -oxidation which may then upregulate the catabolism of fatty acid reserves stored in the body. Similarly, it has been shown that when mice were fasted

for 24 hours, PPAR α transcript abundance was approximately 5-fold higher in the liver compared to the control (fed) mice (Patsouris et al., 2004). In mammals, this could be due to the absence of a dietary fuel source and therefore a switch from dietary fatty acids to stored fatty acids as the main fuel source (McGarry and Foster, 1980). Evidence of a switch from dietary sources of energy to stored fatty acids has previously been reported for YTK (Barreto-Curiel et al., 2017). It has been reported that when YTK were fasted for a period of 35 days there was significantly reduced lipid content in the muscle (56% lower) and liver (52%) but muscle protein was largely conserved, being neither catabolized nor replenished (Barreto-Curiel et al., 2017). This is consistent with YTK utilising their fat reserves before using their protein reserves without a dietary energy source, as is true in general in vertebrate animals (Lindgård et al., 1992). The findings of the previous studies indicated that there was an increase in the capacity for β -oxidation of fatty acids in response to fasting in the liver of both mammals and fishes (Patsouris et al., 2004, Olmez et al., 2015, Barreto-Curiel et al., 2017). However, the apparent decrease we observed in PPAR α transcript abundance in the liver of YTK could suggest that the response to feed restriction may have the opposite effect to fasting in fishes. Instead, the decrease in PPAR α transcript abundance in response to feed restriction could be a means of slowing down the transcription of genes that encode the enzymes involved in fatty acid β -oxidation to avoid using the body's fatty acid fuel reserves too quickly.

5.4.11. Effects of tissue type and feed restriction on MCAD transcript abundance

In our study we observed that MCAD transcript abundance in YTK was approximately 2-fold greater in the red muscle compared with the white muscle and approximately 4-fold greater in the liver compared with the white muscle but these differences were not statistically significantly different. Nevertheless, this was consistent with MCAD transcript abundance being greater in tissues that use fatty acids as their main fuel source. In an early study with rats, it was observed that MCAD transcript abundance was greatest in tissues such as the heart, skeletal muscle and small intestines compared to tissues such as the brain, lung and spleen (Kelly et al., 1989). From this it was concluded that

MCAD transcript abundance was high in tissues that use fatty acids as their main fuel source such as the red muscle and to a lesser extent the liver.

We observed that feed restriction had no effect on MCAD transcript abundance in either the red muscle or the white muscle in YTK. However, we did observe an apparent 50% decrease in MCAD transcript abundance in the liver in response to feed restriction but this was not statistically significant. In contrast, it has previously been shown that when goldfish were fasted for three weeks, MCAD transcript abundance remained unchanged in the red muscle, was 2-fold greater in the white muscle and was 50% lower in the liver and these changes were statistically significant (LeMoine et al., 2008). In another previous study, rainbow trout that were feed restricted by being fed to apparent satiation once per week for 31 days, showed no change in the transcript abundance of MCAD in the white muscle (Kondo et al., 2012). Together with our data, this indicated that feed restriction had no effect on the gene expression of MCAD in the white muscle but fasting resulted in an increase in MCAD gene expression. No change in MCAD gene expression in response to feed restriction may be a means of preserving the fatty acid stores within the body, whereas fasting results in more of a dependency on those stores, resulting in increased mobilisation of fatty acids in the white muscle. Interestingly, the opposite was true for the liver of goldfish, where MCAD gene expression decreased in response to fasting, suggesting that fasting may result in a decrease in fatty acid β -oxidation in the liver of fishes (LeMoine et al., 2008). To gain a better understanding of the role of β -oxidation in the liver of YTK in response to restricted feeding, the next logical step would be to analyse the protein expression of enzymes involved in β -oxidation such as MCAD as well as the protein expression of PPAR α and PGC-1 α . This will tell us whether there is an increase in the abundance of the enzymes that break down fatty acids and whether this is regulated by an increase in PPAR α and PGC-1 α protein.

5.4.12. Conclusions

This study investigated the effects of restricted feeding on the aerobic and glycolytic metabolic capacity of YTK red muscle, white muscle and liver in the unfavourably cold conditions of the Australian winter. We found that

mitochondrial abundance and by inference aerobic metabolic capacity were greater in the red muscle compared with the white muscle or the liver. We also found that feed restriction significantly increased mitochondrial enzyme activity in the liver. This suggested that the aerobic metabolic capacity of the liver increased in response to feed restriction. The increase in aerobic metabolic capacity could be a response to enable the fish to respond more rapidly and effectively when feed becomes more readily available in the future. In contrast, the glycolytic metabolic capacity of the fish was greater in the white muscle than in the red muscle or the liver. We also found that there was significantly lower PK enzyme activity in the red muscle of the feed restricted fish compared to the control fish but there was no effect in the white muscle or liver. This suggested that the glycolytic metabolic capacity of the red muscle decreased in response to feed restriction. This response may be a result of feed restricted YTK limiting their physical activity to conserve fuel reserves within the body. In addition, we observed that the YTK PGC-1 α amino acid sequence was highly similar to PGC-1 α amino acid sequences from other ray-finned fishes but substantially different in some respects from these proteins in all other vertebrates. In particular, there were amino acid insertions within the NRF-1, PPAR γ and MEF2 transcription factor binding domains. These inserts are features that are not found in any other class of vertebrates. This suggests that PGC-1 α may interact differently, or not at all with these transcription factors. The highly variable transcript abundance of PGC-1 α , PPAR α and MCAD made it difficult to fully determine the role of these genes in response to feed restriction in YTK. To gain a better understanding of the role of β -oxidation in the liver of YTK in response to restricted feeding the next logical step is to analyse the enzyme activity of enzymes involved in β -oxidation such as MCAD as well as the protein expression of MCAD, PPAR α and PGC-1 α .

CHAPTER 6 - Conclusions and future directions

6.1. Conclusions and future directions

This thesis has first reported on an investigation of the development of regional endothermy in juvenile PBT. Secondly, this thesis has reported on an investigation of the effects of feed restriction/suboptimal water temperatures on the aerobic and glycolytic metabolic capacity in YTK. This chapter presents a summary of the major discoveries reported in this thesis and future research that could further develop what has been presented here.

In Chapter 2 we observed a steep linear increase in the red muscle temperature elevation in our fish between the sizes of ~20-60 cm FL and corresponding to ages ~2 months to ~2 years of age. This indicated that the development of red muscle endothermy was occurring in this size range. More specifically, we estimated that significant temperature elevation in the red muscle of juvenile PBT occurs at a minimum body size of approximately 29 cm FL, corresponding to an age of approximately 5.5 months. This was smaller than previously published data suggested (Kubo et al., 2008). The red muscle mass of PBT scaled slightly less than isometrically with increasing BM indicating that increasing red muscle mass as a proportion of total BM was not the explanation for the increasing red muscle temperature elevation with increasing body size. Instead, a steep linear increase in the length and the maximum number of blood vessel rows of the red muscle *retia* correlated well with the increase in temperature elevation in the red muscle. Therefore, it is likely that the development of the red muscle *retia* is the most important factor supporting the development of red muscle endothermy in PBT.

We also observed a modest linear increase in the temperature elevation of the viscera with increasing body size. The increase in visceral temperature elevation corresponded with a steep linear increase in the total cross-sectional area and therefore the number of blood vessels within the visceral rete. Therefore, it is likely that the development of the visceral rete is the most important factor supporting the development of visceral endothermy in PBT.

Due to the difficulties involved with maintaining PBT in captivity, the specimens used for this investigation were either wild caught or wild caught and then farmed. As a result, the water temperature varied between the times of

sampling for the different sized fish. Thus, to more accurately determine the minimum body size required for regional endothermy in juvenile PBT, temperature measurements of the red muscle, viscera and cranium in fish of the same size range we investigated here could be performed but at a standardised ambient water temperature. A low ambient water temperature of 10-15°C could reveal whether the ability for ~20 cm FL PBT to elevate the temperature of their red muscle, viscera and cranium above the surrounding environment is greater than the specimens we obtained from ~30°C waters. In the future, the continuation of this investigation should include PBT specimens that are both smaller and larger than the specimens we analysed for this study. This will provide an indication of the minimum size/age at which the temperature elevations start to occur in juvenile PBT and the size/age at which the maximum temperature elevation occurs.

In Chapter 3 we investigated the effects of muscle type, body size and water temperature on CS and COX enzyme activity as indicators of aerobic metabolic capacity and PK enzyme activity as an indicator of glycolytic metabolic capacity in red and white muscle of young PBT juveniles undergoing the ontogenetic transition from ectothermy to regional endothermy. We observed that CS and COX enzyme activity was approximately one order of magnitude greater in the red muscle compared with the white muscle in our juvenile PBT specimens. This was consistent with red muscle being more aerobic than the white muscle. The CS enzyme activity, per g tissue, decreased in the red muscle and the white muscle with increasing body size. This suggested that the mitochondrial abundance and therefore aerobic metabolic capacity of the skeletal muscle in PBT decreased with increasing body size. This may be a method of preventing overheating as the surface area to volume ratio decreases with increasing body size. However, unlike the CS enzyme activity, the COX enzyme activity, per g tissue, remained constant in the red muscle and the white muscle with increasing body size. This suggested that the folding of the mitochondrial inner membrane may increase with increasing body size, possibly to compensate for the decrease in mitochondrial abundance (as indicated by the decreasing CS enzyme activity). Overall this suggested that the development of red muscle endothermy in PBT is not a result of an increase in mitochondrial abundance per g tissue and

therefore heat generated by an increase aerobic metabolic activity in the red muscle. The transcript abundance of CS and COX did not correlate well with the enzyme activity regardless of whether the data were expressed relative to the house-keeping gene β -actin or not. This indicated that the differences in enzyme activity we observed were not due to regulation at the transcriptional level.

In the future, electron microscopy could be utilised to directly visualise the mitochondria within PBT red muscle and white muscle samples to determine if the interpretation of our mitochondrial enzyme activities is accurate and mitochondrial abundance decreases while mitochondrial inner membrane folding increases in the red muscle and white muscle of juvenile PBT with increasing body size.

The PK enzyme activity was 4.3-fold greater in the white muscle compared to the red muscle. This was indicative of the white muscle having a much higher glycolytic capacity than red muscle. The PK enzyme activity increased in the white muscle but not the red muscle with increasing body size. This indicated that the glycolytic capacity of the white muscle increased with increasing body size. A possible reason for the increase could be to allow larger-bodied fishes to be able reach the same burst swimming velocities as smaller-bodied fishes. PK transcript abundance was also statistically significantly greater in the white muscle compared to the red muscle. This was consistent with the PK enzyme activity being regulated at the transcriptional level. However, in contrast to the increase in PK transcript abundance with increasing body size in the white muscle, there was a statistically significant decrease in the transcript abundance. This indicated that PK may also be regulated at the post-transcriptional level.

In Chapter 4 we observed that the PBT PGC-1 α protein sequence was highly similar to PGC-1 α protein sequences from other ray-finned fishes, a subclass of the bony fishes. Amino acid insertions within the NRF-1, PPAR γ and MEF2 binding domains of the PGC-1 α protein sequence are a feature that ray-finned fishes have in common and PBT is no exception. This was consistent with the findings of LeMoine et al. (2010a) who observed insertions in the same binding domains. These insertions are not found in any other class of vertebrate or

even within the lobe-finned fishes, the second subclass of bony fishes. This suggests that PGC-1 α may not be involved in regulating mitochondrial biogenesis and function in fishes, as it is in mammals. Co-immunoprecipitation assays with PGC-1 α or PGC-1 β protein from PBT with NRF-1, PPAR γ and MEF2c protein from PBT could be performed to determine whether the interactions with the PGC-1 transcription factors and these transcription factors occur in PBT. This process would use recombinantly expressed proteins all from the same species of fish. Thus, the results would give an accurate representation of what occurs in PBT.

PGC-1 α transcript abundance ranged from ~20- to ~100-fold greater in the red muscle compared to the white muscle. This was much greater than the differences we observed in mitochondrial abundance, indicated by the CS and COX enzyme activity in these tissues. In contrast, PGC-1 β transcript abundance was ~5- to ~9-fold greater in the red muscle than in the white muscle. This was similar to the difference in mitochondrial abundance, which was approximately one order of magnitude greater in the red muscle than in the white muscle. Unlike in mammals, these data suggest that PGC-1 β , not PGC-1 α , may have more of a role in mitochondrial biogenesis in fishes. However, the temperature elevation we observed in the red muscle of our PBT specimens with increasing body size (Chapter 2) was not paralleled with an increase in the transcript abundance of PGC-1 α or PGC-1 β with increasing body size. This suggests that the temperature elevation in the red muscle of our PBT specimens was not influenced by the expression of these genes.

We observed greater PPAR α and MCAD transcript abundance in the red muscle compared to the white muscle. This was consistent with their role in β -oxidation and red muscle being highly aerobic and therefore having a high utilisation of fatty acids as a fuel source in this tissue. There were strong positive correlations between the transcript abundances of PPAR α and MCAD with the PGC-1 α and PGC-1 β transcriptional coactivators, which provides evidence that the PGC-1 transcriptional coactivators may upregulate β -oxidation in these tissues. Similar to the transcript abundance of PGC-1 α and PGC-1 β , the transcript abundance of PPAR α and MCAD did not increase with increasing body size either. This suggests that an increase in mitochondrial

activity (i.e. β -oxidation) was not the reason for the steep linear temperature elevation we observed in the red muscle of our PBT specimens.

This was interesting because it has previously been shown that small (20–25 cm FL) PBT juveniles prey upon small squid and zooplankton and as they grow larger (25–40 cm FL) their diet gradually shifts to epipelagic and mesopelagic fishes (Shimose et al., 2013). This reported shift in diet occurs at approximately the same size at which we estimate the switch from ectothermy to red muscle endothermy occurs in juvenile PBT. Although both temperature elevation in the red muscle and a shift in diet seemingly occur concurrently, it is unknown if this diet shift contributes to the development of red muscle endothermy. Here we have shown that there was no change in PPAR α or MCAD transcript abundance with increasing body size in PBT. Future research could investigate the protein content of PPAR α and MCAD to determine whether protein content correlates with the transcript abundances we reported here or whether it is coincident with a shift in diet.

In Chapter 5 we investigated the effects of feed restriction on the aerobic and glycolytic metabolic capacity of the red muscle, white muscle and liver of farmed YTK cultured at suboptimal water temperatures. We determined that CS and COX enzyme activities per g tissue were 8-fold and 6-fold greater, respectively, in the red muscle compared with the white muscle in our YTK specimens. This was consistent with red muscle being more aerobic than the white muscle, as was observed in PBT (Chapter 3).

Additionally, CS and COX enzyme, per g tissue, were 57% and 20% greater, respectively, in the liver of feed restricted YTK compared to satiated YTK. This suggested that the aerobic capacity of the liver increased in response to feed restriction. This could have been to facilitate an increase the capacity for β -oxidation in response to reduced dietary fatty acid supply. The liver of our feed restricted YTK could have been priming itself to break down fatty acids when they become available.

We observed that the YTK PGC-1 α protein sequence was highly similar to PGC-1 α protein sequences from other ray-finned fishes, including PBT. This included amino acid insertions within the NRF-1, PPAR γ and MEF2 binding

domains. This supported the theory that PGC-1 α may not be involved in regulating mitochondrial biogenesis and function in fishes, as it is in mammals.

Feed restriction resulted in PGC-1 α transcript abundance being 3-fold greater in the red muscle and 7-fold greater in the white muscle compared to the control fish. This increase in PGC-1 α transcript abundance did not correspond with an increase in CS or COX enzyme activity. Therefore, it is unlikely that the feed restriction-induced increase in PGC-1 α transcript abundance was related to an increase in mitochondrial abundance. Further investigation will be required to understand what this increase means.

Fasting and suboptimal water temperatures have been shown to have opposing effects on mitochondrial abundance in the skeletal muscle of fishes, with fasting resulting in an increase in mitochondrial abundance and suboptimal water temperatures resulting in an increase. Additionally, the effects of feed restriction on the aerobic metabolic capacity in fishes have never been explored. This makes it difficult to determine whether the results observed during this study were due to feed restriction or suboptimal water temperature. To gain a better understanding of the effects of feed restriction on the aerobic metabolic capacity of the red muscle, white muscle and liver of YTK, the same experiment could be repeated at the optimal temperature for the growth of YTK (22.8°C) side by side with a suboptimal temperature. Additionally, comparing the aerobic metabolic capacity in the red muscle, white muscle and liver of feed restricted YTK to fasted YTK would provide a better understanding of how energy stores are utilised under the two states of feed deprivation in this species of fish.

In conclusion, this thesis has used a variety of methods to describe the development of regional endothermy in juvenile PBT. The results of this have advanced the current understanding of the anatomical, physiological and molecular changes that occur in juvenile PBT as they transition from being ectothermic to regionally endothermic. Furthermore, the work with PBT has provided a foundation for future researchers to further investigate the development of regional endothermy in PBT and other regionally endothermic fish species. Additionally, this thesis has used a variety of methods to describe the effects of feed restriction in YTK at suboptimal temperatures. The results

of this advanced the current understanding of the effects of feed restriction in fishes compared to fasting.

REFERENCES

- AGAWA, Y., HONRYO, T., ISHII, A., KOBAYASHI, T., OKU, H. & SAWADA, Y. 2012. Molecular identification and tissue distribution of peroxisome proliferators activated receptor gamma transcript in cultured *Thunnus orientalis*. *Aquaculture Research*, 43, 1145-1158.
- ANDERSSON, U. & SCARPULLA, R. C. 2001. PGC-1-related coactivator, a novel, serum-inducible coactivator of nuclear respiratory factor 1-dependent transcription in mammalian cells. *Mol Cell Biol*, 21, 3738-49.
- ARANY, Z. 2008. PGC-1 coactivators and skeletal muscle adaptations in health and disease. *Current opinion in genetics & development*, 18, 426-434.
- ARANY, Z., LEBRASSEUR, N., MORRIS, C., SMITH, E., YANG, W., MA, Y., CHIN, S. & SPIEGELMAN, B. M. 2007. The transcriptional coactivator PGC-1beta drives the formation of oxidative type IIX fibers in skeletal muscle. *Cell Metab*, 5, 35-46.
- BAIN, P. A., HUTCHINSON, R. G., MARKS, A. B., CRANE, M. S. J. & SCHULLER, K. A. 2013. Establishment of a continuous cell line from southern bluefin tuna (*Thunnus maccoyii*). *Aquaculture*, 376-379, 59-63.
- BANSEMER, M. S., STONE, D. A. J., D'ANTIGNANA, T., SKORDAS, P., KUERSCHNER, L. & CURRIE, K.-L. 2018. Optimising feeding strategies for Yellowtail Jack at winter water temperatures. *North American Journal of Aquaculture*, n/a-n/a.
- BARRETO-CURIEL, F., FOCKEN, U., D'ABRAMO, L. R. & VIANA, M. T. 2017. Metabolism of *Seriola lalandi* during starvation as revealed by fatty acid analysis and compound-specific analysis of stable isotopes within amino acids. *PLoS ONE*, 12, e0170124.
- BATTERSBY, B. J. & MOYES, C. D. 1998. Influence of acclimation temperature on mitochondrial DNA, RNA, and enzymes in skeletal muscle. *Am J Physiol*, 275, R905-12.
- BENETTI, D., NAKADA, M., SHOTTON, S., POORTENAAR, C., TRACY, P. L. & HUTCHINSON, W. 2005. *Aquaculture of three species of yellowtail jacks*.
- BERGIN, A. & HAWARD, M. G. 1996. *Japan's Tuna Fishing Industry: A Setting Sun Or New Dawn?*, Nova Science Publishers.
- BERNAL, D., DICKSON, K. A., SHADWICK, R. E. & GRAHAM, J. B. 2001a. Review: Analysis of the evolutionary convergence for high performance swimming in lamnid sharks and tunas. *Comparative Biochemistry and Physiology Part A: Molecular & Integrative Physiology*, 129, 695-726.
- BERNAL, D., SEPULVEDA, C. & GRAHAM, J. B. 2001b. Water-tunnel studies of heat balance in swimming mako sharks. *J Exp Biol*, 204, 4043-54.
- BESTLEY, S., PATTERSON, T. A., HINDELL, M. A. & GUNN, J. S. 2008. Feeding ecology of wild migratory tunas revealed by archival tag records of visceral warming. *J Anim Ecol*, 77, 1223-33.
- BLANK, J. M., FARWELL, C. J., MORRISSETTE, J. M., SCHALLERT, R. J. & BLOCK, B. A. 2007. Influence of swimming speed on metabolic rates of juvenile Pacific bluefin tuna and yellowfin tuna. *Physiological and Biochemical Zoology*, 80, 167-177.
- BLANK, J. M., MORRISSETTE, J. M., FARWELL, C. J., PRICE, M., SCHALLERT, R. J. & BLOCK, B. A. 2008. Temperature effects on metabolic rate of juvenile Pacific bluefin tuna *Thunnus orientalis*. *Journal of Experimental Biology*, 210, 4254-4261.
- BLOCK, B. A. 1987a. BILLFISH BRAIN AND EYE HEATER - A new look at nonshivering heat-production. *News in Physiological Sciences*, 2, 208-213.
- BLOCK, B. A. 1987b. Strategies for regulating brain and eye temperatures: A thermogenic tissue in fish. *Comparative Physiology: Life in the Water and on Land* (ed. P. Dejours, L. Bolis, CR Taylor and ER Weibel), 401-420.

- BLOCK, B. A. 2011. Endothermy in tunas, billfishes, and sharks. *Encyclopedia of Fish Physiology: From Genome to Environment, Vols 1-3, 1914-1920.*
- BLOCK, B. A. & FINNERTY, J. R. 1994. Endothermy in fishes: A phylogenetic analysis of constraints, predispositions, and selection pressures. *Environmental Biology of Fishes*, 40, 283-302.
- BLOCK, B. A., FINNERTY, J. R., STEWART, A. F. & KIDD, J. 1993. Evolution of endothermy in fish: Mapping physiological traits on a molecular phylogeny. *Science*, 260, 210-4.
- BOWYER, J. N., QIN, J. G., ADAMS, L. R., THOMSON, M. J. S. & STONE, D. A. J. 2012a. The response of digestive enzyme activities and gut histology in yellowtail kingfish (*Seriola lalandi*) to dietary fish oil substitution at different temperatures. *Aquaculture*, 368-369, 19-28.
- BOWYER, J. N., QIN, J. G., SMULLEN, R. P., ADAMS, L. R., THOMSON, M. J. S. & STONE, D. A. J. 2013. The use of a soy product in juvenile yellowtail kingfish (*Seriola lalandi*) feeds at different water temperatures: 2. Soy protein concentrate. *Aquaculture*, 410-411, 1-10.
- BOWYER, J. N., QIN, J. G., SMULLEN, R. P. & STONE, D. A. J. 2012b. Replacement of fish oil by poultry oil and canola oil in yellowtail kingfish (*Seriola lalandi*) at optimal and suboptimal temperatures. *Aquaculture*, 356-357, 211-222.
- BRAISSANT, O., FOUFELLE, F., SCOTTO, C., DAUÇA, M. & WAHLI, W. 1996. Differential expression of peroxisome proliferator-activated receptors (PPARs): tissue distribution of PPAR-alpha, -beta, and -gamma in the adult rat. *Endocrinology*, 137, 354-366.
- BREMER, K., KOCHA, K. M., SNIDER, T. & MOYES, C. D. 2016. Sensing and responding to energetic stress: The role of the AMPK-PGC1 α -NRF1 axis in control of mitochondrial biogenesis in fish. *Comparative Biochemistry and Physiology Part B: Biochemistry and Molecular Biology*, 199, 4-12.
- BREMER, K., MONK, C. T., GURD, B. J. & MOYES, C. D. 2012. Transcriptional regulation of temperature-induced remodeling of muscle bioenergetics in goldfish. *American Journal of Physiology - Regulatory, Integrative and Comparative Physiology*, 303, 150-158.
- BREMER, K. & MOYES, C. D. 2011. Origins of variation in muscle cytochrome c oxidase activity within and between fish species. *J Exp Biol*, 214, 1888-95.
- BUBNER, E., FARLEY, J., THOMAS, P., BOLTON, T. & ELIZUR, A. 2012. Assessment of reproductive maturation of southern bluefin tuna (*Thunnus maccoyii*) in captivity. *Aquaculture*, 364-365, 82-95.
- BUCKLEY, L. B., HURLBERT, A. H. & JETZ, W. 2012. Broad-scale ecological implications of ectothermy and endothermy in changing environments. *Global Ecology and Biogeography*, 21, 873-885.
- BURNESS, G. P., LEARY, S. C., HOCHACHKA, P. W. & MOYES, C. D. 1999. Allometric scaling of RNA, DNA, and enzyme levels: an intraspecific study. *American Journal of Physiology - Regulatory, Integrative and Comparative Physiology*, 277, 1164-1170.
- BUSHNELL, P. G. & JONES, D. R. 1994. Cardiovascular and respiratory physiology of tuna - Adaptations for support of exceptionally high metabolic rates. *Environmental Biology of Fishes*, 40, 303-318.
- BUSHNELL, P. G., JONES, D. R. & FARRELL, A. P. 1992. 2 - The arterial system. *In: HOAR, W. S., RANDALL, D. J. & FARRELL, A. P. (eds.) Fish Physiology.* Academic Press.
- CAMÕES, F., BONEKAMP, N. A., DELILLE, H. K. & SCHRADER, M. 2009. Organelle dynamics and dysfunction: A closer link between peroxisomes and mitochondria. *Journal of Inherited Metabolic Disease*, 32, 163-180.
- CAREY, F. G. 1982. A BRAIN HEATER IN THE SWORDFISH. *Science*, 216, 1327-1329.
- CAREY, F. G., KANWISHER, J. W. & STEVENS, E. D. 1984. Bluefin tuna warm their viscera during digestion. *Journal of Experimental Biology*, 109, 1-20.

- CAREY, F. G. & ROBISON, B. H. 1981. Daily patterns in the activities of swordfish, *Xiphias gladius*, observed by acoustic telemetry. *Fishery Bulletin*, 79, 277-292.
- CAREY, F. G. & TEAL, J. M. 1966. Heat conservation in tuna fish muscle. *Proc Natl Acad Sci U S A*, 56, 1464-9.
- CAREY, F. G. & TEAL, J. M. 1969. Regulation of body temperature by the bluefin tuna. *Comparative Biochemistry and Physiology*, 28, 205-213.
- CAREY, F. G., TEAL, J. M. & KANWISHER, J. W. 1981. The visceral temperatures of mackerel sharks (Lamnidae). *Physiological Zoology*, 54, 334-344.
- CASTELLINI, M. 2018. Thermoregulation. In: WÜRSIG, B., THEWISSEN, J. G. M. & KOVACS, K. M. (eds.) *Encyclopedia of Marine Mammals (Third Edition)*. Academic Press.
- CHEDOLOH, R., KARRILA, T. & PAKDEECHANUAN, P. 2011. Fatty acid composition of important aquatic animals in Southern Thailand. *International Food Research Journal*, 18.
- CHEN, Y., JACKSON, D. A. & HARVEY, H. H. 1992. A comparison of von Bertalanffy and polynomial functions in modelling fish growth data. *Canadian Journal of Fisheries and Aquatic Sciences*, 49, 1228-1235.
- CHILDRESS, J. J. & SOMERO, G. N. 1990. Metabolic Scaling: A new perspective based on scaling of glycolytic enzyme activities. *American Zoologist*, 30, 161-173.
- CHOW, S., NOHARA, K., TANABE, T., ITOH, T., TSUJI, S., NISHIKAWA, Y., UYEYANAGI, S. & UCHIKAWA, K. 2003. Genetic and morphological identification of larval and small juvenile tunas (Pisces: Scombridae) caught by a mid-water trawl in the western Pacific. *BULLETIN-FISHERIES RESEARCH AGENCY JAPAN*, 1-14.
- CLARKE, A. & PORTNER, H. O. 2010. Temperature, metabolic power and the evolution of endothermy. *Biological Reviews*, 85, 703-727.
- COLLETTE, B., AMORIM, A. F., BOUSTANY, A., CARPENTER, K. E., DE OLIVEIRA LEITE JR., N., DI NATALE, A., DIE, D., FOX, W., FREDOU, F. L., GRAVES, J., VIERA HAZIN, F. H., HINTON, M., JUAN JORDA, M., KADA, O., MINTE VERA, C., MIYABE, N., NELSON, R., OXENFORD, H., POLLARD, D., RESTREPO, V., SCHRATWIESER, J., TEIXEIRA LESSA, R. P., PIRES FERREIRA TRAVASSOS, P. E. & UOZUMI, Y. 2011a. *Thunnus thynnus*. *The IUCN Red List of Threatened Species* [Online]. Available: <http://dx.doi.org/10.2305/IUCN.UK.2011-2.RLTS.T21860A9331546.en>. [Accessed 7th January 2019].
- COLLETTE, B., CHANG, S.-K., DI NATALE, A., FOX, W., JUAN JORDA, M., MIYABE, N., NELSON, R., UOZUMI, Y. & WANG, S. 2011b. *Thunnus maccoyii*. *The IUCN Red List of Threatened Species* [Online]. Available: <http://dx.doi.org/10.2305/IUCN.UK.2011-2.RLTS.T21858A9328286.en>. [Accessed 7th January 2019].
- COLLETTE, B., FOX, W., JUAN JORDA, M., NELSON, R., POLLARD, D., SUZUKI, N. & TEO, S. 2014. *Thunnus orientalis*. *The IUCN Red List of Threatened Species* [Online]. Available: <http://dx.doi.org/10.2305/IUCN.UK.2014-3.RLTS.T170341A65166749.en> [Accessed 24th April 2018].
- COLLU-MARCHESE, M., SHUEN, M., PAULY, M., SALEEM, A. & HOOD, D. A. 2015. The regulation of mitochondrial transcription factor A (Tfam) expression during skeletal muscle cell differentiation. *Biosci Rep*, 35.
- CORDINER, S. & EGGINTON, S. 1997. Effects of seasonal temperature acclimatization on muscle metabolism in rainbow trout, *Oncorhynchus mykiss*. *Fish Physiology and Biochemistry*, 16, 333-343.
- CST 2016. Annual Report 2015-2016. Clean Seas Tuna Ltd. Company Announcement.
- CST 2018. Annual Report 2017-2018. Clean Seas Tuna Ltd. Company Announcement.

- DALZIEL, A. C., MOORE, S. E. & MOYES, C. D. 2005. Mitochondrial enzyme content in the muscles of high-performance fish: Evolution and variation among fiber types. *Am J Physiol Regul Integr Comp Physiol*, 288, R163-72.
- DAVENPORT, J., JONES, T. T., WORK, T. M. & BALAZS, G. H. 2015. Topsy-turvy: turning the counter-current heat exchange of leatherback turtles upside down. *Biology Letters*, 11, 20150592.
- DAVIES, R. & MOYES, C. D. 2007. Allometric scaling in centrarchid fish: origins of intra-and inter-specific variation in oxidative and glycolytic enzyme levels in muscle. *Journal of Experimental Biology*, 210, 3798-3804.
- DE METRIO, G., BRIDGES, C. R., MYLONAS, C. C., CAGGIANO, M., DEFLORIO, M., SANTAMARIA, N., ZUPA, R., POUISIS, C., VASSALLO-AGIUS, R., GORDIN, H. & CORRIERO, A. 2010. Spawning induction and large-scale collection of fertilized eggs in captive Atlantic bluefin tuna (*Thunnus thynnus* L.) and the first larval rearing efforts. *Journal of Applied Ichthyology*, 26, 596-599.
- DESVERGNE, B. & WAHLI, W. 1999. Peroxisome proliferator-activated receptors: Nuclear control of metabolism. *Endocrine Reviews*, 20, 649-688.
- DHAHBI, J. M., MOTE, P. L., WINGO, J., TILLMAN, J. B., WALFORD, R. L. & SPINDLER, S. R. 1999. Calories and aging alter gene expression for gluconeogenic, glycolytic, and nitrogen-metabolizing enzymes. *American Journal of Physiology-Endocrinology and Metabolism*, 277, E352-E360.
- DHAR, S. S., ONGWIJITWAT, S. & WONG-RILEY, M. T. 2008. Nuclear respiratory factor 1 regulates all ten nuclear-encoded subunits of cytochrome c oxidase in neurons. *J Biol Chem*, 283, 3120-9.
- DICKSON, K. A. 1994. Tunas as small as 207mm fork length can elevate muscle temperatures significantly above ambient water temperature. *Journal of Experimental Biology*, 190, 79-93.
- DICKSON, K. A. 1996. Locomotor muscle of high-performance fishes: What do comparisons of tunas with ectothermic sister taxa reveal? *Comparative Biochemistry and Physiology Part A: Physiology*, 113, 39-49.
- DICKSON, K. A. & GRAHAM, J. B. 2004. Evolution and consequences of endothermy in fishes. *Physiological and Biochemical Zoology*, 77, 998-1018.
- DICKSON, K. A., JOHNSON, N. M., DONLEY, J. M., HOSKINSON, J. A., HANSEN, M. W. & D'SOUZA TESSIER, J. 2000. Ontogenetic changes in characteristics required for endothermy in juvenile black skipjack tuna (*Euthynnus lineatus*). *J Exp Biol*, 203, 3077-87.
- DONLEY, J. M., SEPULVEDA, C. A., KONSTANTINIDIS, P., GEMBALLA, S. & SHADWICK, R. E. 2004. Convergent evolution in mechanical design of lamnid sharks and tunas. *Nature*, 429, 61-65.
- DOWIS, H. J., SEPULVEDA, C. A., GRAHAM, J. B. & DICKSON, K. A. 2003. Swimming performance studies on the eastern Pacific bonito *Sarda chiliensis*, a close relative of the tunas (family Scombridae) II. Kinematics. *J Exp Biol*, 206, 2749-58.
- DUGGAN, A. T., KOCHA, K. M., MONK, C. T., BREMER, K. & MOYES, C. D. 2011. Coordination of cytochrome c oxidase gene expression in the remodelling of skeletal muscle. *J Exp Biol*, 214, 1880-7.
- ELSE, P. L. & HULBERT, A. J. 1985. Mammals: An allometric study of metabolism at tissue and mitochondrial level. *American Journal of Physiology-Regulatory, Integrative and Comparative Physiology*, 248, R415-R421.
- EMMETT, B. & HOCHACHKA, P. W. 1981. Scaling of oxidative and glycolytic enzymes in mammals. *Respir Physiol*, 45, 261-72.
- ENDO, T., ISHIDA, M., YAZAWA, R., TAKEUCHI, Y., KUMAKURA, N., HARA, T. & ADACHI, S. 2016. Mass production of fertilized eggs by artificial insemination from captive-reared Pacific bluefin tuna (*Thunnus orientalis*). *Aquaculture*, 451, 72-77.

- ESTESS, E. E., COFFEY, D. M., SHIMOSE, T., SEITZ, A. C., RODRIGUEZ, L., NORTON, A., BLOCK, B. & FARWELL, C. 2014. Bioenergetics of captive Pacific bluefin tuna (*Thunnus orientalis*). *Aquaculture*, 434, 137-144.
- FIELDER, D. S. 2013. Advances in aquaculture hatchery technology: 18. Hatchery production of yellowtail kingfish (*Seriola lalandi*), Elsevier Science.
- FIELDER, D. S. & HEASMAN, M. 2011. *Hatchery Manual for the Production of Australian Bass, Mulloway and Yellowtail Kingfish*, Industry and Investment NSW.
- FINCK, B. N. & KELLY, D. P. 2006. PGC-1 coactivators: inducible regulators of energy metabolism in health and disease. *Journal of Clinical Investigation*, 116, 615-622.
- FITZGIBBON, Q. P., SEYMOUR, R. S., ELLIS, D. & BUCHANAN, J. 2007. The energetic consequence of specific dynamic action in southern bluefin tuna *Thunnus maccoyii*. *J Exp Biol*, 210, 290-8.
- FOSTER, G. D. & MOON, T. W. 1991. Hypometabolism with fasting in the yellow perch (*Perca flavescens*): A study of enzymes, hepatocyte metabolism, and tissue size. *Physiological Zoology*, 64, 259-275.
- FREITAS, C., OLSEN, E. M., MOLAND, E., CIANNELLI, L. & KNUTSEN, H. 2015. Behavioral responses of Atlantic cod to sea temperature changes. *Ecology and Evolution*, 5, 2070-2083.
- FRITSCHES, K. A., BRILL, R. W. & WARRANT, E. J. 2005. Warm eyes provide superior vision in swordfishes. *Current Biology*, 15, 55-58.
- FROESE, R. & PAULY, D. 2018. *FishBase. World Wide Web electronic publication*. [Online]. Available: www.fishbase.org [Accessed 2 Jan 2019].
- FUDGE, D. S. & STEVENS, E. D. 2005. The visceral retia mirabilia of tuna and sharks: An annotated translation and discussion of the Eschricht & Müller 1835 paper and related papers. 2005, 4.
- FUENTES, E. N., SAFIAN, D., EINARSDOTTIR, I. E., VALDÉS, J. A., ELORZA, A. A., MOLINA, A. & BJÖRNSSON, B. T. 2013. Nutritional status modulates plasma leptin, AMPK and TOR activation, and mitochondrial biogenesis: Implications for cell metabolism and growth in skeletal muscle of the fine flounder. *General and Comparative Endocrinology*, 186, 172-180.
- FUJIOKA, K., FUKUDA, H., FURUKAWA, S., TEI, Y., OKAMOTO, S. & OHSHIMO, S. 2018a. Habitat use and movement patterns of small (age-0) juvenile Pacific bluefin tuna (*Thunnus orientalis*) relative to the Kuroshio. *Fisheries Oceanography*.
- FUJIOKA, K., FUKUDA, H., TEI, Y., OKAMOTO, S., KIYOFUJI, H., FURUKAWA, S., TAKAGI, J., ESTESS, E., FARWELL, C. J., FULLER, D. W., SUZUKI, N., OHSHIMO, S. & KITAGAWA, T. 2018b. Spatial and temporal variability in the trans-Pacific migration of Pacific bluefin tuna (*Thunnus orientalis*) revealed by archival tags. *Progress in Oceanography*, 162, 52-65.
- FURUKAWA, S., FUJIOKA, K., FUKUDA, H., SUZUKI, N., TEI, Y. & OHSHIMO, S. 2017. Archival tagging reveals swimming depth and ambient and peritoneal cavity temperature in age-0 Pacific bluefin tuna, *Thunnus orientalis*, off the southern coast of Japan. *Environmental Biology of Fishes*, 100, 35-48.
- GIBB, A. C. & DICKSON, K. A. 2002. Functional morphology and biochemical indices of performance: Is there a correlation between metabolic enzyme activity and swimming performance? *Integrative and Comparative Biology*, 42, 199-207.
- GLANCY, B. & BALABAN, R. S. 2011. Protein composition and function of red and white skeletal muscle mitochondria. *Am J Physiol Cell Physiol*, 300, C1280-90.
- GLANVILLE, E. J. & SEEBACHER, F. 2006. Compensation for environmental change by complementary shifts of thermal sensitivity and thermoregulatory behaviour in an ectotherm. *Journal of Experimental Biology*, 209, 4869-4877.

- GOOLISH, E. M. 1989. The scaling of aerobic and anaerobic muscle power in rainbow-trout (*Salmo gairdneri*). *Journal of Experimental Biology*, 147, 493-505.
- GRAHAM, J. B. & DICKSON, K. A. 2000. The evolution of thunniform locomotion and heat conservation in scombrid fishes: New insights based on the morphology of *Allothunnus fallai*. *Zoological Journal of the Linnean Society*, 129, 419-466.
- GRAHAM, J. B., KOEHRN, F. J. & DICKSON, K. A. 1983. Distribution and relative proportions of red muscle in scombrid fishes - consequences of body size and relationships to locomotion and endothermy. *Canadian Journal of Zoology-Revue Canadienne De Zoologie*, 61, 2087-2096.
- GREEK-WALKER, M. & PULL, G. A. 1975. A survey of red and white muscle in marine fish. *Journal of Fish Biology*, 7, 295-300.
- GUDERLEY, H. 1990. Functional significance of metabolic responses to thermal acclimation in fish muscle. *Am J Physiol*, 259, R245-52.
- GUDERLEY, H. 2004. Metabolic responses to low temperature in fish muscle. *Biol Rev Camb Philos Soc*, 79, 409-27.
- GULICK, T., CRESCI, S., CAIRA, T., MOORE, D. D. & KELLY, D. P. 1994. The peroxisome proliferator-activated receptor regulates mitochondrial fatty acid oxidative enzyme gene expression. *Proceedings of the National Academy of Sciences*, 91, 11012-11016.
- GUNN, J. & BLOCK, B. 2001. Advances in acoustic, archival, and satellite tagging of tunas. *Fish Physiology*. Academic Press.
- GUPPY, M. & HOCHACHKA, P. W. 1979. Pyruvate kinase functions in hot and cold organs of tuna. *Journal of comparative physiology*, 129, 185-191.
- GUPPY, M., HULBERT, W. C. & HOCHACHKA, P. W. 1979. Metabolic sources of heat and power in tuna muscles .2. Enzyme and metabolite profiles. *Journal of Experimental Biology*, 82, 303-320.
- HANCOCK, C. R., HAN, D.-H., HIGASHIDA, K., KIM, S. H. & HOLLOSZY, J. O. 2011. Does calorie restriction induce mitochondrial biogenesis? A reevaluation. *The FASEB Journal*, 25, 785-791.
- HENDRIKS-BALK, M. C., MICHEL, M. C. & ALEWIJNSE, A. E. 2007. Pitfalls in the normalization of real-time polymerase chain reaction data. *Basic Research in Cardiology*, 102, 195.
- HIGGS, D. A., BALFRY, S. K., OAKES, J. D., ROWSHANDELI, M., SKURA, B. J. & DEACON, G. 2006. Efficacy of an equal blend of canola oil and poultry fat as an alternate dietary lipid source for Atlantic salmon (*Salmo salar* L.) in sea water. I: effects on growth performance, and whole body and fillet proximate and lipid composition. *Aquaculture Research*, 37, 180-191.
- HOLTS, D. Activity patterns of striped marlin in the southern California Bight. In." Planning the future of billfishes, research and management in the 90s and beyond. Proceedings of the second international billfish symposium, Kailua-Kona, Hawaii, August 1-5, 1988. Part 2, 1990. National Coalition for Marine Conservation, 81-93.
- HUMASON, G. L. 1979. Animal tissue techniques.
- HUSS, J. M., KOPP, R. P. & KELLY, D. P. 2002. Peroxisome proliferator-activated receptor coactivator-1alpha (PGC-1alpha) coactivates the cardiac-enriched nuclear receptors estrogen-related receptor-alpha and -gamma. Identification of novel leucine-rich interaction motif within PGC-1alpha. *J Biol Chem*, 40265-40274.
- HUYNH, M. D. & KITTS, D. D. 2009. Evaluating nutritional quality of pacific fish species from fatty acid signatures. *Food Chemistry*, 912-918.
- ICCAT 2017. 9.5 BFT – ATLANTIC BLUEFIN TUNA. International Commission for the Conservation of Atlantic Tunas.
- IKEDA, Y., HALE, D. E., KEESE, S. M., COATES, P. M. & TANAKA, K. 1986. biosynthesis of variant medium chain acyl-CoA dehydrogenase in cultured

- fibroblasts from patients with medium chain Acyl-CoA dehydrogenase deficiency. *Pediatric Research*, 20, 843.
- ITOH, T. 2001. Estimation of total catch in weight and catch-at-age in number of bluefin tuna *Thunnus orientalis* in the whole Pacific Ocean. *Bull. Natl Res. Inst. Far Seas Fish.*, 38, 83-111.
- JAGER, S., HANDSCHIN, C., ST-PIERRE, J. & SPIEGELMAN, B. M. 2007. AMP-activated protein kinase (AMPK) action in skeletal muscle via direct phosphorylation of PGC-1 α . *Proc Natl Acad Sci U S A*, 104, 12017-22.
- JIRSA, D., DAVIS, A., STUART, K. & DRAWBRIDGE, M. 2011. Development of a practical soy-based diet for California yellowtail, *Seriola lalandi*. *Aquaculture Nutrition*, 17, e869-e874.
- JOHANSEN, K. A. & OVERTURF, K. 2006. Alterations in expression of genes associated with muscle metabolism and growth during nutritional restriction and refeeding in rainbow trout. *Comparative Biochemistry and Physiology Part B: Biochemistry and Molecular Biology*, 144, 119-127.
- JOHNSTON, I. A. 1977. A comparative study of glycolysis in red and white muscles of the trout (*Salmo gairdneri*) and mirror carp (*Cyprinus carpio*). *Journal of Fish Biology*, 11, 575-588.
- JOHNSTON, I. A., BOWER, N. I. & MACQUEEN, D. J. 2011. Growth and the regulation of myotomal muscle mass in teleost fish. *The Journal of Experimental Biology*, 214, 1617-1628.
- JORNAYVAZ, F. R. & SHULMAN, G. I. 2010. Regulation of mitochondrial biogenesis. *Essays in biochemistry*, 47, 69-84.
- KAMEI, Y., OHIZUMI, H., FUJITANI, Y., NEMOTO, T., TANAKA, T., TAKAHASHI, N., KAWADA, T., MIYOSHI, M., EZAKI, O. & KAKIZUKA, A. 2003. PPAR γ coactivator 1 β /ERR ligand 1 is an ERR protein ligand, whose expression induces a high-energy expenditure and antagonizes obesity. *Proceedings of the National Academy of Sciences*, 100, 12378-12383.
- KARP, J. R. 2001. Muscle fiber types and training. *Strength and Conditioning Journal*, 23, 21-26.
- KAWAI, H. 1998. *A brief history of recognition of the Kuroshio*.
- KELLY, D. P., GORDON, J. I., ALPERS, R. & STRAUSS, A. W. 1989. The tissue-specific expression and developmental regulation of two nuclear genes encoding rat mitochondrial proteins. Medium chain acyl-CoA dehydrogenase and mitochondrial malate dehydrogenase. *Journal of Biological Chemistry*, 264, 18921-18925.
- KINGFISH-ZEELAND. 2018. *Kingfish Zeeland* [Online]. Available: <https://www.kingfish-zeeland.com> [Accessed 24th July 2018].
- KIRCHHOFF, N. T., ROUGH, K. M. & NOWAK, B. F. 2011. Moving cages further offshore: Effects on southern bluefin tuna, *T. maccoyii*, parasites, health and performance. *PLOS ONE*, 6, e23705.
- KISHINOUE, K. 1923. Contribution to the comparative study of the so-called scombroid fishes. *J. Coll. Agric. Imp. Univ. Tokyo*, 8, 298-475.
- KITAGAWA, T. & FUJIOKA, K. 2017. *Rapid ontogenetic shift in the diet in juvenile Pacific bluefin tuna*.
- KITAGAWA, T., KATO, Y., MILLER, M. J., SASAI, Y., SASAKI, H. & KIMURA, S. 2010. The restricted spawning area and season of Pacific bluefin tuna facilitate use of nursery areas: A modeling approach to larval and juvenile dispersal processes. *Journal of Experimental Marine Biology and Ecology*, 393, 23-31.
- KITAGAWA, T., KIMURA, S., NAKATA, H. & YAMADA, H. 2006a. Thermal adaptation of Pacific bluefin tuna *Thunnus orientalis* to temperate waters (vol 72, pg 149, 2006). *Fisheries Science*, 72, 458-458.
- KITAGAWA, T., SARTIMBUL, A., NAKATA, H., KIMURA, S., YAMADA, H. & NITTA, A. 2006b. The effect of water temperature on habitat use of young Pacific bluefin tuna *Thunnus orientalis* in the East China Sea. *Fisheries Science*, 72, 1166-1176.

- KLEIBER, M. 1947. Body size and metabolic rate. *Physiological reviews*, 27, 511-541.
- KNUTTI, D., KRESSLER, D. & KRALLI, A. 2001. Regulation of the transcriptional coactivator PGC-1 via MAPK-sensitive interaction with a repressor. *Proceedings of the National Academy of Sciences*, 98, 9713-9718.
- KOLKOVSKI, S. & SAKAKURA, Y. 2004. Yellowtail kingfish, from larvae to mature fish—problems and opportunities. *Avances en Nutrición Acuícola VII., Hermosillo, Sonora, México.*
- KONDO, H., SUDA, S., KAWANA, Y., HIRONO, I., NAGASAKA, R., KANEKO, G., USHIO, H. & WATABE, S. 2012. Effects of feed restriction on the expression profiles of the glucose and fatty acid metabolism-related genes in rainbow trout *Oncorhynchus mykiss* muscle. *Fisheries Science*, 78, 1205-1211.
- KOO, S. H., SATOH, H., HERZIG, S., LEE, C. H., HEDRICK, S., KULKARNI, R., EVANS, R. M., OLEFSKY, J. & MONTMINY, M. 2004. PGC-1 promotes insulin resistance in liver through PPAR-alpha-dependent induction of TRB-3. *Nat Med*, 10, 530-4.
- KORSMEYER, K. E. & DEWAR, H. 2001. Tuna metabolism and energetics. *Fish Physiology*. Academic Press.
- KOTTELAT, M. & FREYHOF, J. R. 2007. *Handbook of European freshwater fishes*, Publications Kottelat.
- KRESSLER, D., SCHREIBER, S. N., KNUTTI, D. & KRALLI, A. 2002. The PGC-1-related Protein PERC Is a Selective Coactivator of Estrogen Receptor α . *Journal of Biological Chemistry*, 277, 13918-13925.
- KUBO, T., SAKAMOTO, W., MURATA, O. & KUMAI, H. 2008. Whole-body heat transfer coefficient and body temperature change of juvenile Pacific bluefin tuna *Thunnus orientalis* according to growth. *Fisheries Science*, 74, 995-1004.
- KYPRIANOU, T.-D., PÖRTNER, H. O., ANESTIS, A., KOSTOGLU, B., FEIDANTSIS, K. & MICHAELIDIS, B. 2010. Metabolic and molecular stress responses of gilthead sea bream *Sparus aurata* during exposure to low ambient temperature: An analysis of mechanisms underlying the winter syndrome. *Journal of Comparative Physiology B*, 180, 1005-1018.
- LARKIN, M. A., BLACKSHIELDS, G., BROWN, N. P., CHENNA, R., MCGETTIGAN, P. A., MCWILLIAM, H., VALENTIN, F., WALLACE, I. M., WILM, A., LOPEZ, R., THOMPSON, J. D., GIBSON, T. J. & HIGGINS, D. G. 2007. Clustal W and Clustal X version 2.0. *Bioinformatics*, 23, 2947-8.
- LEARY, S. C., LYONS, C. N., ROSENBERGER, A. G., BALLANTYNE, J. S., STILLMAN, J. & MOYES, C. D. 2003. Fiber-type differences in muscle mitochondrial profiles. *American Journal of Physiology - Regulatory, Integrative and Comparative Physiology*, 285, R817-R826.
- LEAVER, M., BOUKOUVALA, E., ANTONOPOULOU, E., DIEZ, A., FAVRE-KREY, L., EZAZ, T., BAUTISTA, J., TOCHER, D. & KREY, G. 2005. Three Peroxisome Proliferator-Activated Receptor Isoforms from Each of Two Species of Marine Fish. *Endocrinology* 146(7):3150–3162
- LEHMAN, J. J. & KELLY, D. P. 2002. Transcriptional activation of energy metabolic switches in the developing and hypertrophied heart. *Clin Exp Pharmacol Physiol*, 29, 339-45.
- LEMBERGER, T., BRAISSANT, O., JUGE-AUBRY, C., KELLER, H., SALADIN, R., STAELS, B., AUWERX, J., BURGER, A. G., MEIER, C. A. & WAHLI, W. 1996. PPAR tissue distribution and interactions with other hormone-signaling pathways. *Annals of the New York Academy of Sciences*, 804, 231-251.
- LEMOINE, C. M., LOUGHEED, S. C. & MOYES, C. D. 2010a. Modular evolution of PGC-1 α in vertebrates. *J Mol Evol*, 70, 492-505.
- LEMOINE, C. M. R., CRAIG, P. M., DHEKNEY, K., KIM, J. J. & MCCLELLAND, G. B. 2010b. Temporal and spatial patterns of gene expression in skeletal muscles in response to swim training in adult zebrafish (*Danio rerio*). *Journal of Comparative Physiology B*, 180, 151-160.

- LEMOINE, C. M. R., GENGE, C. E. & MOYES, C. D. 2008. Role of the PGC-1 family in the metabolic adaptation of goldfish to diet and temperature. *Journal of Experimental Biology*, 211, 1448-1455.
- LI, Y., PARK, J. S., DENG, J. H. & BAI, Y. 2006. Cytochrome c oxidase subunit IV is essential for assembly and respiratory function of the enzyme complex. *J Bioenerg Biomembr*, 38, 283-91.
- LIANG, H. & WARD, W. F. 2006. PGC-1 α : a key regulator of energy metabolism. *Advances in Physiology Education*, 30, 145-151.
- LIN, J., HANDSCHIN, C. & SPIEGELMAN, B. M. 2005a. Metabolic control through the PGC-1 family of transcription coactivators. *Cell Metab*, 1, 361-70.
- LIN, J., PUIGSERVER, P., DONOVAN, J., TARR, P. & SPIEGELMAN, B. M. 2002a. Peroxisome proliferator-activated receptor γ coactivator 1 β (PGC-1 β), a novel PGC-1-related transcription coactivator associated with host cell factor. *Journal of Biological Chemistry*, 277, 1645-1648.
- LIN, J., TARR, P. T., YANG, R., RHEE, J., PUIGSERVER, P., NEWGARD, C. B. & SPIEGELMAN, B. M. 2003. PGC-1 β in the regulation of hepatic glucose and energy metabolism. *J Biol Chem*, 278, 30843-8.
- LIN, J., WU, H., TARR, P. T., ZHANG, C.-Y., WU, Z., BOSS, O., MICHAEL, L. F., PUIGSERVER, P., ISOTANI, E., OLSON, E. N., LOWELL, B. B., BASSEL-DUBY, R. & SPIEGELMAN, B. M. 2002b. Transcriptional co-activator PGC-1 α drives the formation of slow-twitch muscle fibres. *Nature*, 418, 797-801.
- LIN, J., YANG, R., TARR, P. T., WU, P. H., HANDSCHIN, C., LI, S., YANG, W., PEI, L., ULDRY, M., TONTONOZ, P., NEWGARD, C. B. & SPIEGELMAN, B. M. 2005b. Hyperlipidemic effects of dietary saturated fats mediated through PGC-1 β coactivation of SREBP. *Cell*, 120, 261-73.
- LINDGÅRD, K., STOKKAN, K. A., LE MAHO, Y. & GROSCOLAS, R. 1992. Protein utilization during starvation in fat and lean Svalbard ptarmigan (*Lagopus mutus hyperboreus*). *Journal of Comparative Physiology B*, 162, 607-613.
- LINTHICUM, D. S. & CAREY, F. G. 1972. Regulation of brain and eye temperatures by the bluefin tuna. *Comparative Biochemistry and Physiology Part A: Physiology*, 43, 425-433.
- LIU, C. & LIN, J. D. 2011. PGC-1 coactivators in the control of energy metabolism. *Acta Biochim Biophys Sin (Shanghai)*, 43, 248-57.
- LIVAK, K. J. & SCHMITTGEN, T. D. 2001. Analysis of relative gene expression data using real-time quantitative PCR and the 2- $\Delta\Delta$ CT method. *Methods*, 25, 402-408.
- LONG, Y. C., GLUND, S., GARCIA-ROVES, P. M. & ZIERATH, J. R. 2007. Calcineurin regulates skeletal muscle metabolism via coordinated changes in gene expression. *Journal of Biological Chemistry*, 282, 1607-1614.
- LOVE, R. M. 1970. The chemical biology of fishes : With a key to the chemical literature. London: Academic Press.
- LOVEGROVE, B. G. 2012. The evolution of endothermy in Cenozoic mammals: a plesiomorphic-apomorphic continuum. *Biol Rev Camb Philos Soc*, 87, 128-62.
- LUDWIG, B., BENDER, E., ARNOLD, S., HÜTTEMANN, M., LEE, I. & KADENBACH, B. 2001. Cytochrome c oxidase and the regulation of oxidative phosphorylation. *ChemBioChem*, 2, 392-403.
- MAGNUSON, J. J. 1973. Comparative study of adaptations for continuous swimming and hydrostatic equilibrium of scombroid and xiphoid fishes. *Fishery Bulletin*, 71, 337-356.
- MAGNUSON, J. J. 1978. Locomotion by scombrid fishes: Hydromechanics, morphology, and behavior. In: HOAR, W. S. & RANDALL, D. J. (eds.) *Fish Physiology*. Academic Press.
- MAŁECKI, J., JAKOBSSON, M. E., HO, A. Y. Y., MOEN, A., RUSTAN, A. C. & FALNES, P. Ø. 2017. Uncovering human METTL12 as a mitochondrial methyltransferase that modulates citrate synthase activity through

- metabolite-sensitive lysine methylation. *Journal of Biological Chemistry*, 292, 17950-17962.
- MARCINEK, D. J., BLACKWELL, S. B., DEWAR, H., FREUND, E. V., FARWELL, C., DAU, D., SEITZ, A. C. & BLOCK, B. A. 2001. Depth and muscle temperature of Pacific bluefin tuna examined with acoustic and pop-up satellite archival tags. *Marine Biology*, 138, 869-885.
- MARTÍNEZ, M., GUDERLEY, H., DUTIL, J.-D., WINGER, P. D., HE, P. & WALSH, S. J. 2003. Condition, prolonged swimming performance and muscle metabolic capacities of cod *Gadus morhua*. *Journal of Experimental Biology*, 206, 503-511.
- MASUMA, S., MIYASHITA, S., YAMAMOTO, H. & KUMAI, H. 2008. Status of bluefin tuna farming, broodstock management, breeding and fingerling production in Japan. *Reviews in Fisheries Science*, 16, 385-390.
- MATSUDA, H., TAKENAKA, Y., YAHARA, T. & UOZUMI, Y. 1998. Extinction risk assessment of declining wild populations: The case of the southern bluefin tuna. *Researches on Population Ecology*, 40, 271-278.
- MATSUMOTO, W. M., AHLSTROM, E. H. & JONES, S. 1972. On the clarification of larval tuna identification. *Fish B-NOAA*, 70, 1-12.
- MCCLELLAND, G. B., CRAIG, P. M., DHEKNEY, K. & DIPARDO, S. 2006. Temperature- and exercise-induced gene expression and metabolic enzyme changes in skeletal muscle of adult zebrafish (*Danio rerio*). *Journal of Physiology-London*, 577, 739-751.
- MCGARRY, J. & FOSTER, D. 1980. Regulation of hepatic fatty acid oxidation and ketone body production. *Annual review of biochemistry*, 49, 395-420.
- MEHTA, N. K. & NAYAK, B. B. 2017. Bio-chemical composition, functional, and rheological properties of fresh meat from fish, squid, and shrimp: A comparative study. *International Journal of Food Properties*, 20, S707-S721.
- MEYNIER, L., MOREL, P. C. H., MACKENZIE, D. D. S., MACGIBBON, A., CHILVERS, B. L. & DUIGNAN, P. J. 2008. Proximate composition, energy content, and fatty acid composition of marine species from Campbell Plateau, New Zealand. *New Zealand Journal of Marine and Freshwater Research*, 42, 425-437.
- MICHAEL, L. F., WU, Z., CHEATHAM, R. B., PUIGSERVER, P., ADELMANT, G., LEHMAN, J. J., KELLY, D. P. & SPIEGELMAN, B. M. 2001. Restoration of insulin-sensitive glucose transporter (GLUT4) gene expression in muscle cells by the transcriptional coactivator PGC-1. *Proceedings of the National Academy of Sciences*, 98, 3820-3825.
- MIEGEL, R. P., PAIN, S. J., VAN WETTERE, W. H. E. J., HOWARTH, G. S. & STONE, D. A. J. 2010. Effect of water temperature on gut transit time, digestive enzyme activity and nutrient digestibility in yellowtail kingfish (*Seriola lalandi*). *Aquaculture*, 308, 145-151.
- MILLER, B. F., ROBINSON, M. M., BRUSS, M. D., HELLERSTEIN, M. & HAMILTON, K. L. 2012. A comprehensive assessment of mitochondrial protein synthesis and cellular proliferation with age and caloric restriction. *Aging cell*, 11, 150-161.
- MIYAKE, M., GUILLOTREAU, P., SUN, C.-H. & ISHIMURA, G. 2010. *Recent Developments in Tuna Industry: Stocks, Fisheries, Management, Processing, Trade and Markets*.
- MIZUNO, K. & WHITE, W. B. 1983. Annual and interannual variability in the Kuroshio current system. *Journal of physical oceanography*, 13, 1847-1867.
- MORASH, A. J., VANDERVEKEN, M. & MCCLELLAND, G. B. 2014. Muscle metabolic remodeling in response to endurance exercise in salmonids. *Frontiers in Physiology*, 5, 452.
- MORTENSEN, O. H., PLOMGAARD, P., FISCHER, C. P., HANSEN, A. K., PILEGAARD, H. & PEDERSEN, B. K. 2007. PGC-1 β is downregulated by training in human skeletal muscle: no effect of training twice every second

- day vs. once daily on expression of the PGC-1 family. *Journal of Applied Physiology*, 103, 1536-1542.
- MOYES, C. D., MATHIEU-COSTELLO, O. A., BRILL, R. W. & HOCHACHKA, P. W. 1992. Mitochondrial metabolism of cardiac and skeletal muscles from a fast (*Katsuwonus pelamis*) and a slow (*Cyprinus carpio*) fish. *Canadian Journal of Zoology*, 70, 1246-1253.
- MYLONAS, C. C., DE LA GÁNDARA, F., CORRIERO, A. & RÍOS, A. B. 2010. Atlantic bluefin tuna (*Thunnus Thynnus*) farming and fattening in the Mediterranean sea. *Reviews in Fisheries Science*, 18, 266-280.
- NAOMASA, E., ARITA, S., TAMARU, C. & LEUNG, P. 2013. Assessing hawaii's aquaculture farm and industry performance. *Aquaculture Economics & Management*, 17, 184-207.
- NEWTON, K. C., WRAITH, J. & DICKSON, K. A. 2015. Digestive enzyme activities are higher in the shortfin mako shark, *Isurus oxyrinchus*, than in ectothermic sharks as a result of visceral endothermy. *Fish Physiology and Biochemistry*, 41, 887-898.
- NICHOLAS, K. B., NICHOLAS, H. B. & DEERFIELD, D. W. 1997. GeneDoc: analysis and visualization of genetic variation. *EMBLNEW. NEWS*, 4, 14.
- NISOLI, E., TONELLO, C., CARDILE, A., COZZI, V., BRACALE, R., TEDESCO, L., FALCONE, S., VALERIO, A., CANTONI, O., CLEMENTI, E., MONCADA, S. & CARRUBA, M. O. 2005. Calorie restriction promotes mitochondrial biogenesis by inducing the expression of eNOS. *Science*, 310, 314-7.
- NITANI, H. 1975. Variation of the Kuroshio south of Japan. *Journal of the Oceanographical Society of Japan*, 31, 154-173.
- NODA, T., FUJIOKA, K., FUKUDA, H., MITAMURA, H., ICHIKAWA, K. & ARAI, N. 2016. The influence of body size on the intermittent locomotion of a pelagic schooling fish. *Proc Biol Sci*, 283.
- NORAMBUENA, F., LEWIS, M., HAMID, N. K. A., HERMON, K., DONALD, J. A. & TURCHINI, G. M. 2013. Fish oil replacement in current aquaculture feed: is cholesterol a hidden treasure for fish nutrition? *PLOS ONE*, 8, e81705.
- NORTON, S. F., EPPLEY, Z. A. & SIDELL, B. D. 2000. Allometric scaling of maximal enzyme activities in the axial musculature of striped bass, *Morone saxatilis* (Walbaum). *Physiological and Biochemical Zoology*, 73, 819-828.
- NORWOOD, C. 2017. Kingfish research gathers momentum. *FISH*. 25 3 ed. Australia: Fisheries research and development corporation
- NYACK, A. C., LOCKE, B. R., VALENCIA, A., DILLAMAN, R. M. & KINSEY, S. T. 2007. Scaling of postcontractile phosphocreatine recovery in fish white muscle: effect of intracellular diffusion. *American Journal of Physiology - Regulatory, Integrative and Comparative Physiology*, 292, R2077-R2088.
- O'BRIEN, K. M. 2011. Mitochondrial biogenesis in cold-bodied fishes. *Journal of Experimental Biology*, 214, 275-285.
- OKADA, T., HONRYO, T., SAWADA, Y., AGAWA, Y., MIYASHITA, S. & ISHIBASHI, Y. 2014. The cause of death of juvenile Pacific bluefin tuna (*Thunnus orientalis*) reared in sea net cages. *Aquacultural Engineering*, 59, 23-25.
- OKANO, S., MITSUNAGA, Y., SAKAMOTO, W. & KUMAI, H. 2006. Study on swimming behavior of cultured pacific bluefin tuna using biotelemetry. *Memoirs of the Faculty of Agriculture of Kinki University (Japan)*.
- OLMEZ, A., BAYIR, M., WANG, C. F. & BAYIR, A. 2015. Effects of long-term starvation and refeeding on fatty acid metabolism-related gene expressions in the liver of zebrafish, *Danio rerio*. *Turkish Journal of Veterinary & Animal Sciences*, 39, 654-660.
- ORCZEWSKA, J. I., HARTLEBEN, G. & O'BRIEN, K. M. 2010. The molecular basis of aerobic metabolic remodeling differs between oxidative muscle and liver of threespine sticklebacks in response to cold acclimation. *Am J Physiol Regul Integr Comp Physiol*, 299, R352-64.

- ORELLANA, J., WALLER, U. & WECKER, B. 2014. Culture of yellowtail kingfish (*Seriola lalandi*) in a marine recirculating aquaculture system (RAS) with artificial seawater. *Aquacultural Engineering*, 58, 20-28.
- PATSOURIS, D., MANDARD, S., VOSHOL, P. J., ESCHER, P., TAN, N. S., HAVEKES, L. M., KOENIG, W., MÄRZ, W., TAFURI, S., WAHLI, W., MÜLLER, M. & KERSTEN, S. 2004. PPAR α governs glycerol metabolism. *The Journal of clinical investigation*, 114, 94-103.
- PEDROSA-GERASMIO, I. R., BABARAN, R. P. & SANTOS, M. D. 2012. Discrimination of juvenile yellowfin (*Thunnus albacares*) and bigeye (*T. obesus*) tunas using mitochondrial DNA control region and liver morphology. *PLoS One*, 7, e35604.
- PETER, J. B., BARNARD, R. J., EDGERTON, V. R., GILLESPIE, C. A. & STEMPEL, K. E. 1972. Metabolic profiles of three fiber types of skeletal muscle in guinea pigs and rabbits. *Biochemistry*, 11, 2627-2633.
- PETERS, R. H. 1986. *The Ecological Implications of Body Size*, Cambridge University Press.
- PILEGAARD, H., SALTIN, B. & NEUFER, P. D. 2003. Exercise induces transient transcriptional activation of the PGC-1 α gene in human skeletal muscle. *J Physiol*, 546, 851-8.
- PIRHONEN, J. & FORSMAN, L. 1998. Effect of prolonged feed restriction on size variation, feed consumption, body composition, growth and smolting of brown trout, *Salmo trutta*. *Aquaculture*, 162, 203-217.
- PIROZZI, I. & BOOTH, M. A. 2009. The routine metabolic rate of mulloway (*Argyrosomus japonicus*: Sciaenidae) and yellowtail kingfish (*Seriola lalandi*: Carangidae) acclimated to six different temperatures. *Comparative Biochemistry and Physiology Part A: Molecular & Integrative Physiology*, 152, 586-592.
- PORCH, C. E. 2005. The sustainability of western Atlantic bluefin tuna: A warm-blooded fish in a hot-blooded fishery. *Bulletin of Marine Science*, 76, 363-384.
- PORTER, W. P. & GATES, D. M. 1969. Thermodynamic equilibria of animals with environment. *Ecological Monographs*, 39, 227-244.
- PREMACHANDRA, H. K. A., NGUYEN, N. H., MILLER, A., D'ANTIGNANA, T. & KNIBB, W. 2017. Genetic parameter estimates for growth and non-growth traits and comparison of growth performance in sea cages vs land tanks for yellowtail kingfish *Seriola lalandi*. *Aquaculture*, 479, 169-175.
- PUIGSERVER, P., ADELMANT, G., WU, Z., FAN, M., XU, J., O'MALLEY, B. & SPIEGELMAN, B. M. 1999. Activation of PPAR γ coactivator-1 through transcription factor docking. *Science*, 286, 1368-1371.
- PUIGSERVER, P., WU, Z., PARK, C. W., GRAVES, R., WRIGHT, M. & SPIEGELMAN, B. M. 1998. A cold-inducible coactivator of nuclear receptors linked to adaptive thermogenesis. *Cell*, 92, 829-39.
- QUINN, L. S., ANDERSON, B. G., CONNER, J. D. & WOLDEN-HANSON, T. 2013. IL-15 overexpression promotes endurance, oxidative energy metabolism, and muscle PPAR δ , SIRT1, PGC-1 α , and PGC-1 β expression in male mice. *Endocrinology*, 154, 232-245.
- RANHOTRA, H. S. 2010. Long-term caloric restriction up-regulates PPAR gamma co-activator 1 alpha (PGC-1 alpha) expression in mice. *Indian Journal of Biochemistry & Biophysics*, 47, 272-277.
- REGLERO, P., TITTENSOR, D. P., ÁLVAREZ-BERASTEGUI, D., APARICIO-GONZÁLEZ, A. & WORM, B. 2014. Worldwide distributions of tuna larvae: revisiting hypotheses on environmental requirements for spawning habitats. *Marine Ecology Progress Series*, 501, 207-224.
- REYNOLDS, T., BANERJEE, S., SHARMA, V., DONOHUE, J., COULDWELL, S., SOSINSKY, A., FRULLA, A., ROBINSON, A. & PURI, V. 2015. Effects of a high fat diet and voluntary wheel running exercise on cidea and cidec expression in liver and adipose tissue of mice.

- RHEE, J., GE, H., YANG, W., FAN, M., HANDSCHIN, C., COOPER, M., LIN, J., LI, C. & SPIEGELMAN, B. M. 2006. Partnership of PGC-1 α and HNF4 α in the regulation of lipoprotein metabolism. *Journal of Biological Chemistry*, 281, 14683-14690.
- RIEK, A. & GEISER, F. 2013. Allometry of thermal variables in mammals: consequences of body size and phylogeny. *Biological Reviews*, 88, 564-572.
- RODRIGUEZ-CALVO, R., JOVE, M., COLL, T., CAMINS, A., SANCHEZ, R. M., ALEGRET, M., MERLOS, M., PALLAS, M., LAGUNA, J. C. & VAZQUEZ-CARRERA, M. 2006. PGC-1 β down-regulation is associated with reduced ERR α activity and MCAD expression in skeletal muscle of senescence-accelerated mice. *J Gerontol A Biol Sci Med Sci*, 61, 773-80.
- ROY, B., AGAWA, Y., BRUCE, H., ANDO, M., OKADA, T., SAWADA, Y., ITOH, T. & TSUKAMASA, Y. 2014. Muscle growth in full-cycle cultured Pacific bluefin tuna *Thunnus orientalis* from early larval to juvenile stage: Histochemical, immunohistochemical and ultrastructural observation. *Fisheries Science*, 80, 1009-1020.
- RUBEN, J. 1995. The evolution of endothermy in mammals and birds - From physiology to fossils. *Annual Review of Physiology*, 57, 69-95.
- SADANA, P. & PARK, E. A. 2007a. Characterization of the transactivation domain in the peroxisome-proliferator-activated receptor gamma co-activator (PGC-1). *Biochem J*, 403, 511-8.
- SADANA, P. & PARK, EDWARDS A. 2007b. Characterization of the transactivation domain in the peroxisome-proliferator-activated receptor γ co-activator (PGC-1). *Biochemical Journal*, 403, 511-518.
- SÆTHER, B.-S. & JOBLING, M. 1999. The effects of ration level on feed intake and growth, and compensatory growth after restricted feeding, in turbot *Scophthalmus maximus* L. *Aquaculture Research*, 30, 647-653.
- SAFINA, C. & KLINGER, D. H. 2008. Collapse of bluefin tuna in the western Atlantic. *Conservation Biology*, 22, 243-246.
- SAITOU, N. & NEI, M. 1987. The neighbor-joining method: A new method for reconstructing phylogenetic trees. *Mol Biol Evol*, 4, 406-25.
- SAVAGE, V. M., ALLEN, A. P., BROWN, J. H., GILLOOLY, J. F., HERMAN, A. B., WOODRUFF, W. H. & WEST, G. B. 2007. Scaling of number, size, and metabolic rate of cells with body size in mammals. *Proceedings of the National Academy of Sciences of the United States of America*, 104, 4718-4723.
- SAVAGE, V. M., GILLOOLY, J. F., WOODRUFF, W. H., WEST, G. B., ALLEN, A. P., ENQUIST, B. J. & BROWN, J. H. 2004. The predominance of quarter-power scaling in biology. *Functional Ecology*, 18, 257-282.
- SAWADA, Y., OKADA, T., MIYASHITA, S., MURATA, O. & KUMAI, H. 2005. Completion of the Pacific bluefin tuna *Thunnus orientalis* life cycle. *Aquaculture Research*, 36, 413-421.
- SCARPULLA, R. C. 2002. Nuclear activators and coactivators in mammalian mitochondrial biogenesis. *Biochim Biophys Acta*, 1576, 1-14.
- SCARPULLA, R. C. 2011. Metabolic control of mitochondrial biogenesis through the PGC-1 family regulatory network. *Biochimica et Biophysica Acta (BBA) - Molecular Cell Research*, 1813, 1269-1278.
- SCHIAFFINO, S. & REGGIANI, C. 2011. Fiber types in mammalian skeletal muscles. *Physiological Reviews*, 91, 1447-1531.
- SCHNEIDER, C. A., RASBAND, W. S. & ELICEIRI, K. W. 2012. NIH Image to ImageJ: 25 years of image analysis. *Nature Methods*, 9, 671-675.
- SCHRADER, M., COSTELLO, J., GODINHO, L. & ISLINGER, M. 2015. *Peroxisome-mitochondria interplay and disease*.
- SEEBACHER, F. 2000. Heat transfer in a microvascular network: The effect of heart rate on heating and cooling in reptiles (pogona barbata and varanus varius). *J Theor Biol*, 203, 97-109.

- SEEBACHER, F. 2009. Responses to temperature variation: integration of thermoregulation and metabolism in vertebrates. *J Exp Biol*, 212, 2885-91.
- SEEBACHER, F. & GRIGG, G. 2001. Changes in heart rate are important for thermoregulation in the varanid lizard *Varanus varius*. *Journal of Comparative Physiology B*, 171, 395-400.
- SEPULVEDA, C. A., DICKSON, K. A., FRANK, L. R. & GRAHAM, J. B. 2007. Cranial endothermy and a putative brain heater in the most basal tuna species, *Allothunnus fallai*. *Journal of Fish Biology*, 70, 1720-1733.
- SEPULVEDA, C. A., WEGNER, N. C., BERNAL, D. & GRAHAM, J. B. 2005. The red muscle morphology of the thresher sharks (family Alopiidae). *Journal of Experimental Biology*, 208, 4255-4261.
- SETH, A., STEEL, J. H., NICHOL, D., POCOCK, V., KUMARAN, M. K., FRITAH, A., MOBBERLEY, M., RYDER, T. A., ROWLERSON, A., SCOTT, J., POUTANEN, M., WHITE, R. & PARKER, M. 2007. The transcriptional corepressor RIP140 regulates oxidative metabolism in skeletal muscle. *Cell Metabolism*, 6, 236-245.
- SFAKIOTAKIS, M., LANE, D. M. & DAVIES, J. B. C. 1999. Review of fish swimming modes for aquatic locomotion. *IEEE Journal of Oceanic Engineering*, 24, 237-252.
- SHADWICK, R. E. 2005. How tunas and Lamnid sharks swim: An evolutionary convergence. *American Scientist*, 93, 524-531.
- SHADWICK, R. E. & SYME, D. A. 2008. Thunniform swimming: muscle dynamics and mechanical power production of aerobic fibres in yellowfin tuna (*Thunnus albacares*). *Journal of Experimental Biology*, 211, 1603-1611.
- SHEPPARD, M. 2004. *A Photographic Guide to Diseases of Yellowtail (Seriola) Fish*, M. Sheppard.
- SHIMOSE, T., TANABE, T., CHEN, K.-S. & HSU, C.-C. 2009. Age determination and growth of Pacific bluefin tuna, *Thunnus orientalis*, off Japan and Taiwan. *Fisheries Research*, 100, 134-139.
- SHIMOSE, T., WATANABE, H., TANABE, T. & KUBODERA, T. 2013. Ontogenetic diet shift of age-0 year Pacific bluefin tuna *Thunnus orientalis*. *Journal of Fish Biology*, 82, 263-276.
- SICURO, B. & LUZZANA, U. 2016. The state of seriola spp. Other than yellowtail (*S. quinqueradiata*) farming in the world. *Reviews in Fisheries Science & Aquaculture*, 24, 314-325.
- SIEVERS, F., WILM, A., DINEEN, D., GIBSON, T. J., KARPLUS, K., LI, W., LOPEZ, R., MCWILLIAM, H., REMMERT, M., SÖDING, J., THOMPSON, J. D. & HIGGINS, D. G. 2011. Fast, scalable generation of high-quality protein multiple sequence alignments using Clustal Omega. *Molecular Systems Biology*, 7.
- SKETELJ, J., CRNE-FINDERLE, N., STRUKELJ, B., TRONTELJ, J. V. & PETTE, D. 1998. Acetylcholinesterase mRNA level and synaptic activity in rat muscles depend on nerve-induced pattern of muscle activation. *The Journal of Neuroscience*, 18, 1944-1952.
- SLADEK, R., BADER, J. A. & GIGUÈRE, V. 1997. The orphan nuclear receptor estrogen-related receptor alpha is a transcriptional regulator of the human medium-chain acyl coenzyme A dehydrogenase gene. *Molecular and Cellular Biology*, 17, 5400-5409.
- SOMERO, G. N. & CHILDRESS, J. J. 1980. A violation of the metabolism-size scaling paradigm: Activities of glycolytic enzymes in muscle increase in larger-size fish. *Physiological Zoology*, 53, 322-337.
- SOMERO, G. N. & CHILDRESS, J. J. 1985. Scaling of oxidative and glycolytic enzyme activities in fish muscle. In: GILLES, R. (ed.) *Circulation, Respiration, and Metabolism: Current Comparative Approaches*. Berlin, Heidelberg: Springer Berlin Heidelberg.

- SOTO, I. C., FONTANESI, F., LIU, J. & BARRIENTOS, A. 2012. Biogenesis and assembly of eukaryotic cytochrome I oxidase catalytic core. *Biochimica et Biophysica Acta*, 1817, 883-897.
- SPANGENBURG, E. E. & BOOTH, F. W. 2003. Molecular regulation of individual skeletal muscle fibre types. *Acta Physiologica Scandinavica*, 178, 413-424.
- SPEAKMAN, J. R. & KRÓL, E. 2010. Maximal heat dissipation capacity and hyperthermia risk: neglected key factors in the ecology of endotherms. *Journal of Animal Ecology*, 79, 726-746.
- STANCIC, A., BUZADZIC, B., KORAC, A., OTASEVIC, V., JANKOVIC, A., VUCETIC, M., MARKELIC, M., VELICKOVIC, K., GOLIC, I. & KORAC, B. 2013. Regulatory role of PGC-1 α /PPAR signaling in skeletal muscle metabolic recruitment during cold acclimation. *The Journal of Experimental Biology*, 216, 4233-4241.
- STEVENS, E. D. 2011. The Retia. *Encyclopedia of Fish Physiology: From Genome to Environment, Vols 1-3*, 1119-1131.
- STEVENS, E. D. & FRY, F. E. J. 1971. Brain and muscle temperatures in ocean caught and captive skipjack tuna. *Comparative Biochemistry and Physiology Part A: Physiology*, 38, 203-211.
- STEWART, J., FERRELL, D. J. & VAN DER WALT, B. 2004. Sizes and ages in commercial landings with estimates of growth, mortality and yield per recruit of yellowtail kingfish (*Seriola lalandi*) from New South Wales, Australia. *Marine and Freshwater Research*, 55, 489-497.
- SWANSON, D., BLOCK, R. & MOUSA, S. A. 2012. Omega-3 Fatty Acids EPA and DHA: Health Benefits Throughout Life. *Advances in Nutrition*, 3, 1-7.
- TAKAGI, T., TAMURA, Y. & WEIHS, D. 2013. Hydrodynamics and energy-saving swimming techniques of Pacific bluefin tuna. *Journal of Theoretical Biology*, 336, 158-172.
- TAMURA, K., STECHER, G., PETERSON, D., FILIPSKI, A. & KUMAR, S. 2013. MEGA6: Molecular Evolutionary Genetics Analysis version 6.0. *Mol Biol Evol*, 30, 2725-9.
- TANABE, T., KAYAMA, S. & OGURA, M. 2003. *Precise age determination of young to adult skipjack tuna (Katsuwonus pelamis) with validation of otolith daily increment.*
- TANAKA, Y., SATOH, K., IWAHASHI, M. & YAMADA, H. 2006. *Growth-dependent recruitment of Pacific bluefin tuna Thunnus orientalis in the northwestern Pacific Ocean.*
- TAYLOR, E. B., LAMB, J. D., HURST, R. W., CHESSER, D. G., ELLINGSON, W. J., GREENWOOD, L. J., PORTER, B. B., HERWAY, S. T. & WINDER, W. W. 2005. Endurance training increases skeletal muscle LKB1 and PGC-1 α protein abundance: effects of time and intensity. *American Journal of Physiology-Endocrinology and Metabolism*, 289, 960-968.
- TIAN, X. & QIN, J. G. 2004. Effects of previous ration restriction on compensatory growth in barramundi *Lates calcarifer*. *Aquaculture*, 235, 273-283.
- TOCHER, D. R. 2003. Metabolism and Functions of Lipids and Fatty Acids in Teleost Fish. *Reviews in Fisheries Science*, 11, 107-184.
- TOCHER, D. R. 2010. Fatty acid requirements in ontogeny of marine and freshwater fish. *Aquaculture Research*, 41, 717-732.
- TRIPATHI, G. & VERMA, P. 2003. Starvation-induced impairment of metabolism in a freshwater catfish. *Zeitschrift Fur Naturforschung C-a Journal of Biosciences*, 58, 446-451.
- TSENG, M.-C., SHIAO, J.-C. & HUNG, Y.-H. 2011. Genetic identification of *Thunnus orientalis*, *T. thynnus*, and *T. maccoyii* by a cytochrome *b* gene analysis. *Environmental Biology of Fishes*, 91, 103-115.
- TSUDA, Y., SAKAMOTO, W., YAMAMOTO, S. & MURATA, O. 2012. Effect of environmental fluctuations on mortality of juvenile Pacific bluefin tuna, *Thunnus orientalis*, in closed life-cycle aquaculture. *Aquaculture*, 330-333, 142-147.

- TSUKIHARA, T., AOYAMA, H., YAMASHITA, E., TOMIZAKI, T., YAMAGUCHI, H., SHINZAWAITOH, K., NAKASHIMA, R., YAONO, R. & YOSHIKAWA, S. 1996. The whole structure of the 13-subunit oxidized cytochrome *c* oxidase at 2.8 angstrom. *Science*, 272, 1136-1144.
- TURCHINI, G. M., TORSTENSEN, B. E. & NG, W.-K. 2009. Fish oil replacement in finfish nutrition. *Reviews in Aquaculture*, 1, 10-57.
- UNTERGASSER, A., CUTCUTACHE, I., KORESSAAR, T., YE, J., FAIRCLOTH, B. C., REMM, M. & ROZEN, S. G. 2012. Primer3--new capabilities and interfaces. *Nucleic Acids Res*, 40, e115.
- VEGA, R. B., HUSS, J. M. & KELLY, D. P. 2000. The coactivator PGC-1 cooperates with peroxisome proliferator-activated receptor α in transcriptional control of nuclear genes encoding mitochondrial fatty acid oxidation enzymes. *Molecular and Cellular Biology*, 20, 1868-1876.
- WANG, T., HUNG, C. C. Y. & RANDALL, D. J. 2006. The comparative physiology of food deprivation: From feast to famine. *Annual Review of Physiology*. Palo Alto: Annual Reviews.
- WARD, R. D., ZEMLAK, T. S., INNES, B. H., LAST, P. R. & HEBERT, P. D. N. 2005. DNA barcoding Australia's fish species. *Philosophical Transactions of the Royal Society B: Biological Sciences*, 360, 1847-1857.
- WEBSTER, C. D. & LIM, C. 2002. *Nutrient Requirements and Feeding of Finfish for Aquaculture*, CABI.
- WEGNER, N. C., SNODGRASS, O. E., DEWAR, H. & HYDE, J. R. 2015. Whole-body endothermy in a mesopelagic fish, the opah, *Lampris guttatus*. *Science*, 348, 786-789.
- WOLF, N. G., SWIFT, P. R. & CAREY, F. G. 1988. Swimming muscle helps warm the brain of lamnid sharks. *Journal of Comparative Physiology B*, 157, 709-715.
- WU, Z., PUIGSERVER, P., ANDERSSON, U., ZHANG, C., ADELMANT, G., MOOTHA, V., TROY, A., CINTI, S., LOWELL, B., SCARPULLA, R. C. & SPIEGELMAN, B. M. 1999. Mechanisms Controlling Mitochondrial Biogenesis and Respiration through the Thermogenic Coactivator PGC-1. *Cell*, 98, 115-124.
- YANG, T. H. & SOMERO, G. N. 1993. Effects of feeding and food deprivation on oxygen consumption, muscle protein concentration and activities of energy metabolism enzymes in muscle and brain of shallow-living (*Scorpaena guttata*) and deep-living (*Sebastolobus alascanus*) scorpaenid fishes. *The Journal of Experimental Biology*, 181, 213-232.
- YOON, J. C., PUIGSERVER, P., CHEN, G., DONOVAN, J., WU, Z., RHEE, J., ADELMANT, G., STAFFORD, J., KAHN, C. R., GRANNER, D. K., NEWGARD, C. B. & SPIEGELMAN, B. M. 2001. Control of hepatic gluconeogenesis through the transcriptional coactivator PGC-1. *Nature*, 413, 131-8.
- YÚFERA, M., ORTIZ-DELGADO, J. B., HOFFMAN, T., SIGUERO, I., URUP, B. & SARASQUETE, C. 2014. Organogenesis of digestive system, visual system and other structures in Atlantic bluefin tuna (*Thunnus thynnus*) larvae reared with copepods in mesocosm system. *Aquaculture*, 426-427, 126-137.
- ZHANG, Y., TIMMERHAUS, G., ANTTILA, K., MAUDUIT, F., JØRGENSEN, S. M., KRISTENSEN, T., CLAIREAUX, G., TAKLE, H. & FARRELL, A. P. 2016. Domestication compromises athleticism and respiratory plasticity in response to aerobic exercise training in Atlantic salmon (*Salmo salar*). *Aquaculture*, 463, 79-88.

APPENDICES

Appendix 1. Confirmation of the species identity of the PBT specimens

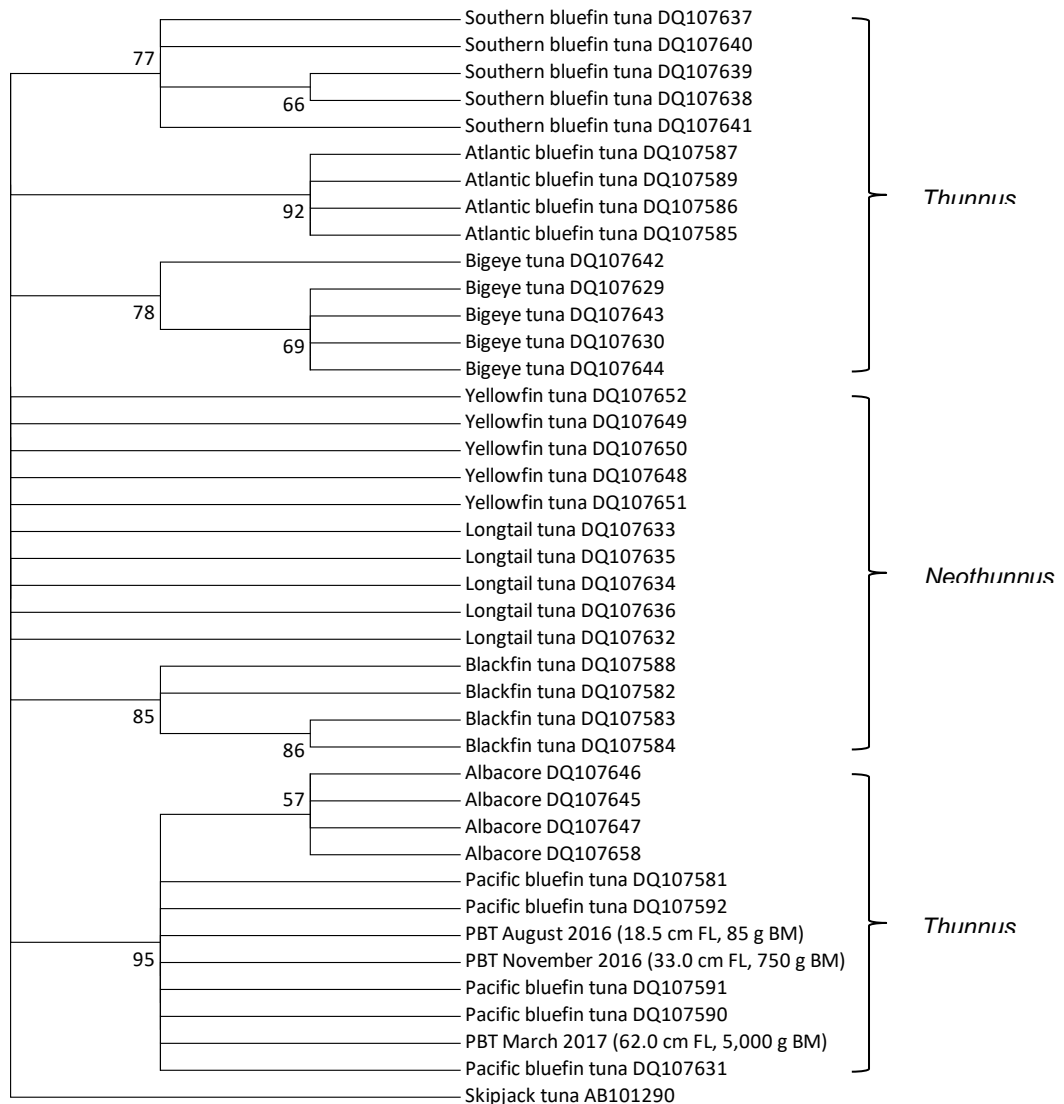


Fig. A1.1. A phylogeny of COXI nucleotide sequences from the eight species that make up the genus *Thunnus*, including three sequences from the fish sampled in this study. The sequences were obtained from the GenBank database (available at <http://www.ncbi.nlm.nih.gov/>). *Katsuwonus pelamis* (skipjack tuna) was used as the outgroup to root the tree. Evaluation of statistical confidence was based on 1,000 bootstrap replicates. Branches with bootstrap values of less than 50 have been collapsed.

Appendix 2. PCR primer validations

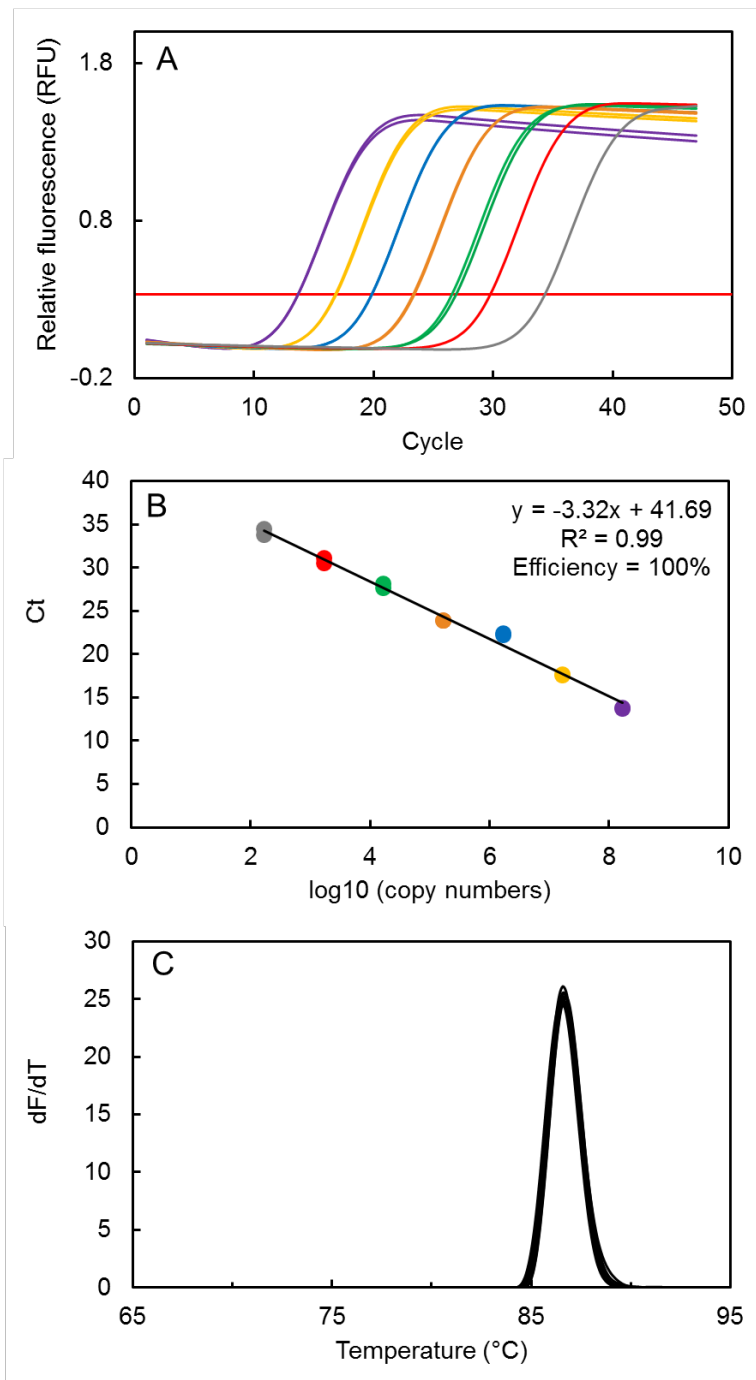


Fig. A2.1 β -actin (A) Fluorescence curve, threshold indicated by red line (B) Standard curve, colours correspond to the curves in part A (C) Melt curve rate of change in fluorescence relative to temperature

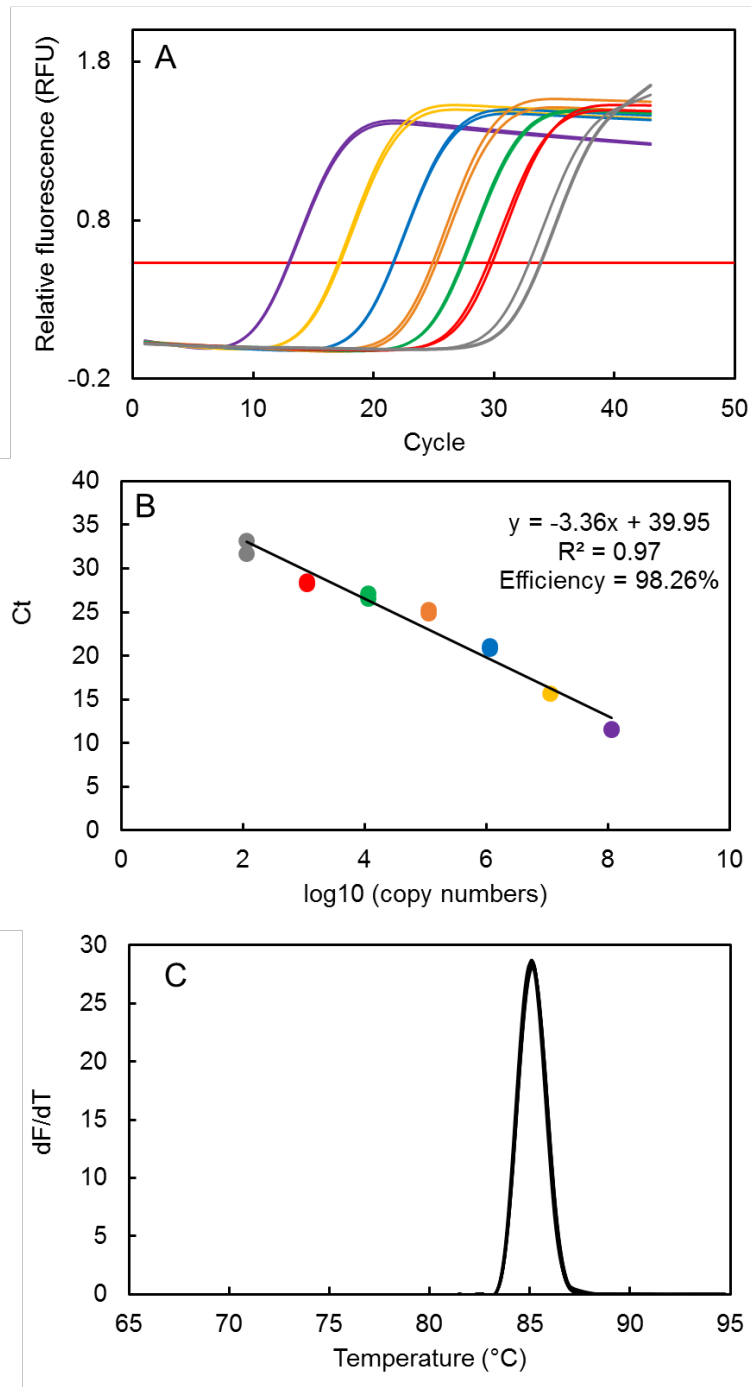


Fig. A2.2 CS (A) Fluorescence curve, threshold indicated by red line (B) Standard curve, colours correspond to the curves in part A (C) Melt curve rate of change in fluorescence relative to temperature

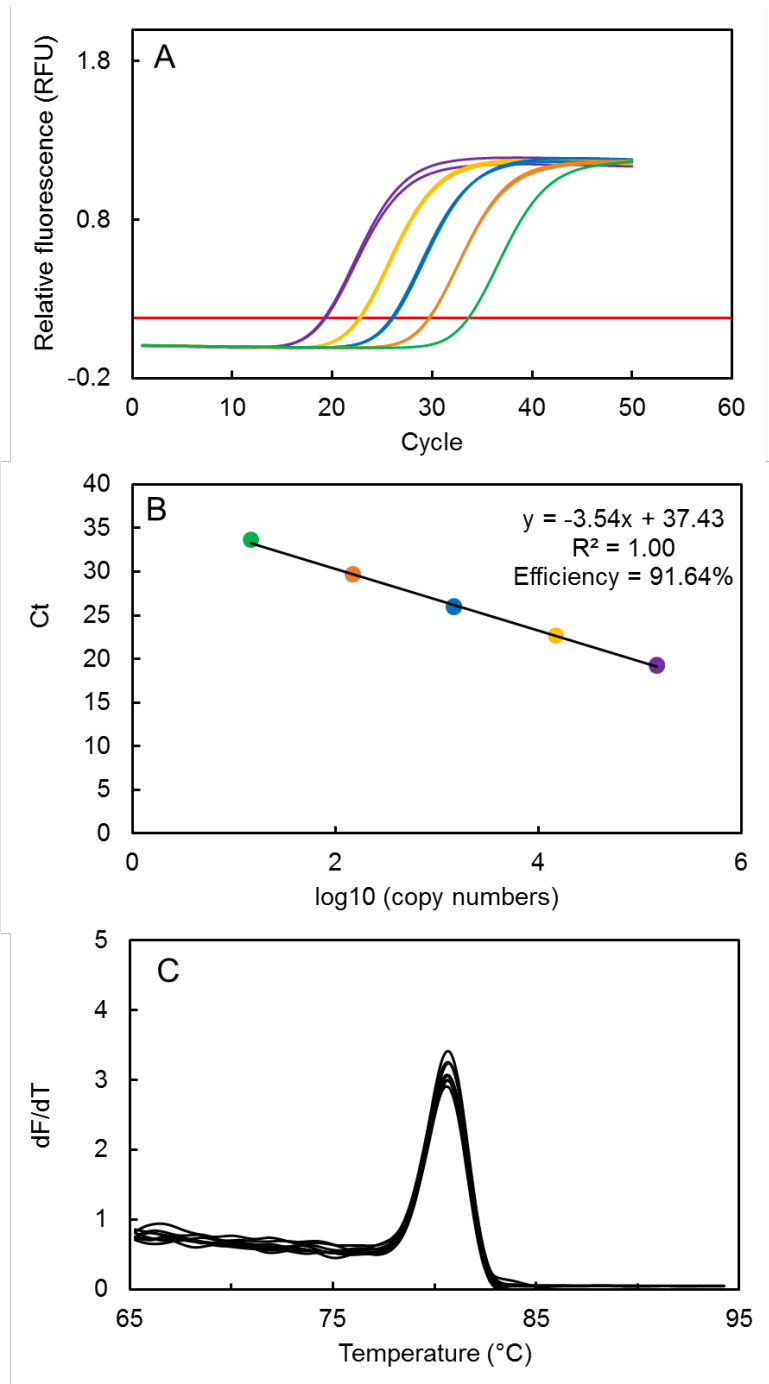


Fig. A2.3 PBT COXI (A) Fluorescence curve, threshold indicated by red line (B) Standard curve, colours correspond to the curves in part A (C) Melt curve rate of change in fluorescence relative to temperature

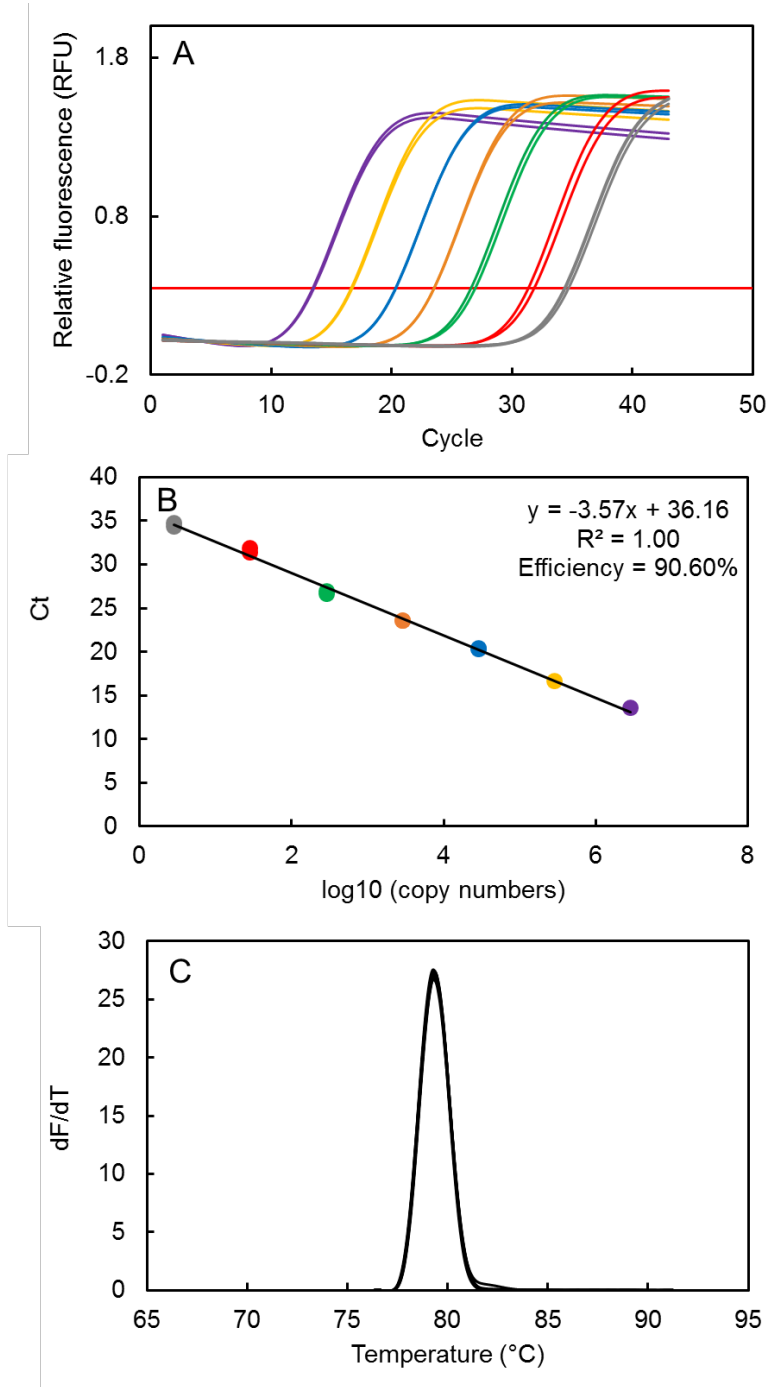


Fig. A2.4 PBT COXIV-1 (A) Fluorescence curve, threshold indicated by red line (B) Standard curve, colours correspond to the curves in part A (C) Melt curve rate of change in fluorescence relative to temperature

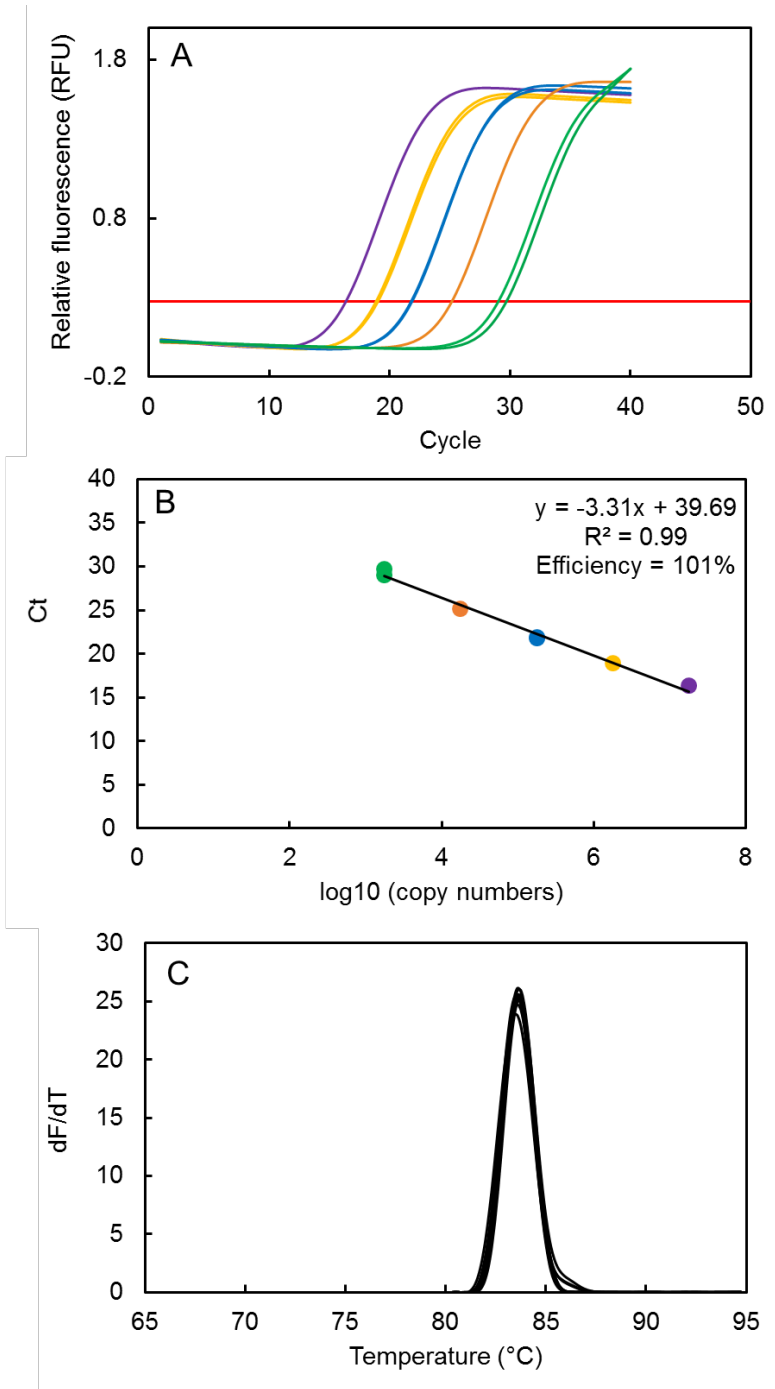


Fig. A2.5 PK (A) Fluorescence curve, threshold indicated by red line (B) Standard curve, colours correspond to the curves in part A (C) Melt curve rate of change in fluorescence relative to temperature

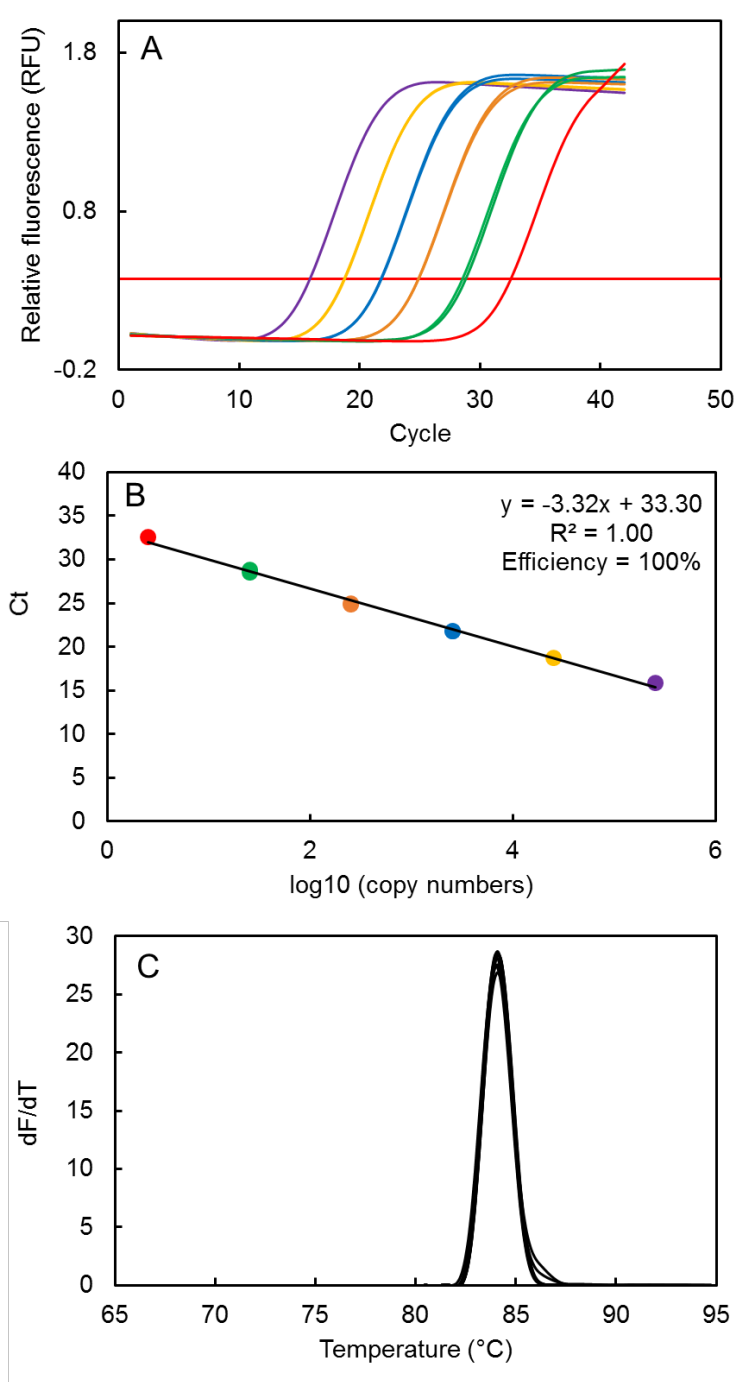


Fig. A2.6 PBT PGC-1 α (A) Fluorescence curve, threshold indicated by red line (B) Standard curve, colours correspond to the curves in part A (C) Melt curve rate of change in fluorescence relative to temperature

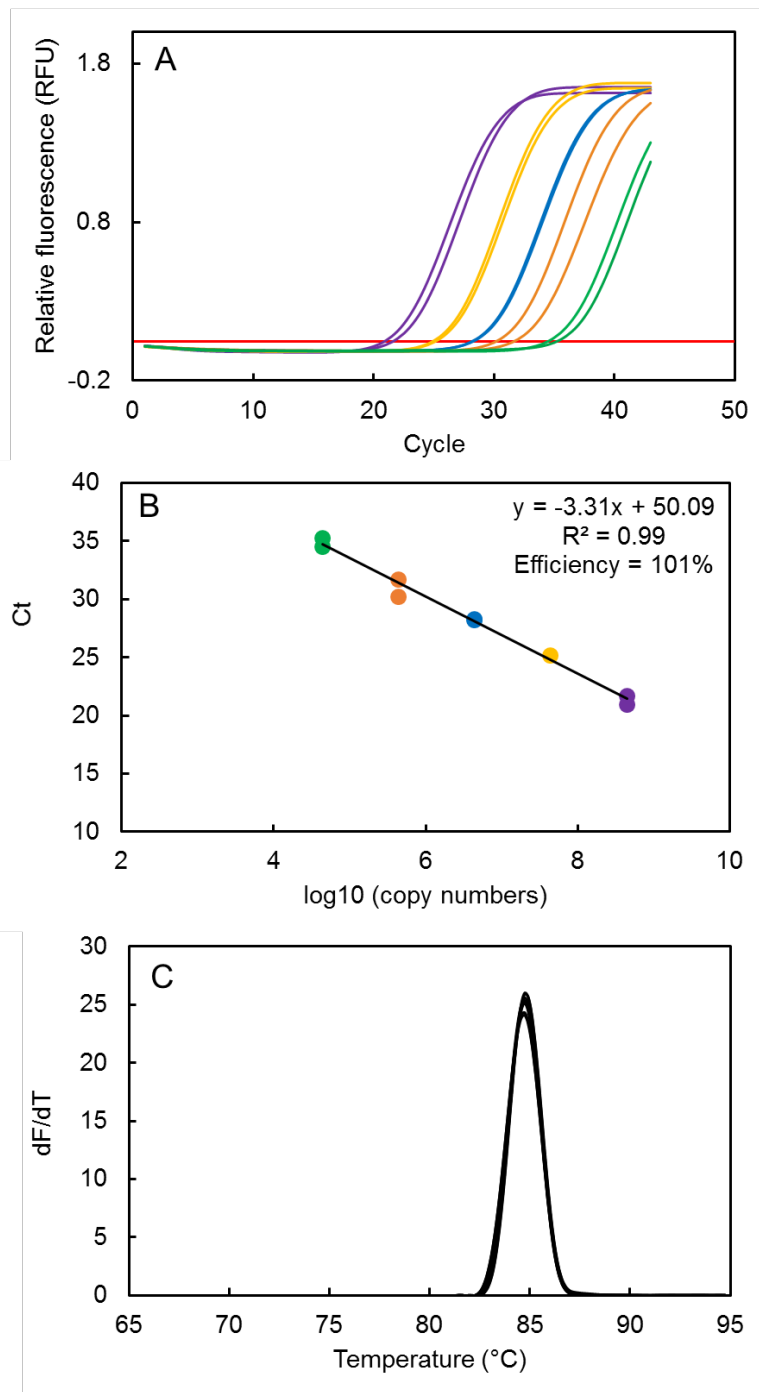


Fig. A2.7 PBT PGC-1 β (A) Fluorescence curve, threshold indicated by red line (B) Standard curve, colours correspond to the curves in part A (C) Melt curve rate of change in fluorescence relative to temperature

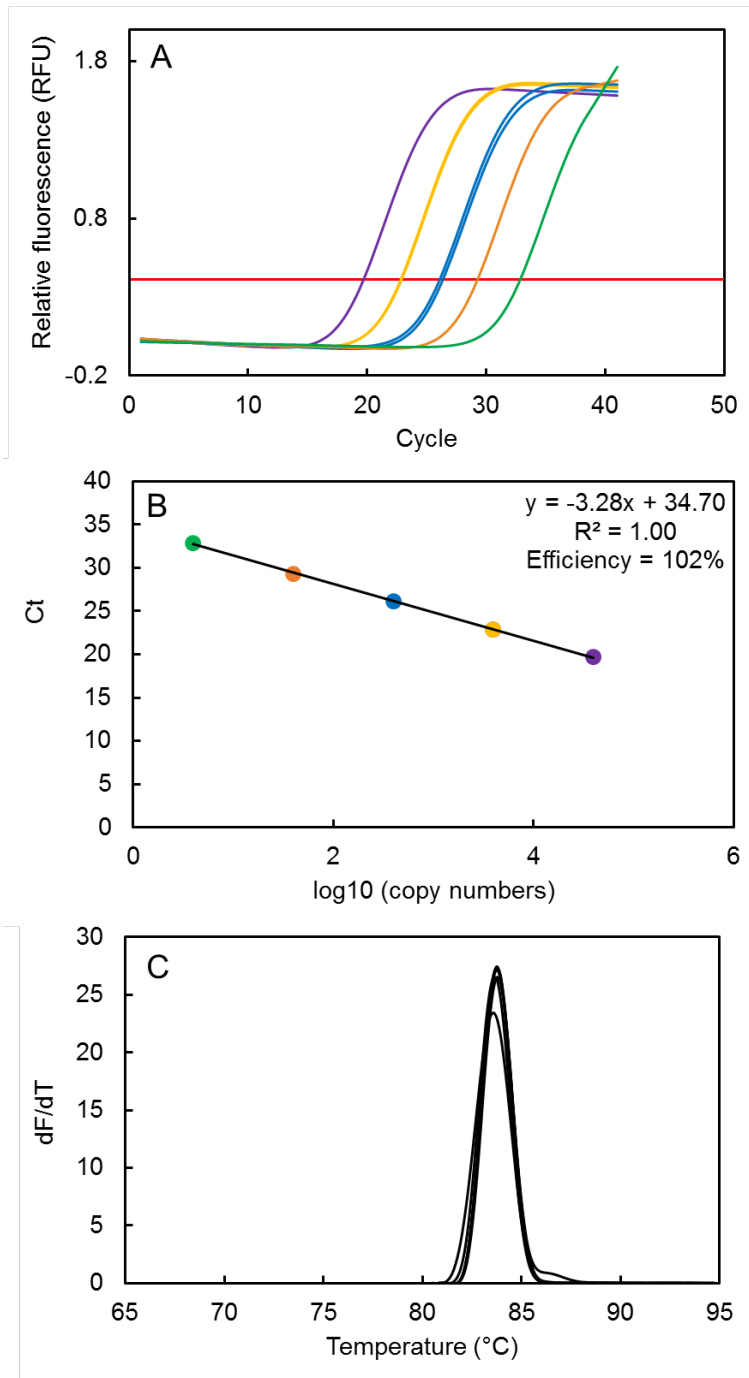


Fig. A2.8 PBT PPAR α (A) Fluorescence curve, threshold indicated by red line (B) Standard curve, colours correspond to the curves in part A (C) Melt curve rate of change in fluorescence relative to temperature

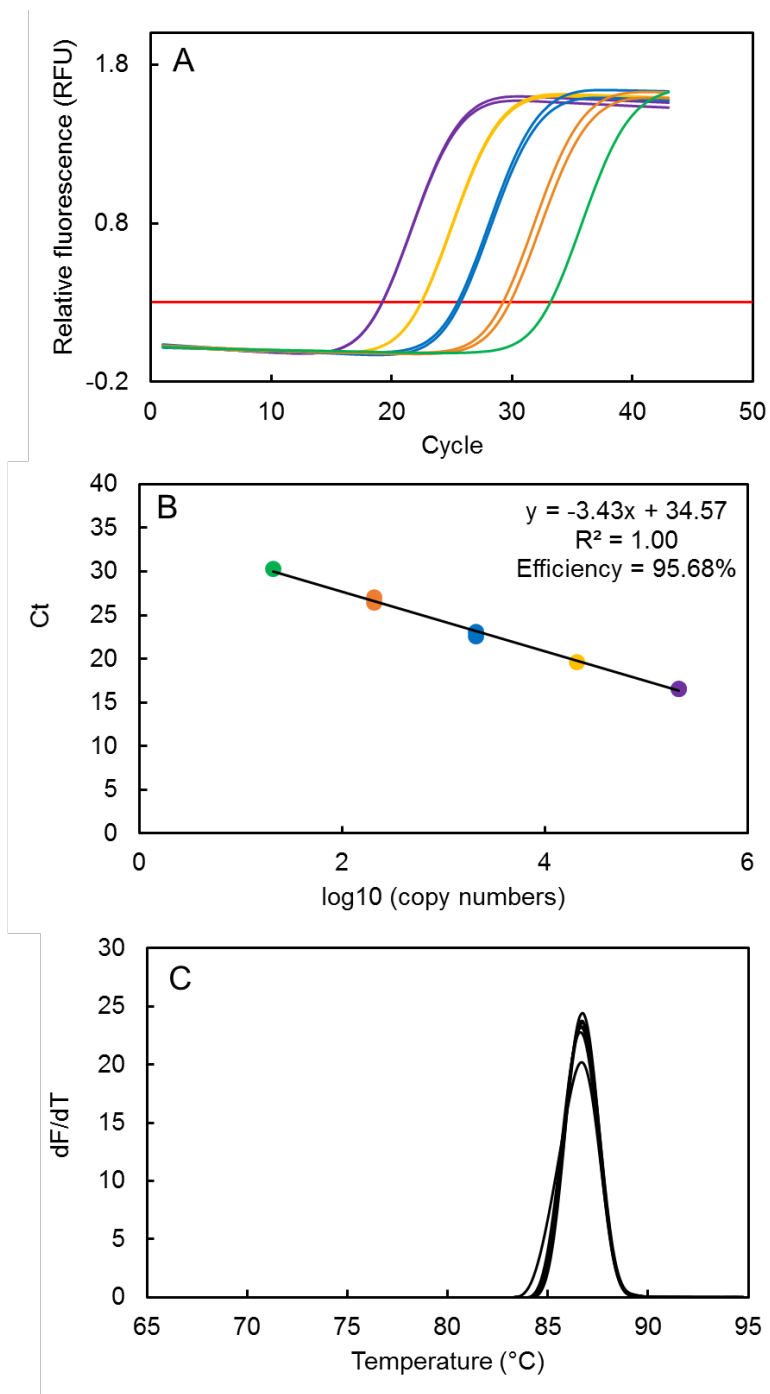


Fig. A2.9 PBT MCAD (A) Fluorescence curve, threshold indicated by red line (B) Standard curve, colours correspond to the curves in part A (C) Melt curve rate of change in fluorescence relative to temperature

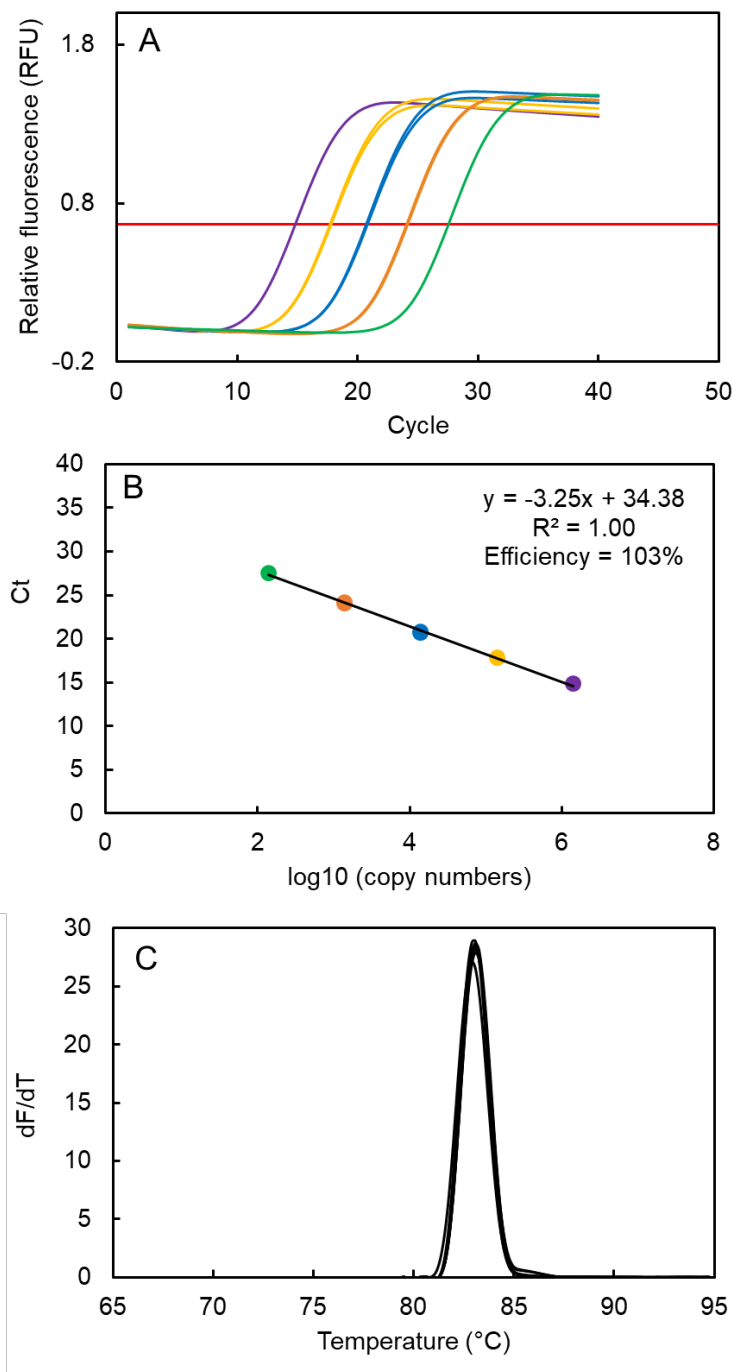


Fig. A2.10 YTK COXI (A) Fluorescence curve, threshold indicated by red line (B) Standard curve, colours correspond to the curves in part A (C) Melt curve rate of change in fluorescence relative to temperature

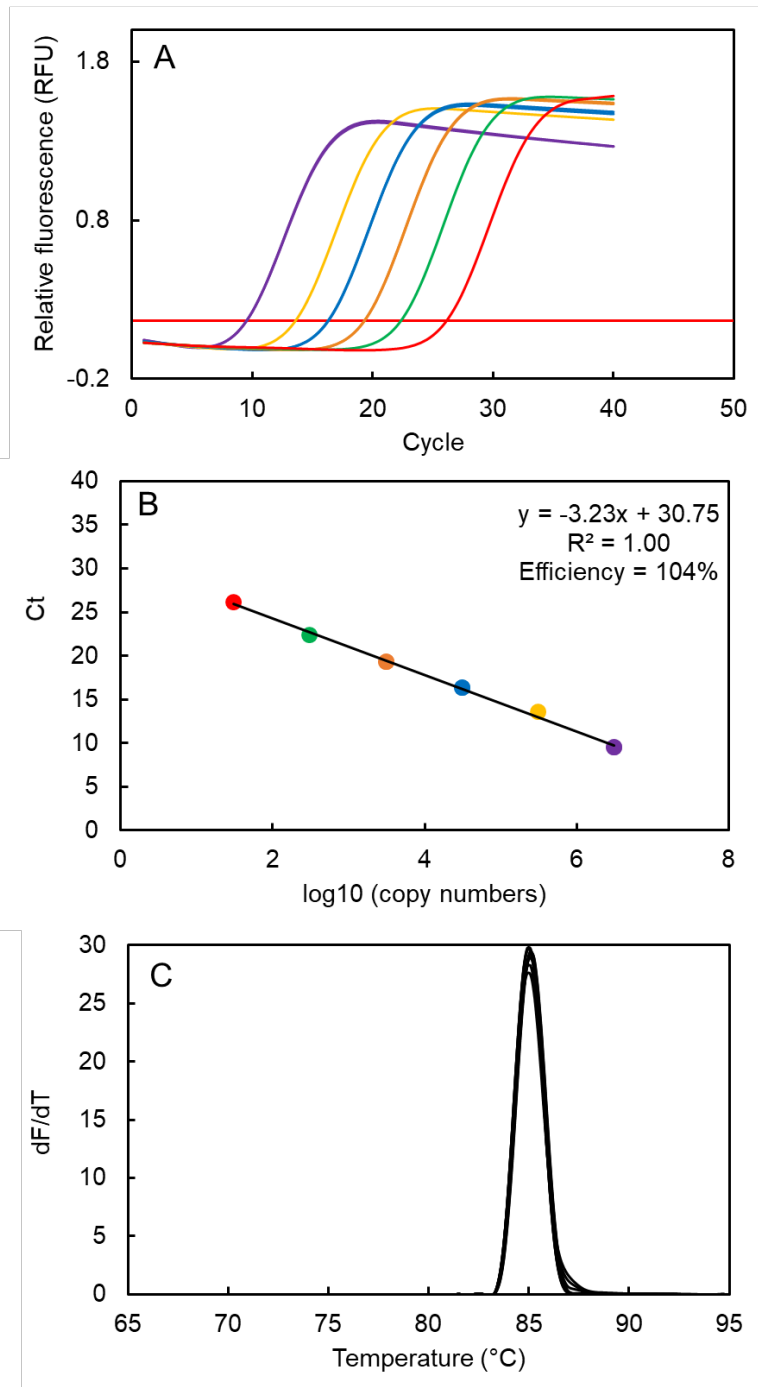


Fig. A2.11 YTK PGC-1 α (A) Fluorescence curve, threshold indicated by red line (B) Standard curve, colours correspond to the curves in part A (C) Melt curve rate of change in fluorescence relative to temperature

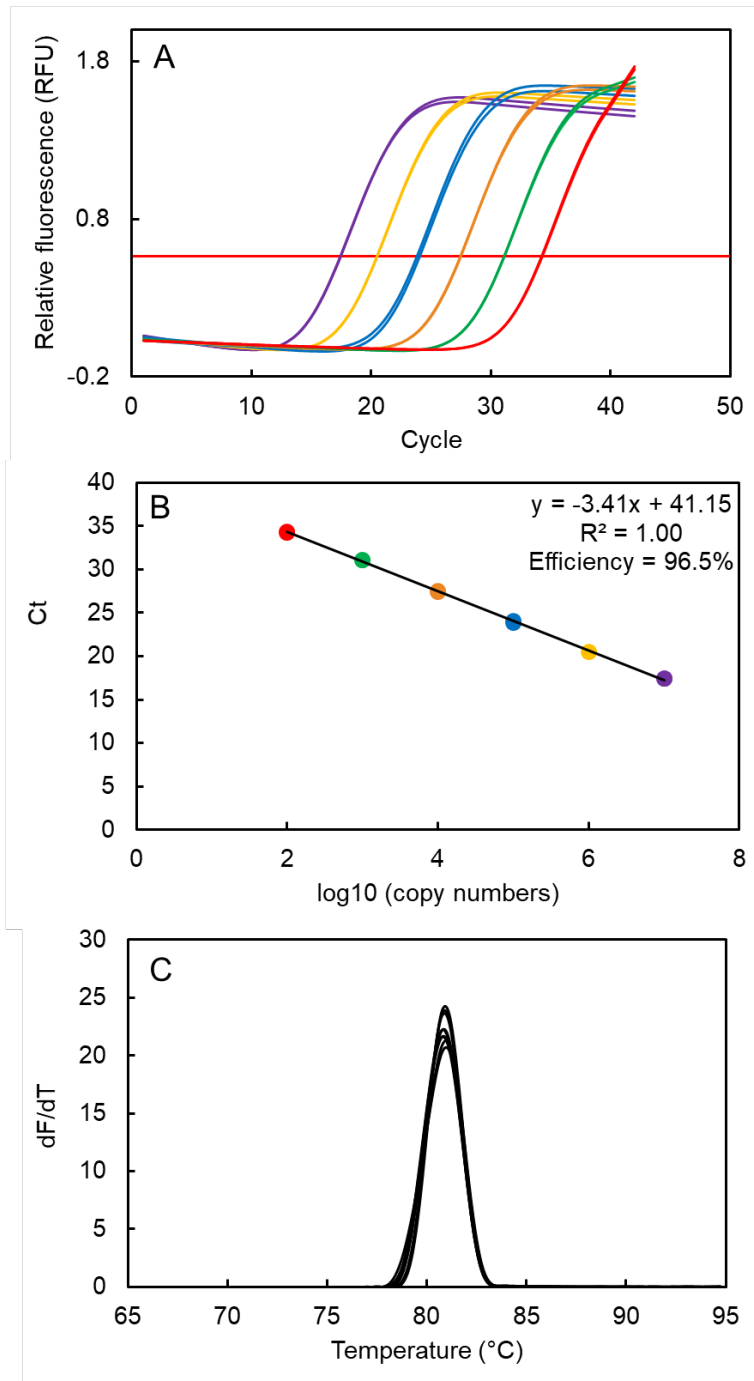


Fig. A2.12 YTK PPAR α (A) Fluorescence curve, threshold indicated by red line (B) Standard curve, colours correspond to the curves in part A (C) Melt curve rate of change in fluorescence relative to temperature

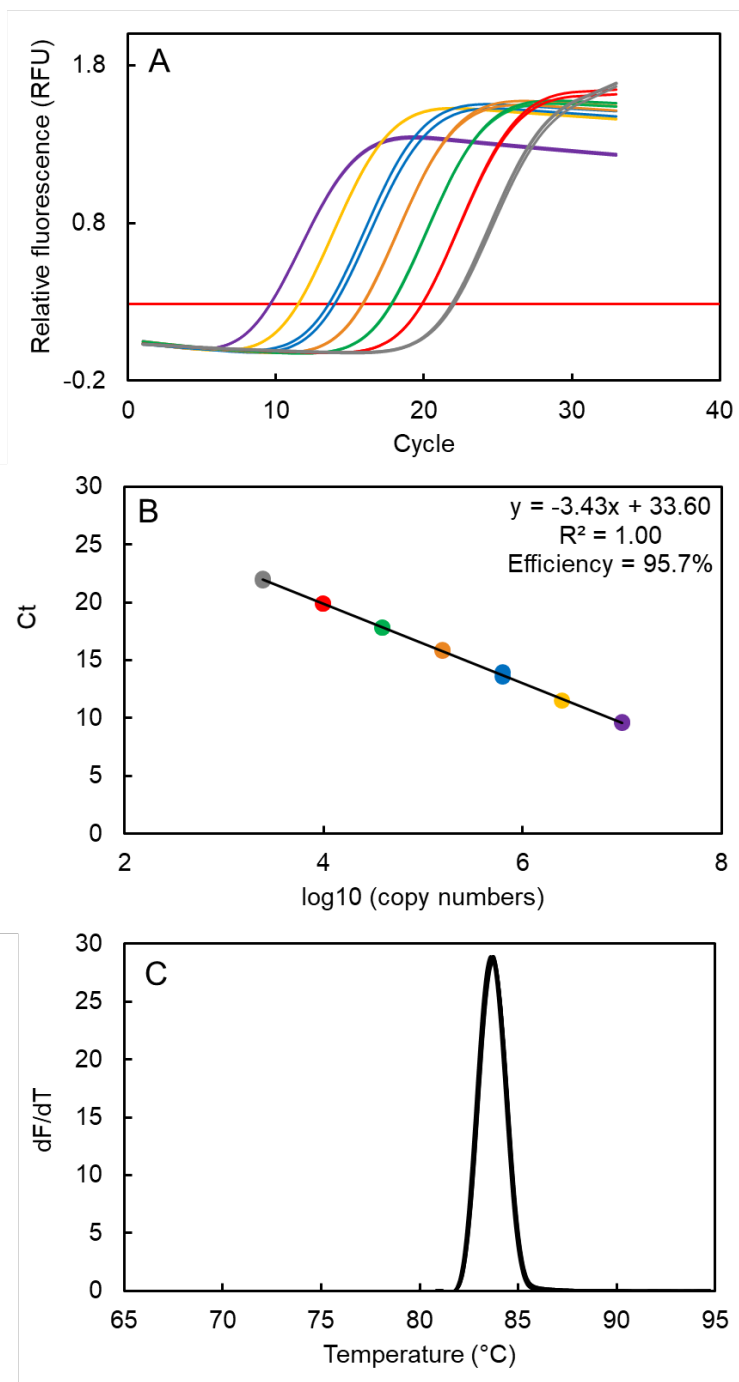


Fig. A2.13 YTK MCAD (A) Fluorescence curve, threshold indicated by red line (B) Standard curve, colours correspond to the curves in part A (C) Melt curve rate of change in fluorescence relative to temperature

Appendix 3. Identity matrix of PGC-1 α amino acid sequences

Table A3.1. PGC-1 α amino acid sequence identity matrix, constructed using Clustal Omega (Sievers et al., 2011), comparing YTK and PBT with other vertebrate species (for scientific names and GenBank accession numbers refer to Table. 5.3).

	YTK	PBT	Swordfish	Clownfish	Japanese medaka	Arctic char	Rainbow trout	Bowfin	Zebrafish	Golden shiner	Black ghost knifefish	Goldfish	White sturgeon	Nile bichir	Chicken	Southern ostrich	Cow	Chinese alligator	Rat	Green sea turtle	Mouse	African clawed frog	Spiny dogfish	Burmese python	Central bearded dragon
YTK	100	95	96.21	92.99	85.4	75.88	74.54	71.09	70.36	69.44	69.37	69.2	67.77	64.88	60.32	59.97	59.89	59.66	59.58	59.66	59.37	57.67	55.74	55.61	55.03
PBT	95	100	93.05	91.5	82.99	71.23	71.88	68.8	69.26	69.48	69.87	69.03	65.42	61.73	58.52	58.52	58.48	57.21	58.82	56.99	58.91	56.51	52.42	53.19	55.12
Swordfish	96.21	93.05	100	92.09	83.86	74.53	73.46	69.77	69.13	68.31	68.1	67.95	67.14	63.79	59.79	59.54	59.1	58.99	59.04	59.25	58.83	57.18	55.17	54.8	54.86
Clownfish	92.99	91.5	92.09	100	86.9	75.49	73.63	70.8	69.75	68.32	68.72	68.44	67.35	64.53	60.98	60.65	60.95	60.21	60.38	60.21	60.18	58.03	55.52	56.4	55.97
Japanese medaka	85.4	82.99	83.86	86.9	100	73.62	71.41	69.42	67.49	66.14	66.42	66.06	66.54	63.07	60.16	59.95	59.61	59.51	58.91	59.12	58.84	58.02	54.8	55.43	54.85
Arctic char	75.88	71.23	74.53	75.49	73.62	100	96.33	71.95	72.74	71.6	71.11	70.55	69.77	65.49	61.69	61.24	60.57	61.04	60.7	61.04	60.62	59.03	56.86	56.98	56.55
Rainbow trout	74.54	71.88	73.46	73.63	71.41	96.33	100	70.22	71.55	70.05	69.65	69.53	68.24	64.04	59.73	59.47	58.55	59.04	58.96	58.9	58.88	57.76	56.47	55.57	55.13
Bowfin	71.09	68.8	69.77	70.8	69.42	71.95	70.22	100	76.21	74.69	75.28	74.69	74.21	70.2	66.58	66.17	64.99	65.35	64.44	65.48	64.35	61.22	63.02	60.48	61.85
Zebrafish	70.36	69.26	69.13	69.75	67.49	72.74	71.55	76.21	100	91.8	89.93	89.68	67.92	65.87	61.43	61.47	60.99	61.02	60.52	61.29	60.16	59.5	58.83	57.74	57.22
Golden shiner	69.44	69.48	68.31	68.32	66.14	71.6	70.05	74.69	91.8	100	89.68	89.56	66.33	64.81	60.03	59.92	59.19	59.49	58.6	59.89	58.52	58.02	57.55	56.76	55.91
Black ghost knifefish	69.37	69.87	68.1	68.72	66.42	71.11	69.65	75.28	89.93	89.68	100	99.4	66.36	64.1	59.67	59.95	58.69	58.98	58.63	59.4	58.41	57.58	57.16	56.35	56.3
Goldfish	69.2	69.03	67.95	68.44	66.06	70.55	69.53	74.69	89.68	89.56	99.4	100	66.16	63.71	59.54	59.56	58.57	58.73	58.51	59.27	58.3	57.1	56.88	56.13	55.27
White sturgeon	67.77	65.42	67.14	67.35	66.54	69.77	68.24	74.21	67.92	66.33	66.36	66.16	100	77.17	68.46	68.08	66.62	67.79	65.55	67.25	65.46	63.86	64.57	61.35	62.85
Nile bichir	64.88	61.73	63.79	64.53	63.07	65.49	64.04	70.2	65.87	64.81	64.1	63.71	77.17	100	67.31	67.31	66.53	66.48	65.7	67.17	65.28	62.36	63.73	60.16	61.69
Chicken	60.32	58.52	59.79	60.98	60.16	61.69	59.73	66.58	61.43	60.03	59.67	59.54	68.46	67.31	100	96.29	87.28	93.84	86.04	92.45	85.79	75.82	66.62	81.44	83.86
Southern ostrich	59.97	58.52	59.54	60.65	59.95	61.24	59.47	66.17	61.47	59.92	59.95	59.56	68.08	67.31	96.29	100	87.69	95.26	86.56	94.11	86.3	76.38	67.88	82.13	86.78
Cow	59.89	58.48	59.1	60.95	59.61	60.57	58.55	64.99	60.99	59.19	58.69	58.57	66.62	66.53	87.28	87.69	100	86.4	92.45	86.52	91.95	74.25	66.53	78.91	79.32
Chinese alligator	59.66	57.21	58.99	60.21	59.51	61.04	59.04	65.35	61.02	59.49	58.98	58.73	67.79	66.48	93.84	95.26	86.4	100	85.28	93.33	85.16	76.47	66.76	82.07	83.98
Rat	59.58	58.82	59.04	60.38	58.91	60.7	58.96	64.44	60.52	58.6	58.63	58.51	65.55	65.7	86.04	86.56	92.45	85.28	100	85.41	98.37	73.46	64.99	77.9	78.81
Green sea turtle	59.66	56.99	59.25	60.21	59.12	61.04	58.9	65.48	61.29	59.89	59.4	59.27	67.25	67.17	92.45	94.11	86.52	93.33	85.41	100	85.28	76.08	67.18	81.19	83.35
Mouse	59.37	58.91	58.83	60.18	58.84	60.62	58.88	64.35	60.16	58.52	58.41	58.3	65.46	65.28	85.79	86.3	91.95	85.16	98.37	85.28	100	72.94	64.71	77.27	78.18
African clawed frog	57.67	56.51	57.18	58.03	58.02	59.03	57.76	61.22	59.5	58.02	57.58	57.1	63.86	62.36	75.82	76.38	74.25	76.47	73.46	76.08	72.94	100	61.2	69.9	71.37
Spiny dogfish	55.74	52.42	55.17	55.52	54.8	56.86	56.47	63.02	58.83	57.55	57.16	56.88	64.57	63.73	66.62	67.88	66.53	66.76	64.99	67.18	64.71	61.2	100	60.76	62.36
Burmese python	55.61	53.19	54.8	56.4	55.43	56.98	55.57	60.48	57.74	56.76	56.35	56.13	61.35	60.16	81.44	82.13	78.91	82.07	77.9	81.19	77.27	69.9	60.76	100	82.24
Central bearded dragon	55.03	55.12	54.86	55.97	54.85	56.55	55.13	61.85	57.22	55.91	56.3	55.27	62.85	61.69	83.86	86.78	79.32	83.98	78.81	83.35	78.18	71.37	62.36	82.24	100

